

RECENT ADVANCES IN PHEOCHROMOCYTOMA AND PARAGANGLIOMA: MOLECULAR PATHOGENESIS, CLINICAL IMPACTS, AND THERAPEUTIC PERSPECTIVE

EDITED BY: Farhadul Islam, Ichiro Abe, Alfred King-yin Lam and Suja Pillai
PUBLISHED IN: Frontiers in Endocrinology





frontiers

Frontiers eBook Copyright Statement

The copyright in the text of individual articles in this eBook is the property of their respective authors or their respective institutions or funders. The copyright in graphics and images within each article may be subject to copyright of other parties. In both cases this is subject to a license granted to Frontiers.

The compilation of articles constituting this eBook is the property of Frontiers.

Each article within this eBook, and the eBook itself, are published under the most recent version of the Creative Commons CC-BY licence.

The version current at the date of publication of this eBook is CC-BY 4.0. If the CC-BY licence is updated, the licence granted by Frontiers is automatically updated to the new version.

When exercising any right under the CC-BY licence, Frontiers must be attributed as the original publisher of the article or eBook, as applicable.

Authors have the responsibility of ensuring that any graphics or other materials which are the property of others may be included in the CC-BY licence, but this should be checked before relying on the CC-BY licence to reproduce those materials. Any copyright notices relating to those materials must be complied with.

Copyright and source acknowledgement notices may not be removed and must be displayed in any copy, derivative work or partial copy which includes the elements in question.

All copyright, and all rights therein, are protected by national and international copyright laws. The above represents a summary only. For further information please read Frontiers' Conditions for Website Use and Copyright Statement, and the applicable CC-BY licence.

ISSN 1664-8714

ISBN 978-2-88971-482-7

DOI 10.3389/978-2-88971-482-7

About Frontiers

Frontiers is more than just an open-access publisher of scholarly articles: it is a pioneering approach to the world of academia, radically improving the way scholarly research is managed. The grand vision of Frontiers is a world where all people have an equal opportunity to seek, share and generate knowledge. Frontiers provides immediate and permanent online open access to all its publications, but this alone is not enough to realize our grand goals.

Frontiers Journal Series

The Frontiers Journal Series is a multi-tier and interdisciplinary set of open-access, online journals, promising a paradigm shift from the current review, selection and dissemination processes in academic publishing. All Frontiers journals are driven by researchers for researchers; therefore, they constitute a service to the scholarly community. At the same time, the Frontiers Journal Series operates on a revolutionary invention, the tiered publishing system, initially addressing specific communities of scholars, and gradually climbing up to broader public understanding, thus serving the interests of the lay society, too.

Dedication to Quality

Each Frontiers article is a landmark of the highest quality, thanks to genuinely collaborative interactions between authors and review editors, who include some of the world's best academicians. Research must be certified by peers before entering a stream of knowledge that may eventually reach the public - and shape society; therefore, Frontiers only applies the most rigorous and unbiased reviews.

Frontiers revolutionizes research publishing by freely delivering the most outstanding research, evaluated with no bias from both the academic and social point of view. By applying the most advanced information technologies, Frontiers is catapulting scholarly publishing into a new generation.

What are Frontiers Research Topics?

Frontiers Research Topics are very popular trademarks of the Frontiers Journals Series: they are collections of at least ten articles, all centered on a particular subject. With their unique mix of varied contributions from Original Research to Review Articles, Frontiers Research Topics unify the most influential researchers, the latest key findings and historical advances in a hot research area! Find out more on how to host your own Frontiers Research Topic or contribute to one as an author by contacting the Frontiers Editorial Office: frontiersin.org/about/contact

RECENT ADVANCES IN PHEOCHROMOCYTOMA AND PARAGANGLIOMA: MOLECULAR PATHOGENESIS, CLINICAL IMPACTS, AND THERAPEUTIC PERSPECTIVE

Topic Editors:

Farhadul Islam, Rajshahi University, Bangladesh

Ichiro Abe, Fukuoka University Chikushi Hospital, Japan

Alfred King-yin Lam, Griffith University, Australia

Suja Pillai, The University of Queensland, Australia

Citation: Islam, F., Abe, I., Lam, A. K.-Y., Pillai, S., eds. (2021). Recent Advances in Pheochromocytoma and Paraganglioma: Molecular Pathogenesis, Clinical Impacts, and Therapeutic Perspective. Lausanne: Frontiers Media SA. doi: 10.3389/978-2-88971-482-7

Table of Contents

- 05 Editorial: Recent Advances in Pheochromocytoma and Paraganglioma: Molecular Pathogenesis, Clinical Impacts, and Therapeutic Perspective**
Farhadul Islam, Ichiro Abe, Suja Pillai, Robert A. Smith and Alfred King-Yin Lam
- 08 Preoperative Management of Pheochromocytoma and Paraganglioma**
Fang Fang, Li Ding, Qing He and Ming Liu
- 18 Recent Advances in Histopathological and Molecular Diagnosis in Pheochromocytoma and Paraganglioma: Challenges for Predicting Metastasis in Individual Patients**
Yuto Yamazaki, Xin Gao, Alessio Pecori, Yasuhiro Nakamura, Yuta Tezuka, Kei Omata, Yoshikiyo Ono, Ryo Morimoto, Fumitoshi Satoh and Hironobu Sasano
- 29 Histopathological Analysis of Tumor Microenvironment and Angiogenesis in Pheochromocytoma**
Xin Gao, Yuto Yamazaki, Alessio Pecori, Yuta Tezuka, Yoshikiyo Ono, Kei Omata, Ryo Morimoto, Yasuhiro Nakamura, Fumitoshi Satoh and Hironobu Sasano
- 39 The VHL/HIF Axis in the Development and Treatment of Pheochromocytoma/Paraganglioma**
Song Peng, Jun Zhang, Xintao Tan, Yiqiang Huang, Jing Xu, Natalie Silk, Dianzheng Zhang, Qiuli Liu and Jun Jiang
- 52 Glucose Intolerance on Pheochromocytoma and Paraganglioma—The Current Understanding and Clinical Perspectives**
Ichiro Abe, Farhadul Islam and Alfred King-Yin Lam
- 58 A Durable Response With the Combination of Nivolumab and Cabozantinib in a Patient With Metastatic Paraganglioma: A Case Report and Review of the Current Literature**
Minas P. Economides, Amishi Y. Shah, Camilo Jimenez, Mouhammed A. Habra, Monica Desai and Matthew T. Campbell
- 65 Genetic and Clinical Profiles of Pheochromocytoma and Paraganglioma: A Single Center Study**
Xiaosen Ma, Ming Li, Anli Tong, Fen Wang, Yunying Cui, Xuebin Zhang, Yushi Zhang, Shi Chen and Yuxiu Li
- 78 A Predictive Nomogram for Red Blood Cell Transfusion in Pheochromocytoma Surgery: A Study on Improving the Preoperative Management of Pheochromocytoma**
Ying Guo, Lili You, Huijun Hu, Anli Tong, Xiaoyun Zhang, Li Yan and Shaoling Zhang

- 86 *Succinate Mediates Tumorigenic Effects via Succinate Receptor 1: Potential for New Targeted Treatment Strategies in Succinate Dehydrogenase Deficient Parangliomas***
Dieter M. Matlac, Katerina Hadrava Vanova, Nicole Bechmann, Susan Richter, Julica Folberth, Hans K. Ghayee, Guang-Bo Ge, Luma Abunimer, Robert Wesley, Redouane Aherrahrou, Margo Dona, Ángel M. Martínez-Montes, Bruna Calsina, Maria J. Merino, Markus Schwaninger, Peter M. T. Deen, Zhengping Zhuang, Jiri Neuzil, Karel Pacak, Hendrik Lehnert and Stephanie M. J. Fliedner
- 97 *Seven Novel Genes Related to Cell Proliferation and Migration of VHL-Mutated Pheochromocytoma***
Shuai Gao, Longfei Liu, Zhuolin Li, Yingxian Pang, Jiaqi Shi and Feizhou Zhu
- 112 *Identification of Clinical Relevant Molecular Subtypes of Pheochromocytoma***
Umair Ali Khan Saddozai, Fengling Wang, Muhammad Usman Akbar, Lu Zhang, Yang An, Wan Zhu, Longxiang Xie, Yongqiang Li, Xinying Ji and Xiangqian Guo



Editorial: Recent Advances in Pheochromocytoma and Paraganglioma: Molecular Pathogenesis, Clinical Impacts, and Therapeutic Perspective

Farhadul Islam^{1*}, Ichiro Abe², Suja Pillai³, Robert A. Smith⁴ and Alfred King-Yin Lam^{3,5*}

¹ Department of Biochemistry and Molecular Biology, University of Rajshahi, Rajshahi, Bangladesh, ² Department of Endocrinology and Diabetes Mellitus, Fukuoka University Chikushi Hospital, Chikushino, Japan, ³ School of Biomedical Sciences, Faculty of Medicine, University of Queensland, Herston, QLD, Australia, ⁴ Genomics Research Centre, Centre for Genomics and Personalised Health, Queensland University of Technology, Brisbane, QLD, Australia, ⁵ Cancer Molecular Pathology of School of Medicine and Dentistry, Griffith University, Gold Coast, QLD, Australia

OPEN ACCESS

Edited and reviewed by:

Hubert Vaudry,
Université de Rouen, France

*Correspondence:

Farhadul Islam
farhad_bio83@ru.ac.bd
Alfred King-Yin Lam
a.lam@griffith.edu.au

Specialty section:

This article was submitted to
Neuroendocrine Science,
a section of the journal
Frontiers in Endocrinology

Received: 05 June 2021

Accepted: 28 June 2021

Published: 23 August 2021

Citation:

Islam F, Abe I, Pillai S, Smith RA and
Lam AK (2021) Editorial: Recent
Advances in Pheochromocytoma and
Paraganglioma: Molecular
Pathogenesis, Clinical Impacts, and
Therapeutic Perspective.
Front. Endocrinol. 12:720983.
doi: 10.3389/fendo.2021.720983

Keywords: pheochromocytoma, paraganglioma, neuroendocrine tumors, cancer therapeutics, cancer management

Editorial on the Research Topic

Recent Advances in Pheochromocytoma and Paraganglioma: Molecular Pathogenesis, Clinical Impacts, and Therapeutic Perspective

In this Research Topic, we have collected recent developments in research into Pheochromocytomas and Paragangliomas (PPGLs), highlighting their molecular mechanisms, clinical manifestations, and improved therapeutic management.

PPGLs are the primary types of neuroendocrine tumors, and are relatively rare, originating from chromaffin tissue in the adrenal medulla and/or autonomic nervous system ganglia (1). The symptoms experienced by PPGL patients include, but are not limited to, secretion of excess catecholamines, which can manifest as various cardiovascular-related indications such as hypertension *via* increased total peripheral resistance, heart attack without previous history, shock (non-cardiogenic pulmonary), arrhythmias, and oedemas (2). Also, pseudo-bowel obstructions, diabetic ketoacidosis, and multisystem crises involving lactic acidosis have been associated with PPGL patients (3). Since PPGLs are rare and symptoms are non-specific, they have potential for underdiagnosis. This may lead to the progression of undetected tumors into highly metastatic phenotypes in patients with PPGLs. Recent advances in understanding of the molecular biology of PPGLs, however, offer potential to open pathways to improve therapeutic interventions for PPGL tumors (4–9).

In this Research Topic, Ma et al. reported the genetic profiling of Chinese PPGL patients (n=314) examined by next-generation and Sanger sequencing. They noted that 29% of patients with PPGLs had shown mutations in one of several pathogenic genes. Among the tested genes, *SDHB* was the most

frequently (14.6%) mutated. In addition, Ma et al. observed that metastatic PPGLs, paragangliomas, and younger patients (under 30 years of age) were more likely to harbor pathogenic mutations of the tested genes. Furthermore, Yamazaki et al. summarized the clinical significance of genetic abnormalities and their association with the phenotype of patients with PPGLs. Moreover, Saddozai et al. identified two distinct subtypes of PPGLs based on the expression of genes in two cohorts (data retrieved from the TCGA and GSE19422 databases).

Surgery is the mainstay of treatment for patients with PPGLs. Without proper preoperative preparation, the excessive release of catecholamines during tumor surgery can result in lethal cardiovascular complications (Fang et al.). Thus, Fang et al. reviewed the recent advancements in preoperative management including hypertension control and improvement of blood volume for patients with PPGLs. They summarize the available approaches and evidence for preoperative management of PPGLs with or without α adrenergic-receptor antagonists, which could facilitate improvements in outcomes for patients with PPGLs. Another study in this Research Topic reported on effective preoperative management approaches, in particular red blood cell transfusion during surgery on patients with PPGLs (Guo et al.). Therefore, the new methodologies detailed in the papers in this Research Topic could facilitate the understanding of physicians for better management of patients with PPGLs. In addition, Abe et al. reviewed the current development of glucose intolerance in PPGLs for this Research Topic, and summarized its clinical significance in patients with PPGLs.

Pseudohypoxia plays important roles in the tumorigenesis of PPGLs (6). Mutations in Von Hippel-Lindau (VHL) and hypoxia-induced factor (HIF) related genes, including *PHD*, *VHL*, *HIF-2A* (*EPAS1*), and *SDHx*, which are known as VHL/HIF axis genes, are common in PPGLs (10). Also, VHL/HIF-mediated pseudohypoxia has a critical role in the pathogenesis of PPGLs (10). Peng et al. reviewed the recent studies highlighting the VHL/HIF axis and its genetic alterations in PPGLs. In addition, they discussed the underlying mechanisms of VHL/HIF axis-driven PPGL pathogenesis and summarized the therapeutics targeting this axis in cancer (Peng et al.). Furthermore, Gao et al. reported that the suppression of VHL

induced increased cell proliferation and migration of pheochromocytoma cell lines by modulating genes associated with cell proliferation.

An effective histological risk stratification for prediction of clinical outcomes for patients with PPGLs has not yet been established. However, Yamazaki et al. summarized the proposed histopathological and clinicopathological scoring systems in the present Research Topic. In their work, they listed the limitations of each scoring method, such as their ability to predict the metastatic potential of tumors (Yamazaki et al.). Another study in this series examined the relationship between the tumor microenvironment in the form of immune and sustentacular cell makeup, as well as the angiogenic potential of PPGLs with histopathology using the scoring methods. They identified several relationships, such as an association between intratumoral hemorrhage and its pathological malignancy scores (Gao et al.).

Succinate plays critical roles in PPGL pathogenesis and the accumulation of succinate receptor 1 (SUCNR1) in *SDHx* mutated PPGLs has been previously reported (11). In this Research Topic, Matlac et al. reported the oncometabolic function of succinate in *SDHx* mutation driven PPGLs via SUCNR1 stimulation of the ERK pathway, and the capacity of SUCNR1 inhibitors to abrogate this effect.

Another paper in this Research Topic reported a case study of a patient undergoing systemic therapies for metastatic PPGL and reviewed the current development of novel agents under clinical trials, including therapeutics for metastatic PPGLs (Economides et al.).

In conclusion, the information presented in this Research Topic provides an underlying molecular and genetic spectrum of PPGLs, unveiling their clinical implications, thereby enriching our understanding of the pathogenesis of the disease, which could improve clinical outcomes in patients with PPGLs.

AUTHOR CONTRIBUTIONS

FI, IA, SP, RS, and AL conceptualized, designed, wrote, and approved the editorial. All the authors contributed to the manuscript and approved the submitted version.

REFERENCES

- Kantorovich V, Pacak K. Pheochromocytoma and Paranglioma. *Prog Brain Res* (2010) 182:343–73. doi: 10.1016/S0079-6123(10)82015-1
- Aygun N, Uludag M. Pheochromocytoma and Paranglioma: From Clinical Findings to Diagnosis. *Sisli Etfal Hastan Tip Bul* (2020) 54(3):271–80. doi: 10.14744/SEMB.2020.14826
- Yen K, Lodish M. Pheochromocytomas and Parangliomas. *Curr Opin Pediatr* (2021) 32(1):134–53. doi: 10.1097/MOP.0000000000001029
- Papathomas TG, Suurd DPD, Pacak K, Tischler AS, Vriens MR, Lam AK, et al. What Have We Learned From Molecular Biology of Parangliomas and Pheochromocytomas? *Endocr Pathol* (2021) 32(1):134–53. doi: 10.1007/s12022-020-09658-7
- Abe I, Islam F, Lo CY, Liew V, Pillai S, Lam AK. VEGF-A/VEGF-B/VEGF-C Expressions in non-Hereditary, non-Metastatic Pheochromocytoma. *Histol Histopathol* (2021) 18:18329. doi: 10.14670/HH-18-329
- Islam F, Pillai S, Gopalan V, Lam AK. Identification of Novel Mutations and Expressions of *EPAS1* in Pheochromocytomas and Parangliomas. *Genes (Basel)* (2020) 11(11):1254. doi: 10.3390/genes11111254
- Pillai S, Gopalan V, Smith RA, Lam AK. Updates on the Genetics and the Clinical Impacts on Pheochromocytoma and Paranglioma in the New Era. *Crit Rev Oncol Hematol* (2016) 100:190–208. doi: 10.1016/j.critrevonc.2016.01.022
- Pillai S, Gopalan V, Lo CY, Liew V, Smith RA, Lam AK. Silent Genetic Alterations Identified by Targeted Next-Generation Sequencing in Pheochromocytoma/Paranglioma: A Clinicopathological Correlations. *Exp Mol Pathol* (2017) 102:41–6. doi: 10.1016/j.yexmp.2016.12.007
- Pillai S, Lo CY, Liew V, Laloz M, Smith RA, Gopalan V, et al. microRNA 183 Family Profiles in Pheochromocytomas are Related to Clinical Parameters and SDHB Expression. *Hum Pathol* (2017) 64:91–7. doi: 10.1016/j.humpath.2017.03.017
- Kantorovich V, Pacak K. New Insights on the Pathogenesis of Paranglioma and Pheochromocytoma. *F1000Res* (2018) 7:F1000 Faculty Rev–1500. doi: 10.12688/f1000research.14568.1

11. Shankavaram U, Fliedner SM, Elkahoul AG, Barb JJ, Munson PJ, Huynh TT, et al. Genotype and Tumor Locus Determine Expression Profile of Pseudohypoxic Pheochromocytomas and Paragangliomas. *Neoplasia* (2013) 15(4):435–47. doi: 10.1593/neo.122132

Conflict of Interest: The authors declare that the research was conducted in the absence of any commercial or financial relationships that could be construed as a potential conflict of interest.

Publisher's Note: All claims expressed in this article are solely those of the authors and do not necessarily represent those of their affiliated organizations, or those of

the publisher, the editors and the reviewers. Any product that may be evaluated in this article, or claim that may be made by its manufacturer, is not guaranteed or endorsed by the publisher.

Copyright © 2021 Islam, Abe, Pillai, Smith and Lam. This is an open-access article distributed under the terms of the Creative Commons Attribution License (CC BY). The use, distribution or reproduction in other forums is permitted, provided the original author(s) and the copyright owner(s) are credited and that the original publication in this journal is cited, in accordance with accepted academic practice. No use, distribution or reproduction is permitted which does not comply with these terms.



Preoperative Management of Pheochromocytoma and Paraganglioma

Fang Fang, Li Ding, Qing He and Ming Liu*

Department of Endocrinology and Metabolism, Tianjin Medical University General Hospital, Tianjin, China

Pheochromocytoma and paraganglioma (PPGL) are rare neuroendocrine tumors, characterized by excessive release of catecholamines (CAs), and manifested as the classic triad of headaches, palpitations, profuse sweating, and a variety of other signs and symptoms. The diagnosis of PPGL requires both evidence of excessive release of CAs and anatomical localization of CA-secreting tumor. Surgery is the mainstay of treatment for all patients with PPGL unless contraindicated. However, without proper preparation, the release of excessive CAs, especially during surgery, can result in lethal cardiovascular complications. Herein, we briefly reviewed the pathogenesis of this disease, discussed the current approaches and evidence available for preoperative management, summarizing the results of the latest studies which compared the efficacies of preoperative management with or without α adrenergic-receptor antagonists, aiming to facilitate better understanding of the preoperative management of PPGL for the physicians.

Keywords: pheochromocytoma, paraganglioma, preoperative management, catecholamines, adrenergic receptors, α -adrenergic receptor antagonists, hypertension

OPEN ACCESS

Edited by:

Farhadul Islam,
University of Rajshahi, Bangladesh

Reviewed by:

Nils Lambrecht,
VA Long Beach Healthcare System,
United States
Letizia Canu,
University of Florence, Italy

*Correspondence:

Ming Liu
mingliu@tmu.edu.cn

Specialty section:

This article was submitted to
Neuroendocrine Science,
a section of the journal
Frontiers in Endocrinology

Received: 24 July 2020

Accepted: 14 September 2020

Published: 29 September 2020

Citation:

Fang F, Ding L, He Q and Liu M (2020)
Preoperative Management of
Pheochromocytoma and
Paraganglioma.
Front. Endocrinol. 11:586795.
doi: 10.3389/fendo.2020.586795

INTRODUCTION

A pheochromocytoma is a tumor derived from catecholamine (CA)-producing chromaffin cells in the adrenal medulla, while a paraganglioma is a tumor arising from extra-adrenal chromaffin cells. Since the two tumor types have similar histologic characteristics, they can only be differentiated by anatomical location (intra-adrenal or extra-adrenal). Sympathetic paragangliomas (CAs-producing) derive from paravertebral ganglia of thorax, abdomen, and pelvis, while parasympathetic paragangliomas (rarely produce CAs) arise from vagal and glossopharyngeal nerves at the base of skull and in the neck. Pheochromocytoma and paraganglioma are together referred to as PPGL. Approximately 80%–85% of PPGL are pheochromocytomas, while about 15%–20% are paragangliomas (1). The prevalence of PPGL is about 6 cases per 1 million person-years (2). Almost 5% of patients with adrenal incidentaloma proved to be pheochromocytoma (3). Besides sustained or paroxysmal hypertension and the classic triad of headaches, palpitations, and profuse sweating, a variety of other signs and symptoms may present in PPGL, including tachycardia, fatigue, pallor, nausea, weight loss, and anxiety (4). The biochemical diagnosis of PPGL requires evidence of excessive release of CAs, and then imaging examinations are necessary to detect the anatomical localization of the catecholamine-secreting tumor. The biochemical testing indexes of CAs include CAs (plasma or urine epinephrine-E, norepinephrine-NE, and dopamine-DA), intermediate metabolites of CAs (plasma or urine metanephrine-MN and normetanephrine-

NMN), and terminal metabolites of CAs (urine vanillylmandelic acid-VMA). With a mean sensitivity of 97% and a specificity of 93%, the measurements of plasma free MNs are proved by compelling evidence to be the primary test of excessive CAs for diagnosis of PPGL. Therefore, the values of other biochemical tests are limited (1, 5). Once there is clear evidence of excessive CAs, imaging studies should be initiated to locate PPGL. Because of its excellent spatial resolution, computed tomography (CT) should be the first-choice for detection of tumors in thorax, abdomen, and pelvis in most conditions. In patients with metastatic PPGL, an allergy to CT contrast and in whom radiation exposure should be avoided, and for detection of neck and skull paragangliomas, magnetic resonance imaging (MRI) is recommended. ^{123}I -metaiodobenzylguanidine (MIBG) scintigraphy, ^{18}F -fluorodeoxyglucose (^{18}F -FDG) positron emission tomography (PET)/CT scanning, and somatostatin receptor imaging are all functional imaging modalities, and they can be used for occult lesions which failed to be detected by conventional imaging modalities and patients with metastatic PPGL (1). At least one-third of all patients with PPGL carry disease-causing germline mutations, and PPGL may often be part of some hereditary syndromes, such as multiple endocrine neoplasia (MEN) type 2, von Hippel-Lindau (VHL) syndrome and neurofibromatosis type 1 (NF1). Therefore, genetic testing are recommended for all patients with PPGL (6). Surgery is the mainstay of treatment for all patients with PPGL unless contraindicated. And for patients with a hormonally functional PPGL, preoperative management is critical to prevent perioperative complications. The α -adrenergic receptor blockers are the first choice for preoperative management of PPGL (1, 4).

CATECHOLAMINES AND ADRENERGIC RECEPTORS

The naturally occurring CAs consist of E, NE, and DA, and they are not only important neurotransmitters in the central and peripheral nervous systems, but also play key roles as circulating neurohormones (7). In PPGL, many pheochromocytomas produce both E and NE, and few produces predominantly E, while paragangliomas which arising from extra-adrenal chromaffin cells, produce predominantly NE. In rare cases, sympathetic paragangliomas and pheochromocytomas may produce DA (7, 8). The CAs take effect by interacting with adrenergic receptors (ARs) which express on cell membranes of smooth muscles and visceral organs. Upon binding of CAs to ARs, the signaling pathways are activated, resulting in alterations in smooth muscle tone and organ function (7). There are mainly four kinds of ARs, including α_1 , α_2 , β_1 , and β_2 . They distribute over different effector organs and tissues, thus mediate different biological responses and correlate with various clinical manifestations (**Table 1**) (8, 9). α_1 -ARs are primarily expressed at postsynapses of sympathetic nerves and vascular smooth muscle. The activation of α_1 -ARs causes vasoconstriction, resulting in hypertension. While α_2 -ARs are primarily localized on presynaptic nerve terminals of sympathetic nerves, resulting in

feedback inhibition of NE release. Therefore, activation of α_2 -ARs dampens the functions of sympathetic nerves. α_2 -ARs are also expressed at the nonsynaptic sites of vascular smooth muscles, mediating vasoconstriction when activated. β_1 -ARs are mainly localized in the heart, and they mediate positive inotropic and chronotropic responses, thus resulting in hypertension and tachycardia. β_2 -ARs are present in smooth muscles of most other organs, such as tracheal and bronchial, gallbladder, and uterus. They mediate relaxation of these smooth muscles, thus playing an important role in spasmolysis. Both α and β_1 -AR subtypes have high affinity for E and NE, but β_2 -AR subtype has much higher affinity for E than NE (7). Although these properties of ARs allow us to better understand their functions and response to E and NE, the actual effects/outcomes are much more complex, since the proximity of sites of E and NE release to ARs and the concentrations at effector sites are also significant determinants of AR-mediated actual effects of CAs (8). The effects of CAs on target organs exert a dose-dependent manner by acting on different receptors. NE predominantly acts on α and β_1 -ARs, and the higher concentrations of NE mediate more severe systemic vascular resistance (SVR), thus patients with PPGL secreting high concentrations of NE may present with sustained hypertension, headache, palpitation, and sweating. For low and medium concentrations of E, β_2 -ARs, which mediate vasodilatation in skeletal muscle, are the dominant receptors, thus hypotension may manifest. While high concentration of E primarily acts on α -ARs which may cause SVR, patients with predominantly E-secreting PPGL may present with paroxysmal hypertension resulting from different concentrations of E. Moreover, E is an important metabolic hormone, which stimulates lipolysis, thermogenesis, and glycolysis, and plasma glucose concentrations may be increased by stimulating glycogenolysis and gluconeogenesis. Physiological concentration of DA acts primarily on DA receptors, leading to negative cardiac inotropic action and renal artery dilatation. As DA concentration increases, DA can act on α and β -ARs, causing variable degrees of hypertension and tachycardia. Therefore, patients with DA-secreting PPGL may present with different manifestations, varying from hypotension to normotension and hypertension (8, 10, 11). CAs synthetic pathway and effects in dose-dependent manner are shown in **Figure 1** (10). These CA-specific effects on ARs can explain the various presentations of patients with PPGLs and are the foundation for appropriate preoperative management.

PREOPERATIVE MANAGEMENT OF PPGL

PPGL is characterized by hypertension and low blood volume, resulting from excessive concentration of CAs in the plasma. With insufficient preoperative antihypertensive management or untreated hypovolemia, the hemodynamic instability during surgical treatment of PPGL may be lethal. Therefore, preoperative management, which includes hypertension control and expansion of blood volume, is extremely important (12, 13). The main goal of preoperative management of PPGL is to normalize blood pressure and heart rate, restore effective circulating blood volume, improve metabolic condition, and

TABLE 1 | Adrenergic receptors-mediated responses of effector organs (9).

Effector organs	Receptor type	Responses	Most relevant clinical manifestations
Eye			
Radial muscle, iris	$\alpha 1$	Contraction (mydriasis) ++	Blurry vision
Ciliary muscle	$\beta 2$	Relaxation for far vision +	
Heart			
SA node	$\beta 1, \beta 2$	Increase in heart rate ++	Palpitations, angina
Atria	$\beta 1, \beta 2$	Increase in contractility and conduction velocity ++	
AV node	$\beta 1, \beta 2$	Increase in contractility and conduction velocity +++	
His-Purkinje system	$\beta 1, \beta 2$	Increase in contractility and conduction velocity +++	
Ventricles	$\beta 1, \beta 2$	Increase in contractility and conduction velocity, automaticity, and rate of idioventricular pacemakers +++	
Arterioles			
Coronary	$\alpha 1, \alpha 2, \beta 2$	Constriction +, dilations ++	Angina
Skin and mucosa	$\alpha 1, \alpha 2$	Constriction +++	Pallor
Skeletal muscle	$\alpha 1, \beta 2$	Constriction ++, dilations +	Hypertension
Cerebral	$\alpha 1$	Constriction (slight)	Stroke
Pulmonary	$\alpha 1, \beta 2$	Constriction +, dilations ++	Edema
Abdominal viscera	$\alpha 1, \beta 2$	Constriction +, dilations +	E.g., Bowel ischemia
Salivary glands	$\alpha 1, \alpha 2$	Constriction +++	
Renal	$\alpha 1, \alpha 2, \beta 1, \beta 2$	Constriction +, dilations +	Renal failure
Veins (systemic)	$\alpha 1, \alpha 2, \beta 2$	Constriction ++, dilations +	Orthostatic hypotension
Lung			
Tracheal and bronchial muscle	$\beta 2$	Relaxation +	
Bronchial glands	$\alpha 1, \beta 2$	Decreased secretion; increased secretion	
Stomach			
Motility and tone	$\alpha 1, \alpha 2, \beta 2$	Decrease (usually) +	Early satiety, discomfort
Sphincters	$\alpha 1$	Contraction (usually) +	
Intestine			
Motility and tone	$\alpha 1, \alpha 2, \beta 1, \beta 2$	Decrease +	Constipation, ileus
Sphincters	$\alpha 1$	Contraction (usually) +	
Secretion	$\alpha 2$	Inhibition	Constipation
Gallbladder and ducts	$\beta 2$	Relaxation +	Gallstones
Kidney			
Renin secretion	$\alpha 1, \beta 2$	Decrease +, increase ++	
Urinary bladder			
Detrusor	$\beta 2$	Relaxation (usually) +	Urinary retention
Trigone and sphincter	$\alpha 1$	Contraction ++	
Ureter			
Motility and tone	$\alpha 1$	Increase	
Uterus	$\alpha 1, \beta 2$	Pregnant: contraction; relaxation Nonpregnant: relaxation	
Sex organs, male	$\alpha 1$	Ejaculation ++	
Skin			
Pilomotor muscles	$\alpha 1$	Contraction ++	Sweating
Sweat glands	$\alpha 1$	Localized secretion +	

(Continued)

TABLE 1 | Continued

Effector organs	Receptor type	Responses	Most relevant clinical manifestations
Spleen capsule	$\alpha 1, \beta 2$	Contraction ++, relaxation +	
Skeletal muscle	$\beta 2$	Increased contractility; glycogenolysis; K^+ uptake	Hyperglycemia, glycosuria
Pancreas			
Acini	α	Decreased secretion +	
Islet (β cells)	$\alpha 2$	Decreased secretion +++	Hyperglycemia, glycosuria
Fat cells	$\beta 2$	Increased secretion +	Hypoglycemia
Salivary glands	$\alpha 2, \beta 1, \beta 2$	Lipolysis +++ (thermogenesis)	Feeling warm
Lacrimal glands	$\alpha 1$	K^+ and water secretion +	
Pineal gland	β	Amylase secretion +	
Posterior pituitary	α	Secretion +	Lacrimation
	β	Melatonin synthesis	
	$\beta 1$	Antidiuretic hormone secretion	Decreased diuresis

SA, Sinoatrial; AV, atrioventricular. Highest (+++) to lowest (+) intensity of adrenergic nerve activity in the control of various organs and functions. Where (+) is not given, intensity is not specified (8, 9).

prevent a patient from CA storm and hemodynamic instability during surgery (8). However, since the low incidence of PPGL, evidence-based studies (such as large-scale randomized controlled trials-RCTs) comparing different treatments are scarce, and there is still no consensus for the most appropriate preoperative management of PPGL (8, 13). However, the most common approach is to block the function of excessive plasma CAs, and α -AR antagonists are the first choice. β -AR antagonists, calcium channel blockers (CCBs), and CA synthesis inhibitors are also recommended when necessary, but β -AR antagonists can only be used after sufficient pretreatment with α -AR antagonists to avoid unopposed α -AR overstimulation. Brief instructions of preoperative drugs for PPGL are shown in **Table 2**. In the meantime, a high-sodium diet and fluid intake are recommended to reverse CA-induced blood volume contraction to prevent severe hypotension (1, 8).

At present, there is no consensus for when preoperative management should be started to ensure adequate preparation for surgery. In most circumstances, α -AR antagonists are usually initiated 1–2 weeks preoperatively to normalize blood pressure, heart rate and to replete contracted blood volume. In patients with CA-induced cardiomyopathy or other organ damage, α -AR antagonists should be start much earlier (8). There is not enough evidence from RCTs to determine the optimal target blood pressure and cardiac condition, and the present recommendations are from institutional experience and retrospective studies. In 1983, Roizen proposed the Roizen criteria to assess for adequate α -AR blockade: 1. No blood pressure >160/90mmHg should be evident for 24 h before surgery; 2. For patients with orthostatic hypotension, readings >80/45mmHg should be present; 3. No ST-T changes is present in electrocardiogram for at least 1 week; 4. No more than one premature ventricular contraction for every 5 min (14). In 2007, the Endocrine Society recommended that the goal is to achieve target blood pressure of less than 130/80 mmHg when sitting and

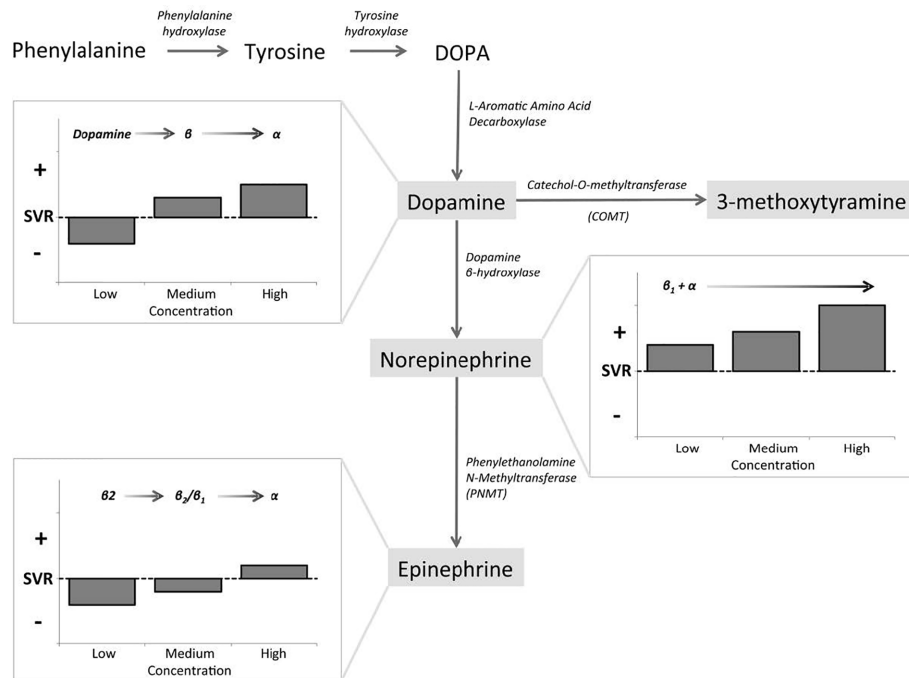


FIGURE 1 | Catecholamines (CAs) synthetic pathway and dose-dependent effects. Epinephrine (E), norepinephrine (NE), and dopamine (DA) exert dose-dependent effects at low, medium, and high circulating concentrations, as governed by affinity to α -AR, β -AR, and DA receptors (10).

no less than 80/45 mmHg when standing, and target heart rate is about 60–70 beat per minute (bpm) when sitting and 70–80 bpm when standing (8). These targets should be individualized according to age, general conditions and complications. However, it should be clearly noted that complete prevention of perioperative hypertension and tachycardia cannot be achieved by any doses or combinations of drugs (1).

α -AR ANTAGONISTS

Two types of α -AR antagonists are widely used clinically, non-selective and selective α -AR antagonists. Phenoxybenzamine is a non-selective, non-competitive α -AR antagonist, which binds irreversibly with both α_1 and α_2 -AR. Phenoxybenzamine is long-acting and its effects persist long after it has been discontinued, since the effect diminishes only after α -AR resynthesis (15, 16). The starting dose of phenoxybenzamine is usually 10 mg twice a day and the dose can be increased in increments of 10–20 mg every 2–3 days, until the clinical manifestations are well controlled or adverse effects appear. Generally speaking, a total daily dose of 1 mg/kg is adequate for most patients of PPGL, while for some patients, larger doses may be required. Phenoxybenzamine can also be administered 3 days before operation by infusion (0.5 mg/kg/d) for 5 h a day, but this approach requires closely monitoring of the patient (8). The advantage of phenoxybenzamine is that its effect is profound

and long-acting, even when excessive amounts of CAs reach the circulation, since the combination of phenoxybenzamine and α -AR is non-competitive and non-selective. Orthostatic hypotension is the common adverse effect of nearly all the α -AR antagonists. Another disadvantage of phenoxybenzamine is the high incidence of reflex tachycardia, as a result of the inhibition of α_2 -AR which localized in the presynaptic membrane and participate in the negative feedback of NE release. Blockade of the presynaptic α_2 -AR results in the release of NE into circulation and an increase in chronotropic activity of the heart, leading to tachycardia. Therefore, β -AR antagonist is often required to control tachycardia after the use of phenoxybenzamine. Other side effects related to inhibition of α_2 -AR include nasal congestion and retrograde ejaculation. Moreover, phenoxybenzamine can cause prolonged hypotension postoperatively due to its long-acting features, which should draw the clinicians' attention. Since it can pass the blood-brain barrier, it may cause central sedation occasionally (17).

Selective α -AR antagonists, including prazosin, terazosin, and doxazosin, competitively inhibit only α_1 -AR, and they are short-acting drugs used for patients with PPGL as well. The initial dose of prazosin is 0.5–1 mg, 2–3 times a day, and the dose can be gradually increased to 6–15 mg per day. Terazosin is usually given in doses of 2–10 mg per day. For both prazosin and terazosin, the doses of higher than 20mg per day may not bring extra benefit. Doxazosin, with a half-life much longer than the other selective α -AR antagonists, can be dosed once daily, and is the most commonly

TABLE 2 | Brief instructions of preoperative drugs for pheochromocytoma and paraganglioma (PPGL).

Drugs		Doses	Starting time	Advantages	Adverse effects and points for attention
α -AR antagonists	Phenoxybenzamine	Initially 10mg BID, usually 1mg/kg/d	1–2 weeks before surgery	The effect is profound and long-acting.	Prolonged hypotension postoperatively, orthostatic hypotension, reflex tachycardia, nasal congestion, central sedation
	Prazosin	Initially 0.5–1 mg BID-TID, usually 6–15 mg/d, maximum dose of 20 mg/d		Lower risk of postoperative hypotension, seldom cause reflex tachycardia, nasal congestion and central sedation	Orthostatic hypotension, the anti-hypertensive effect may not as profound as phenoxybenzamine
	Perazosin	Usually 2–10 mg/d, maximum dose of 20 mg/d			
	Doxazosin	Initially 1mg QD, usually 2–8 mg/d, maximum dose of 16 mg/d			
β -AR antagonists	Propranolol	Initially 10 mg TID-QID, maximum dose of 200 mg/d	After adequate α -AR blockade	Long-acting	Never be used alone or before adequate α -AR blockade, should not be used for patients with asthma, severe atrioventricular block or bradycardia, sick sinus syndrome, severe heart failure, and cardiogenic shock
	Atenolol	Usually 12.2–25 mg BID-TID			
	Metoprolol	Usually 25–50 mg BID-TID			
	Metoprolol controlled release tablets	25–200 mg QD			
CCBs	Nicardipine	Initially 20 mg TID, maximum dose of 120 mg/d	1–2 weeks before surgery if necessary	Do not cause drug-induced orthostatic hypotension and reflex tachycardia, prevention of CA-mediated coronary vasospasm and myocarditis	Monotherapy of CCBs may not be effective enough for patients with biochemically active PPGL, which should be combined with α -AR antagonists.
	Amlodipine	5–10 mg QD			
	Nifedipine	Initially 10mg TID, maximum dose of 120mg/d			
	Nifedipine controlled release tablets	30-60mg QD			
CA synthesis inhibitor	Metyrosine	Initially 500 mg/d, maximum dose of 4 g/d	At least 1-3 weeks before surgery	Directly inhibit the CAs biosynthesis	Sedation, somnolence, anxiety, depression, and rarely leading to extrapyramidal signs (such as parkinsonism)

used selective α -AR antagonist in recent years. The starting dose of doxazosin is usually 1 mg per day, and the most commonly used doses are 2–8 mg per day. The maximum recommended dose is 16 mg per day (8). Since all the α -AR antagonists may cause orthostatic hypotension, they are recommended to be given just before bedtime when used for the first time, and the patients should be reminded of slow body position changes. Unlike phenoxybenzamine, selective α_1 -AR antagonists do not cause reflex tachycardia, and seldom cause nasal congestion, because they do not inhibit α_2 -AR. Due to the nature of competitive inhibition of α_1 -AR, they have a shorter duration of action and lower risk of postoperative hypotension. Furthermore, they minimally pass the blood-brain barrier, and central sedation is rare. Compared to phenoxybenzamine, selective α_1 -AR antagonists have fewer side effects. However, as competitive inhibition may be overcome by excessive concentration of CAs, the anti-hypertensive effect is not as profound as phenoxybenzamine (17, 18).

NON-SELECTIVE OR SELECTIVE α -AR ANTAGONISTS?

Evidence from RCTs or systematic reviews comparing the effectiveness of non-selective and selective α -AR antagonists

for patients of PPGL is unavailable (1). However, many retrospective and prospective studies have made efforts to compare these two types of drugs. Some studies show that non-selective α -AR antagonists, phenoxybenzamine, and selective α -AR antagonist, doxazosin, have similar effects on controlling blood pressure (16, 19, 20), while some studies report that hypertension is better controlled by phenoxybenzamine than by doxazosin (15, 21, 22). With respect to hemodynamic instability, some studies reveal that phenoxybenzamine is as effective as doxazosin (15, 23). However, most studies report that doxazosin is associated with less adverse effects than phenoxybenzamine, such as reflex tachycardia, postoperative hypotension, edema, and nasal congestion (16, 19, 20, 22). In general, both phenoxybenzamine and doxazosin are able to effectively control perioperative blood pressure and to prevent hemodynamic instability in patients of PPGL. Hypertension may be slightly better controlled by phenoxybenzamine for some patients, at the cost of higher risk of postoperative hypotension. To control reflex tachycardia, phenoxybenzamine more often required co-treatment by β -AR antagonists. While doxazosin is more likely to require additional antihypertensive drugs, such as calcium channel blockers (CCBs) (17), for blood pressure control, and is proved to have much less adverse effects. At present, choice of medication depends on institutional preference whether to use a non-selective or selective α -AR

antagonist, because there is still no consensus according to the existing evidences.

IS α -AR BLOCKADE NECESSARY FOR ALL PATIENTS OF PPGL?

Many retrospective studies have reported the use α -AR antagonists as the first-choice to prevent perioperative complications of PPGL, including intraoperative hypertension, tachycardia, and hemodynamic instability (24–28). North American neuroendocrine tumor society consensus guidelines recommended that all patients with PPGL (even those with normal levels of CAs) should use appropriate management to block effects of released CAs (29). The Endocrine Society clinical practice guideline also recommended that all patients with a hormonally functional PPGL should receive α -AR antagonists to prevent perioperative cardiovascular complications (1). It is recommended that even normotensive patients of PPGL should receive preoperative α -AR blockade to prevent potential risk of intraoperative hypertension. While for patients with parasympathetic-derived head and neck paragangliomas or biochemically silent PPGL, α -AR blockade may not be necessary, and there should be a collaborative decision with anaesthetist and surgeon, considering cardiovascular status and intraoperative risks of the patients (1, 10). However, there are some studies question the necessity of α -AR blockade, and report successful PPGL resection without this kind of drug. It is reported by some studies that there is no significant difference of perioperative blood pressure and hemodynamic stability with or without the use of α -AR antagonists (30–33). Especially in 2017, Groeben et al. (34) assessed hemodynamic conditions and perioperative complications in 110 patients with and 166 patients without α -AR blockade. Only a slight difference in mean maximal systolic pressure was reported between groups. There was no significant difference in the incidence of hypertensive episodes between patients with and without α -AR blockade, and no severe complications occurred in either group. It is so far the largest number of patients of PPGL without α -AR blockade reported, and this study demonstrated that surgery of PPGL without preoperative α -AR blockade is feasible. In 2019, a review about PPGL in New England Journal of Medicine (5) quoted this study and agreed that α -AR antagonists may be not necessary. Possible reasons for the idea of adrenergic receptor blockade-free management are as follows. Firstly, the guidelines (1, 29) which recommended necessity of α -AR antagonists for patients with PPGL stated that there was no RCTs or other high quality evidences available for this statement, and scientific investigations were unable to be carried out because of the very low incidence of the disease. Moreover, α -AR antagonists are not without adverse effects, and there are even significant side aspects sometimes (35). Secondly, in a patient with PPGL who has had side effects associated with long-term, episodic hypertension without α -AR blockade, it seems impossible that decompensation would occur several days before operation, and other short-acting anti-hypertensive drugs may be appropriate during aesthesia (5).

Thirdly, with the improvement of diagnostic tools for identification and localization of the lesions, modern minimally invasive surgical techniques, and highly effective, short-acting drugs without severe side effects to control intraoperative conditions, the necessity of the unreliable, time-consuming preoperative management with potential significant adverse effects should be questioned (34).

β -AR ANTAGONISTS

The use of β -AR antagonists is determined by the extent of CA-induced tachycardia or reflex tachycardia after the initiation of phenoxybenzamine. It is noteworthy that β -AR antagonists should never be treated alone or before adequate α -AR blockade. Since for patients with PPGL, loss of β -AR-mediated vasodilatation with unopposed CA-induced vasoconstriction can cause dramatic increase in blood pressure, or even hypertensive crisis (1, 12). Propranolol, a non-selective β -AR antagonist, which is often used in the past, is given in doses of 10 mg, three to four times a day initially, and usually no higher than 200 mg/d. Nowadays, more cardio-selective β_1 -AR antagonists are recommended, such as atenolol (12.2–25 mg two to three times a day), metoprolol (25–50 mg two to three times a day), and metoprolol controlled release tables (Toprol) (25–200 mg once a day) (8). However, there is no ample evidence to support the use of β_1 -selective AR antagonists over non-selective AR antagonists in patients with PPGL (1). There are also some combined α and β -AR antagonists, such as labetalol and carvedilol. They have fixed ratio but more potent β than α antagonistic activities, such as α : β of labetalol is 1:5, but it is reported that α - to β -antagonistic activity should be at least 4:1 to achieve sufficient antihypertensive effect. Therefore, they are not recommended as the initial therapy for PPGL to take the place of α and β -AR antagonists separately, to avoid episodes of hypertension or even hypertensive crisis (8). For patients with CA-induced cardiomyopathy, it is reported that β -AR antagonists can lead to severe hypotension, bradycardia and even cardiac arrest, which warrant extra caution (36).

CALCIUM CHANNEL BLOCKERS (CCBs)

CCBs are the most commonly used drugs, in combination with α -AR antagonists, to further improve blood pressure control in patients with PPGL (1). Some studies consider this kind of drugs as the primary choice of preoperative management of PPGL, especially for normotensive patients or those with very mild hypertension, and for patients experiencing severe side effects with α -AR antagonists (8, 30, 37). These drugs can relax vascular smooth muscle and reduce peripheral vascular resistance by inhibiting NE-induced intracellular and transmembrane calcium influx in vascular smooth muscle (18). Compared to α -AR antagonists, CCBs do not cause drug-induced orthostatic hypotension and reflex tachycardia, and exert additional protective effects of the heart by preventing CA-mediated coronary vasospasm and myocarditis (38). A retrospective study

showed no differences in intraoperative hemodynamic stability and short-term postoperative outcomes in patients with PPGL using nicardipine compared with phenoxybenzamine (39). Another study showed similar improvements in intraoperative hemodynamic instability between α -AR blockade and CCBs (40). It is reported in a study that the monotherapy of CCBs for the perioperative management of PPGL did not prevent all hemodynamic instability, but was associated with a lower morbidity and mortality (41). The most often used CCBs are nicardipine (60–120 mg per day), amlodipine (5–10 mg per day), and nifedipine (30–120 mg per day) (8). Nowadays, nifedipine controlled release tables (30–60 mg once a day) have become a good choice by its effective and long-acting profiles.

CA SYNTHESIS INHIBITOR

It is proved that excessive CAs release results in perioperative cardiovascular instability in the patients with PPGL, so the administration of drugs which inhibit the CA biosynthesis may be beneficial for the treatment of PPGL (42). Metyrosine, a CA synthesis inhibitor, inhibits tyrosine hydroxylase, which catalyzes the conversion of tyrosine to dihydroxyphenylalanine (DOPA) (**Figure 1**), the rate-limiting step of the CA synthesis pathway (12, 43). Therefore, metyrosine has been used as one of the approaches for the management of PPGL, especially when phenoxybenzamine is unavailable in some areas, such as Italy. It takes effect at about 3 days and should be used at least 1–3 weeks before surgery, at initial dose of 500 mg per day and titrated as necessary to a maximum dose of 4 g per day (8, 44, 45). It was shown that a dose range of 1–2 g per day is well tolerated with relatively low incidence of side effects (46). Metyrosine can readily cross the blood-brain barrier, and inhibits CA synthesis in the brain as well as in the periphery, thus resulting in sedation, somnolence, anxiety, depression, and rarely leading to extrapyramidal signs, such as parkinsonism. It should also be used with caution for patients with renal dysfunction, since metyrosine is excreted through kidney and the pharmacokinetics of metyrosine are significantly affected by renal dysfunction. Most adverse effects would disappear after cessation of administration (8, 45). It was shown that urine MNs have been reduced for at least 50% from baseline after the administration of metyrosine (45, 46). Although Butz et al. reported that patients treated with metyrosine and phenoxybenzamine had wider range of intraoperative blood pressure variations than phenoxybenzamine-only patients (47), it has been reported by most studies that the combination of metyrosine and α -AR antagonists lead to better blood pressure control, decreased intraoperative blood loss, and reduced volume replacement during operation compared with the classical method of monotherapy of α -AR blockade (45, 46, 48, 49). In a case report of a patient with PPGL, the administration of metyrosine alone was unable to satisfactorily control intraoperative blood pressure (50), which was probably due to the incomplete depletion of CA stores no matter what dose used. Therefore, metyrosine is always used in combination with α -AR antagonists in patients with serious symptoms which cannot be well controlled by other medications, such as those with biochemically active tumors or

extensive metastatic tumors (8, 45). However, the limited availability of this drug and its adverse effects at high doses limit its widely use (8).

CARDIOVASCULAR EVALUATION AND BLOOD VOLUME RESTORATION

The excessive CAs release and resultant hypertension can lead to significant changes in the cardiovascular system, such as vasoconstriction of the coronary arteries, increased arterial stiffness, arrhythmias, and cardiomyopathy (13). Moreover, it was shown that normotensive patients with PPGL had similar perioperative hemodynamic instability to those with significant preoperative hypertension (51). Therefore, it is essential to perform cardiovascular evaluation for every patient with PPGL. The evaluation should include a thorough history, physical examination, complete laboratory tests, electrocardiogram (ECG), and echocardiography. An ECG may reveal pathologic findings such as nonspecific ST-T wave changes, arrhythmias, and signs of left ventricular hypertrophy, which may be related to the CA-induced coronary artery vasoconstriction that obstructs myocardial blood flow. An ecocardiography is recommended to evaluate the presence of cardiomyopathy, and may be helpful to determine improvement after therapy (13).

Restoration of blood volume decreases the risk of protracted hypotension or shock as a result of sudden vasodilation during surgery. However, the management with α -AR antagonists alone will lead to blood volume restoration in only approximately 60% patients with PPGL (8). Therefore, it is recommended by the Endocrine Society clinical practice guidelines that treatment of PPGL should also include fluid intake and a high-sodium diet to restore blood volume preoperatively and prevent perioperative hypotension, although evidence from RCTs is not available. A high-sodium diet (e.g., 5,000 mg per day) is usually initiated 3 days after the administration of α -AR blockade, and continuous saline infusion (e.g., 2,500 ml per day) is usually started in the evening before surgery. For patients with heart or renal failure, special caution is required for volume loading (1, 5).

OTHER RECOMMENDATIONS

The administration of drugs that provoke the release of CAs produced by the tumor or interfere with CAs metabolism should be avoided for patients with PPGL. E and NE release can be provoked by steroids, histamine, glucagon, vasopressin, and angiotensin II. Drugs that are used for obesity management, such as phentermine, phendimetrazine, and phenylethylamine, are sympathomimetic amines with a direct action on adrenoceptors. NE reuptake inhibitors, such as tricyclic antidepressants and amitriptyline, cocaine, and those that interfere with NE metabolism, all result in high circulating NE levels, and should be avoided by PPGL patients (8). Moreover, strenuous physical activities, smoking, and alcohol consumption should also be avoided, since they all significantly increase CAs release from a

tumor. To ensure optimal preoperative management for patients with PPGL, multidisciplinary teamwork, including endocrine, surgical, cardiology, anesthesia, and oncology teams, is essential (8).

IS PREOPERATIVE MANAGEMENT NECESSARY FOR PATIENTS WITH CLINICALLY SILENT AND BIOCHEMICALLY SILENT PPGL?

It was reported that patients with clinically silent (normotensive) but biologically active PPGL had relatively lower levels of CAs than those with hypertensive PPGL, since the expression of multiple genes which were involved in key processes of CA synthesis was decreased in these tumors (10, 52). Studies that evaluating the value of preoperative management for patients with normotensive PPGL are scarce. Although one study showed that preoperative α -AR antagonist had no benefit for patients with normotensive PPGL (31), another study revealed that normotensive PPGL had similar perioperative hemodynamic instability with hypertensive PPGL, which differed significantly from nonfunctioning adrenal adenomas (51). Therefore, as recommended by the Endocrine society, patients with normotensive PPGL should also receive α -AR antagonists or CCBs to prevent unpredictable hypertension during surgery (1).

For biochemically silent PPGL, which do not secrete CAs, hemodynamic instability resulting from the tumors should not occur theoretically. However, malignant hypertension during surgery has been reported by several cases in patients with biochemically silent PPGL not receiving preoperative management (53–55). Mechanisms remain unclear. It is speculated that some could be a result of undetected dopamine secretion by the tumor, and others may originate from the intratumoral CA release during surgery (10). There is no consensus about the necessity of preoperative management for patients with biochemically silent PPGL, but it is recommended that before clinicians choose not to pre-medicate preoperatively, cardiovascular status and perceived intraoperative risks should be evaluated, and decision should be made by multidisciplinary teamwork (10).

MANAGEMENT OF HYPERTENSIVE CRISIS

PPGL may cause potentially lethal hypertensive crisis due to the effects of the excessive released CAs. Hypertensive crisis is an acute, life-threatening situation associated with severe increase in blood pressure, requiring special attention. It is defined as a systolic blood pressure higher than 180 mmHg or a diastolic blood pressure higher than 120 mmHg, with or without acute target organ damage (56). Hypertensive crisis may develop as a consequence of postural changes, urination, emotional stress, and use of certain drugs which may provoke the release of CAs. It may also be induced by administration of a β -AR antagonist

without sufficient α -AR blockade, or during a surgery without proper preparation. The clinical presentation may vary, including headaches, nausea, vomiting, visual disturbances, and palpitations. In this case, control of blood pressure may be achieved by a continuous infusion of sodium nitroprusside at 0.5–10.0 μ g/kg/min, or phentolamine, a short-acting α -AR blockade, given as an intravenous bolus of 2.5–5 mg at the rate of 1 mg/min, which can be repeated every 3–5 min. Urapidil, a selective α_1 -AR antagonist, can also be used to control blood pressure during hypertensive crisis at the dose of 10–15 ml/h in continuous infusion, or as a bolus of 25 or 50 mg intravenously (57). If conventional antihypertensive treatments do not achieve optimal effects, magnesium sulfate can be used. It is an effective arteriolar dilator, and can inhibit the function of excessive CAs release. Magnesium sulfate should be administered with a loading dose of 40–60 mg/kg followed by an continuous infusion of 1–2 g/h (58).

CONCLUSIONS

In summary, preoperative management of PPGL, which includes hypertension control and improvement of blood volume, is crucial. The most common approach is to block the function of excessive plasma CAs, and α -AR antagonists are the first choice. Hypertension may be slightly better controlled by non-selective α -AR antagonist, phenoxybenzamine, for some patients, at the cost of higher risk of postoperative hypotension and other side effects. While selective α -AR antagonist, doxazosin, is proved to have much less adverse effects, but is more likely to be used in combination with additional antihypertensive drugs. With the improvement of diagnostic tools for identification and localization of the lesions, modern minimally invasive surgical techniques, and highly effective, short-acting drugs without severe side effects, the necessity of the preoperative management of α -AR antagonists with potential significant adverse effects should be questioned. The use of β -AR antagonists is determined by the extent of CA-induced tachycardia or reflex tachycardia after the prescription of phenoxybenzamine. It is noteworthy that β -AR antagonists should never be treated alone or before adequate α -AR blockade. CCBs are the most often used drugs in combination with α -AR antagonists, to further improve blood pressure control in patients with PPGL. Some studies considered this kind of drugs as the primary choice of preoperative management of PPGL, especially for normotensive patients or those with very mild hypertension, and for patients with severe side effects when using α -AR antagonists. CA synthesis inhibitor, metyrosine, is used combined with α -AR antagonists to patients with serious symptoms which cannot be well controlled by other medications, such as those with biochemically active tumors or extensive metastatic tumors. It is essential to make cardiovascular evaluation for every patient with PPGL and it is recommended that treatment of PPGL should also include a high-sodium diet and fluid intake to restore blood volume preoperatively and

prevent perioperative hypotension. However, PPGL is a rare disease, so large RCTs or meta-analyses are not available at present. Therefore, more convincing evidence is needed to determine the most proper preoperative management strategies.

AUTHOR CONTRIBUTIONS

FF, LD, QH, and ML conducted a review of the literature and wrote the review. FF and ML contributed to conception and

design of the review, and ML finalized the review. All authors contributed to the article and approved the submitted version.

FUNDING

This study was support by the National Key R&D Program of China (2019YFA0802502) and Natural Science Foundation of China (81830025 and 81620108004). We acknowledge support from Tianjin Municipal Science and Technology Commission (17ZXMFSY00150 and 18JCYBJC93900).

REFERENCES

- Lenders JW, Duh QY, Eisenhofer G, Gimenez-Roqueplo AP, Grebe SK, Murad MH, et al. Pheochromocytoma and paraganglioma: an endocrine society clinical practice guideline. *J Clin Endocrinol Metab* (2014) 99:1915–42. doi: 10.1210/jc.2014-1498
- Berends A, Buitenwerf E, de Krijger RR, Veeger N, van der Horst-Schrivers A, Links TP, et al. Incidence of pheochromocytoma and sympathetic paraganglioma in the Netherlands: A nationwide study and systematic review. *Eur J Intern Med* (2018) 51:68–73. doi: 10.1016/j.iejim.2018.01.015
- Mantero F, Terzolo M, Arnaldi G, Osella G, Masini AM, Ali A, et al. A survey on adrenal incidentaloma in Italy. Study Group on Adrenal Tumors of the Italian Society of Endocrinology. *J Clin Endocrinol Metab* (2000) 85:637–44. doi: 10.1210/jcem.85.2.6372
- Fishbein L. Pheochromocytoma and Paraganglioma: Genetics, Diagnosis, and Treatment. *Hematol Oncol Clin North Am* (2016) 30:135–50. doi: 10.1016/j.hoc.2015.09.006
- Neumann H, Young WJ, Eng C. Pheochromocytoma and Paraganglioma. *N Engl J Med* (2019) 381:552–65. doi: 10.1056/NEJMra1806651
- Buffet A, Venisse A, Nau V, Roncellin I, Boccio V, Le Pottier N, et al. A Decade (2001–2010) of Genetic Testing for Pheochromocytoma and Paraganglioma. *Hormone Metab Res* (2012) 44:359–66. doi: 10.1055/s-0032-1304594
- Tank AW, Lee WD. Peripheral and central effects of circulating catecholamines. *Compr Physiol* (2015) 5:1–15. doi: 10.1002/cphy.c140007
- Pacak K. Preoperative management of the pheochromocytoma patient. *J Clin Endocrinol Metab* (2007) 92:4069–79. doi: 10.1210/jc.2007-1720
- Pacak K, Keiser HR, Eisenhofer G. “Pheochromocytoma” in: *Endocrinology*. Eds. LJ DeGroot, JL Jamenson, G Eisenhofer, (Philadelphia: Elsevier Saunders) (2006). pp. 2501–34.
- Isaacs M, Lee P. Preoperative alpha-blockade in phaeochromocytoma and paraganglioma: is it always necessary? *Clin Endocrinol (Oxf)* (2017) 86:309–14. doi: 10.1111/cen.13284
- Mamilla D, Araque KA, Brofferio A, Gonzales MK, Sullivan JN, Nilubol N, et al. Postoperative Management in Patients with Pheochromocytoma and Paraganglioma. *Cancers (Basel)* (2019) 11:936. doi: 10.3390/cancers11070936
- Farrugia FA, Charalampopoulos A. Pheochromocytoma. *Endocr Regul* (2019) 53:191–212. doi: 10.2478/enr-2019-0020
- Naranjo J, Dodd S, Martin YN. Perioperative Management of Pheochromocytoma. *J Cardiothorac Vasc Anesth* (2017) 31:1427–39. doi: 10.1053/j.jvca.2017.02.023
- Roizen MF, Hunt TK, Beaupre PN, Kremer P, Firmin R, Chan CN, et al. The effect of alpha-adrenergic blockade on cardiac performance and tissue oxygen delivery during excision of pheochromocytoma. *Surgery* (1983) 94:941–5.
- Liu C, Lv Q, Chen X, Ni G, Hu L, Tong N, et al. Preoperative selective vs non-selective α -blockade in PPGL patients undergoing adrenalectomy. *Endocr Connect* (2017) 6:830–8. doi: 10.1530/EC-17-0232
- Prys-Roberts C, Farndon JR. Efficacy and safety of doxazosin for perioperative management of patients with pheochromocytoma. *World J Surg* (2002) 26:1037–42. doi: 10.1007/s00268-002-6667-z
- van der Zee PA, de Boer A. Pheochromocytoma: a review on preoperative treatment with phenoxybenzamine or doxazosin. *Neth J Med* (2014) 72:190–201.
- Bravo EL, Tagle R. Pheochromocytoma: state-of-the-art and future prospects. *Endocr Rev* (2003) 24:539–53. doi: 10.1210/er.2002-0013
- Kocak S, Aydinoglu S, Canakci N. Alpha blockade in preoperative preparation of patients with pheochromocytomas. *Int Surg* (2002) 87:191–4.
- Malec K, Miśkiewicz P, Witkowska A, Krajewska E, Toutouchi S, Galazka Z, et al. Comparison of phenoxybenzamine and doxazosin in perioperative management of patients with pheochromocytoma. *Kardiol Pol* (2017) 75:1192–8. doi: 10.5603/KP.a2017.0147
- Weingarten TN, Cata JP, O'Hara JF, Prybilla DJ, Pike TL, Thompson GB, et al. Comparison of two preoperative medical management strategies for laparoscopic resection of pheochromocytoma. *Urology* (2010) 76:506–8. doi: 10.1016/j.urology.2010.03.032
- Zhu Y, He HC, Su TW, Wu YX, Wang WQ, Zhao JP, et al. Selective α 1-adrenoceptor antagonist (controlled release tablets) in preoperative management of pheochromocytoma. *Endocrine* (2010) 38:254–9. doi: 10.1007/s12020-010-9381-x
- Bruynzeel H, Feelders RA, Groenland TH, van den Meiracker AH, van Eijk CH, Lange JF, et al. Risk Factors for Hemodynamic Instability during Surgery for Pheochromocytoma. *J Clin Endocrinol Metab* (2010) 95:678–85. doi: 10.1210/jc.2009-1051
- Plouin PF, Duclos JM, Soppelsa F, Boulblil G, Chatellier G. Factors associated with perioperative morbidity and mortality in patients with pheochromocytoma: analysis of 165 operations at a single center. *J Clin Endocrinol Metab* (2001) 86:1480–6. doi: 10.1210/jcem.86.4.7392
- Goldstein RE, O'Neill JJ, Holcomb GR, Morgan WR, Neblett WR, Oates JA, et al. Clinical experience over 48 years with pheochromocytoma. *Ann Surg* (1999) 229:755–66. doi: 10.1097/0000658-199906000-00001
- Ross EJ, Prichard BN, Kaufman L, Robertson AI, Harries BJ. Preoperative and operative management of patients with phaeochromocytoma. *Br Med J* (1967) 1:191–8. doi: 10.1136/bmj.1.5534.191
- Perry LB, Gould AJ. The anesthetic management of pheochromocytoma effect of preoperative adrenergic blocking drugs. *Anesth Analg* (1972) 51:36–40. doi: 10.1213/0000539-197201000-00010
- Young WJ. Pheochromocytoma: 1926–1993. *Trends Endocrinol Metab* (1993) 4:122–7. doi: 10.1016/1043-2760(93)90035-d
- Chen H, Sippel RS, O'Dorisio MS, Vinik AI, Lloyd RV, Pacak K. The North American Neuroendocrine Tumor Society consensus guideline for the diagnosis and management of neuroendocrine tumors: pheochromocytoma, paraganglioma, and medullary thyroid cancer. *Pancreas* (2010) 39:775–83. doi: 10.1097/MPA.0b013e3181ebb4f0
- Ulchaker JC, Goldfarb DA, Bravo EL, Novick AC. Successful outcomes in pheochromocytoma surgery in the modern era. *J Urol* (1999) 161:764–7. doi: 10.1016/S0022-5347(01)61762-2
- Shao Y, Chen R, Shen ZJ, Teng Y, Huang P, Rui WB. Preoperative alpha blockade for normotensive pheochromocytoma: is it necessary? *J Hypertens* (2011) 29:2429–32. doi: 10.1097/HJH.0b013e32834d24d9
- Lentschener C, Gaujoux S, Thillois JM, Duboc D, Bertherat J, Ozier Y, et al. Increased arterial pressure is not predictive of haemodynamic instability in patients undergoing adrenalectomy for phaeochromocytoma. *Acta Anaesthesiol Scand* (2009) 53:522–7. doi: 10.1111/j.1399-6576.2008.01894.x
- Boutros AR, Bravo EL, Zanetti G, Straffon RA. Perioperative management of 63 patients with pheochromocytoma. *Cleve Clin J Med* (1990) 57:613–7. doi: 10.3949/ccjm.57.7.613

34. Groeben H, Nottebaum BJ, Alesina PF, Traut A, Neumann HP, Walz MK. Perioperative α -receptor blockade in pheochromocytoma surgery: an observational case series. *Br J Anaesth* (2017) 118:182–9. doi: 10.1093/bja/aew392
35. Sprung J, Weingarten TN. Sometimes too much of a good thing may not be that good. *Urology* (2011) 78:478–9. doi: 10.1016/j.urology.2011.04.053
36. Shupak RC. Difficult anesthetic management during pheochromocytoma surgery. *J Clin Anesth* (1999) 11:247–50. doi: 10.1016/s0952-8180(99)00014-8
37. Bravo EL. Evolving concepts in the pathophysiology, diagnosis, and treatment of pheochromocytoma. *Endocr Rev* (1994) 15:356–68. doi: 10.1210/edrv-15-3-356
38. Bravo EL. Pheochromocytoma. *Cardiol Rev* (2002) 10:44–50. doi: 10.1097/00045415-200201000-00009
39. Siddiqi HK, Yang HY, Laird AM, Fox AC, Doherty GM, Miller BS, et al. Utility of oral nicardipine and magnesium sulfate infusion during preparation and resection of pheochromocytomas. *Surgery* (2012) 152:1027–36. doi: 10.1016/j.surg.2012.08.023
40. Brunaud L, Boutami M, Nguyen-Thi PL, Finnerty B, Germain A, Weryha G, et al. Both preoperative alpha and calcium channel blockade impact intraoperative hemodynamic stability similarly in the management of pheochromocytoma. *Surgery* (2014) 156:1410–18. doi: 10.1016/j.surg.2014.08.022
41. Lebuffe G, Dosseh ED, Tek G, Tytgat H, Moreno S, Tavernier B, et al. The effect of calcium channel blockers on outcome following the surgical treatment of pheochromocytomas and paragangliomas. *Anaesthesia* (2005) 60:439–44. doi: 10.1111/j.1365-2044.2005.04156.x
42. Russell WJ, Metcalfe IR, Tonkin AL, Frewin DB. The preoperative management of pheochromocytoma. *Anaesth Intensive Care* (1998) 26:196–200. doi: 10.1177/0310057X9802600212
43. Sjoerdsma A, Engelman K, Spector S, Udenfriend S. Inhibition of catecholamine synthesis in man with alpha-methyl-tyrosine, an inhibitor of tyrosine hydroxylase. *Lancet* (1965) 2:1092–4. doi: 10.1016/s0140-6736(65)90062-0
44. Brogden N, Heel RC, Speight TM, Avery GS. alpha-Methyl-p-tyrosine: a review of its pharmacology and clinical use. *Drugs* (1981) 21:81–9. doi: 10.2165/00003495-198121020-00001
45. Naruse M, Satoh F, Tanabe A, Okamoto T, Ichihara A, Tsuiji M, et al. Efficacy and safety of metyrosine in pheochromocytoma/paraganglioma: a multi-center trial in Japan. *Endocr J* (2018) 65:359–71. doi: 10.1507/endocrj.EJ17-0276
46. Steinsapir J, Carr AA, Prisant LM, Bransome EJ. Metyrosine and pheochromocytoma. *Arch Intern Med* (1997) 157:901–6. doi: 10.1001/archinte.157.8.901
47. Butz JJ, Weingarten TN, Cavalcante AN, Bancos I, Young WJ, McKenzie TJ, et al. Perioperative hemodynamics and outcomes of patients on metyrosine undergoing resection of pheochromocytoma or paraganglioma. *Int J Surg* (2017) 46:1–6. doi: 10.1016/j.ijsu.2017.08.026
48. Perry RR, Keiser HR, Norton JA, Wall RT, Robertson CN, Travis W, et al. Surgical management of pheochromocytoma with the use of metyrosine. *Ann Surg* (1990) 212:621–8. doi: 10.1097/0000658-199011000-00010
49. Wachtel H, Kennedy EH, Zaheer S, Bartlett EK, Fishbein L, Roses RE, et al. Preoperative Metyrosine Improves Cardiovascular Outcomes for Patients Undergoing Surgery for Pheochromocytoma and Paraganglioma. *Ann Surg Oncol* (2015) 22(Suppl 3):S646–54. doi: 10.1245/s10434-015-4862-z
50. Thanapaalasingham K, Pollmann AS, Schelew B. Failure of metyrosine therapy for preoperative management of pheochromocytoma: a case report. *Can J Anaesth* (2015) 62:1303–7. doi: 10.1007/s12630-015-0480-2
51. Lafont M, Fagour C, Haissaguerre M, Daracette G, Wagner T, Corcuff JB, et al. Per-operative hemodynamic instability in normotensive patients with incidentally discovered pheochromocytomas. *J Clin Endocrinol Metab* (2015) 100:417–21. doi: 10.1210/jc.2014-2998
52. Haissaguerre M, Courel M, Caron P, Denost S, Dubessy C, Gosse P, et al. Normotensive incidentally discovered pheochromocytomas display specific biochemical, cellular, and molecular characteristics. *J Clin Endocrinol Metab* (2013) 98:4346–54. doi: 10.1210/jc.2013-1844
53. Song G, Joe BN, Yeh BM, Meng MV, Westphalen AC, Coakley FV. Risk of catecholamine crisis in patients undergoing resection of unsuspected pheochromocytoma. *Int Braz J Urol* (2011) 37:35–40. doi: 10.1590/s1677-55382011000100005
54. Kota SK, Kota SK, Panda S, Modi KD. Pheochromocytoma: an uncommon presentation of an asymptomatic and biochemically silent adrenal incidentaloma. *Malays J Med Sci* (2012) 19:86–91.
55. El-Doueih RZ, Salti I, Maroun-Aouad M, Hajj AE. Bilateral biochemically silent pheochromocytoma, not silent after all. *Urol Case Rep* (2019) 24:100876. doi: 10.1016/j.eucr.2019.100876
56. Chobanian AV, Bakris GL, Black HR, Cushman WC, Green LA, Izzo JJ, et al. The Seventh Report of the Joint National Committee on Prevention, Detection, Evaluation, and Treatment of High Blood Pressure: the JNC 7 report. *JAMA* (2003) 289:2560–72. doi: 10.1001/jama.289.19.2560
57. Mazza A, Armigliato M, Marzola MC, Schiavon L, Montemurro D, Vescovo G, et al. Anti-hypertensive treatment in pheochromocytoma and paraganglioma: current management and therapeutic features. *Endocrine* (2014) 45:469–78. doi: 10.1007/s12020-013-0007-y
58. James MF, Cronjé L. Pheochromocytoma crisis: the use of magnesium sulfate. *Anesth Analg* (2004) 99:680–6. doi: 10.1213/01.ANE.0000133136.01381.52

Conflict of Interest: The authors declare that the research was conducted in the absence of any commercial or financial relationships that could be construed as a potential conflict of interest.

Copyright © 2020 Fang, Ding, He and Liu. This is an open-access article distributed under the terms of the Creative Commons Attribution License (CC BY). The use, distribution or reproduction in other forums is permitted, provided the original author(s) and the copyright owner(s) are credited and that the original publication in this journal is cited, in accordance with accepted academic practice. No use, distribution or reproduction is permitted which does not comply with these terms.



Recent Advances in Histopathological and Molecular Diagnosis in Pheochromocytoma and Paraganglioma: Challenges for Predicting Metastasis in Individual Patients

OPEN ACCESS

Edited by:

Ichiro Abe,
Fukuoka University Chikushi Hospital,
Japan

Reviewed by:

Takeshi Nigawara,
Tsugaru General Hospital, Japan
Hiroko Fujita,
Tama Hokubu Medical Center, Japan

*Correspondence:

Hironobu Sasano
hsasano@patholo2.med.tohoku.ac.jp

Specialty section:

This article was submitted to
Neuroendocrine Science,
a section of the journal
Frontiers in Endocrinology

Received: 27 July 2020

Accepted: 30 September 2020

Published: 27 October 2020

Citation:

Yamazaki Y, Gao X, Pecori A,
Nakamura Y, Tezuka Y, Omata K,
Ono Y, Morimoto R, Satoh F and
Sasano H (2020) Recent Advances in
Histopathological and Molecular
Diagnosis in Pheochromocytoma
and Paraganglioma: Challenges
for Predicting Metastasis
in Individual Patients.
Front. Endocrinol. 11:587769.
doi: 10.3389/fendo.2020.587769

Yuto Yamazaki¹, Xin Gao¹, Alessio Pecori^{1,2}, Yasuhiro Nakamura³, Yuta Tezuka^{2,4},
Kei Omata^{2,4}, Yoshikiyo Ono^{2,4}, Ryo Morimoto⁴, Fumitoshi Satoh^{2,4}
and Hironobu Sasano^{1*}

¹ Department of Pathology, Tohoku University Graduate School of Medicine, Sendai, Japan, ² Division of Clinical Hypertension, Endocrinology and Metabolism, Tohoku University Graduate School of Medicine, Sendai, Japan, ³ Division of Pathology, Faculty of Medicine, Tohoku Medical and Pharmaceutical University, Sendai, Japan, ⁴ Division of Nephrology, Endocrinology, and Vascular Medicine, Tohoku University Hospital, Sendai, Japan

Pheochromocytomas and paragangliomas (PHEO/PGL) are rare but occasionally life-threatening neoplasms, and are potentially malignant according to WHO classification in 2017. However, it is also well known that histopathological risk stratification to predict clinical outcome has not yet been established. The first histopathological diagnostic algorithm for PHEO, “PASS”, was proposed in 2002 by Thompson et al. Another algorithm, GAPP, was then proposed by Kimura et al. in 2014. However, neither algorithm has necessarily been regarded a ‘gold standard’ for predicting post-operative clinical behavior of tumors. This is because the histopathological features of PHEO/PGL are rather diverse and independent of their hormonal activities, as well as the clinical course of patients. On the other hand, recent developments in wide-scale genetic analysis using next-generation sequencing have revealed the molecular characteristics of pheochromocytomas and paragangliomas. More than 30%–40% of PHEO/PGL are reported to be associated with hereditary genetic abnormalities involving > 20 genes, including *SDH*Xs, *RET*, *VHL*, *NF1*, *TMEM127*, *MAX*, and others. Such genetic alterations are mainly involved in the pathogenesis of pseudohypoxia, *Wnt*, and kinase signaling, and other intracellular signaling cascades. In addition, recurrent somatic mutations are frequently detected and overlapped with the presence of genetic alterations associated with hereditary diseases. In addition, therapeutic strategies specifically targeting such genetic abnormalities have been proposed, but they are not clinically applicable at this

time. Therefore, we herein review recent advances in relevant studies, including histopathological and molecular analyses, to summarize the current status of potential prognostic factors in patients with PHEO/PGL.

Keywords: adrenal, pheochromocytoma, paraganglioma, genotype, pathology, SDHB, PASS, GAPP

INTRODUCTION

Pheochromocytomas (PHEOs)/paragangliomas (PGLs) or PPGLs are not only oncological diseases due to their invasive or metastatic properties, but also life-threatening endocrinological disorders associated with medical therapy resistant hypertension due to catecholamine excess (1–4). Differentiation between “PHEOs” and “PGLs” is defined based on the sites of the primary lesion as follows; PHEOs are derived from chromaffin cells in the adrenal medulla, and PGLs from sympathetic or parasympathetic paraganglion cells located in extra-adrenal tissues (5).

Distant metastasis is detected in 5%–20% of PHEOs, and relatively higher in PGLs, ranging from 15% to 35% (6–9). The five-year survival rate of metastatic disease has been reported to be approximately 50% or less (10–12). However, it is difficult to predict metastatic potential based on histopathological findings alone, and none of the previously proposed histopathological scoring systems can reach the levels of accurate metastasis prediction. Therefore, all PPGLs were proposed to have malignant potential according to the WHO classification in 2017, because of the absence of hallmark diagnostic markers (5).

In contrast, recent developments in molecular analysis have clarified the genetic landscape or characteristics of PPGLs, which could reflect the risks of metastatic potential (1–4, 6). The results of those studies revealed a higher incidence of genetic abnormalities associated with hereditary diseases, spanning more than 20 relevant genes in > 40% of all cases (1–4, 6). Among the genes above, the presence of *SDHX* mutations is reported to increase the risks of developing aggressive disease behavior by altering intracellular metabolism, especially the tricarboxylic acid (TCA) cycle (4, 13–17).

In this review, we therefore summarized the previously proposed histopathological/clinicopathological scoring systems, including their limitations for predicting the metastatic potential of the disease, and pitfalls when interpreting the findings. In addition, the clinical significance of recently reported genetic abnormalities and genotype-phenotype associations are also summarized.

GENETIC ABNORMALITIES IN PPGLS

PPGLs were previously called “10%-diseases” associated with hereditary disorders. However, recent developments in genetic analysis using next-generation sequencing and large-scale integrated analysis by The Cancer Genome Atlas (TCGA) database has identified a much larger number of relevant genetic abnormalities (6, 18). The prevalence of PPGLs

associated with hereditary diseases involves approximately 40% of all patients (6). Pathogenic variants with genetic alterations in relevant genes are generally exclusive to each other, but it is also true that somatically mutated driver genes are involved in further development of PPGLs in a minor population with germline mutations (6), which is considered unique to this tumor. In addition, comprehensive genetic analysis by Fishbein et al. further demonstrated that 27% of PPGLs have germline mutations, 39% somatic mutations (with 5%–10% overlap with germline mutations), 7% gene fusions, and 89% copy number alterations (6). PPGLs are sub-classified into three different groups, according to their genotype-related pathophysiology (4, 6, 19–21). The most prevalent subtype is the “pseudohypoxia type”, with genetic alterations in *SDHX* families, *FH*, *VHL*, and *EPAS1* (13–17, 22–27). The second is the “Wnt-signal type” associated with somatic alterations in genes involved in Wnt-signaling pathways, including *CSDE1* mutation and *MAML3* gene translocation (6, 28). The third is the “kinase signal type” with genetic alterations involving *RET*, *NF1*, *MAX*, and *TMEM127*, and which is frequently associated with MEN2 (multiple endocrine neoplasia type 2) gene abnormalities (4, 6, 29–35). In addition, a fourth group was also recently proposed as a cortical admixture subtype, although the detailed features involved have remained uncertain compared to the three major subtypes indicated above (6). Therefore, in this paper, individual genotypes and their pathophysiological characteristics are briefly reviewed. Previously reported genetic alterations associated with PPGLs are also summarized in **Table 1**.

“Pseudohypoxia Type”

“Pseudohypoxia type” is the most prevalent phenotype in PPGLs, and the great majority of genetic abnormalities involving this phenotype have been detected in genes involved in the TCA cycle, including *SDHX* family, *FH*, *VHL*, *EPAS1*, *SLC25A11*, and others (13–17, 22–27). Chromaffin cells are physiologically involved in oxidative metabolism status, with abundant aerobic respiration by mitochondria synthesizing ATP by activating the TCA cycle. However, genetic alterations in genes encoding catalyzing enzymes involved in the TCA cycle, such as succinate dehydrogenase, are known to result in loss of their physiological functions. These altered genes subsequently promote anaerobic metabolism by tumor cells, shifting ATP resources from the TCA cycle into the system of metabolic glycolysis (62–64). These alterations in intracellular metabolism eventually result in degradation of chromatin remodeling, reactive oxygen species production, and DNA methylation (62–66). These intracellular changes also enable tumor cells to efficiently synthesize ATP, although the amounts of ATP synthesized from glycolysis per reaction does not reach

TABLE 1 | Previously identified mutated driver genes associated with PPGLs.

Type	Gene	Condong Protein	Chromosome location	Germline or Somatic	Predominant tumor site	Contribution to metastatic potential	Associated hereditary diseases	Reference
1	<i>SDHA</i>	Succinate Dehydrogenase Complex Flavoprotein Subunit A	5p15.33	Germline	PGL>PHEO	Low	Familial PGL type 5	(6, 13),
1	<i>SDHB</i>	Succinate Dehydrogenase Complex Iron Sulfur Subunit B	1p36.13	Germline	PGL>PHEO	Intermediate	Familial PGL type 4	(14)
1	<i>SDHC</i>	Succinate Dehydrogenase Complex Subunit C	1q23.3	Germline	PGL>>PHEO	Very low	Familial PGL type 3	(15)
1	<i>SDHD</i>	Succinate Dehydrogenase Complex Subunit D	11q23.1	Germline	PGL>PHEO	Low	Familial PGL type 1	(6, 16)
1	<i>SDHAF2</i>	Succinate Dehydrogenase Complex Assembly Factor 2	11q12.2	Germline	PGL>>PHEO	Very Low	Familial PGL type 2	(17, 36)
1	<i>FH</i>	Fumarate Hydratase	1q43	Germline	PHEO, PGL	Low	FH-deficient HLRCC (Hereditary leiomyomatosis and renal cell carcinoma)	(37)
1	<i>VHL</i>	Von Hippel-Lindau Tumor Suppressor	3p25.3	Germline	PHEO>PGL	Low-Intermediate	Von-Hippel-Lindau disease	(6, 25),
1	<i>EPAS1 (HIF2A)</i>	Endothelial PAS Domain Protein 1	2p21	Germline, Somatic	PHEO, PGL	Low-Intermediate	Pacak-Zhuang syndrome	(6, 26, 27)
1	<i>EGLN1 (PHD1)</i>	Egl-9 Family Hypoxia Inducible Factor 1	1q42.2	Germline	PHEO, PGL	Not characterized	Polycythemia	(6, 38)
1	<i>EGLN2 (PHD2)</i>	Egl-9 Family Hypoxia Inducible Factor 2	19q13.2	Germline	PHEO, PGL	Not characterized	Polycythemia	(38)
1	<i>MDH2</i>	Malate Dehydrogenase 2	7q11.23	Germline	PHEO, PGL	Not characterized	Not characterized	(23, 39),
1	<i>SLC25A11</i>	Solute Carrier Family 25 Member 11	17p13.2	Germline	PGL	Low-Intermediate	Not characterized	(40)
1	<i>DLST</i>	Dihydrolipoamide S-Succinyltransferase	14q24.3	Germline	PHEO, PGL	Not characterized	Not characterized	(41)
1	<i>DNMT3A</i>	DNA Methyltransferase 3 Alpha	2p23.3	Germline, Somatic	PHEO, PGL	Not characterized	Acute Myeloid Leukemia (AML) (42)	(43)
1	<i>GOT2</i>	Glutamic-Oxaloacetic Transaminase 2	16q21	Germline	PHEO, PGL	Not characterized	Not characterized	(44)
2	<i>CSDE1</i>	Cold Shock Domain Containing E1	1p13.2	Somatic	PHEO, PGL	Not characterized	—	(6)
2	<i>MAML3</i>	Mastermind Like Transcriptional Coactivator 3	4q31.1	Somatic, Transfusion	PHEO, PGL	Low-Intermediate	—	(6, 28),
3	<i>KIF1B</i>	Kinesin Family Member 1B	1p36.22	Germline	PHEO?	Not characterized	Ganglioneuroma, leiomyosarcoma, lung adenocarcinoma, neuroblastoma, ganglioneuroma	(45)
3	<i>RET</i>	Proto-Oncogene Tyrosine-Protein Kinase Receptor Ret	10q11.21	Germline, Somatic	PHEO>>PGL	Low	Multiple endocrine neoplasia type 2	(6, 29–31),
3	<i>NF1</i>	Neurofibromin 1	17q11.2	Germline, Somatic	PHEO>PGL	Low	Nuerofibromatosis type 1	(6, 29–32),
3	<i>MAX</i>	MYC Associated Factor X	14q23.3	Germline	PHEO>PGL	Low	Familial PCC	(6, 34, 35),
3	<i>TMEM127</i>	Transmembrane Protein 127	2q11.2	Germline	PHEO>PGL	Low	Familial PCC	(6, 33),
3	<i>HRAS</i>	GTPase HRas	11p15.5	Somatic	PHEO?	Not characterized	—	(6)
3	<i>BRAF</i>	Serine/Threonine-Protein Kinase B-Raf	7q34	Somatic	PHEO, PGL	Not characterized	—	(6)
Others	<i>MEN1</i>	Menin 1	11q13.1	Germline	PHEO, PGL	Not characterized	Multiple endocrine neoplasia type 1	(46)
Somatic	<i>IRP1</i>	Iron Regulatory Protein 1	9p21.1	Somatic	PHEO, PGL	Not characterized	—	(47)
Somatic	<i>SETD2</i>	Histone-Lysine N-Methyltransferase SETD2	3p21.31	Somatic	PHEO, PGL	Low-Intermediate	—	(6, 18, 48),
Somatic	<i>FGFR1</i>	Fibroblast Growth Factor Receptor 1	8p11.23	Somatic	PHEO, PGL	Not characterized	—	(6, 49),

(Continued)

TABLE 1 | Continued

Type	Gene	Condong Protein	Chromosome location	Germline or Somatic	Predominant tumor site	Contribution to metastatic potential	Associated hereditary diseases	Reference
Somatic	<i>MET</i>	Hepatocyte Growth Factor Receptor	7q31.2	Somatic	PHEO, PGL	Not characterized	—	(50)
Somatic	<i>TP53</i>	Cellular Tumor Antigen P53	17p13.1	Somatic, Germline	PHEO, PGL	Not characterized	Li-Fraumeni Syndrome	(6)
Somatic	<i>ARNT</i>	Aryl Hydrocarbon Receptor Nuclear Translocator	1q21.3	Somatic	PGL	Not characterized	—	(6)
Somatic	<i>MYO5B</i>	Myosin VB	18q21.1	Somatic	PHEO, PGL	Not characterized	—	(51, 52),
Somatic	<i>MYCN</i>	N-Myc Proto-Oncogene Protein	2p24.3	Somatic	PHEO, PGL	Not characterized	—	(51)
Somatic	<i>VCL</i>	Vinculin	10q22.2	Somatic	PHEO, PGL	Not characterized	—	(51)
Somatic	<i>KMT2D</i>	Histone-Lysine N-Methyltransferase 2D	12q13.12	Somatic	PHEO, PGL	Not characterized	—	(53)
Somatic	<i>TERT</i>	Telomerase Reverse Transcriptase	5p15.33	Somatic	PHEO, PGL	Low-Intermediate	—	(54–57),
Somatic	<i>ATRX</i>	Transcriptional regulator ATRX	Xq21.1	Somatic	PHEO, PGL	Low-Intermediate	—	(6, 36, 58–60)
Somatic	<i>IDH1</i>	Isocitrate Dehydrogenase (NADP(+)) 1	2q34	Somatic	PHEO, PGL	Not characterized	—	(6, 59)
Somatic	<i>IDH2</i>	Isocitrate Dehydrogenase (NADP(+)) 2	15q26.1	Somatic	PHEO, PGL	Not characterized	—	(61)
Somatic	<i>H3F3A</i>	H3 Histone Family Member 3A	1q42.12	Somatic	PHEO, PGL	Not characterized	—	(50)

Type 1 Pseudohypoxia type, Type 2: Wnt signal type, Type 3: Kinase signal type.

In addition to more than 20 genes with germline mutations, recently detected genes with somatic variants are also summarized in this table. Some genes with somatic variants were classified into three previously known types if the detailed function of the mutated genes was clarified.

the same levels as those from the TCA cycle (62–66). This phenomenon has attracted considerable interest because of its possible associations with Warburg effects detected in some neoplastic cells (65, 66). Therefore, sub-typing based on intracellular metabolism in PPGLs has also been proposed. Some clinical studies exploring the ability of glucose absorption in PPGLs by FDG-PET imaging have been reported, and are proposed to be practically useful as a noninvasive diagnostic tool, especially for detecting pseudohypoxic phenotypes of tumors, and those manifesting potentially malignant behavior over their clinical course (67, 68).

“Wnt-Signal Type”

The “Wnt-signal type” is known as the most prevalent phenotype among sporadic PPGLs, with somatic alterations to driver genes (4, 6). Wnt-/Shh-related pathways are widely reported to be involved in cell proliferation in various types of diseases (69, 70). The activation of Wnt-related signals is not necessarily specific for PPGLs, but the presence of this particular type of genetic abnormality has been reported to result in relatively frequent distant metastasis or recurrence, especially in cases involving *MAML3* gene fusions (6). Somatic mutations of the *CSDE1* gene and transfection of *MAML3* are both classified as exhibiting this phenotype. *CSDE1* frameshift and splice-site mutations have been reported in a minor population of PPGLs with previously known germline mutations, including *VHL*, *NF1*, and *RET* (6). These *CSDE1* genetic alterations result in loss-of-function (6). *CSDE1* is well known in regulating translation initiation, apoptosis, RNA stability, and differentiation/development of neuronal tissue (71, 72). The functional roles of mutated

variants of *CSDE1* were also previously validated by microarray analysis using mouse embryonic stem cells (73, 74).

PPGLs with *MAML3* gene fusions are reported to be associated with a higher prevalence of metastatic diseases, frequently in conjunction with SDH loss (6, 28). Comprehensive genetic analysis revealed that the *UBTF-MAML3* fusion gene activates *Wnt-Shh* signaling, but only a small number of studies have investigated the clinical significance of this chimeric fusion gene (6, 28). Therefore, the detailed underlying mechanisms, as well as their prevalence, have not been thoroughly studied, and further investigations are warranted.

“Kinase Signal Type”

The “kinase signal type” is associated with systemic hereditary diseases such as MEN2A/2B (*RET* mutation) and neurofibromatosis type 1 (*NF1* mutation) (29–32). Familial PHEOs with *TMEM127* or *MAX* mutations are also categorized into this subtype (33–35). Among them, the gain-of-function caused by *RET* gene mutation has been studied in the most detail. *RET* encodes a transmembrane receptor tyrosine kinase involved in the development of the neural crest. *RET* mutations detected in MEN2A are reported to cause homodimerization, which subsequently activates PI3K-AKT, RAS, p38-MAPK, and JUN N-terminal kinase pathways in a ligand-independent manner, promoting abnormal cell proliferation (75–77). Recently, somatic mutations detected involving *FGFR1*, *NF1*, *BRAF*, *HRAS*, and others have also been reported to contribute to the activation of the relevant pathways indicated above (6). However, the underlying

mechanisms involving the kinase signaling pathway remain unknown, especially whether these pathways possibly interact with the downstream pathways of other subtypes.

Others (Somatic Abnormalities)

With the exception of three major subgroups, multiple somatic genetic abnormalities have been reported, involving *IRP1* (47), *SETD2* (6, 18, 48), *FGFR1* (6, 49), *MET* (50), *TP53* (6), *ARNT* (6), *MYO5B* (51, 52), *MYCN* (51), *VCL* (51), *KMT2D* (53), *TERT* (54–57), *ATRX* (6, 57–59), *IDH1* (6, 58), *IDH2* (36), and *H3F3A* (50). However, it is also true that majority of newly reported somatic gene abnormalities are detected in only a minor proportion of patients with PPGLs. Among these somatic gene abnormalities, aberrant telomere maintenance mechanism (TMM), which is caused by *TERT* (telomerase reverse transcriptase) structural rearrangement, genetic abnormalities, and *ATRX* mutations, has been reported to be associated with poor clinical outcomes in patients (54–57). Structural rearrangement of *TERT* has also been reported to result in its over-expression as a result of the placement of enhancers proximal to the *TERT* promoter (56). The presence of somatic mutations detected in the *TERT* promoter is not necessarily concordant with *TERT* overexpression, but a specific hot-spot, C228T, is reported to be associated with adverse clinical outcomes in patients (57, 78). However, its cross-interaction with *SDHX*-related pseudohypoxic pathways cannot be ruled out.

CHALLENGES OF PREDICTIVE CLINICOPATHOLOGICAL/HISTOPATHOLOGICAL SCORING SYSTEMS FOR MALIGNANT BEHAVIOR/METASTASIS IN PPGLS

Histopathological risk stratification, or discerning malignancy, in PPGL patients is very challenging and is generally considered one of the most difficult differential diagnoses in the field of surgical pathology. Several histopathological scoring systems have been proposed, including PASS and GAPP scores, but it is also true that those above could by no means precisely predict the clinical outcome and/or the degree of aggressive clinical behavior in PPGL patients (5, 79–81). As a basis for these two established representative histological scoring systems, several combined scoring systems with genetic abnormalities and immunohistochemical findings have also been recently proposed, such as M-GAPP (Modified-GAPP) score (82), ASES (Age, Size, Extra-adrenal location, and Secretory type) score (83) and COPPs (Composite Pheochromocytoma/paraganglioma Prognostic score) (84). However, further investigations are needed to clarify the practical value of such systems in discerning the clinical behavior of patient tumors.

Therefore, in this section, previously proposed histopathological/clinicopathological scoring systems and the recent validation studies of these systems were covered to clarify the usefulness

and limitations of histopathological findings to predict the clinical behavior of tumors, as well as the potential pitfalls involving interpretation of such findings with high inter-/intra-observer variation by both pathologists and clinicians.

PASS (Pheochromocytoma of the Adrenal Gland Scale Score)

PASS was the first histopathological scoring system proposed by the group of Armed Forces Institute of Pathology led by Thompson in 2002, and this system was composed of twelve findings based on histological features as follows (summarized in **Figure 1A**): 1) large cell nests or diffuse growth of >10%, 2) central or confluent tumor necrosis, 3) high cellularity, 4) cell monotony, 5) tumor cell spindling (even if focal), 6) mitotic figures >3 figures/10 high power fields, 7) atypical mitotic figure(s), 8) extension into adipose tissue, 9) vascular invasion, 10) capsular invasion, 11) profound nuclear polymorphism, 12) and nuclear hyperchromasia (79). Tumors with 4 points or more were proposed to be associated with a high prevalence of distant metastasis, and those with less than 4 points considered as benign (never metastatic) (79). Of particular note, the use of PASS in extra-adrenal PGLs was limited because this particular scoring system was designed only for PHEOs, and included those criteria only applicable to intra-adrenal tumors such as extension into adipose tissue (81).

After the proposal of PASS, several validation studies were reported in the literature (82, 85–87). The presence of relatively high inter-/intra-observer variation has been reported in the confirmatory studies indicated above. Among those 12 histological features above, the presence of capsular and vascular invasion, extension into adipose tissue, and atypical mitosis could reach relatively high inter-observer concordance in > 80% of the examined cases (88). However, the histological features of high cellularity, profound nuclear polymorphism, and nuclear hyperchromasia resulted in low inter- and intra- observer concordance in their interpretation, even among pathologists with sufficient experience and knowledge in this field (88). Furthermore, it is also pivotal to note that the gradients of scoring points of individual histological features did not necessarily match the degree of inter-/intra-observer variation (88). Scoring systems based only on morphological or histological findings could become more subjective and, therefore, some studies employing combined PASS and genetic abnormality, as well as immunohistochemistry, have been proposed in recent years in order to overcome potential disadvantages or pitfalls of the system, as described above.

GAPP Score (Grading of Adrenal Pheochromocytoma and Paraganglioma) and M-GAPP (Modified GAPP)

The GAPP score was proposed by Kimura et al. in 2014 and required not only morphological findings, but also clinically proven catecholamine-producing types and proliferative ability of tumor cells by Ki-67 (MIB-1) labeling index (LI), in contrast to PASS, which could be performed only on hematoxylin-eosin

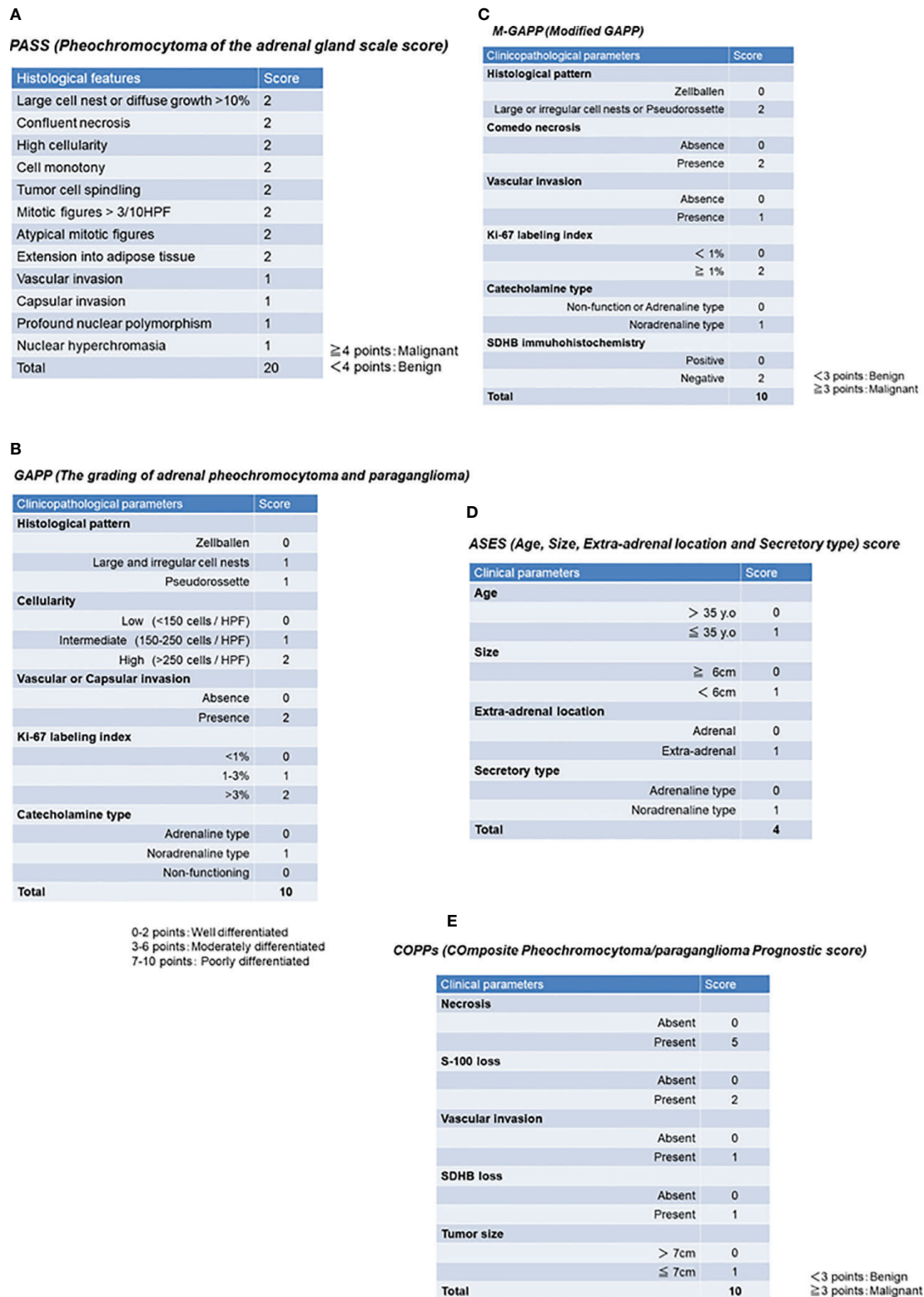


FIGURE 1 | Previously proposed histopathological/clinicopathological scoring system. **(A)** PASS (Pheochromocytoma of the adrenal gland scale score). **(B)** GAPP (Grading of adrenal pheochromocytoma and paraganglioma). **(C)** M-GAPP (Modified GAPP). **(D)** ASES (Age, Size, Extra-adrenal location and Secretory type) score. **(E)** COPPs (Composite Pheochromocytoma/paraganglioma Prognostic score).

stained tissue slides. This GAPP scoring system classified PPGLs into three different grades: well- (0-2 points), moderately (3-6 points), and poorly differentiated (7-10 points) PPGLs (80). The details of this scoring system are summarized in **Figure 1B**. The five-year survival rates of these three groups are 100% (well-differentiated), 66.8% (moderately differentiated), and 22.4% (poorly differentiated) (80). GAPP has been used in some diagnostic pathology laboratories, but several limitations or pitfalls have been raised regarding its clinical utility (4, 5, 81). In particular, MEN2A-associated PPGLs are over-diagnosed by both PASS and GAPP in predicting the potential malignant behavior of tumors (85). MEN2A-associated PPGLs rarely metastasize, although large cell nests or diffuse growth patterns (MEN2A-associated: 77% vs. benign: 30%, malignant: 90%) and increased Ki-67 LI of > 3% (MEN2A-associated: 31% vs. sporadic: 11%) are frequently detected in such cases, which result in high scores (85). In addition, the original GAPP system did not include finding regarding *SDHX* status (80). Therefore, Koh et al. subsequently proposed a modified GAPP score, modifying the gradient of the scoring points, and added the findings of SDHB immunohistochemistry (82). The details of M-GAPP are summarized in **Figure 1C**. The sensitivity of GAPP and M-GAPP is relatively high, while their specificity only reaches 50%–60% in terms of predicting distant metastasis in PPGL patients (82). The area under the curve (AUC) of these scoring systems resulted in 0.822 for M-GAPP, 0.728 for GAPP, and 0.753 for PASS (82), and there were no differences among the predictive values for patients. Therefore, other clinicopathological factors such as tumor size or patient age should be considered when determining the malignant potential of PPGLs. Further improvements in histopathological evaluation are warranted to more precisely predict the malignant potential of tumors.

ASES (Age, Size, Extra-Adrenal Location, and Secretory Type) Score

ASES (Age, Size, Extra-adrenal location and Secretory type) scoring was recently proposed by Cho et al. in 2018 (83). They performed a retrospective analysis using a relatively large number of cases, including 333 PPGLs (83). In contrast to other histopathological predictive models, ASES is entirely composed of only 4 clinical parameters (**Figure 1D**). The AUC to predict malignant behavior is reported to be 0.735 (88), and the practical advantages of using this scoring system includes no requirement for surgical specimens, which could apply this scoring system to all PPGLs, regardless of clinical stage (83). However, the sensitivity and specificity of these histology-based scoring systems remain unknown.

COPPs (Composite Pheochromocytoma/Paranglioma Prognostic Score)

COPPs (Composite Pheochromocytoma/paranglioma Prognostic score) was recently proposed by Pierre et al. in 2019, integrating morphological features and immunohistochemical findings of S-100 and SDHB (84). They examined a total of 147 PPGLs and performed multivariate analysis, including incorporation of the

morphological features listed in PASS, immunohistochemical findings of S-100, Ki-67, and MCM6, clinicopathological factors (tumor size, age, and hypertension) and genotype (84). Finally, COPPs were defined according to the following criteria: three clinicopathological parameters (tumor size > 7 cm, necrosis, and vascular invasion), loss of S-100 immunoreactivity (loss of intervening sustentacular cells), and loss of SDHB immunoreactivity (suggesting *SDHB* mutation) (84) (**Figure 1E**). When compared with previously proposed scoring systems, COPPs could provide a high AUC to predict potential metastasis in patients (sensitivity: 100%, specificity: 94.7%) (84). However, prospective validation studies involving COPPs have not been reported, and not all of the parameters proposed in this scoring system are readily available in clinical practice. Thus, COPPs could not reach the levels suitable for practical usage in current clinical settings and awaits validation.

PRACTICAL IMMUNOHISTOCHEMICAL (IHC) PPGL MARKERS

In addition to the above previously proposed clinicopathological scoring systems, several immunohistochemical (IHC) markers have also been reported in the literature to be able to differentiate metastatic from non-metastatic PPGLs. In this paper, the practical usefulness of IHC and its limitations and pitfalls in daily clinical settings are summarized.

Conventional Markers

SDHB IHC has been employed to detect *SDHB* gene mutations with relatively high concordance (sensitivity: 100% [95% CI: 87%–100%], specificity: 84% [95% CI: 60%–97%]) as demonstrated by the total absence of immunoreactivity, with positive immunoreactivity in endothelial cells as a positive IHC control (89). However, it is pivotal to note that interpretation of SDHB IHC is sometimes difficult because of the presence of false-negative findings, caused by various pre-analytical factors such as inappropriate fixation, which results in various staining patterns, including potential false-negative findings (89, 90). In particular, patterns of SDHB immunoreactivity with a complete absence, or weak but diffuse dot-like cytoplasmic staining patterns were detected in *SDHB*-mutated PPGLs (90). Therefore, confirmatory genetic analysis is practically mandatory for cases with equivocal immunoreactivity.

Both S-100 and Ki-67 are well-known and widely used markers for evaluation of the malignant potential of PPGLs (80, 81, 84). S-100 is generally immunolocalized in sustentacular cells surrounding tumor cells (91). Absence or attenuation of S-100 immunoreactivity (sustentacular cells) is generally considered to reflect diffuse growth patterns that deviate from the structure of Zellballen, possibly resulting in the aggressive clinical behavior of tumors (84, 91). S-100 positive sustentacular cells have recently been reported as non-neoplastic cells because SOX-10 and SDHB are both positive only in sustentacular cells in the cases of *SDHB*-mutated PPGLs (91). However, detailed characterization of sustentacular cells remains to be conducted.

The Ki-67 LI is also listed as one of the parameters in GAPP and M-GAPP. However, it is also important to note that Ki-67 LI is generally low (< 3%) in > 80% of PPGLs, and its intratumoral heterogeneity is also marked (80–82). In addition, the guidelines to obtaining Ki-67 LI, such as whether counting should be performed in “hot spots” or “averages”, have not necessarily been standardized, and inter-observer or -laboratory differences in Ki-67 LI results might be unavoidable.

Thus, these IHC markers are marginally useful for predicting the clinical behavior of tumors, but none of the previously proposed IHC markers are by no means independent predictive markers in patients.

Catecholamine-Synthesizing Enzymes

In addition to broadly used IHC markers, analyses of hormonal activities and IHC analysis of catecholamine-synthesizing enzymes such as tyrosine hydroxylase (TH), dopamine beta hydroxylase (DBH), dopa decarboxylase (DDC) and phenylethanolamine N-methyltransferase (PNMT) have also been reported in the literature. The expression profiles of these enzymes do not only characterize the secretory phenotypes of norepinephrine or epinephrine, but also reflect differentiation of the tumor cells in PPGLs (80, 92). PNMT catalyzes the final step of catecholamine biosynthesis from norepinephrine into epinephrine. Of particular interest, pseudohypoxic PPGLs are generally negative for PNMT, and have silent clinical and hormonal phenotypes, which could delay therapeutic intervention in such patients (93). Fukaya et al. reported that lower DDC immunoreactivity was detected in poorly differentiated PPGLs, histologically representing confluent necrosis, diffuse growth, nuclear polymorphism, and tumor cell spindling (94). Therefore, it is considered worthwhile to incorporate IHC analysis of these four catecholamine-producing enzymes into routine clinical practice in institutions treating relatively large volumes of patients with PPGLs because antibodies against all four enzymes used for IHC are commercially available (94).

Newly Proposed Markers

In addition to the classical markers above, several relatively unique IHC markers have recently been proposed for predicting the presence of distant metastasis in PPGLs. Deng et al. reported lower immunoreactivity of Snail, Galectin-3, and IGF-1R in benign PHEOs without local invasion and distant metastasis, based on a study of 226 PPGL cases (95). Leijon et al. immunolocalized SSTR (somatostatin receptor) family as a potential prognostic factor or a therapeutic target, and reported that 71.4% (10/14) of cases of metastasized PPGLs abundantly expressed SSTR2 (96). Among them, different immunoprofiles were detected between metastasized PGLs and PHEOs (PGLs: 100% (9/9 cases), PHEOs: 20% (1/5 cases). In contrast, SSTR4 and SSTR5 were IHC-negative in the majority of the cases examined, and both SSTR1 and SSTR3 were divergent and independent of *SDHX* deficiency, as well as the presence of metastases (96). However, the usefulness of somatostatin analogs in the treatment of patients with PPGLs has not been established, and the clinicopathological value of SSTR IHC should be validated by

further studies. Surrogate markers associated with tumor immune microenvironmental factors have been studied recently, especially PD-1/PD-L1 in PPGLs (97, 98). Guo et al. examined PD-L1 immunoreactivity in 77 PPGL cases using an anti-PD-L1 antibody (clone E1L3N) and reported that 59.74% (46/77 cases) of PPGLs were IHC-positive for PD-L1, with high co-efficiency of Ki-67 LI, as well as the presence of hypertension (97). On the other hand, Pinato et al. examined 100 PPGL cases using the same anti-PD-L1 antibody (clone E1L3N) and anti-PD-L2 antibody (polyclonal) (98). They reported that PD-L1 was IHC-positive in 18% (18/100 cases) and PD-L2 in 16% (16/100 cases) of PPGLs, respectively (98). Of particular interest, PD-L2 immunoreactivity in tumor cells was significantly correlated with overall survival of patients in their study (98). The presence of PD-L1 immunoreactivity in tumor cells could potentially indicate the utility of immune-checkpoint inhibitors, but standardization of histopathological evaluation of such markers, as well as unification of IHC antibody clones, are mandatory before various immune checkpoint inhibitors can be used therapeutically in PPGLs. In addition, few studies have reported histopathological surrogate markers of the tumor-immune microenvironment in PPGLs, and the clinical therapeutic efficacy of immune-checkpoint inhibitors remains unknown.

In summary, with a possible exception of SDHB, IHC-based analysis was less predictive than genetic analysis and past clinical history of the relevant hereditary diseases, and none of the above could be an independent predictive marker or a therapeutic target molecule. Therefore, future clinical trials as well as investigations of novel therapeutic targets are warranted in PPGLs.

SUMMARY

Recent advances in genetic and molecular characterization have classified PPGLs into subgroups based on their genotype-related pathophysiology. These genetic abnormalities are frequently detected in approximately 40% of PPGLs, far more than proposed over the past decades. Among them, *SDHX* mutations are the most frequently detected, resulting in pseudohypoxic status of tumor cells and which correlate with patient clinical outcomes, especially in detecting metastatic potential. Several histopathological and clinicopathological scoring systems have been proposed, but it is still challenging for diagnostic pathologists to predict malignant behavior based on histopathological findings of resected specimens alone, in contrast to other tumors such as adrenocortical neoplasms. Therefore, comprehensive scoring systems, combined with histopathological findings, genotyping, IHC, hormonal activities (metabolic phenotypes), the sites of involvement, and other clinical parameters have recently been proposed in the literature. However, none of the scoring systems reported could reach the necessary levels of practical usage or incorporation into clinical guidelines with high accuracy. In addition, no surrogate markers of specific therapy in patients with PPGL have been identified. Further investigations are required to clarify detailed pathophysiology of PPGLs, as well as more precise patient risk stratification.

AUTHOR CONTRIBUTIONS

All authors contributed to the article and approved the submitted version.

REFERENCES

1. Neumann HPH, Young WF Jr, Eng C. Pheochromocytoma and Paraganglioma. *N Engl J Med* (2019) 381:552–65. doi: 10.1056/NEJMra1806651
2. Alrezk R, Suarez A, Tena I, Pacak K. Update of Pheochromocytoma Syndromes: Genetics, Biochemical Evaluation, and Imaging. *Front Endocrinol (Lausanne)* (2018) 9:515. doi: 10.3389/fendo.2018.00515
3. Nölting S, Ullrich M, Pietzsch J, Ziegler CG, Eisenhofer G, Grossman A, et al. Current Management of Pheochromocytoma/Paraganglioma: A Guide for the Practicing Clinician in the Era of Precision Medicine. *Cancers* (2019) 11:1505. doi: 10.3390/cancers11101505
4. Crona J, Taïeb D, Pacak K. New Perspectives on Pheochromocytoma and Paraganglioma: Toward a Molecular Classification. *Endocr Rev* (2017) 38:489–515. doi: 10.1210/er.2017-00062
5. WHO classification. *Endocrine Tumor*. IARC (International Agency for Research on Cancer) (2017).
6. Fishbein L, Leshchiner I, Walter V, Danilova L, Robertson AG, Johnson AR, et al. Comprehensive molecular characterization of pheochromocytoma and paraganglioma. *Cancer Cell* (2017) 31:181–93. doi: 10.1016/j.ccr.2017.01.001
7. Burnichon N, Vescovo L, Amar L, Libe R, De RA, Venisse A, et al. Integrative genomic analysis reveals somatic mutations in pheochromocytoma and paraganglioma. *Hum Mol Genet* (2011) 20:3974–85. doi: 10.1093/hmg/ddr324
8. Korevaar TI, Grossman AB. Pheochromocytomas and paragangliomas: assessment of malignant potential. *Endocrine* (2011) 40:354–65. doi: 10.1007/s12020-011-9545-3
9. Goffredo P, Sosa JA, Roman SA. Malignant pheochromocytoma and paraganglioma: a population level analysis of long-term survival over two decades. *J Surg Oncol* (2013) 107:659–64. doi: 10.1002/jso.23297
10. Ziegler RG, Weinstein SJ, Fears TR. Nutritional and genetic inefficiencies in one-carbon metabolism and cervical cancer risk. *J Nutr* (2002) 132:2345S–9S. doi: 10.1093/jn/132.8.2345S
11. Turkova H, Prodanov T, Maly M, Martucci V, Adams K, Widimsky J, et al. Characteristics and outcomes of metastatic SDHB and sporadic pheochromocytoma/ paraganglioma: an National Institutes of Health study. *Endocr Pract* (2016) 22:302–14. doi: 10.4158/EP15725.0R
12. Hamidi O. Metastatic pheochromocytoma and paraganglioma: recent advances in prognosis and management. *Curr Opin Endocrinol Diabetes Obes* (2019) 26:146–54. doi: 10.1097/MED.0000000000000476
13. Burnichon N, Brière JJ, Libe R, Vescovo L, Rivi`ere J, Tissier F, et al. SDHA is a tumor suppressor gene causing paraganglioma. *Hum Mol Genet* (2010) 19 (15):3011–20. doi: 10.1093/hmg/ddq206
14. Astuti D, Latif F, Dallol A, Dahia PL, Douglas F, George E, et al. Gene mutations in the succinate dehydrogenase subunit SDHB cause susceptibility to familial pheochromocytoma and to familial paraganglioma. *Am J Hum Genet* (2001) 69(1):49–54. doi: 10.1086/321282
15. Niemann S, Müller U. Mutations in SDHC cause autosomal dominant paraganglioma, type 3. *Nat Genet* (2000) 26(3):268–70. doi: 10.1038/81551
16. Baysal BE, Ferrell RE, Willett-Brozick JE, Lawrence EC, Myssiorek D, Bosch A, et al. Mutations in SDHD, a mitochondrial complex II gene, in hereditary paraganglioma. *Science* (2000) 287(5454):848–51. doi: 10.1126/science.287.5454.848
17. Bayley JP, Kunst HP, Cascon A, Sampietro ML, Gaal J, Korpershoek E, et al. SDHAF2 mutations in familial and sporadic paraganglioma and phaeochromocytoma. *Lancet Oncol* (2010) 11(4):366–72. doi: 10.1016/S1470-2045(10)70007-3
18. Suh YJ, Choe J-Y, Park HJ. Malignancy in Pheochromocytoma or Paraganglioma: Integrative Analysis of 176 Cases in TCGA. *Endocr Pathol* (2017) 28:159–64. doi: 10.1007/s12022-017-9479-2
19. Antonio K, Valdez MMN, Mercado-Asis L, Taïeb D, Pacak K. Pheochromocytoma/paraganglioma: recent updates in genetics,

FUNDING

This work was supported by a Health Labour Sciences Research Grant (No. H29-Nanji-Ippan-046).

- biochemistry, immunohistochemistry, metabolomics, imaging and therapeutic options. *Gland Surg* (2020) 9(1):105–23. doi: 10.21037/gs.2019.10.25
20. Dahia PLM. Pheochromocytoma and paraganglioma pathogenesis: learning from genetic heterogeneity. *Nat Rev Cancer* (2014) 14(2):108–19. doi: 10.1038/nrc3648
 21. Turchini J, Cheung VKY, Tischler AS, Krijger RRD, Gill AJ. Pathology and genetics of phaeochromocytoma and paraganglioma. *Histopathology* (2018) 72:97–105. doi: 10.1111/his.13402
 22. Letouze E, Martinelli C, Lorient C, Burnichon N, Abermil N, Ottolenghi C, et al. SDH mutations establish a hypermethylator phenotype in paraganglioma. *Cancer Cell* (2013) 23(6):739–52. doi: 10.1016/j.ccr.2013.04.018
 23. Cascón A, Comino-Méndez I, Currás-Freixes M, de Cubas AA, Contreras L, Richter S, et al. Whole-exome sequencing identifies MDH2 as a new familial paraganglioma gene. *J Natl Cancer Inst* (2015) 107(5):107. doi: 10.1093/jnci/djv053
 24. Selak MA, Armour SM, MacKenzie ED, Boulahbel H, Watson DG, Mansfield KD, et al. Succinate links TCA cycle dysfunction to oncogenesis by inhibiting HIF α prolyl hydroxylase. *Cancer Cell* (2005) 7(1):77–85. doi: 10.1016/j.ccr.2004.11.022
 25. Latif F, Tory K, Gnarr J, Yao M, Duh FM, Orcutt ML, et al. Identification of the von Hippel-Lindau disease tumor suppressor gene. *Science* (1993) 260 (5112):1317–20. doi: 10.1126/science.8493574
 26. Tella SH, Taïeb D, Pacak K. HIF-2 α : Achilles' heel of pseudohypoxic subtype paraganglioma and other related conditions. *Eur J Cancer* (2017) 86:1–4. doi: 10.1016/j.ejca.2017.08.023
 27. Zhuang Z, Yang C, Lorenzo F, Merino M, Fojo T, Kebebew E, et al. Somatic HIF2A gain-of-function mutations in paraganglioma with polycythemia. *N Engl J Med* (2012) 367:922–30. doi: 10.1056/NEJMoa1205119
 28. Smestad JA, Maher LJ. Master regulator analysis of paragangliomas carrying SDHx, VHL, or MAML3 genetic alterations. *BMC Cancer* (2019) 19:619. doi: 10.1186/s12885-019-5813-z
 29. Welander J, Soderkvist P and Gimm O. Genetics and clinical characteristics of hereditary pheochromocytomas and paragangliomas. *Endocr Relat Cancer* (2011) 18:R253–76. doi: 10.1530/ERC-11-0170
 30. Gimenez-Roqueplo A-P, Dahia PL, Robledo M. An update on the genetics of paraganglioma, pheochromocytoma, and associated hereditary syndromes. *Horm Metab Res* (2012) 44:328–33. doi: 10.1055/s-0031-1301302
 31. Neumann HP, Bausch B, McWhinney SR, Bender BU, Gimm O, Franke G, et al. Germ-line mutations in nonsyndromic pheochromocytoma. *N Engl J Med* (2002) 346:1459–66. doi: 10.1056/NEJMoa020152
 32. Burnichon N, Buffet A, Parfait B, Letouze E, Laurendeau I, Lorient C, et al. Somatic NF1 inactivation is a frequent event in sporadic pheochromocytoma. *Hum Mol Genet* (2012) 21:5397–405. doi: 10.1093/hmg/ddc374
 33. Qin Y, Yao L, King EE, Buddavarapu K, Lenci RE, Chocron ES, et al. Germline mutations in TMEM127 confer susceptibility to pheochromocytoma. *Nat Genet* (2010) 42(3):229–33. doi: 10.1038/ng.533
 34. Burnichon N, Cascón A, Schiavi F, Morales NP, Comino-Méndez I, Abermil N, et al. MAX mutations cause hereditary and sporadic pheochromocytoma and paraganglioma. *Clin Cancer Res* (2012) 18(10):2828–37. doi: 10.1158/1078-0432
 35. Comino-Méndez I, Gracia-Aznárez FJ, Schiavi F, Landa I, Leandro-García LJ, Letón R, et al. Exome sequencing identifies MAX mutations as a cause of hereditary pheochromocytoma. *Nat Genet* (2011) 43(7):663–7. doi: 10.1038/ng.861
 36. Job S, Draskovic I, Burnichon N, Buffet A, Cros J, Lépine C, et al. Telomerase Activation and ATRX Mutations Are Independent Risk Factors for Metastatic Pheochromocytoma and Paraganglioma. *Clin Cancer Res* (2019) 25(2):760–70. doi: 10.1158/1078-0432.CCR-18-0139
 37. Letouze E, Martinelli C, Lorient C, Burnichon N, Abermil N, Ottolenghi C, et al. SDH mutations establish a hypermethylator phenotype in paraganglioma. *Cancer Cell* (2013) 23:739–52. doi: 10.1016/j.ccr.2013.04.018

38. Yang C, Zhuang Z, Flidner SM, Shankavaram U, Sun MG, Bullova P, et al. Germ-line PHD1 and PHD2 mutations detected in patients with pheochromocytoma/paranglioma-polycythemia. *J Mol Med (Berl)* (2015) 93:93–104. doi: 10.1007/s00109-014-1205-7
39. Calsina B, Currás-Freixes M, Buffet A, Pons T, Contreras L, Letón R, et al. Role of MDH2 pathogenic variant in pheochromocytoma and paraganglioma patients. *Genet Med* (2018) 20(12):1652–62. doi: 10.1038/s41436-018-0068-7
40. Buffet A, Morin A, Castro-Vega LJ, Habarou F, Lussey-Lepoutre C, Letouze E, et al. Germline Mutations in the Mitochondrial 2-Oxoglutarate/Malate Carrier SLC25A11 Gene Confer a Predisposition to Metastatic Parangliomas. *Cancer Res* (2018) 78:1914–22. doi: 10.1158/0008-5472.CAN-17-2463
41. Remacha L, Pirman D, Mahoney CE, Coloma J, Calsina B, Currás-Freixes M, et al. Recurrent Germline DLST Mutations in Individuals with Multiple Pheochromocytomas and Parangliomas. *Am J Hum Genet* (2019) 104:1008–10. doi: 10.1016/j.ajhg.2019.04.010
42. Sandoval JE, Huang YH, Muise A, Goodell MA, Reich NO. Mutations in the DNMT3A DNA methyltransferase in acute myeloid leukemia patients cause both loss and gain of function and differential regulation by protein partners. *J Biol Chem* (2019) 294(13):4898–910. doi: 10.1074/jbc.RA118.006795
43. Remacha L, Currás-Freixes M, Torres-Ruiz R, Schiavi F, Torres-Pérez R, Calsina B, et al. Gain-of-function mutations in DNMT3A in patients with paraganglioma. *Genet Med* (2018) 20(12):1644–51. doi: 10.1038/s41436-018-0003-y
44. Remacha L, Comino-Méndez I, Richter S, Contreras L, María Currás-Freixes M, Pita G, et al. Targeted Exome Sequencing of Krebs Cycle Genes Reveals Candidate Cancer-Predisposing Mutations in Pheochromocytomas and Parangliomas. *Clin Cancer Res* (2017) 23(20):6315–24. doi: 10.1158/1078-0432.CCR-16-2250
45. Yeh I-T, Lenci RE, Qin Y, Buddavarapu K, Ligon AH, Leteurtre E, et al. Germline mutation of the KIF1B gene on 1p36 in a family with neural and nonneural tumors. *Hum Genet* (2008) 124:279–85. doi: 10.1007/s00439-008-0553-1
46. Pillai S, Gopalan V, Lo CY, Liew V, Smith RA, Lam AFK. Silent genetic alterations identified by targeted next-generation sequencing in pheochromocytoma/paranglioma: A clinicopathological correlations. *Exp Mol Pathol* (2017) 102(1):41–6. doi: 10.1016/j.yexmp.2016.12.007
47. Pang Y, Gupta G, Yang C, Wang H, Huynh T-T, Abdullaev Z, et al. A novel splicing site IRP1 somatic mutation in a patient with pheochromocytoma and JAK2 V617F positive polycythemia vera: a case report. *BMC Cancer* (2018) 18(1):286. doi: 10.1186/s12885-018-4127-x
48. Snezhkina AV, Lukyanova EN, Kalinin DV, Pokrovsky AV, Dmitriev AA, Koroban NV, et al. Exome analysis of carotid body tumor. *BMC Med Genomics* (2018) 11(Suppl 1):17. doi: 10.1186/s12920-018-0327-0
49. Welander J, Lysiak M, Brauckhoff M, Brunaud L, Soëderkvist P, Gimm O. Activating FGFR1 Mutations in Sporadic Pheochromocytomas. *World J Surg* (2018) 42:482–9. doi: 10.1007/s00268-017-4320-0
50. Toledo RA, Qin Y, Cheng ZM, Gao Q, Iwata S, Silva GM, et al. Recurrent mutations of chromatin-remodeling genes and kinase receptors in pheochromocytomas and paragangliomas. *Clin Cancer Res* (2016) 22(9):2301–10. doi: 10.1158/1078-0432.CCR-15-1841
51. Wilén A, Rehammar A, Muth A, Nilsson O, Tešanj Tomić T, Wängberg B, et al. Malignant pheochromocytomas/parangliomas harbor mutations in transport and cell adhesion genes. *Int J Cancer* (2016) 138(9):2201–11. doi: 10.1002/ijc.29957
52. Tomić TT, Olausson J, Rehammar A, Deland L, Muth A, Ejeskär K, et al. MYO5B mutations in pheochromocytoma/paranglioma promote cancer progression. *PLoS Genet* (2020) 16(6):e1008803. doi: 10.1371/journal.pgen.1008803
53. Juhlin CC, Stenman A, Haglund F, Clark VE, Brown TC, Baranoski J, et al. Whole-exome sequencing defines the mutational landscape of pheochromocytoma and identifies KMT2D as a recurrently mutated gene. *Genes Chromosomes Cancer* (2015) 54(9):542–54. doi: 10.1002/gcc.22267
54. Hsu YR, Torres-Mora J, Kipp BR, Sukov WR, Jenkins SM, Voss JS, et al. Clinicopathological, immunophenotypic and genetic studies of mediastinal paragangliomas. *Eur J Cardiothorac Surg* (2019) 56(5):867–75. doi: 10.1093/ejcts/ezz115
55. Papatomas TG, Oudijk L, Zwarthoff EC, Post E, Duijkers FA, van Noesel MM, et al. Telomerase reverse transcriptase promoter mutations in tumors originating from the adrenal gland and extra-adrenal paraganglia. *Endocr Relat Cancer* (2014) 21(4):653–61. doi: 10.1530/ERC-13-0429
56. Dwight T, Flynn A, Amarasinghe K, Benn DE, Lupat R, Li J, et al. TERT structural rearrangements in metastatic pheochromocytomas. *Endocr Relat Cancer* (2018) 25(1):1–9. doi: 10.1530/ERC-17-0306
57. Liu T, Brown TC, Juhlin CC, Andreasson A, Wang N, Backdahl M, et al. The activating TERT promoter mutation C228T is recurrent in subsets of adrenal tumors. *Endocr Related Cancer* (2014) 21:427–34. doi: 10.1530/ERC-14-0016
58. Irwin T, Konnick EQ, Tretiakova MS. Malignant Intrarenal/Renal Pelvis Paranglioma with Co-Occurring SDHB and ATRX Mutations. *Endocr Pathol* (2019) 30:270–5. doi: 10.1007/s12022-019-09594-1
59. Zhang J, Jiang J, Luo Y, Li X, Lu Z, Liu Y, et al. Molecular evaluation of a sporadic paraganglioma with concurrent IDH1 and ATRX mutations. *Endocrine* (2018) 61(2):216–23. doi: 10.1007/s12020-018-1617-1
60. Fishbein L, Khare S, Wubbenhorst B, Desloover D, D'andrea K, Merrill S, et al. Whole-exome sequencing identifies somatic ATRX mutations in pheochromocytomas and paragangliomas. *Nat Commun* (2015) 6:6140. doi: 10.1038/ncomms7140
61. Yao L, Barontini M, Niederle B, Jech M, Pfragner R, Dahia PLM. Mutations of the Metabolic Genes IDH1, IDH2, and SDHAF2 Are Not Major Determinants of the Pseudohypoxic Phenotype of Sporadic Pheochromocytomas and Parangliomas. *J Clin Endocrinol Metab* (2010) 95:1469–72. doi: 10.1210/jc.2009-2245
62. Favier J, Brière J-J, Burnichon N, Rivière J, Vescovo L, Benit P, et al. The Warburg Effect Is Genetically Determined in Inherited Pheochromocytomas. *PLoS One* (2009) 4(9):e7094. doi: 10.1371/journal.pone.0007094
63. Vicha A, Taieb D, Pacak K. Current views on cell metabolism in SDHx-related pheochromocytoma and paraganglioma. *Endocr Relat Cancer* (2014) 21(3):R261–77. doi: 10.1530/ERC-13-0398
64. Neumann HP, de Herder W. Energy and metabolic alterations in predisposition to pheochromocytomas and paragangliomas: the so-called Warburg (and more) effect, 15 years on. *Endocr Relat Cancer* (2015) 22(4):E5–7. doi: 10.1530/ERC-15-0340
65. Lu J, Tan M, Cai Q. The Warburg effect in tumor progression: Mitochondrial oxidative metabolism as an anti-metastasis mechanism. *Cancer Lett* (2015) 356(2 Pt A):156–64. doi: 10.1016/j.canlet.2014.04.001
66. Grasso D, Zampieri LX, Capelôa T, Van de Velde JA, Sonveaux P. Mitochondria in cancer. *Cell Stress* (2020) 4(6):114–46. doi: 10.15698/cst2020.06.221
67. van Berkel A, Rao JU, Kusters B, Demir T, Visser E, Mensenkamp AR, et al. Correlation between in vivo 18F-FDG PET and immunohistochemical markers of glucose uptake and metabolism in pheochromocytoma and paraganglioma. *J Nucl Med* (2014) 55(8):1253–9. doi: 10.2967/jnumed.114.137034
68. van Berkel A, Vriens D, Visser EP, Janssen MJR, Gotthardt M, Hermus ARMM, et al. Metabolic Subtyping of Pheochromocytoma and Paranglioma by (18)F-FDG Pharmacokinetics Using Dynamic PET/CT Scanning. *J Nucl Med* (2019) 60(6):745–51. doi: 10.2967/jnumed.118.216796
69. Katoh Y, Katoh M. Hedgehog target genes: mechanisms of carcinogenesis induced by aberrant hedgehog signaling activation. *Curr Mol Med* (2009) 9(7):873–86. doi: 10.2174/156652409789105570
70. Wilson NH, Stoeckli ET. Sonic Hedgehog regulates Wnt activity during neural circuit formation. *Vitam Horm* (2012) 88:173–209. doi: 10.1016/B978-0-12-394622-5.00008-0
71. Kobayashi H, Kawauchi D, Hashimoto Y, Ogata T, Murakami F. The control of precerebellar neuron migration by RNA-binding protein Csd1. *Neuroscience* (2013) 253:292–303. doi: 10.1016/j.neuroscience.2013.08.055
72. Mihailovich M, Militti C, Gabaldon T, Gebauer F. Eukaryotic cold shock domain proteins: highly versatile regulators of gene expression. *Bioessays* (2010) 32:109–18. doi: 10.1002/bies.200900122
73. Dormoy-Raclet V, Markovits J, Malato Y, Huet S, Lagarde P, Montaudon D, et al. Unr. A cytoplasmic RNA-binding protein with cold-shock domains, is involved in control of apoptosis in ES and HuH7 cells. *Oncogene* (2007) 26:2595–605. doi: 10.1038/sj.onc.1210068
74. Elatmani H, Dormoy-Raclet V, Dubus P, Dautry F, Chazaud C, Jacquemin-Sablon H. The RNA-binding protein Unr prevents mouse embryonic stem cells differentiation toward the primitive endoderm lineage. *Stem Cells* (2011) 29:1504–16. doi: 10.1002/stem.712

75. Schuchardt A, D'Agati V, Larsson-Blomberg L, Costantini F, Pachnis V. The c-ret receptor tyrosine kinase gene is required for the development of the kidney and enteric nervous system. *Nature* (1994) 367:380–3. doi: 10.1038/367380a0
76. Asai N, Iwashita T, Matsuyama M, Takahashi M. Mechanism of activation of the ret proto-oncogene by multiple endocrine neoplasia 2A mutations. *Mol Cell Biol* (1995) 3:1613–9. doi: 10.1128/MCB.15.3.1613
77. Santoro M, Carlomagno F, Romano A, Bottaro DP, Dathan NA, Grieco M, et al. Activation of RET as a dominant transforming gene by germline mutations of MEN 2A. *Science* (1995) 267(5196):381–3. doi: 10.1126/science.7824936
78. Dahia PLM, Clifton-Bligh R, Gimenez-Roqueplo AP, Robledo M, Jimenez C. HEREDITARY ENDOCRINE TUMOURS: CURRENT STATE-OF-THE-ART AND RESEARCH OPPORTUNITIES. Metastatic pheochromocytomas and paragangliomas: proceedings of the MEN2019 workshop. *Endocr Relat Cancer* (2020) 27(8):T41–52. doi: 10.1530/ERC-19-0435
79. Thompson LDR. Pheochromocytoma of the Adrenal Gland Scaled Score (PASS) to Separate Benign From Malignant Neoplasms A Clinicopathologic and Immunophenotypic Study of 100 Cases. *Am J Surg Pathol* (2002) 26(5):551–66. doi: 10.1097/00000478-200205000-00002
80. Kimura N, Takayanagi R, Takizawa N, Itagaki E, Katabami T, Kakoi N, et al. Phaeochromocytoma Study Group in Japan. Pathological grading for predicting metastasis in phaeochromocytoma and paraganglioma. *Endocr Relat Cancer* (2014) 21(3):405–14. doi: 10.1530/ERC-13-0494
81. Wang Y, Li M, Deng H, Pang Y, Liu L, Guan X. The systems of metastatic potential prediction in pheochromocytoma and paraganglioma. *Am J Cancer Res* (2020) 10(3):769–80.
82. Koh J-M, Ahn SH, Kim H, Kim B-J, Sung T-Y, Kim YH, et al. Validation of pathological grading systems for predicting metastatic potential in pheochromocytoma and paraganglioma. *PLoS One* (2017) 12(11):e0187398. doi: 10.1371/journal.pone.0187398
83. Cho YY, Kwak MK, Lee SE, Ahn SH, Kim H, Suh S, et al. A clinical prediction model to estimate the metastatic potential of pheochromocytoma/paraganglioma: ASES score. *Surgery* (2018) 164(3):511–7. doi: 10.1016/j.surg.2018.05.001
84. Pierre C, Agopianz M, Brunaud L, Battaglia-Hsu S-F, Max A, Pouget C, et al. COPPS, a composite score integrating pathological features, PS100 and SDHB losses, predicts the risk of metastasis and progression-free survival in pheochromocytomas/paragangliomas. *Virch Arch* (2019) 474:721–34. doi: 10.1007/s00428-019-02553-5
85. Stenman A, Zedenius J, Juhlin CC. Over-diagnosis of potential malignant behavior in MEN 2A-associated pheochromocytomas using the PASS and GAPP algorithms. *Langenbecks Arch Surg* (2018) 403(6):785–90. doi: 10.1007/s00423-018-1679-9
86. Gao B, Meng F, Bian W, Chen J, Zhao H, Ma G, et al. Development and validation of pheochromocytoma of the adrenal gland scaled score for predicting malignant pheochromocytomas. *Urology* (2006) 68(2):282–6. doi: 10.1016/j.urol.2006.02.019
87. Kulkarni MM, Khandeparkar SG, Deshmukh SD, Karekar RR, Gaopande VL, Joshi AR, et al. Risk Stratification in Paragangliomas with PASS (Pheochromocytoma of the Adrenal Gland Scaled Score) and Immunohistochemical Markers. *J Clin Diagn Res* (2016) 10(9):EC01–4. doi: 10.7860/JCDR/2016/20565.8419
88. Wu D, Tischler AS, Lloyd RV, DeLellis RA, de Krijger R, van Nederveen F, et al. Observer variation in the application of the Pheochromocytoma of the Adrenal Gland Scaled Score. *Am J Surg Pathol* (2009) 33(4):599–608. doi: 10.1097/PAS.0b013e318190d12e
89. van Nederveen FH, Gaal J, Favier J, Korpershoek E, Oldenburg RA, de Bruyn EM, et al. An immunohistochemical procedure to detect patients with paraganglioma and pheochromocytoma with germline SDHB, SDHC, or SDHD gene mutations: a retrospective and prospective analysis. *Lancet Oncol* (2009) 10(8):764–71. doi: 10.1016/S1470-2045(09)70164-0
90. Castelblanco E, Santacana M, Valls J, Cubas A, Cascón A, Robledo M, et al. Usefulness of Negative and Weak-Diffuse Pattern of SDHB Immunostaining in Assessment of SDH Mutations in Paragangliomas and Pheochromocytomas. *Endocr Pathol* (2013) 24:199–205. doi: 10.1007/s12022-013-9269-4
91. Zhou YY, Coffey M, Mansur D, Wasman J, Asa SL, Couce M. Images in Endocrine Pathology: Progressive Loss of Sustentacular Cells in a Case of Recurrent Jugulotympanic Paraganglioma over a Span of 5 years. *Endocr Pathol* (2020) 31(3):310–4. doi: 10.1007/s12022-020-09632-3
92. Kimura N, Takekoshi K, Naruse M. Risk Stratification on Pheochromocytoma and Paraganglioma from Laboratory and Clinical Medicine. *J Clin Med* (2018) 7:242. doi: 10.3390/jcm7090242
93. Sue M, Martucci V, Frey F, Lenders JM, Timmers HJ, Peczkowska M, et al. Lack of utility of SDHB mutation testing in adrenergic metastatic pheochromocytoma. *Eur J Endocrinol* (2015) 172(2):89–95. doi: 10.1530/EJE-14-0756
94. Konosu-Fukaya S, Omata K, Tezuka Y, Ono Y, Aoyama Y, Satoh F, et al. Catecholamine-Synthesizing Enzymes in Pheochromocytoma and Extraadrenal Paraganglioma. *Endocr Pathol* (2018) 29(4):302–9. doi: 10.1007/s12022-018-9544-5
95. Deng L, Chen T, Xu H, Li Y, Deng M, Mo D, et al. The Expression of Snail, Galectin-3, and IGF1R in the Differential Diagnosis of Benign and Malignant Pheochromocytoma and Paraganglioma. *BioMed Res Int* (2020) 27:4150735. doi: 10.1155/2020/4150735
96. Leijon H, Remes S, Hagström J, Louhimo J, Mäenpää H, Schalin-Jäntti C, et al. Variable somatostatin receptor subtype expression in 151 primary pheochromocytomas and paragangliomas. *Hum Pathol* (2019) 86:66–75. doi: 10.1016/j.humpath.2018.11.020
97. Guo D, Zhao X, Wang A, Xie Q, Xu X, Sun J, Guo D, et al. PD-L1 expression and association with malignant behavior in pheochromocytomas/paragangliomas. *Hum Pathol* (2019) 86:155–62. doi: 10.1016/j.humpath.2018.10.041
98. Pinato DJ, Black JR, Trousil S, Dina RE, Trivedi P, Mauri FA, et al. Programmed cell death ligands expression in pheochromocytomas and paragangliomas: Relationship with the hypoxic response, immune evasion and malignant behavior. *Oncoimmunology* (2017) 6(11):e1358332. doi: 10.1080/2162402X.2017.1358332

Conflict of Interest: The authors declare that the research was conducted in the absence of any commercial or financial relationships that could be construed as a potential conflict of interest.

Copyright © 2020 Yamazaki, Gao, Pecori, Nakamura, Tezuka, Omata, Ono, Morimoto, Satoh and Sasano. This is an open-access article distributed under the terms of the Creative Commons Attribution License (CC BY). The use, distribution or reproduction in other forums is permitted, provided the original author(s) and the copyright owner(s) are credited and that the original publication in this journal is cited, in accordance with accepted academic practice. No use, distribution or reproduction is permitted which does not comply with these terms.



Histopathological Analysis of Tumor Microenvironment and Angiogenesis in Pheochromocytoma

Xin Gao¹, Yuto Yamazaki¹, Alessio Pecori¹, Yuta Tezuka^{2,3}, Yoshikiyo Ono³, Kei Omata^{2,3}, Ryo Morimoto³, Yasuhiro Nakamura⁴, Fumitoshi Satoh^{2,3} and Hironobu Sasano^{1*}

¹ Department of Pathology, Tohoku University Graduate School of Medicine, Sendai, Japan, ² Division of Clinical Hypertension, Endocrinology and Metabolism, Tohoku University Graduate School of Medicine, Sendai, Japan, ³ Division of Nephrology, Endocrinology, and Vascular Medicine, Tohoku University Hospital, Sendai, Japan, ⁴ Division of Pathology, Faculty of Medicine, Tohoku Medical and Pharmaceutical University, Sendai, Japan

OPEN ACCESS

Edited by:

Ichiro Abe,
Fukuoka University Chikushi Hospital,
Japan

Reviewed by:

Michio Otsuki,
Osaka University Hospital, Japan
Wataru Kameda,
Yamagata University, Japan

*Correspondence:

Hironobu Sasano
hsasano@pathol2.med.tohoku.ac.jp

Specialty section:

This article was submitted to
Neuroendocrine Science,
a section of the journal
Frontiers in Endocrinology

Received: 27 July 2020

Accepted: 09 October 2020

Published: 10 November 2020

Citation:

Gao X, Yamazaki Y, Pecori A, Tezuka Y, Ono Y, Omata K, Morimoto R, Nakamura Y, Satoh F and Sasano H (2020) Histopathological Analysis of Tumor Microenvironment and Angiogenesis in Pheochromocytoma. *Front. Endocrinol.* 11:587779. doi: 10.3389/fendo.2020.587779

Pheochromocytomas (PHEOs) are relatively rare catecholamine-producing tumors derived from adrenal medulla. Tumor microenvironment (TME) including neoangiogenesis has been explored in many human neoplasms but not necessarily in PHEOs. Therefore, in this study, we examined tumor infiltrating lymphocytes (CD4 and CD8), tumor associated macrophages (CD68 and CD163), sustentacular cells (S100p), and angiogenic markers (CD31 and areas of intratumoral hemorrhage) in 39 cases of PHEOs in the quantitative fashion. We then compared the results with pheochromocytoma of the adrenal gland scaled score (PASS), grading system for pheochromocytoma and paraganglioma (GAPP) and the status of intra-tumoral catecholamine-synthesizing enzymes (TH, DDC, and PNMT) as well as their clinicopathological factors. Intratumoral CD8 ($p = 0.0256$), CD31 ($p = 0.0400$), and PNMT ($p = 0.0498$) status was significantly higher in PHEOs with PASS <4 than PASS ≥ 4 . In addition, intratumoral CD8⁺ lymphocytes were also significantly more abundant in well-than moderately differentiated PHEO according to GAPP score ($p = 0.0108$) and inversely correlated with tumor size ($p = 0.0257$). Intratumoral CD68⁺ cells were significantly higher in PHEOs with regular or normal histological patterns than those not ($p = 0.0370$) and inversely correlated with tumor size ($p = 0.0457$). The status of CD163 was significantly positively correlated with that of CD8 positive cells ($p = 0.0032$). The proportion of intratumoral hemorrhage areas was significantly higher in PHEOs with PASS ≥ 4 ($p = 0.0172$). DDC immunoreactivity in tumor cells was significantly positively correlated with PASS score ($p = 0.0356$) and TH status was significantly higher in PHEOs harboring normal histological patterns ($p = 0.0236$) and cellular monotony ($p = 0.0219$) than those not. Results of our present study did demonstrate that abundant CD8⁺ and CD68⁺ cells could represent a histologically low-scored tumor. In particular, PHEOs with increased intratumoral hemorrhage should be considered rather malignant. In addition, abnormal catecholamine-producing status of tumor cells such as deficient PNMT and TH and increased DDC could also represent more aggressive PHEOs.

Keywords: pheochromocytoma, pathology, immunohistochemistry, tumor microenvironment, angiogenesis

INTRODUCTION

Pheochromocytomas (PHEOs) and paragangliomas (PGLs) are relatively rare tumors originating from the adrenal medulla at proximately 2 to 9.1 per 1 million adults frequently associated with cardiovascular complications due to excessive catecholamine production (1–3). The difference between PHEOs and PGLs depends on the primary sites, *i.e.*, intra- or extra-adrenal glands (4), and the former one termed as PHEOs (5). It is generally extremely difficult to differentiate benign from malignant PHEOs based upon clinical or even histopathological findings, and all PHEOs are currently considered potentially malignant tumor in the WHO 2017 classification (6). However, toward establishing more accurate histopathological diagnosis of PHEOs, Thompson et al., proposed a novel scoring system for the patients with PHEOs, *i.e.*, PASS (pheochromocytoma of the adrenal gland scaled score) system, composed of twelve different histological features (7). This system has been frequently used for discerning malignancy in PHEOs, and PASS of ≥ 4 was proposed to be malignant or biologically more aggressive than those with PASS < 4 (7). However, it is also true that there have been controversies regarding the application of this system into the differential diagnosis between benign and malignant PHEOs including its reproducibility (7). Kimura et al. subsequently proposed another system to assess malignant potential of PHEOs, *i.e.*, GAPP (grading system for pheochromocytoma and paraganglioma) (8). This system used both histological and clinical parameters including histological patterns, cellularity, comedo-type necrosis, capsular/vascular invasion, proliferative index (Ki-67) and catecholamine type. According to the GAPP system, PHEOs were subclassified into well-differentiated (WD), moderately differentiated (MD), or poorly differentiated tumor (PD), and this classification has been then used widely.

The tumor microenvironment (TME) has been reported to play pivotal roles in many human malignancies in tumorigenesis, progression, and metastasis and recently also explored as therapeutic targets (9). Histopathologically, TME is well known to be composed of a number of cellular components including inflammatory cells, blood vessels, fibroblasts, and others (10, 11). Of those components above, both T lymphocytes and macrophages have been generally considered to play pivotal roles in biological features of the patients (12, 13). In benign adrenocortical tumors, we previously demonstrated that cortisol-producing adenomas harbored higher immune cell infiltration and angiogenic markers than other hormone-producing adenomas (14). In adrenocortical carcinomas, tumor infiltrating T cells were also reported to be correlated with better overall survival (15). However, little has been known on TME in PHEOs at this juncture even in contrast to adrenocortical neoplasms above, although aggressive PHEOs were reported to harbor lower number of S100 positive sustentacular cells and increased angiogenesis (16–18). Therefore, in this study, we explored various TME relevant markers (CD4, CD8, CD68, CD163, and S100p), angiogenic markers (CD31, intratumoral hemorrhage area) and catecholamine-synthesizing enzymes (TH, DDC, and PNMT) of the tumors and compared the results with GAPP and PASS scoring systems, other clinicopathological factors of individual cases of 39 PHEOs in order to explore the possible

correlation between the status of catecholamine production and TME and angiogenesis.

MATERIALS AND METHODS

Pheochromocytoma Cases

We studied 39 adrenal PHEO patients operated at Tohoku University Hospital, Sendai, Japan from 2012 to 2019. Following the evaluation of 24 h urinary levels of metanephrine and normetanephrine, the diagnosis of PHEO was confirmed by their increased levels of at least three times than the normal range (2). We also applied PASS and GAPP in their histological diagnosis. Clinicopathological features of these patients examined were summarized in **Table 1**. Clinical information is not available due to the relatively new cases. Two patients experienced recurrence and one of them died. The present research protocol was approved by the Institutional Review Board (IRB) of Tohoku University School of Medicine (2018-1-669).

Immunohistochemistry and Its Evaluation

Hematoxylin and eosin (H&E) staining and immunohistochemistry (IHC) were both performed in the specimens fixed in 10% buffered formalin and embedded in paraffin. The protocols for individual IHC markers used in our present study were summarized in **Table 2**. All the H&E and IHC sections were digitally scanned by Image Scope AT2 (Leica, Wetzlar, Germany). Nuclear immunoreactivity of CD4, CD8, CD68, CD163, and S100p were all evaluated by the percentage of positive cells in tumoral parenchyma by manual analysis (19–22). Ki-67 labeling index was evaluated after identifying hot spot of the whole tumor (23). Microvascular density (MVD) was evaluated by counting the number of CD31-positive vessels within 0.75 mm² and highest expressed tumor area (24). Immunoreactivity of catecholamine-synthesizing enzymes including tyrosine hydroxylase (TH), dopa-decarboxylase (DDC), and phenolamine-N-methyltransferase (PNMT) was all digitally and quantitatively evaluated by using “HALO™ CytoNuclear ver.1.5” (Indica Laboratories, Corrales, NM, USA) image analysis (25, 26). The positive cells were tentatively classified into the

TABLE 1 | Clinicopathological factors in PHEO patients.

Clinical factors	Average (range)
Age (years)	56 (39–79)
Gender: Female/Gender	25/14
BMI (kg/m ²)	22.7 (15.48–31.49)
Tumor size (mm)	45.3 (20–100)
Tumor location: left/right	24/15
Duration of hypertension (years)	9.3 (0–25)
Plasma AD (ng/ml)	0.16 (0.01–0.742)
Plasma NAD (ng/ml)	1.8 (0.1–12)
24-h urine MN (mg/day)	1.7 (0.01–11)
24-h urine NMN (mg/day)	4.1 (0.01–26)
24-h urine AD (μg/day)	115.7 (1.9–510)
24-h urine NAD (μg/day)	775.9 (42.6–4200)

Gender and tumor location were described as the number of persons.

AD, adrenaline; NAD, noradrenaline; DA, dopamine; MN, metanephrine; NMN, normetanephrine; BMI, body mass index.

Normal range reference: plasma AD: 0–0.17 ng/ml; plasma NAD, 0.15–0.57 ng/ml; 24-h urine adrenaline, 1.1–22.5 mcg/day; 24-h urine noradrenaline, 29.2–118.0 mcg/day; 24-h urine metanephrine, 0.05–0.20 mg/day; 24-h urine normetanephrine, 0.10–0.28 mg/day.

TABLE 2 | IHC protocols.

Antibody	Host	Clone	Dilution	Antigen retrieval	Source
CD4	Rabbit	EPR6855	1:400	AC	Abcam
CD8	Mouse	M7103	1:50	AC	Dako
CD68	Mouse	M0876	1:100	Trypsin	Dako
CD163	Mouse	M3527	1:600	AC	Dako
S100p	Rabbit	—	1:9,000	—	Dako
CD31	Mouse	M0823	1:100	AC	Dako
Ki67	Mouse	M7240	1:100	AC	Dako
TH	Mouse	T1299	1:2,000	MW	Sigma
DDC	Rabbit	AB136	1:500	—	Millipore
PNMT	Mouse	Ab119784	1:2,000	—	Abcam

AC, autoclave 121°C 5 min, pH = 6 buffer; MW, microwave 500 W 20 min, pH = 6 buffer.

following four categories based on the levels of their relative immunointensity: negative as “0”, weak as “+1”, moderate as “+2”, and strong as “+3”. H-score was subsequently calculated based on the following formula; Σ (Number of the individual gradients of the positive cells X Score 1+, 2+, 3+)/Total cells) X100 (27–29). The evaluation of intratumoral hemorrhage area was also performed by using HALO software above according to the classifier system on H&E stained tissue sections (25). Under this system, tumor areas were tentatively classified into two portions: tumor and intratumoral hemorrhage areas (**Figure 1**). Hemorrhage in the central vein and ubiquitous necrosis were both carefully

excluded in this analysis. The final value of intratumoral hemorrhage was the ratio of intratumoral hemorrhage against the whole tumor area.

Statistical Analysis

We analyzed the correlations among TME relevant markers, angiogenic markers, catecholamine-synthesizing enzymes, histopathological score, and clinicopathological factors by *Spearman's test*. The differences of TME relevant markers, angiogenic markers, and catecholamine-synthesizing enzymes in individual PASS and GAPP factors were all analyzed using *Mann–Whitney's test*. We defined the significance as P-value <0.05. All the tests were analyzed using the software “JMP Pro ver. 14.0.0”.

RESULTS

Comparison of PHEOs Between PASS ≥ 4 and PASS <4

Representative images were illustrated in **Figure 2**. Results were summarized in **Figure 3**. CD31-positive vessels ($p = 0.0400$), CD8 positive cells ($p = 0.0256$), S100p positive cells ($p = 0.0353$), and PNMT immunoreactivity ($p = 0.0498$) were all significantly higher in PHEOs with PASS <4 than those with PASS ≥ 4 . The

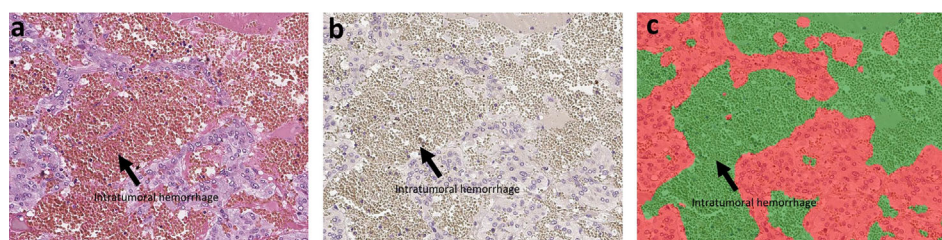


FIGURE 1 | The analysis of intratumoral hemorrhage area. H&E stained section and hematoxylin-stained section are present in (A, B). There were several intratumoral hemorrhage areas with gray color in (B). Because the hemorrhage is composed of red blood cells that did not have a nucleus, it cannot be stained by hematoxylin. We used classifier system in HALO software to recognize the normal tumor area (blue) and the intratumoral hemorrhage area (gray). After analysis, the software can divide the tissue into two colors: red for tumor and green for hemorrhage (C). Finally, we can calculate the ratio of intratumoral hemorrhage area against the whole tumor area.

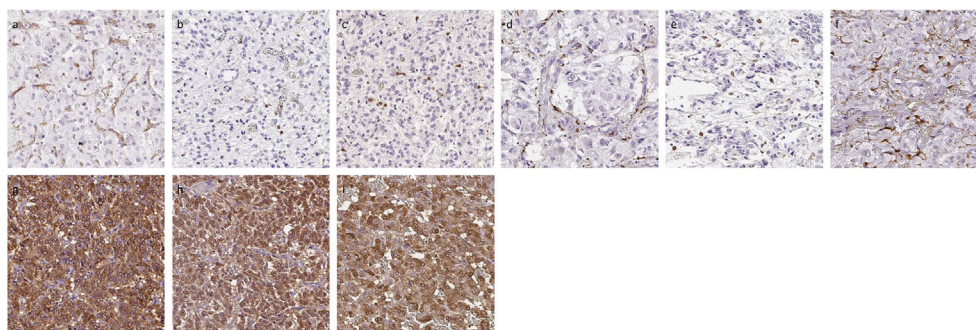


FIGURE 2 | Representative IHC images of PHEOs. (A) CD31, (B) CD4, (C) CD8, (D) CD68, (E) CD163, (F) S100p, (G) TH, (H) DDC, (I) PNMT.

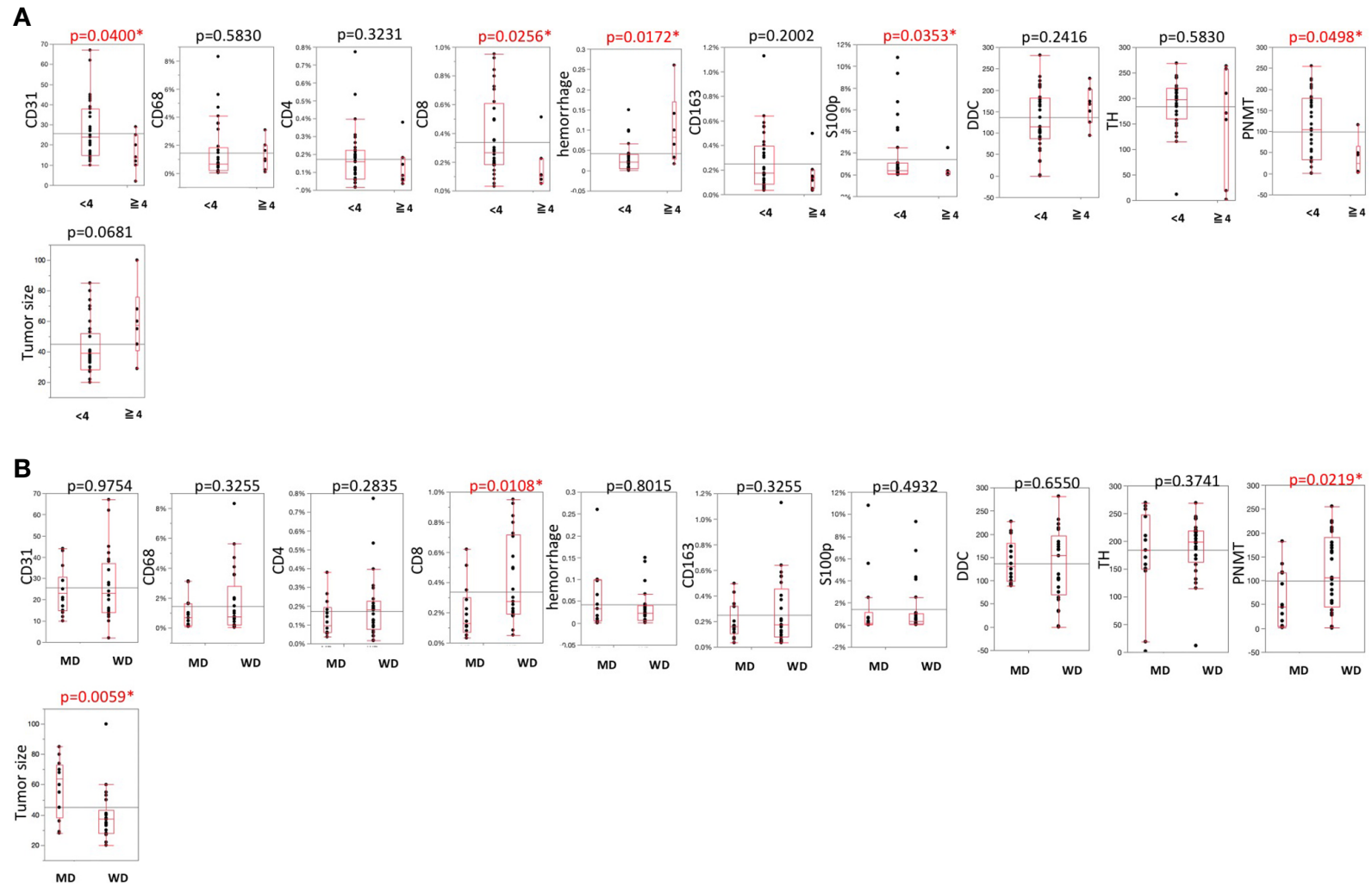


FIGURE 3 | (A) Comparisons of TME-relevant markers, angiogenic marker, and catecholamine-synthesizing enzymes between PASS <4 and PASS \geq 4. **(B)** Comparisons of TME-relevant markers, angiogenic marker, and catecholamine-synthesizing enzymes between WD and MD according to the GAPP system. All of the comparisons are presented **Figure 3**. P value was on the head of each factor.

ratio of intratumoral hemorrhage was significantly higher in PHEOs with PASS ≥ 4 than PASS < 4 ($p = 0.0172$).

Comparison Between Well and Moderately Differentiated PHEOs According to GAPP Analysis

Analysis based on GAPP scores revealed as follows: 26 well-differentiated (WD), 13 moderately differentiated, and no poorly differentiated PHEOs (Figure 3). Both PNMT immunoreactivity ($p = 0.0219$) and CD8 positive cells ($p = 0.0108$) were significantly higher in WD- than MD-PHEOs. Tumor size was significantly smaller in WD- than MD-PHEOs ($p = 0.0059$). No other significant correlations were detected.

Comparison of TME, Angiogenesis, and Catecholamine-Synthesizing Enzymes With Results of PASS and GAPP Factors in Individual PHEOs

The histopathological factors of PASS and GAPP scoring systems were summarized in Table 3. Among individual factors of the PASS systems, the following were the numbers of positive individual cases per each factor: large nests of cells or diffuse growth in 10% of tumor: six; necrosis: three; high cellularity: four; cellular monotony: two; presence of spindle shaped tumor cells: two; increased mitotic figure (> 3 per 10 high power fields): zero; atypical mitosis: one; extension of tumor into adjacent fat: three; vascular invasion: 13; capsular invasion: five cases; profound nuclear pleomorphism: five; nuclear hyperchromasia: three (Supplemental File 1).

Among the six GAPP factors examined in 39 PHEOs in our present study, 13 demonstrated abnormal histological features, 11 low cellularity ($< 150/\text{HPF}$), 19 moderate cellularity ($150\text{--}250/\text{HPF}$) and nine high cellularity ($> 250/\text{HPF}$), one comedo-necrosis, 13 capsule or vascular invasion, 26 low Ki-67 LI ($< 1\%$), nine moderate Ki-67 LI ($1\text{--}3\%$) and four high Ki-67 LI ($> 3\%$), 10 norepinephrine predominant secretion (Supplemental File 2). CD68 positive cells were significantly higher in PHEOs with normal histological patterns than those with abnormal patterns ($p = 0.0370$). DDC in tumor cells was significantly more abundant in PHEOs with capsule or vascular invasion than those without ($p = 0.0172$). TH in tumor cells was significantly more abundant in PHEOs with normal histological patterns than PHEOs with abnormal patterns ($p = 0.0236$).

Correlations Among TME Relevant Markers, Angiogenic Markers, and Catecholamine-Synthesizing Enzymes

Results were summarized in Table 4. CD163 positive cells were significantly positively correlated with CD4 ($p = 0.0405$) and CD8 ($p = 0.0032$) positive cells in the tumor. The ratio of intratumoral hemorrhage areas was inversely correlated with CD31-positive vessels ($p = 0.0785$). CD8 positive cells were significantly inversely correlated with GAPP score ($p = 0.0018$). CD68 positive cells were positively correlated with TH ($p = 0.0901$) and DDC ($p = 0.0168$) immunoreactivity in tumor cells. S100p positive cells were significantly inversely correlated with PASS ($p = 0.0205$) and GAPP ($p = 0.0217$) scores. Hemorrhage score was significantly positively correlated with PASS score ($p = 0.0059$). DDC was positively correlated with

TABLE 3 | PASS and GAPP systems.

PASS factors	Score
Large nests or diffuse growth ($> 10\%$ of tumor volume)	2
Necrosis	2
High cellularity	2
Cellular monotony	2
Presence of spindle-shaped tumor cells	2
Atypical mitotic figures	2
Greater than 3 mitotic figures	2
Extension of tumor into adjacent fat	2
Vascular invasion	1
Capsular invasion	1
Profound nuclear pleomorphism	1
Nuclear hyperchromasia	1
Total	20
GAPP factors	Score
Histological pattern:	
Zellballen	0
Large and irregular cell nest	1
Pseudorosette	1
Cellularity:	
Low (< 150 cells/U)	0
Moderate ($150\text{--}250$ cells/U)	1
High (> 250 cells/U)	2
Comedo necrosis:	
Absence	0
Presence	2
Vascular or capsular invasion:	
Absence	0
Presence	1
Ki-67 labeling index:	
$< 1\%$	0
$1\text{--}3\%$	1
$> 3\%$	2
Catecholamine type:	
Epinephrine type (E or E + NE)	0
Norepinephrine type (NE or NE + AD)	1
Non-functioning type	0
Total maximum score	10

U, number of tumor cells under $\times 400$ magnification; E, epinephrine; NE, norepinephrine.

PASS score ($p = 0.0365$) but PNMT was inversely significantly correlated with PASS ($p = 0.0632$) and GAPP score ($p = 0.0003$).

Correlations of TME Relevant Markers, Angiogenic Markers With Clinicopathological Factors in PHEOs

The correlations among TME relevant markers, angiogenic markers and catecholamine-synthesizing enzymes and clinicopathological factors were summarized in Table 5.

TABLE 4 | Correlations among TME-relevant, angiogenetic markers, and catecholamine-synthesizing enzymes.

	CD31	CD4	CD8	CD68	CD163	S100	Ki-67	TH	DDC	PNMT	PASS score	GAPP score
CD31								$\rho = 0.0013$ $\rho = 0.9938$	$\rho = -0.0277$ $\rho = 0.8688$	$\rho = -0.0737$ $\rho = 0.6647$	$\rho = -0.1980$ $\rho = 0.2333$	$\rho = -0.0119$ $\rho = 0.9436$
CD4	$\rho = 0.1069$ $\rho = 0.5230$							$\rho = -0.1340$ $\rho = 0.4160$	$\rho = -0.1138$ $\rho = 0.4905$	$\rho = 0.2804$ $\rho = 0.0881$	$\rho = -0.1894$ $\rho = 0.2482$	$\rho = -0.1110$ $\rho = 0.5013$
CD8	$\rho = -0.0650$ $\rho = 0.6982$	$\rho = 0.0395$ $\rho = 0.8114$						$\rho = -0.0312$ $\rho = 0.8505$	$\rho = -0.1795$ $\rho = 0.2743$	$\rho = 0.1672$ $\rho = 0.3156$	$\rho = -0.1714$ $\rho = 0.2969$	$\rho = -0.4839$ $\rho = 0.0018^*$
CD68	$\rho = -0.0629$ $\rho = 0.7077$	$\rho = 0.0759$ $\rho = 0.6460$	$\rho = 0.1822$ $\rho = 0.2669$					$\rho = 0.2751$ $\rho = 0.0901$	$\rho = 0.3806$ $\rho = 0.0168^*$	$\rho = 0.2041$ $\rho = 0.2191$	$\rho = 0.0612$ $\rho = 0.7113$	$\rho = -0.1848$ $\rho = 0.2600$
CD163	$\rho = 0.0460$ $\rho = 0.7839$	$\rho = 0.3296$ $\rho = 0.0405^*$	$\rho = 0.4604$ $\rho = 0.0032^*$	$\rho = -0.0200$ $\rho = 0.9036$				$\rho = 0.0435$ $\rho = 0.7925$	$\rho = 0.0022$ $\rho = 0.9893$	$\rho = 0.0058$ $\rho = 0.9724$	$\rho = -0.1593$ $\rho = 0.3327$	$\rho = -0.1668$ $\rho = 0.3103$
S100p	$\rho = 0.1404$ $\rho = 0.4005$	$\rho = 0.2008$ $\rho = 0.2203$	$\rho = 0.2642$ $\rho = 0.1041$	$\rho = 0.0277$ $\rho = 0.8669$	$\rho = 0.1054$ $\rho = 0.5232$			$\rho = -0.0108$ $\rho = 0.9478$	$\rho = -0.0420$ $\rho = 0.7996$	$\rho = 0.2185$ $\rho = 0.1875$	$\rho = -0.3699$ $\rho = 0.0205^*$	$\rho = -0.3665$ $\rho = 0.0217^*$
Ki-67	$\rho = -0.0841$ $\rho = 0.6206$	$\rho = 0.1014$ $\rho = 0.5445$	$\rho = 0.0039$ $\rho = 0.9813$	$\rho = 0.0863$ $\rho = 0.6063$	$\rho = 0.1623$ $\rho = 0.3304$	$\rho = -0.2206$ $\rho = 0.1832$		$\rho = 0.1977$ $\rho = 0.2341$	$\rho = -0.0012$ $\rho = 0.9943$	$\rho = 0.0028$ $\rho = 0.9867$	$\rho = 0.2319$ $\rho = 0.1612$	$\rho = 0.2909$ $\rho = 0.0764$
Hemorrhage	$\rho = -0.2955$ $\rho = 0.0758$	$\rho = -0.1605$ $\rho = 0.3358$	$\rho = 0.0630$ $\rho = 0.7070$	$\rho = 0.0667$ $\rho = 0.6909$	$\rho = 0.0454$ $\rho = 0.7865$	$\rho = -0.1501$ $\rho = 0.3684$	$\rho = -0.1555$ $\rho = 0.3581$	$\rho = 0.0055$ $\rho = 0.9740$	$\rho = 0.1228$ $\rho = 0.4625$	$\rho = -0.0125$ $\rho = 0.9417$	$\rho = 0.4385$ $\rho = 0.0059^*$	$\rho = 0.0575$ $\rho = 0.7317$
PASS score								$\rho = -0.1492$ $\rho = 0.3648$	$\rho = 0.3376$ $\rho = 0.0356^*$	$\rho = -0.3044$ $\rho = 0.0632$		
GAPP score								$\rho = -0.1598$ $\rho = 0.3313$	$\rho = 0.1808$ $\rho = 0.2708$	$\rho = -0.5580$ $\rho = 0.0003^*$		

* $p < 0.05$.

TABLE 5 | Correlations among TME-relevant markers, plasma, and urine catecholamines and clinicopathological factors.

	Plasma AD	Plasma NAD	Urine AD	Urine NAD	Tumor size
CD31	$\rho = 0.0415$	$\rho = 0.1527$	$\rho = -0.0875$	$\rho = 0.1179$	$\rho = -0.0226$
	$\rho = 0.8075$	$\rho = 0.3668$	$\rho = 0.6119$	$\rho = 0.4935$	$\rho = 0.8957$
CD4	$\rho = -0.0677$	$\rho = -0.0748$	$\rho = 0.0937$	$\rho = 0.0254$	$\rho = -0.0235$
	$\rho = 0.6863$	$\rho = 0.6556$	$\rho = 0.5814$	$\rho = 0.8815$	$\rho = 0.8901$
CD8	$\rho = 0.3175$	$\rho = -0.0718$	$\rho = 0.2197$	$\rho = -0.1190$	$\rho = -0.3665$
	$\rho = 0.0521$	$\rho = 0.6683$	$\rho = 0.1914$	$\rho = 0.4829$	$\rho = 0.0257^*$
CD68	$\rho = 0.2738$	$\rho = 0.1993$	$\rho = 0.1496$	$\rho = -0.1107$	$\rho = -0.3305$
	$\rho = 0.0962$	$\rho = 0.2303$	$\rho = 0.3768$	$\rho = 0.5142$	$\rho = 0.0457^*$
CD163	$\rho = 0.0359$	$\rho = 0.0638$	$\rho = -0.0211$	$\rho = 0.0318$	$\rho = 0.0638$
	$\rho = 0.8304$	$\rho = 0.7035$	$\rho = 0.9013$	$\rho = 0.8519$	$\rho = 0.7077$
S100p	$\rho = 0.0141$	$\rho = 0.0464$	$\rho = 0.0598$	$\rho = 0.0537$	$\rho = -0.4676$
	$\rho = 0.9331$	$\rho = 0.7820$	$\rho = 0.7254$	$\rho = 0.7523$	$\rho = 0.0035^*$
Ki-67	$\rho = -0.0145$	$\rho = -0.1544$	$\rho = 0.0049$	$\rho = -0.2530$	$\rho = -0.0181$
	$\rho = 0.9322$	$\rho = 0.3616$	$\rho = 0.9774$	$\rho = 0.1365$	$\rho = 0.9168$
Hemorrhage	$\rho = 0.0425$	$\rho = -0.2718$	$\rho = 0.0644$	$\rho = -0.2752$	$\rho = 0.0595$
	$\rho = 0.8028$	$\rho = 0.1037$	$\rho = 0.7091$	$\rho = 0.1043$	$\rho = 0.7301$
TH	$\rho = -0.0956$	$\rho = 0.1085$	$\rho = -0.2388$	$\rho = -0.1183$	$\rho = -0.3171$
	$\rho = 0.5679$	$\rho = 0.5169$	$\rho = 0.1547$	$\rho = 0.4856$	$\rho = 0.0558$
DDC	$\rho = -0.1402$	$\rho = 0.1288$	$\rho = -0.1721$	$\rho = 0.0782$	$\rho = -0.1125$
	$\rho = 0.4010$	$\rho = 0.4408$	$\rho = 0.3083$	$\rho = 0.6453$	$\rho = 0.5075$
PNMT	$\rho = 0.2564$	$\rho = -0.2727$	$\rho = 0.3052$	$\rho = -0.3586$	$\rho = -0.5290$
	$\rho = 0.1256$	$\rho = 0.1025$	$\rho = 0.0703$	$\rho = 0.0318^*$	$\rho = 0.0009^*$
PASS score	$\rho = -0.0269$	$\rho = -0.1252$	$\rho = -0.0056$	$\rho = -0.1274$	$\rho = 0.2961$
	$\rho = 0.8726$	$\rho = 0.4539$	$\rho = 0.9739$	$\rho = 0.4523$	$\rho = 0.0710$
GAPP score	$\rho = -0.3787$	$\rho = 0.0396$	$\rho = -0.3115$	$\rho = 0.0977$	$\rho = 0.5316$
	$\rho = 0.0191^*$	$\rho = 0.8136$	$\rho = 0.0605$	$\rho = 0.5653$	$\rho = 0.0006^*$

* $p < 0.05$.

Plasma adrenaline levels were significantly positively correlated with CD8 ($p = 0.0521$) and CD68 ($p = 0.0962$) positive cells and significantly inversely correlated with GAPP score ($p = 0.0191$). Urinary AD was inversely correlated with GAPP score ($p = 0.0605$). PNMT expression was significantly inversely correlated with urinary NAD ($p = 0.0318$). Tumor size was significantly inversely correlate with CD8 ($p = 0.0257$), CD68 ($p = 0.0457$), S100 ($p = 0.0035$), PNMT ($p = 0.0009$) and positively correlated with PASS ($p = 0.0710$) and GAPP score ($p = 0.0006$).

DISCUSSION

TME including tumor infiltrating lymphocytes (TILs), tumor-associated macrophages (TAMs) as well as angiogenesis has all been reported to play pivotal roles in not only clinical but also therapeutic outcomes in various human malignancies. However, TME and other relevant phenomena have not necessarily been well studied in adrenal medullary tumor including PHEOs although decreased S100 was detected in benign PHEOs (17, 18, 30). In our present study, we did compare the status of S100 positive cells with results of PASS analysis and obtained similar findings reported above (7). Both PASS and GAPP scoring systems have been used relatively widely for surgical pathologists to evaluate the malignant potential of the patients with PHEOs. PASS score could be obtained only from routinely available histopathological findings and tumor with PASS of four or more than four score was considered malignant (7). However,

relatively marked inter- and intra-observer variations have been reported in application of PASS scoring system (31). Therefore, we also employed GAPP system as well, which included not only morphological features but also catecholamine secretory phenotypes and Ki-67 labeling index (8), in order to further explore the malignant potential of PHEOs in a more precise fashion (32).

In this study, we firstly evaluated the details of TILs. The status of CD8⁺ TILs has been generally reported to be correlated with better prognosis (33–35). Our results did demonstrate that CD8⁺ TILs could play pivotal roles in possible biological behavior of PHEOs and its abundance could also represent relatively benign tumors as reported in other human malignancies (33–35). However, it awaits further investigations for clarification.

Dendritic cells activated anti-tumor CD8⁺ T lymphocytes (CTLs) by presenting tumor antigen and then effector CTLs executed its roles of eliminating tumor cells (36). CTLs can induce an apoptosis of tumor cell by FasL pathway and can also release some cytokines to induce cytotoxicity in tumor cells (37). In our present study, we demonstrated an inverse correlation between CTLs and tumor size, which indicated that CTLs could suppress the expansion of tumor. However, CTLs were also suppressed in malignant PHEOs possibly by excessive catecholamine derived from tumor cells, themselves (38). Catecholamine was reported to suppress T lymphocyte such as T-helper 1/2, cytotoxic CD8⁺T-lymphocytes and NK cells (39–41). Both epinephrine and norepinephrine were also reported to

exert inhibitory effects on T-cell proliferation due to chronic mild stress in mice (42). Therefore, results of our present study also indicated that CTLs could be suppressed by excessive catecholamine produced by malignant PHEOs. In addition, in our present study, CD68⁺ cells were significantly higher in PHEOs with normal histological patterns and negatively correlated with tumor size. Intratumoral CD163 positive cells were significantly positively correlated with the status of intratumoral CD4 and CD8 infiltrating cells. Macrophages constituted the great majority of cellular components in tumor stroma with noticeable plasticity and could be further subclassified into M1 and M2 phenotypes (37). M1 macrophages were classically defined as activated macrophages and reported to play pro-inflammation roles resulting in overall antitumor effects (37, 43, 44). On the other hand, M2 macrophages were reported to have opposite roles toward M1 macrophages resulting in pro-tumor effects (37, 44, 45). In addition, the differentiation to M1 or M2 macrophages was reported to be dependent on cytokines (44). For instance, differentiation to M1 macrophages could be induced by IFN- γ , TNF- α , IL-8, and IL-12 secreted from CTLs. M2 macrophages were reported to be induced by STAT3, IL4, and IL-10 and to subsequently suppress T cell function. In addition, M2 macrophages were the representative subtypes of macrophages in TME of most human malignancies including breast, urinary bladder, and prostate carcinoma (46, 47). Results of our present study did demonstrate that TAMs in PHEOs could be predominantly reprogrammed into CD68⁺M1 rather than CD163⁺M2 macrophages, which exerted potential anti-tumoral effects by secreting different cytokines (44, 48). However further investigations are required to clarify the details.

Recently, TILs have been also reported to be associated with overall survival and recurrence-free survival of the patients with adrenocortical carcinomas (ACCs). However, of particular interest, the difference between ACCs and PHEOs was that not only CD8⁺ but also CD4⁺ T lymphocytes were related to relatively better clinical outcome in the patients with ACCs (15). CD4⁺ T cells are helper T cells, stimulating CTLs activities (37). In addition, ACCs were also relatively frequently detected in childhood and increased TILs were reported in those young ACCs patients than adults (49). The most notable difference between ACCs and PHEOs was considered the effects of different hormones on TILs. The great majority of PHEOs were characterized by catecholamine excess, which could suppress T-cell activity. On the other hand, ACC was characterized by the excessive steroids including relatively abundant precursor steroids and steroid hormones could in general hamper anti-tumor roles of T-cells (50–53). Therefore, tumor microenvironment could be influenced by those hormones secreted by tumor cells, but it awaits further investigations for clarification.

Angiogenesis is indispensable and pivotal for tumor growth, invasion and metastasis (54). Hypoxia has been reported one of the most pivotal causes of angiogenesis in PHEOs (55). Increased endothelial growth factor (VEGF) has been reported in

malignant PHEOs and to be associated with hypoxia inducible factor (HIF) (56–59). PHEOs have been well known to be associated with increased angiogenesis due to pseudohypoxic signaling pathway (60). Among the factors involved in this pathway, *SDHXs* were the most susceptible genes (60). Pseudohypoxic subtype has been also reported to be associated with aggressive biological behavior (60). The pathophysiological features of this particular phenotype could therefore promote the neoplastic angiogenesis. In our present study, intratumoral hemorrhage was abundantly detected in histologically high-graded tumors, which could also result in relatively low CD31 status in histologically low-graded tumors. However, genetic testing was not performed as a routine in our institution and this could also represent the limitation of our present study.

In general, norepinephrine-producing PHEOs were reported to accompany PNMT deficiency which is considered to be less differentiated than epinephrine-producing PHEOs (7, 17). Dopamine-secreting PHEOs were also considered less differentiated or immature and had a high prevalence of malignancy (59, 60). Results of our present study were also consistent with those findings above. The absence of TH in some PHEOs in our present study could not only result in non-functional nature of the tumors but also in increased aggressive biological behavior (61, 62). Therefore, the abnormal elevation of plasma dopamine or the absence of TH immunoreactivity in PHEOs could indicate more aggressive biological behavior of the tumor.

It is true that there are several limitations in our present study. The number of the cases examined was relatively small. In addition, the cases examined were relatively new cases which could make it difficult to obtain the long-term clinical outcome of the patients. Genetic testing was not performed routinely in our hospital. Therefore, those above were considered limitations of this study. Further investigations are also required to clarify the detailed mechanisms of interaction between TME and tumor cells in PHEOs.

In summary, we firstly presented detailed features of TILs and TAMs in PHEOs. CD8 and CD68 could also serve as biomarkers of well-differentiated or histologically low-scored PHEOs. Benign PHEOs harbored smaller sized tumor than malignant ones, also related both TILs and TAMs. Poorly differentiated PHEOs had increased incidence of intratumoral hemorrhage and the absence of TH in tumor cells.

DATA AVAILABILITY STATEMENT

The raw data supporting the conclusions of this article will be made available by the authors, without undue reservation.

ETHICS STATEMENT

The studies involving human participants were reviewed and approved by the Institutional Review Board of Tohoku

University School of Medicine (2018-1-669). The patients/participants provided their written informed consent to participate in this study.

AUTHOR CONTRIBUTIONS

XG, YY, and AP contributed to staining and evaluation of H&E and IHC sections. YT, KO, YO, and RM contributed to the collection of clinical data from Tohoku University hospital. YN, FS, and HS supervised all of the present study. All authors contributed to the article and approved the submitted version.

REFERENCES

- Farrugia FA, Charalampopoulos A. Pheochromocytoma. *Endocr Regul* (2019) 53:191–212. doi: 10.2478/enr-2019-0020
- Farrugia FA, Martikos G, Tzanetis P, Charalampopoulos A, Misiakos E, Zavras N, et al. Pheochromocytoma, diagnosis and treatment: Review of the literature. *Endocr Regul* (2017) 51:168–81. doi: 10.1515/enr-2017-0018
- Farrugia FA, Georgios M, Panagiotis T, Nikolaos Z, Anestis C, Dimitrios S, et al. Adrenal incidentaloma or epinephroma and review of the literature. Differential diagnosis of adrenal incidentaloma. *Khirurgiia (Sofia)* (2016) 82:120–8.
- Lam AK. Update on Adrenal Tumours in 2017 World Health Organization (WHO) of Endocrine Tumours. *Endocr Pathol* (2017) 28:213–27. doi: 10.1007/s12022-017-9484-5
- Bravo EL. Pheochromocytoma: new concepts and future trends. *Kidney Int* (1991) 40:544–56. doi: 10.1038/ki.1991.244
- Lloyd RVOR, Kloppel G, Rosai J. *WHO classification of tumours: pathology and genetics of tumours of endocrine organs*. (2017).
- Thompson LD. Pheochromocytoma of the Adrenal gland Scaled Score (PASS) to separate benign from malignant neoplasms: a clinicopathologic and immunophenotypic study of 100 cases. *Am J Surg Pathol* (2002) 26:551–66. doi: 10.1097/0000478-200205000-00002
- Kimura N, Takayanagi R, Takizawa N, Itagaki E, Katabami T, Kakoi N, et al. Pathological grading for predicting metastasis in pheochromocytoma and paraganglioma. *Endocr Relat Cancer* (2014) 21:405–14. doi: 10.1530/ERC-13-0494
- Chew V, Toh HC, Abastado JP. Immune microenvironment in tumor progression: characteristics and challenges for therapy. *J Oncol* (2012) 2012:608406. doi: 10.1155/2012/608406
- Quail DF, Joyce JA. Microenvironmental regulation of tumor progression and metastasis. *Nat Med* (2013) 19:1423–37. doi: 10.1038/nm.3394
- Hanahan D, Coussens LM. Accessories to the crime: functions of cells recruited to the tumor microenvironment. *Cancer Cell* (2012) 21:309–22. doi: 10.1016/j.ccr.2012.02.022
- Joyce JA, Fearon DT. T cell exclusion, immune privilege, and the tumor microenvironment. *Science* (2015) 348:74–80. doi: 10.1126/science.aaa6204
- Rahat MA, Coffelt SB, Granot Z, Muthana M, Amedei A. Macrophages and Neutrophils: Regulation of the Inflammatory Microenvironment in Autoimmunity and Cancer. *Mediators Inflamm* (2016) 2016:5894347. doi: 10.1155/2016/5894347
- Kitawaki Y, Nakamura Y, Kubota-Nakayama F, Yamazaki Y, Miki Y, Hata S, et al. Tumor microenvironment in functional adrenocortical adenomas: immune cell infiltration in cortisol-producing adrenocortical adenoma. *Hum Pathol* (2018) 77:88–97. doi: 10.1016/j.humpath.2018.03.016
- Landwehr LS, Altieri B, Schreiner J, Sbiera I, Weigand I, Kroiss M, et al. Interplay between glucocorticoids and tumor-infiltrating lymphocytes on the prognosis of adrenocortical carcinoma. *J Immunother Cancer* (2020) 8. doi: 10.1136/jitc-2019-000469
- Liu Q, Djuricin G, Staren ED, Gattuso P, Gould VE, Shen J, et al. Tumor angiogenesis in pheochromocytomas and paragangliomas. *Surgery* (1996) 120:938–42; discussion 942–933. doi: 10.1016/s0039-6060(96)80037-7

FUNDING

XG was supported by Global Hagi scholarship by Tohoku University. This work was supported by a Health Labour Sciences Research Grant (No. H29-Nanji-Ippan-046).

SUPPLEMENTARY MATERIAL

The Supplementary Material for this article can be found online at: <https://www.frontiersin.org/articles/10.3389/fendo.2020.587779/full#supplementary-material>

- Kulkarni MM, Khandeparkar SG, Deshmukh SD, Karekar RR, Gaopande VL, Joshi AR, et al. Risk Stratification in Paragangliomas with PASS (Pheochromocytoma of the Adrenal Gland Scaled Score) and Immunohistochemical Markers. *J Clin Diagn Res* (2016) 10:EC01–4. doi: 10.7860/JCDR/2016/20565.8419
- Konosu-Fukaya S, Omata K, Tezuka Y, Ono Y, Aoyama Y, Satoh F, et al. Catecholamine-Synthesizing Enzymes in Pheochromocytoma and Extraadrenal Paraganglioma. *Endocr Pathol* (2018) 29:302–9. doi: 10.1007/s12022-018-9544-5
- Chan MS, Chen SF, Felizola SJ, Wang L, Nemoto N, Tamaki K, et al. Correlation of tumor-infiltrative lymphocyte subtypes alteration with neoangiogenesis before and after neoadjuvant chemotherapy treatment in breast cancer patients. *Int J Biol Markers* (2014) 29:e193–203. doi: 10.5301/ijbm.5000082
- Konno-Kumagai T, Fujishima F, Nakamura Y, Nakano T, Nagai T, Kamei T, et al. Programmed death-1 ligands and tumor infiltrating T lymphocytes in primary and lymph node metastasis of esophageal cancer patients. *Dis Esophagus* (2019) 32. doi: 10.1093/dote/doy063
- Chan MS, Wang L, Chanplakorn N, Tamaki K, Ueno T, Toi M, et al. Effects of estrogen depletion on angiogenesis in estrogen-receptor-positive breast carcinoma—an immunohistochemical study of vasohibin-1 and CD31 with correlation to pathobiological response of the patients in neoadjuvant aromatase inhibitor therapy. *Expert Opin Ther Targets* (2012) 16 Suppl 1: S69–78. doi: 10.1517/14728222.2011.628938
- Yazdani S, Kasajima A, Tamaki K, Nakamura Y, Fujishima F, Ohtsuka H, et al. Angiogenesis and vascular maturation in neuroendocrine tumors. *Hum Pathol* (2014) 45:866–74. doi: 10.1016/j.humpath.2013.09.024
- Oka N, Kasajima A, Konukiewicz B, Sakurada A, Okada Y, Kameya T, et al. Classification and Prognostic Stratification of Bronchopulmonary Neuroendocrine Neoplasms. *Neuroendocrinology* (2020) 110:393–403. doi: 10.1159/000502776
- Yazdani S, Miki Y, Tamaki K, Ono K, Iwabuchi E, Abe K, et al. Proliferation and maturation of intratumoral blood vessels in non-small cell lung cancer. *Hum Pathol* (2013) 44:1586–96. doi: 10.1016/j.humpath.2013.01.004
- Yamazaki Y, Omata K, Tezuka Y, Ono Y, Morimoto R, Adachi Y, et al. Tumor Cell Subtypes Based on the Intracellular Hormonal Activity in KCNJ5-Mutated Aldosterone-Producing Adenoma. *Hypertension* (2018) 72:632–40. doi: 10.1161/HYPERTENSIONAHA.118.10907
- Gao X, Yamazaki Y, Tezuka Y, Onodera Y, Ogata H, Omata K, et al. The crosstalk between aldosterone and calcium metabolism in primary aldosteronism: A possible calcium metabolism-associated aberrant “neoplastic” steroidogenesis in adrenals. *J Steroid Biochem Mol Biol* (2019) 193:105434. doi: 10.1016/j.jsbmb.2019.105434
- Konosu-Fukaya S, Nakamura Y, Satoh F, Felizola SJ, Maekawa T, Ono Y, et al. 3beta-Hydroxysteroid dehydrogenase isoforms in human aldosterone-producing adenoma. *Mol Cell Endocrinol* (2015) 408:205–12. doi: 10.1016/j.mce.2014.10.008
- McCarty KS Jr., Miller LS, Cox EB, Konrath J, McCarty KSSr. Estrogen receptor analyses. Correlation of biochemical and immunohistochemical methods using monoclonal antireceptor antibodies. *Arch Pathol Lab Med* (1985) 109:716–21.
- Yamazaki Y, Nakamura Y, Omata K, Ise K, Tezuka Y, Ono Y, et al. Histopathological Classification of Cross-Sectional Image-Negative

- Hyperaldosteronism. *J Clin Endocrinol Metab* (2017) 102:1182–92. doi: 10.1210/jc.2016-2986
30. Farhat NA, Powers JF, Shepard-Barry A, Dahia P, Pacak K, Tischler AS. A Previously Unrecognized Monocytic Component of Pheochromocytoma and Paraganglioma. *Endocr Pathol* (2019) 30:90–5. doi: 10.1007/s12022-019-9575-6
 31. Wu D, Tischler AS, Lloyd RV, DeLellis RA, de Krijger R, van Nederveen F, et al. Observer variation in the application of the Pheochromocytoma of the Adrenal Gland Scaled Score. *Am J Surg Pathol* (2009) 33:599–608. doi: 10.1097/PAS.0b013e318190d12e
 32. Fishbein L. Pheochromocytoma and Paraganglioma: Genetics, Diagnosis, and Treatment. *Hematol Oncol Clin North Am* (2016) 30:135–50. doi: 10.1016/j.hoc.2015.09.006
 33. Troiano G, Caponio VCA, Adipietro I, Tepedino M, Santoro R, Laino L, et al. Prognostic significance of CD68(+) and CD163(+) tumor associated macrophages in head and neck squamous cell carcinoma: A systematic review and meta-analysis. *Oral Oncol* (2019) 93:66–75. doi: 10.1016/j.oraloncology.2019.04.019
 34. Ni YH, Ding L, Huang XF, Dong YC, Hu QG, Hou YY. Microlocalization of CD68+ tumor-associated macrophages in tumor stroma correlated with poor clinical outcomes in oral squamous cell carcinoma patients. *Tumour Biol* (2015) 36:5291–8. doi: 10.1007/s13277-015-3189-5
 35. Lin Z, Gu J, Cui X, Huang L, Li S, Feng J, et al. Deciphering Microenvironment of NSCLC based on CD8+ TIL Density and PD-1/PD-L1 Expression. *J Cancer* (2019) 10:211–22. doi: 10.7150/jca.26444
 36. Nouri-Shirazi M, Banchereau J, Bell D, Burkeholder S, Kraus ET, Davoust J, et al. Dendritic cells capture killed tumor cells and present their antigens to elicit tumor-specific immune responses. *J Immunol* (2000) 165:3797–803. doi: 10.4049/jimmunol.165.7.3797
 37. Farhood B, Najafi M, Mortezaee K. CD8(+) cytotoxic T lymphocytes in cancer immunotherapy: A review. *J Cell Physiol* (2019) 234:8509–21. doi: 10.1002/jcp.27782
 38. Sarkar C, Chakroborty D, Basu S. Neurotransmitters as regulators of tumor angiogenesis and immunity: the role of catecholamines. *J Neuroimmune Pharmacol* (2013) 8:7–14. doi: 10.1007/s11481-012-9395-7
 39. Madden KS, Sanders VM, Felten DL. Catecholamine influences and sympathetic neural modulation of immune responsiveness. *Annu Rev Pharmacol Toxicol* (1995) 35:417–48. doi: 10.1146/annurev.pa.35.040195.002221
 40. Nasi G, Ahmed T, Rasini E, Fenoglio D, Marino F, Filaci G, et al. Dopamine inhibits human CD8+ Treg function through D1-like dopaminergic receptors. *J Neuroimmunol* (2019) 332:233–41. doi: 10.1016/j.jneuroim.2019.02.007
 41. Inbar S, Neeman E, Avraham R, Benish M, Rosenne E, Ben-Eliyahu S. Do stress responses promote leukemia progression? An animal study suggesting a role for epinephrine and prostaglandin-E2 through reduced NK activity. *PLoS One* (2011) 6:e19246. doi: 10.1371/journal.pone.0019246
 42. Edgar VA, Silberman DM, Cremaschi GA, Zieher LM, Genaro AM. Altered lymphocyte catecholamine reactivity in mice subjected to chronic mild stress. *Biochem Pharmacol* (2003) 65:15–23. doi: 10.1016/s0006-2952(02)01457-0
 43. Parayath NN, Parikh A, Amiji MM. Repolarization of Tumor-Associated Macrophages in a Genetically Engineered Nonsmall Cell Lung Cancer Model by Intraperitoneal Administration of Hyaluronic Acid-Based Nanoparticles Encapsulating MicroRNA-125b. *Nano Lett* (2018) 18:3571–9. doi: 10.1021/acs.nanolett.8b00689
 44. Wang N, Liang H, Zen K. Molecular mechanisms that influence the macrophage m1-m2 polarization balance. *Front Immunol* (2014) 5:614. doi: 10.3389/fimmu.2014.00614
 45. Genard G, Wera AC, Huat C, Le Calve B, Penninckx S, Fattaccoli A, et al. Proton irradiation orchestrates macrophage reprogramming through NFκB signaling. *Cell Death Dis* (2018) 9:728. doi: 10.1038/s41419-018-0757-9
 46. Mantovani A, Marchesi F, Malesci A, Laghi L, Allavena P. Tumour-associated macrophages as treatment targets in oncology. *Nat Rev Clin Oncol* (2017) 14:399–416. doi: 10.1038/nrclinonc.2016.217
 47. Ruffell BC, Coussens LM. Macrophages and therapeutic resistance in cancer. *Cancer Cell* (2015) 27:462–72. doi: 10.1016/j.ccell.2015.02.015
 48. Yamate J, Izawa T, Kuwamura M. Histopathological Analysis of Rat Hepatotoxicity Based on Macrophage Functions: in Particular, an Analysis for Thioacetamide-induced Hepatic Lesions. *Food Saf (Tokyo)* (2016) 4:61–73. doi: 10.14252/foodsafetyfscj.2016012
 49. Parise IZS, Parise GA, Noronha L, Surakhy M, Woiski TD, Silva DB, et al. The Prognostic Role of CD8(+) T Lymphocytes in Childhood Adrenocortical Carcinomas Compared to Ki-67, PD-1, PD-L1, and the Weiss Score. *Cancers (Basel)* (2019) 11. doi: 10.3390/cancers11111730
 50. Trigunaite A, Dimo J, Jorgensen TN. Suppressive effects of androgens on the immune system. *Cell Immunol* (2015) 294:87–94. doi: 10.1016/j.cellimm.2015.02.004
 51. Rasmuson T, Ljungberg B, Grankvist K, Jacobsen J, Olsson T. Increased serum cortisol levels are associated with high tumour grade in patients with renal cell carcinoma. *Acta Oncol* (2001) 40:83–7. doi: 10.1080/028418601750071118
 52. Taves MD, Hamden JE, Soma KK. Local glucocorticoid production in lymphoid organs of mice and birds: Functions in lymphocyte development. *Horm Behav* (2017) 88:4–14. doi: 10.1016/j.yhbeh.2016.10.022
 53. Trenti A, Tedesco S, Boscaro C, Trevisi L, Bolego C, Cignarella A. Estrogen, Angiogenesis, Immunity and Cell Metabolism: Solving the Puzzle. *Int J Mol Sci* (2018) 19. doi: 10.3390/ijms19030859
 54. Sasano H, Suzuki T. Pathological evaluation of angiogenesis in human tumor. *BioMed Pharmacother* (2005) 59 Suppl 2:S334–336. doi: 10.1016/s0753-3322(05)80068-x
 55. Favier J, Gimenez-Roqueplo AP. Pheochromocytomas: the (pseudo)-hypoxia hypothesis. *Best Pract Res Clin Endocrinol Metab* (2010) 24:957–68. doi: 10.1016/j.beem.2010.10.004
 56. Pollard PJ, El-Bahrawy M, Poulson R, Elia G, Killick P, Kelly G, et al. Expression of HIF-1α, HIF-2α (EPAS1), and their target genes in paraganglioma and pheochromocytoma with VHL and SDH mutations. *J Clin Endocrinol Metab* (2006) 91:4593–8. doi: 10.1210/jc.2006-0920
 57. Salmenkivi K, Heikkilä P, Liu J, Haglund C, Arola J. VEGF in 105 pheochromocytomas: enhanced expression correlates with malignant outcome. *APMIS* (2003) 111:458–64. doi: 10.1034/j.1600-0463.2003.1110402.x
 58. Ziehlke A, Middeke M, Hoffmann S, Colombo-Benkmann M, Barth P, Hassan I, et al. VEGF-mediated angiogenesis of human pheochromocytomas is associated to malignancy and inhibited by anti-VEGF antibodies in experimental tumors. *Surgery* (2002) 132:1056–63; discussion 1063. doi: 10.1067/msy.2002.128613
 59. Feng F, Zhu Y, Wang X, Wu Y, Zhou W, Jin X, et al. Predictive factors for malignant pheochromocytoma: analysis of 136 patients. *J Urol* (2011) 185:1583–90. doi: 10.1016/j.juro.2010.12.050
 60. Amorim-Pires D, Peixoto J, Lima J. Hypoxia Pathway Mutations in Pheochromocytomas and Paragangliomas. *Cytogenet Genome Res* (2016) 150:227–41. doi: 10.1159/000457479
 61. Takahashi H, Nakashima S, Kumanishi T, Kura F. Paragangliomas of the craniocervical region. An immunohistochemical study on tyrosine hydroxylase. *Acta Neuropathol* (1987) 73:227–32. doi: 10.1007/BF00686615
 62. Kimura N, Miura Y, Nagatsu I, Nagura H. Catecholamine synthesizing enzymes in 70 cases of functioning and non-functioning pheochromocytoma and extra-adrenal paraganglioma. *Virchows Arch A Pathol Anat Histopathol* (1992) 421:25–32. doi: 10.1007/BF01607135

Conflict of Interest: The authors declare that the research was conducted in the absence of any commercial or financial relationships that could be construed as a potential conflict of interest.

Copyright © 2020 Gao, Yamazaki, Pecori, Tezuka, Ono, Omata, Morimoto, Nakamura, Satoh and Sasano. This is an open-access article distributed under the terms of the Creative Commons Attribution License (CC BY). The use, distribution or reproduction in other forums is permitted, provided the original author(s) and the copyright owner(s) are credited and that the original publication in this journal is cited, in accordance with accepted academic practice. No use, distribution or reproduction is permitted which does not comply with these terms.



The VHL/HIF Axis in the Development and Treatment of Pheochromocytoma/Paraganglioma

Song Peng¹, Jun Zhang¹, Xintao Tan¹, Yiqiang Huang¹, Jing Xu¹, Natalie Silk², Dianzheng Zhang², Qiuli Liu^{1*} and Jun Jiang^{1*}

¹ Department of Urology, Daping Hospital, Army Medical University, Chongqing, China, ² Department of Bio-Medical Sciences, Philadelphia College of Osteopathic Medicine, Philadelphia, PA, United States

OPEN ACCESS

Edited by:

Alfred King-yin Lam,
Griffith University, Australia

Reviewed by:

Judith Favier,
Institut National de la Santé et de la
Recherche Médicale (INSERM), France
Kan Gong,
Peking University First Hospital, China

*Correspondence:

Jun Jiang
jiangjun_64@163.com
Qiuli Liu
liuqiuli900827@163.com

Specialty section:

This article was submitted to
Neuroendocrine Science,
a section of the journal
Frontiers in Endocrinology

Received: 24 July 2020

Accepted: 23 October 2020

Published: 24 November 2020

Citation:

Peng S, Zhang J, Tan X, Huang Y,
Xu J, Silk N, Zhang D, Liu Q and
Jiang J (2020) The VHL/HIF Axis in the
Development and Treatment of
Pheochromocytoma/Paraganglioma.
Front. Endocrinol. 11:586857.
doi: 10.3389/fendo.2020.586857

Pheochromocytomas and paragangliomas (PPGLs) are rare neuroendocrine tumors originating from chromaffin cells in the adrenal medulla (PCCs) or extra-adrenal sympathetic or parasympathetic paraganglia (PGLs). About 40% of PPGLs result from germline mutations and therefore they are highly inheritable. Although dysfunction of any one of a panel of more than 20 genes can lead to PPGLs, mutations in genes involved in the VHL/HIF axis including *PHD*, *VHL*, *HIF-2A* (*EPAS1*), and *SDHx* are more frequently found in PPGLs. Multiple lines of evidence indicate that pseudohypoxia plays a crucial role in the tumorigenesis of PPGLs, and therefore PPGLs are also known as metabolic diseases. However, the interplay between VHL/HIF-mediated pseudohypoxia and metabolic disorder in PPGLs cells is not well-defined. In this review, we will first discuss the VHL/HIF axis and genetic alterations in this axis. Then, we will dissect the underlying mechanisms in VHL/HIF axis-driven PPGL pathogenesis, with special attention paid to the interplay between the VHL/HIF axis and cancer cell metabolism. Finally, we will summarize the currently available compounds/drugs targeting this axis which could be potentially used as PPGLs treatment, as well as their underlying pharmacological mechanisms. The overall goal of this review is to better understand the role of VHL/HIF axis in PPGLs development, to establish more accurate tools in PPGLs diagnosis, and to pave the road toward efficacious therapeutics against metastatic PPGLs.

Keywords: pheochromocytomas, paragangliomas, VHL, HIF, metabolism, inhibitor

INTRODUCTION

Pheochromocytomas (PCCs) are catecholamine-secreting tumors that originated from the chromaffin cells in the adrenal medulla. Paragangliomas (PGLs) are neural crest-derived neuroendocrine neoplasms originating from extra-adrenal sympathetic or parasympathetic ganglia (1). Both PCCs and PGLs are collectively known as PPGLs. PPGLs are rare tumors with the incidence rate between 0.2 and 0.8 per 100,000 (2–4) with great clinical manifestations (5). Due to elevated levels of catecholamines in the circulation, the common clinical presentations of PPGLs include episodes of headache, sweating, palpitation, and hypertension. In addition, about 10% of PCCs are metastatic (6) and 40% of PGLs are considered as metastatic disease (7, 8).

Etiologically, about 70%–80% of PPGLs are caused by genetic abnormalities which affect different signaling pathways (9). Approximately, 40% of PPGLs result from germline mutations, and therefore they are highly inheritable (10). Although dysfunction of any of these related susceptible gene products can lead to PPGLs, mutations in the genes encoding the VHL/HIF axis such as *VHL*, *HIF*, and *PHD* are more commonly found in PPGLs (11). Moreover, multiple lines of evidence suggest that pseudohypoxia plays a crucial role in the tumorigenesis of PPGLs. In this review, we will discuss the genetic alterations affecting the VHL/HIF axis and dissect the underlying molecular mechanisms in pseudohypoxia signaling and PPGLs. We will also summarize the currently available compounds or drugs targeting VHL/HIF axis, their specific targets, and pharmacological mechanisms.

THE VHL/HIF AXIS

The Von Hippel-Lindau (*VHL*) gene located on 3p25.5 encodes an ancient tumor suppressor, pVHL. Although pVHL functions in both physiology and pathology, as a component of an E3 ubiquitin-ligase complex, pVHL plays a determinant role in the degradation of hypoxia-induced factors (HIFs) including HIF-1 α , HIF-2 α , and HIF-3 α . The roles of HIF-1 α and HIF-2 α in sensing and facilitating cellular adaptation to hypoxic conditions as well as their underlying molecular mechanisms are well-established (12). However, much less is known about HIF-3 α . Functionally, HIF-1 α and HIF-2 α heterodimerize with HIF- β by HLH domain, which is also known as ARNT, to transcriptionally regulate a wide spectrum of HIF target genes. Both HIF- α and

HIF- β belong to the basic helix-loop-helix-Per-ARNT-Sim (bHLH-PAS) family. They contain a basic DNA binding domain, a conserved NH₂-terminal domain (N-TAD), and two specialized transactivation domains located in their variable COOH-terminal domains (C-TAD) (13) (**Figure 1**). The asparagine residue (N803) in the C-TAD of HIF- α can be hydroxylated by factor-inhibiting HIF (FIH) to interrupt its interaction with CREB-binding protein (CBP)/p300, an essential coactivator of HIF (14–16). The N-TAD also contains an oxygen-dependent domain (ODDD), in which a few prolyl residues (Pro-402 and Pro-564 in HIF-1 α ; Pro-405 and Pro-531 in HIF-2 α) are selectively hydroxylated under normoxic condition and hydroxylated HIFs are subsequently degraded (17–20). The enzymes responsible for HIF- α hydroxylation belong to the egg-laying-defective nine (*EGLN*) family known as PHD1, PHD2, and PHD3 because they all contain a prolyl-4-hydroxylase domain. These enzymes are dioxygenases and use both molecular oxygen and Fe²⁺ as their co-substrates to catalyze HIF- α hydroxylation.

The VHL/HIF axis responds to reduced oxygen concentration or hypoxia. Although HIF-1 α and HIF-2 α have about 48% sequence similarity, they regulate two different groups of target genes with limited overlap mainly due to their dissimilar transactivation domains (21, 22). In addition, HIF-1 α is widely expressed, while HIF-2 α is only expressed in certain cell types (23, 24). For example, the genes involved in glucose metabolism are mainly regulated by HIF-1 α . HIF-2 α plays a more important role in the adjustment to high altitudes and the regulation of EPO expression (25, 26). As mentioned above that compared to HIF-1 α and HIF-2 α , much less is known about HIF-3 α . Since it lacks the transactivation domain (27), HIF-3 α likely does not

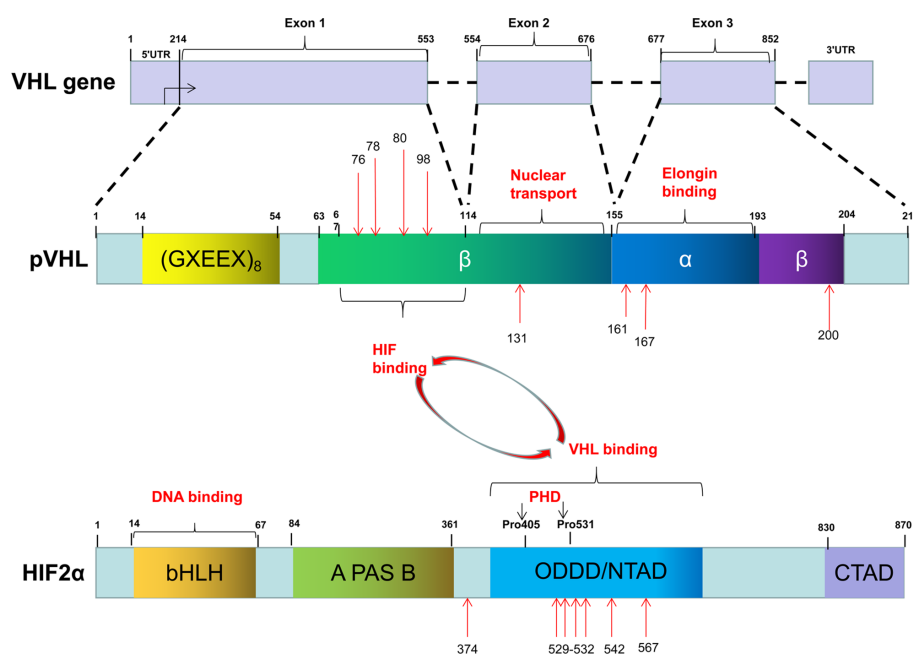


FIGURE 1 | The common mutation sites of VHL and EPAS1 genes in PPGLs.

transcriptionally regulate its target genes. Overall, the levels and functions of both HIF-1 α and HIF-2 α are oxygen-concentration dependent. Specific proline residues of HIF-1 α and HIF-2 α are hydroxylated by PHD under normoxic conditions. With the involvement of the molecules such as elongin B, elongin C, cul2, the hydroxylated HIFs are recognized by the pVHL (28–30), subsequently ubiquitinated and ultimately degraded (31, 32). Under hypoxic conditions, the non-hydroxylated HIFs are dissociated from pVHL, accumulated in the cells, and subsequently upregulate their target genes transcriptionally. However, failure in the degradation of HIFs due to either deletion or mutation of either *VHL*, *HIFs*, or *PHDs* can lead to dysregulation of HIFs-regulated genes in a variety of diseases including PPGLs (**Figure 2**).

DYSREGULATION OF THE VHL/HIF AXIS AND PPGLs

As mentioned above that mutation in either the three genes encoding pVHL, HIFs and PHDs can lead to abnormal accumulation of HIFs. Minor alteration of this axis usually causes erythrocytosis; whereas major dysregulation of the axis is associated with tumorigenesis (33). Although a wide spectrum of tumors including hemangioblastomas, renal cell carcinoma (RCC), pancreatic neuroendocrine tumor, and PPGLs can result from dysregulation of the VHL/HIF axis (34–37), this review will only focus on the relationship between aberrations of these genes and PPGLs.

VHL Mutations

After the *VHL* mutations were first described in an ophthalmic disease (34), multiple studies subsequently confirmed that *VHL* mutations can cause a variety of diseases including cancers (35–37). To honor the contributions of the German ophthalmologist Eugen von Hippel and the Swedish pathologist Arvid Lindau, the gene responsible for these diseases is, therefore, named as *VHL*. Of note, VHL disease caused by heterozygous germline mutations is autosomal dominant and almost completely penetrant (97%) (38). VHL diseases are generally classified into two types, type 1 (without PCCs) and type 2 (with PCCs). The type 2 disease is manifested as RCCs, PCCs, central nervous system, retinal hemangioblastomas, pancreatic neuroendocrine tumors and pancreatic and renal cysts and can be further divided into three subtypes (34), PCCs with all types of VHL disease manifestations without RCC (Type 2A), PCC with all types of VHL disease including RCC (Type 2B), and isolated PCCs (Type 2C).

To date, more than 1,000 mutations in *VHL* gene have been identified. These mutations can be categorized as missense mutation (52%), frameshift mutation (13%), nonsense mutation (11%), in-frame deletion/insertion mutation (6%), large/complete deletion mutation (11%), and splicing mutation (7%) (39). The common germline mutations in *VHL* are delPhe76, Asn78Ser, Arg161Stop, Arg167Gln, Arg167Trp, and Leu178Pro (40) (**Figure 1**). Recently, we reported four missense mutations in five Chinese unrelated families c.239G>T (p.Ser80Ile), c.232A>T (p.As78Tyr), c.500G>A (p.Arg167Gln), c.293A>G (p.Try98Cys), and all four mutations

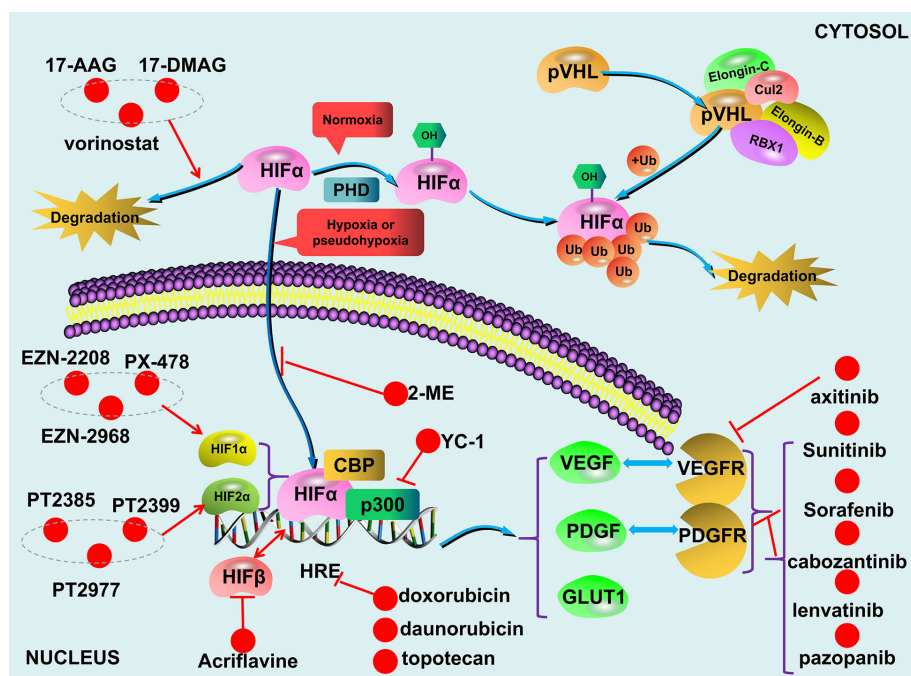


FIGURE 2 | The VHL/HIF axis and compounds targeting the axis.

predispose the patients to VHL disease (41). Notably, type 2 VHL disease mainly resulted from missense mutations (85%–92%) (40, 42), especially mutations in codons 167 and 238, are mainly associated with PPGLs (43, 44). In contrast, homozygous germline mutations are rare or barely cause tumors. Sonny et al. found a c.598C>T (p.Arg200Trp) homozygous missense germline mutation of *VHL* caused Chuvash polycythemia (45). In addition, somatic *VHL* mutations were found in majority (50%–70%) of clear-cell RCC cases (38).

It has been reported that different mutations in *VHL* lead to diverse clinical symptoms (41, 46–49), and sometimes even the same mutation can lead to different phenotypes (50–53). Since pVHL has multiple functional domains, one of the potential explanations for this phenomenon is that a specific mutation causes particular dysfunction. It appears that missense mutations are more likely linked with type 2 disease and truncating mutations are responsible for type 1 disease (54). However, Liu et al. further stratified the missense mutations as HIF- α binding site missense mutations (HM) group and non-HIF- α binding site missense mutations (nHM) group, and found that the missense mutations in HM group had similar risks of most tumors with truncating mutations with the exception that the HM group had a lower risk of RCC. Moreover, compared to nHM, missense mutations in HM had a higher risk of pancreatic cyst or tumor and a lower risk of PCCs (55). Secondly, some functions of pVHL are O₂-independent (56, 57) or unrelated to HIF regulation, these functions may also be involved in PPGLs pathogenesis. Michael et al. found that RCCs with deficient pVHL exhibited deficiency in fibronectin matrix assembly (58). Intriguingly, Clifford et al. reported that mutations associated with type 2C phenotype could even promote, rather than inhibit, HIF- α ubiquitylation and degradation (39). These findings altogether supported the notion that disturbing the functions of pVHL contributes to the development of PPGLs. Additionally, based on Knudson's Two-Hit model (59), it is understandable that the diverse phenotypes of VHL diseases could be the result of two different "hits".

The VHL/HIF axis also can be affected by dysregulated epigenetic modifications such as gene silencing by methylation of the CpG islands in the promoter of related genes. Indeed, promoter hypermethylation occurs in about 3%–42% of clear-cell RCC (60). Adam Andreasson found that the promoter methylation of the *VHL* gene is not only elevated in PPGLs compared with normal tissue (57% vs. 27%) but also significantly higher in malignancies than that in tumors (63% vs. 55%) (61). However, the precise molecular mechanisms in the pathogenesis of PPGLs related to loss-of-function of pVHL are still largely unknown and therefore need further investigation.

HIF-A Mutations

As mentioned above that HIF- α family composed three members, HIF-1 α , HIF-2 α , and HIF-3 α . But little is known about HIF-3 α . Compared with *HIF-2A*, *HIF-1A* has relatively few mutations, ClinVar database (<https://www.ncbi.nlm.nih.gov/clinvar/>) only collects 30 records. Morris et al. reported a somatic mutation (p.Val116Glu) and a germline missense mutation (p.Ala475Ser) of *HIF-1A* in a clear-cell RCC with *VHL*

inactivation. Of note, the germline mutation (p.Ala475Ser) was likely to be a benign variant (62). Furthermore, Gladek et al. found that *HIF-1A* Single-Nucleotide Polymorphisms (SNPs) are association with the phenotypes of many tumors (63). In PPGLs patients, only copy number aberration (TCGA-QT-A5XP, <https://portal.gdc.cancer.gov/>), not *HIF-1A* mutation, have been found. On the other hand, both germline and somatic mutation in *HIF-2A* have been identified in patients with polycythemia and/or PPGLs. However, it appears that germline mutations of *HIF-2A* including p.Met535Val, p.Gly537Arg, p.Gly537Trp only leads to polycythemias, not tumors (64, 65). A gain-of-function germline mutation in *HIF-2A* alone is not sufficient for tumorigenesis presumably that simultaneous loss-of-function in some tumor suppressors is needed. In fact, we recently reported that germline mutations in *HIF-2A* (c.1609G>A, p.Gly537Arg) are responsible for polycythemia formation and additional somatic *VHL* mutations are needed for the development of clear-cell RCC (66). Similarly, a germline mutation in *HIF-2A* exon 9 (c.1121T>A, p.F374Y) leads to polycythemia and predisposes the patients for PPGLs development (67). In addition, somatic mutations in *HIF-2A* appear to be more frequent genetic events in PPGLs (68). For example, Zhang et al. reported two gain-of-function somatic mutations (c.1588G>A, p.Ala530Thr and c.1589C>T, p.Ala530Val) in exon 12 of *HIF-2A* resulting in paraganglioma and polycythemia, respectively. Further analyses suggest that mutations in the vicinity of the hydroxylation site Pro-531 affect the catalytic activity of PHD and then lead to the interrupted interaction between HIF-2 α and pVHL (69). Moreover, Karel Pacak et al. reported two somatic mutations of *HIF-2A* (c.1595A>G p.Y532C and c.1586T>C p.L529P) in patients with either congenital polycythemia, multiple recurrent PPGLs, or somatostatinoma (70). We recently found that a gain-of-function mutation of *HIF-2A* (c.1589C>T) leads to PPGLs with polycythemia simultaneously (26) and a mutation in *HIF-2A* immediately distal to its DNA binding domain (p.Ser71Tyr) has been identified in sporadic PPGLs (71) (**Figure 1**). Germline or somatic mutations of *HIF-2A* can be mosaic. Buffet et al. reported two cases of *HIF-2A*-related Polycythemia-Paraganglioma Syndrome resulted from mosaicism mutations. They found that these patients could present with young age and multiplicity; and also the mutations could be transmitted to the offspring (72). In addition, *HIF-2A* mosaic mutation might be involved in high secretion of catecholamines and cyanotic congenital heart disease (73).

Mutation in PHD and Other Related Factors

Heterozygous germline mutations in *PHD2* gene were first reported in familial erythrocytosis (74, 75). Later, Ladroue et al. reported a heterozygous loss-of-function mutation of *PHD2* (c.1121A>G, p.His374Arg) with the development of both erythrocytosis and recurrent paraganglioma. Functional analysis indicates that His374 is important in the binding of cofactor Fe²⁺, and mutation of this residue is expected to impair the catalytic function of PHDs (76). Yang et al. reported heterozygous germline mutations in *PHD1* (c.188T>A,

p.Ser61Arg and c.682G>T, p.Ala228Ser) in patients with polycythemia and PPGLs, respectively. Further research found that the half-lives of both PHD1 and PHD2 are reduced with these *PHD1* mutants (77). These findings collectively demonstrated that mutant *PHDs* are indeed associated with susceptibility to PPGLs. However, compared to *VHL* and *HIF-A*, mutations in *PHDs* are relatively rare in patients with PPGLs (78). Additionally, mutations of enzymes in the TCA cycle can affect VHL/HIF axis indirectly. For example, elevated levels of HIFs can be caused by the mutations in *SDHx*, *FH*, *MDH*, and *IDH* with subsequent accumulation of specific metabolites and reactive oxygen species (31, 79–89). In addition, multiple lines of evidence indicated that mutations in cluster 2 (Kinase Signaling Cluster) genes, including *NF1*, *RET*, *TMEM127*, *ERK*, *MAX*, and *H-RAS* could affect the VHL/HIF axis indirectly (90–94), although these mutations were initially thought to drive PPGLs through the oxygen-independent kinase signaling pathway, such as mTOR axis.

THE MECHANISMS IN DYSREGULATED VHL/HIF AXIS AND PPGLS

Under normal physiological conditions, HIFs are degraded during normoxic condition and HIFs accumulation only occur during hypoxia. The undegraded HIF- α translocates to the nucleus and dimerizes with HIF- β (95). Together with p300/CBP, the HIF- α /HIF- β heterodimer is recruited to the hypoxia-responsive elements (HREs) located on the promoter regions of HIF-regulated targets to transcriptionally upregulate the expression of the genes including vascular endothelial growth factor (*VEGF*), platelet-derived growth factor (*PDGF*), and glucose transporter (*GLUT*) (93, 96–98) (**Figure 2**). The combined effects of these upregulated gene products result in an increased supply of blood and nutrients to the hypoxic tissues and switch glucose metabolism from aerobic to anaerobic glycolysis. Due to the fast growth of tumor tissues, this process occurs in all solid tumors (99, 100), and dysregulated VHL/HIF axis further exacerbate the development of certain tumors such as PPGLs.

Aerobic glycolysis, also known as Warburg Effect (9, 101, 102), occurs in all solid tumor cells. However, dysregulated VHL/HIF axis plays a more important role in certain cancer types such as clear-cell RCC and PPGLs. Pseudohypoxia, mimicking the hypoxic condition, can affect different cancer processes including tumorigenesis and malignant transformation by promoting epithelial-mesenchymal transition and enhancing stem cell-like property. Of note, metabolic reprogramming can affect each of these processes and the role of VHL/HIF axis in cancer metabolic reprogramming has been well defined. HIF-1 aberrant activation due to either *VHL* or *PHD* mutations increases glucose uptake and glycolysis with a concomitant decrease in mitochondrial mass (103). HIF- α , especially HIF-1 α , controls a wide spectrum of enzymes including *GLUT1*, *GLUT3*, hexokinase 1/2, lactate dehydrogenase-A (*LDH-A*), and pyruvate dehydrogenase kinase

1 (*PDK1*) (104–108). Upregulating these enzymes collectively shifts glycolysis from aerobic to anaerobic (109).

PPGLs are also considered as metabolic diseases due to the increased secretion of one or more catecholamines (epinephrine, norepinephrine, and dopamine). Catecholamines play a crucial role in the regulation of multiple metabolic pathways. Patients with PPGLs usually manifest with impaired insulin secretion, increased insulin resistance, elevated lipolysis, and the bone resorption marker C-terminal telopeptide of type I collagen (110). Many studies have revealed that oncometabolite such as succinate, fumarate, and 2-hydroxyglutarate (2HG) are increased in PPGLs (83, 111, 112). Another study found that compared to PPGLs without *SDHx* mutation, PPGLs with a deficient SDH have 25-fold higher succinate and 80% lower levels of fumarate, cis-aconitate, and isocitrate (113). Mutation in *FH* and *IDH* lead to the accumulation of fumarate and (R)-2-hydroxyglutarate, respectively (88, 114). Mechanistically, these oncometabolite modulate the activity of α -ketoglutarate-dependent dioxygenases such as PDH, which are involved in the induction of the pseudohypoxia pathway and activation of HIF axis (10, 31, 115). In addition, PPGLs with a germline mutation in genes encoding enzymes in the TCA cycle belong to Cluster I tumors, characterized by a pseudohypoxia signature (31). Together with the other intermediate metabolites of the TCA cycle, succinate can increase the chance of tumor development and progression through an ill-defined mechanism (83).

Results from more recent researches indicate that HIFs can regulate non-coding RNA (ncRNA) either directly or indirectly. Direct regulation is achieved by the recruiting HIFs to the HREs located on the promoter regions of ncRNAs. Whereas indirect regulation of ncRNA is achieved by epigenetic modification (116). One of the HIFs targets microRNA 210 (miR-210) (117) participates in a variety of biological processes including carcinogenesis, cancer cell proliferation, apoptosis, angiogenesis, and metastasis (118–120). On the other hand, miRNA can also activate HIF *via* mTOR indirectly. Calsina et al. reported miR-21-3p can regulate TSC2/mTOR axis in metastatic PPGLs and proposed that miR-21-3p can be the predictive markers of metastases (121). In addition, some lncRNA such as H19, MALAT1, HOTAIR, and lncRNA-SARCC play important roles in the activity of VHL/HIF axis (122).

INHIBITORS TARGETING THE VHL/HIF AXIS

Since the VHL/HIF axis plays a critical role in the development of PPGLs, targeting this axis could be a promising therapeutic strategy. Multiple reagents targeting the VHL/HIF axis have been explored and some of them have been applied clinically (123–127). Among them, the tyrosine kinase inhibitors (TKIs) are most widely used because TKIs can repress angiogenesis by inhibiting the VEGF pathway (128–130). Some compounds targeting the VHL/HIF axis can inhibit tumor growth in both animal models and clinical trials (**Table 1**).

TABLE 1 | The inhibitors targeting the VHL/HIF axis.

	Drugs or compounds	Targets or mechanisms	Clinical trials for PPGLs (www.clinicaltrials.gov)
Tyrosine kinase inhibitors	Sunitinib	Targeting VEGFR-1,2, PDGFR- β , RET, FGFR	NCT01371201, NCT00843037
	Sorafenib	Targeting RAF kinase, c-KIT, FLT-3, RET, VEGFR1-3, and PDGFR- β	None
	Cabozantinib	Targeting VEGFR, MET, RET	NCT02592356, NCT04400474, NCT02302833
	Axitinib	Targeting VEGFR	NCT01967576, NCT03839498
	Lenvatinib	Targeting VEGFR, FGFR, RET, c-Kit, PDGF α	NCT03008369, NCT02592356
Non-selective HIFs inhibitors	Pazopanib	Targeting VEGFR1-3, PDGFR- α , β , c-Kit	NCT01340794
	17-AAG	Promoting protein degradation	None
	17-DMAG	Promoting protein degradation	None
	Vorinostat	Promoting protein degradation	None
	Topotecan	Inhibiting translation and transcription activity	None
	Acriflavine	Inhibiting heterodimerization	None
	2-Methoxyestradiol	Inhibiting nuclear translocation and transcriptional activity	None
	YC-1	Inhibiting protein accumulation and transcription activity	None
	Doxorubicin/daunorubicin	Inhibiting DNA binding	NCT00002764, NCT00002608, NCT00002641
HIF-1 α inhibitors	PX-478	Inhibiting mRNA expression and translation	None
	EZN-2208	Inhibiting mRNA expression	None
	Chetomin	Disrupting binding to p300	None
	Echinomycin	Inhibiting DNA binding	None
	KC7F2	Inhibiting protein synthesis	None
	Glyceollins	Inhibiting protein synthesis and stability	None
	Bisphenol A	Promoting protein degradation	None
	LW6	Promoting protein degradation	None
	PX-12	Promoting protein degradation	None
	Cryptotanshinone	Blocking nuclear translocation	None
	cyclo-CLLFVY	Inhibiting heterodimerization	None
	Indenopyrazole 21	Inhibiting transcriptional activity	None
	EZN-2968	Inhibiting mRNA expression and translation	None
	PT2385	Inhibiting heterodimerization	None
	PT2399	Inhibiting heterodimerization	None
	PT2977	Inhibiting heterodimerization	None

Tyrosine Kinase Inhibitors

To date, more than 40 protein kinase inhibitors have been approved by the FDA for cancer treatment (131). Several TKIs including sunitinib, cabozantinib, axitinib, Lenvatinib, and pazopanib are currently being evaluated in phase II clinical trials (www.ClinicalTrials.gov). By repressing the tyrosine kinase receptors, these reagents can inhibit cancer cell growth, metastasis, and the development of therapeutic resistance (132). More recently, several case studies and/or clinical trials in small cohorts suggest that TKIs could be a promising treatment for metastatic PPGLs or the syndrome-associated PPGLs.

Sunitinib, an orally administered TKI, can target both VEGFR and PDGFR (133), and therefore, it could potentially serve as a therapeutic reagent for PPGLs treatment. Early *in vitro* studies showed that sunitinib can repress the growth of PCCs (134), inhibit both synthesis and secretion of catecholamine (135). Several clinical trials have suggested that patients with metastatic PPGLs responded well to sunitinib (136–140). Results from one of our recent studies also suggested that sunitinib could be an optional therapy for patients with VHL disease-associated PCCs (141). Results from the SNIPP trial showed that sunitinib at 50mg daily benefited most patients with progressive PPGLs. Of 23 evaluable cases, the disease control rate (DCR) was 83% and median progression free survival (PFS) was 13.4 months, 3 (13%)

patients with germline variants in *RET* or *SDHx* achieved a partial response (PR), 16 (70%) patients had stable disease (SD) (142). Currently, a phase II clinical trial (the First International Randomized Study in Malignant Progressive Pheochromocytoma and Paraganglioma, FIRSTMAP) studying the effect of sunitinib on PPGLs is ongoing. In addition, results from *sdhb* knockout tumors bearing mice showed that sunitinib treatment can prevent tumor growth and vessel development in the first 2 weeks; thereafter, resistance will develop (143). Another study by using both *in vivo* and *in vitro* models demonstrated that sunitinib and sorafenib can inhibit the growth of PCCs (144, 145). Previous study reported that a patient with recurrence and metastatic PPGLs responded well to 12 weeks of sorafenib treatment evidenced by regressed metastatic and decreased catecholamine level (146).

In addition, cabozantinib also appears to be a promising TKI for patients with PPGLs, especially for those with bone metastases. A trial (NCT02302833) enrolled 11 PPGLs patients with bone metastases is currently ongoing. Preliminary results identified 4 patients with PR (37%) and 6 patients with SD (55%); all patients with SD had tumor regression (18%–29%). The DCR was 92%, PFS was 16 months. None of the patients had any serious hypertension or cardiovascular events (147). A recent trial (NCT01967576) showed that 36% of patients with metastatic PPGLs achieved a PR when treated with axitinib

(148); while only one of seven patients with metastatic PPGLs who received pazopanib showed a PR (149). Finally, recruitment for a phase II clinical trial has just begun to test if lenvatinib can be used as an anti-angiogenic medication for metastatic PPGLs (www.ClinicalTrials.gov) (**Figure 2**).

Although the promising therapeutic effects of TKIs on PPGLs have been widely reported, the toxicity of TKIs should also be mentioned. The side effects of TKIs include fatigue, nausea, thrombocytopenia, hypertension, myocardial infarction, and restrictive cardiomyopathy and so on. O'Kane et al. reported that due to severe adverse events, several patients needed to reduce the dose of sunitinib, and even 20% patients discontinued trial participation (142). A phase III clinical trial compared the safety of pazopanib and sunitinib in metastatic RCC, the results showed that patients treated with sunitinib had a higher incidence of fatigue, the hand-foot syndrome and thrombocytopenia than patients treated with pazopanib. Although the rate of cardiovascular adverse events of pazopanib were similar to that of sunitinib, the abnormal liver tests leading to discontinuation in pazopanib-treatment patients should be noted (139). Furthermore, the tolerance of axitinib was similar to that of other VEGFR inhibitors. Rini et al. reported that axitinib more frequently causes hypertension than sorafenib (40% vs. 29%) (NCT00678392) (140). Similarly, Van Geel et al. reported that the incidence of hypertension in axitinib-treatment patients was higher than that in pazopanib-treatment patients (150). Burotto Pichun et al. reported that even 80% axitinib-treatment patients developed severe hypertension (148). Recently, a phase III randomized ATLAS trial assessed the safety of axitinib versus placebo, axitinib-treated patients had more grade 3/4 adverse events and discontinuations (151). Taken together, the safety of TKIs needs to be further evaluated in the future.

HIFs Inhibitors

Transcription factors including HIFs have been historically considered undruggable. This is one of the reasons that research in the pharmaceutical field has been mainly focusing on HIF's downstream pathways, such as VEGF. However, based on the structure of HIF-2 α (152), two compounds PT2385 and PT2399 targeting HIF-2 α were successfully identified (145, 153). Subsequent *in vitro* and *in vivo* studies showed that these compounds can inhibit the growth of clear-cell RCC (154). A phase I trial found that for patients with progressive clear-cell RCC the complete response, partial response, and stabilized disease to PT2385 were 2%, 12%, and 52%, respectively (155). It has been proposed that HIF-2 α inhibitors possess a great potential for the treatment of advanced PPGLs (156). These initial results could also spearhead a multitude of preclinical and clinical studies assessing the efficiency of the compounds in other tumor types. In fact, PT2385 has entered its phase II clinical trial (NCT03108066) evaluating its efficacy in patients with advanced cancers carrying a *VHL* germline mutation. Recently, second-generation allosteric inhibitor of HIF-2 α PT2977 (MK-6482) was identified. Compared to PT2385, PT2977 have increased potency and improved pharmacokinetic profile (157). The result of phase I/II trial of PT2977 in 55 patients with advanced RCCs

revealed that 24% patients experienced a confirmed PR and 54% had SD, with a clinical benefit rate of 78%. Moreover, a PT2977 monotherapy Phase III trial in patients with previously treated advanced RCC is planned (158). Notably, previous studies reported that HIF-2 α was overexpressed in *VHL* and in *SDH*-related PPGLs compared to HIF-1 α (159, 160). Therefore, inhibitors targeting HIF-2 α appear to be more promising than inhibitors targeting HIF-1 α .

Other Compounds Targeting VHL/HIF Axis

Theoretically, any compounds capable of inhibiting the VHL/HIF axis can potentially become therapeutic reagents for the treatment of metastatic PPGLs. For example, the HSP90 inhibitors, 17-N-allylamino-17-demethoxy geldanamycin (17-AAG) and 17-dimethylaminoethylamino-17-demethoxygeldanamycin (17-DMAG) (161–163), and histone deacetylase inhibitor, vorinostat (164, 165), are capable of inducing HIF- α degradation. Topotecan can downregulate HIF- α by inhibiting topoisomerase I (TOP-I) (166–168). Of note, topotecan has already been used as a therapeutic reagent for the treatment of metastatic ovarian carcinoma, recurrent small cell lung cancer, and recurrent cervical cancer (169–171). Acriflavine can inhibit dimerization between HIF- α and HIF- β and subsequently repress the expression of HIFs target genes (172). 2-Methoxyestradiol (2-ME), an active metabolite of 17 β -estradiol, can inhibit the synthesis, nuclear translocation, and transcriptional activity of HIF- α (173, 174). In addition, an antiplatelet aggregation agent YC-1 can not only suppress HIFs transcriptional activity by inhibiting p300 recruitment but also promote HIF- α degradation by enhancing FIH binding (175). Finally, two anthracyclines, doxorubicin and daunorubicin, have been demonstrated to inhibit the expression of HIFs targets efficiently by interrupting HIF- α recruitment (176).

There are also compounds inhibiting HIF-1 α synthesis. For example, PX-478 is capable of downregulating both the mRNA and protein levels of HIF-1 α (177–179). EZN-2208 (PEG-SN38) can downregulate the expression of HIF-1 α in lymphocytic leukemia (180). By hybridizing with HIF-1 α mRNA, EZN-2968, a 3rd generation antisense oligonucleotide, can specifically inhibit HIF-1 α translation (181, 182). Chetomin is capable of repressing xenograft growth *in vivo* by disrupting HIF-1 α and p300 interaction (183). Finally, there is a myriad of compounds including echinomycin, CAY10585, KC7F2, glyceollins, bisphenol A, LW6, PX-12, cryptotanshinone (CPT), cyclo-CLLFVY, and indenopyrazoles 21 that have all been validated as selective inhibitors of HIF-1 α with different molecular mechanisms (184–196).

CONCLUSION

The VHL/HIF axis plays an important role in oxygen homeostasis and cellular metabolism in both physiology and pathology. Dysregulation of this axis due to either germline mutations, somatic mutations, and epigenetic dysregulation can be involved in tumorigenesis and progression of different cancer types

including PPGLs. Mechanistically, by reprogramming metabolic pathways the abnormally activated HIFs drive cancer cells toward aerobic glycolysis. Based on the underlying molecular mechanisms of VHL/HIF axis in PPGLs development, a wide spectrum of drugs specifically targeting this axis have been and will continue to be developed as PPGL therapeutics. With a better understanding of the relationship between VHL/HIF axis and PPGLs, more accurate diagnosis and prognosis of PPGLs, as well as efficacious therapeutics against PPGLs, are expected in the near future.

AUTHOR CONTRIBUTIONS

SP, QL, JZ, XT, JX, and YH contributed to the writing of the manuscript. NS, JJ, and DZ provided consultation and

contributed to the revising of the manuscript. All authors contributed to the article and approved the submitted version.

FUNDING

This work was supported by the National Natural Science Foundation of China (81972398, JJ) and University Research Project of Army Medical University (218XLC3073, JZ).

ACKNOWLEDGMENTS

The authors thank Drs. Farhadul Islam, Ichiro Abe, Alfred King-yin Lam, and Suja Pillai for inviting this review submission.

REFERENCES

- Lenders JW, Eisenhofer G, Mannelli M, Pacak K. Pheochromocytoma. *Lancet* (2005) 366(9486):665–75. doi: 10.1016/S0140-6736(05)67139-5
- Stenstrom G, Svardsudd K. Pheochromocytoma in Sweden 1958–1981. An analysis of the National Cancer Registry Data. *Acta Med Scand* (1986) 220 (3):225–32. doi: 10.1111/j.0954-6820.1986.tb02755.x
- Ariton M, Juan CS, AvRuskin TW. Pheochromocytoma: clinical observations from a Brooklyn tertiary hospital. *Endocr Pract* (2000) 6 (3):249–52. doi: 10.4158/EP.6.3.249
- Beard CM, Sheps SG, Kurland LT, Carney JA, Lie JT. Occurrence of pheochromocytoma in Rochester, Minnesota, 1950 through 1979. *Mayo Clin Proc* (1983) 58(12):802–4.
- Eisenhofer G, Pacak K, Huynh TT, Qin N, Bratslavsky G, Linehan WM, et al. Catecholamine metabolomic and secretory phenotypes in pheochromocytoma. *Endocr Relat Cancer* (2011) 18(1):97–111. doi: 10.1677/ERC-10-0211
- Nomura K, Kimura H, Shimizu S, Kodama H, Okamoto T, Obara T, et al. Survival of patients with metastatic malignant pheochromocytoma and efficacy of combined cyclophosphamide, vincristine, and dacarbazine chemotherapy. *J Clin Endocrinol Metab* (2009) 94(8):2850–6. doi: 10.1210/jc.2008-2697
- Welander J, Soderkvist P, Gimm O. Genetics and clinical characteristics of hereditary pheochromocytomas and paragangliomas. *Endocr Relat Cancer* (2011) 18(6):R253–76. doi: 10.1530/ERC-11-0170
- Ayala-Ramirez M, Feng L, Johnson MM, Ejaz S, Habra MA, Rich T, et al. Clinical risk factors for malignancy and overall survival in patients with pheochromocytomas and sympathetic paragangliomas: primary tumor size and primary tumor location as prognostic indicators. *J Clin Endocrinol Metab* (2011) 96(3):717–25. doi: 10.1210/jc.2010-1946
- Taieb D, Pacak K. Genetic Determinants of Pheochromocytoma and Paraganglioma Imaging Phenotypes. *J Nucl Med* (2020) 61(5):643–5. doi: 10.2967/jnumed.120.245613
- Dahia PL. Pheochromocytoma and paraganglioma pathogenesis: learning from genetic heterogeneity. *Nat Rev Cancer* (2014) 14(2):108–19. doi: 10.1038/nrc3648
- Fishbein L, Leshchiner I, Walter V, Danilova L, Robertson AG, Johnson AR, et al. Comprehensive Molecular Characterization of Pheochromocytoma and Paraganglioma. *Cancer Cell* (2017) 31(2):181–93. doi: 10.1016/j.ccell.2017.01.001
- Samanta D, Prabhakar NR, Semenza GL. Systems biology of oxygen homeostasis. *Wiley Interdiscip Rev Syst Biol Med* (2017) 9(4). doi: 10.1002/wsbm.1382
- Wu D, Rastinejad F. Structural characterization of mammalian bHLH-PAS transcription factors. *Curr Opin Struct Biol* (2017) 43:1–9. doi: 10.1016/j.sbi.2016.09.011
- Yamashita K, Discher DJ, Hu J, Bishopric NH, Webster KA. Molecular regulation of the endothelin-1 gene by hypoxia. Contributions of hypoxia-inducible factor-1, activator protein-1, GATA-2, AND p300/CBP. *J Biol Chem* (2001) 276(16):12645–53. doi: 10.1074/jbc.M011344200
- Dayan F, Roux D, Brahimi-Horn MC, Pouyssegur J, Mazure NM. The oxygen sensor factor-inhibiting hypoxia-inducible factor-1 controls expression of distinct genes through the bifunctional transcriptional character of hypoxia-inducible factor-1alpha. *Cancer Res* (2006) 66 (7):3688–98. doi: 10.1158/0008-5472.CAN-05-4564
- Kaelin WJ Jr., Ratcliffe PJ. Oxygen sensing by metazoans: the central role of the HIF hydroxylase pathway. *Mol Cell* (2008) 30(4):393–402. doi: 10.1016/j.molcel.2008.04.009
- Bruick RK, McKnight SL. A conserved family of prolyl-4-hydroxylases that modify HIF. *Science* (2001) 294(5545):1337–40. doi: 10.1126/science.1066373
- Favier J, Buffet A, Gimenez-Roqueplo AP. HIF2A mutations in paraganglioma with polycythemia. *N Engl J Med* (2012) 367(22):2161. doi: 10.1056/NEJMc1211953
- Ivan M, Haberberger T, Gervasi DC, Michelson KS, Gunzler V, Kondo K, et al. Biochemical purification and pharmacological inhibition of a mammalian prolyl hydroxylase acting on hypoxia-inducible factor. *Proc Natl Acad Sci USA* (2002) 99(21):13459–64. doi: 10.1073/pnas.192342099
- Baek JH, Mahon PC, Oh J, Kelly B, Krishnamachary B, Pearson M, et al. OS-9 interacts with hypoxia-inducible factor 1alpha and prolyl hydroxylases to promote oxygen-dependent degradation of HIF-1alpha. *Mol Cell* (2005) 17 (4):503–12. doi: 10.1016/j.molcel.2005.01.011
- Keith B, Johnson RS, Simon MC. HIF1alpha and HIF2alpha: sibling rivalry in hypoxic tumour growth and progression. *Nat Rev Cancer* (2011) 12(1):9–22. doi: 10.1038/nrc3183
- Al Tameemi W, Dale TP, Al-Jumaily RMK, Forsyth NR. Hypoxia-Modified Cancer Cell Metabolism. *Front Cell Dev Biol* (2019) 7:4. doi: 10.3389/fcell.2019.00004
- Bertout JA, Patel SA, Simon MC. The impact of O2 availability on human cancer. *Nat Rev Cancer* (2008) 8(12):967–75. doi: 10.1038/nrc2540
- Triner D, Shah YM. Hypoxia-inducible factors: a central link between inflammation and cancer. *J Clin Invest* (2016) 126(10):3689–98. doi: 10.1172/JCI84430
- Hu CJ, Wang LY, Chodosh LA, Keith B, Simon MC. Differential roles of hypoxia-inducible factor 1alpha (HIF-1alpha) and HIF-2alpha in hypoxic gene regulation. *Mol Cell Biol* (2003) 23(24):9361–74. doi: 10.1128/mcb.23.24.9361-9374.2003
- Liu Q, Wang Y, Tong D, Liu G, Yuan W, Zhang J, et al. A Somatic HIF2alpha Mutation-Induced Multiple and Recurrent Pheochromocytoma/Paraganglioma with Polycythemia: Clinical Study with Literature Review. *Endocr Pathol* (2017) 28(1):75–82. doi: 10.1007/s12022-017-9469-4
- Heikkila M, Pasanen A, Kivirikko KI, Myllyharju J. Roles of the human hypoxia-inducible factor (HIF)-3alpha variants in the hypoxia response. *Cell Mol Life Sci* (2011) 68(23):3885–901. doi: 10.1007/s00018-011-0679-5
- Jaakkola P, Mole DR, Tian YM, Wilson MI, Gielbert J, Gaskell SJ, et al. Targeting of HIF-alpha to the von Hippel-Lindau ubiquitylation complex by

- O₂-regulated prolyl hydroxylation. *Science* (2001) 292(5516):468–72. doi: 10.1126/science.1059796
29. Loboda A, Jozkowicz A, Dulak J. HIF-1 and HIF-2 transcription factors—similar but not identical. *Mol Cells* (2010) 29(5):435–42. doi: 10.1007/s10059-010-0067-2
 30. Semenza GL. Oxygen sensing, homeostasis, and disease. *N Engl J Med* (2011) 365(6):537–47. doi: 10.1056/NEJMra1011165
 31. Jochmanova I, Zhuang Z, Pacak K. Pheochromocytoma: Gasping for Air. *Horm Cancer* (2015) 6(5-6):191–205. doi: 10.1007/s12672-015-0231-4
 32. Kaelin WG Jr. The von Hippel-Lindau tumour suppressor protein: O₂ sensing and cancer. *Nat Rev Cancer* (2008) 8(11):865–73. doi: 10.1038/nrc2502
 33. Pouyssegur J, Dayan F, Mazure NM. Hypoxia signalling in cancer and approaches to enforce tumour regression. *Nature* (2006) 441(7092):437–43. doi: 10.1038/nature04871
 34. Gossage L, Eisen T, Maher ER. VHL, the story of a tumour suppressor gene. *Nat Rev Cancer* (2015) 15(1):55–64. doi: 10.1038/nrc3844
 35. Richard S, Graff J, Lindau J, Resche F. Von Hippel-Lindau disease. *Lancet* (2004) 363(9416):1231–4. doi: 10.1016/S0140-6736(04)15957-6
 36. Lonser RR, Glenn GM, Walther M, Chew EY, Libutti SK, Linehan WM, et al. von Hippel-Lindau disease. *Lancet* (2003) 361(9374):2059–67. doi: 10.1016/S0140-6736(03)13643-4
 37. Chittiboina P, Lonser RR. Von Hippel-Lindau disease. *Handb Clin Neurol* (2015) 132:139–56. doi: 10.1016/B978-0-444-62702-5.00010-X
 38. Richards FM. Molecular pathology of von Hippel-Lindau disease and the VHL tumour suppressor gene. *Expert Rev Mol Med* (2001) 2001:1–27. doi: 10.1017/S1462399401002654
 39. Clifford SC, Cockman ME, Smallwood AC, Mole DR, Woodward ER, Maxwell PH, et al. Contrasting effects on HIF-1 α regulation by disease-causing pVHL mutations correlate with patterns of tumorigenesis in von Hippel-Lindau disease. *Hum Mol Genet* (2001) 10(10):1029–38. doi: 10.1093/hmg/10.10.1029
 40. Zbar B, Kishida T, Chen F, Schmidt L, Maher ER, Richards FM, et al. Germline mutations in the Von Hippel-Lindau disease (VHL) gene in families from North America, Europe, and Japan. *Hum Mutat* (1996) 8(4):348–57. doi: 10.1002/(SICI)1098-1004(1996)8:4<348::AID-HUMU8>3.0.CO;2-3
 41. Liu Q, Yuan G, Tong D, Liu G, Yi Y, Zhang J, et al. Novel genotype-phenotype correlations in five Chinese families with Von Hippel-Lindau disease. *Endocr Connect* (2018) 7(7):870–8. doi: 10.1530/EC-18-0167
 42. Nordstrom-O'Brien M, van der Luijt RB, van Rooijen E, van den Ouweland AM, Majoor-Krakauer DF, Lolkema MP, et al. Genetic analysis of von Hippel-Lindau disease. *Hum Mutat* (2010) 31(5):521–37. doi: 10.1002/humu.21219
 43. Beroud C, Joly D, Gallou C, Staroz F, Orfanelli MT, Junien C. Software and database for the analysis of mutations in the VHL gene. *Nucleic Acids Res* (1998) 26(1):256–8. doi: 10.1093/nar/26.1.256
 44. Garcia A, Matias-Guiu X, Cabezas R, Chico A, Prat J, Baiget M, et al. Molecular diagnosis of von Hippel-Lindau disease in a kindred with a predominance of familial pheochromocytoma. *Clin Endocrinol (Oxf)* (1997) 46(3):359–63. doi: 10.1046/j.1365-2265.1997.00149.x
 45. Ang SO, Chen H, Hirota K, Gordeuk VR, Jelinek J, Guan Y, et al. Disruption of oxygen homeostasis underlies congenital Chuvash polycythemia. *Nat Genet* (2002) 32(4):614–21. doi: 10.1038/ng1019
 46. Gallou C, Chauveau D, Richard S, Joly D, Giraud S, Olschwang S, et al. Genotype-phenotype correlation in von Hippel-Lindau families with renal lesions. *Hum Mutat* (2004) 24(3):215–24. doi: 10.1002/humu.20082
 47. Weirich G, Klein B, Wohl T, Engelhardt D, Brauch H. VHL2C phenotype in a German von Hippel-Lindau family with concurrent VHL germline mutations P81S and L188V. *J Clin Endocrinol Metab* (2002) 87(11):5241–6. doi: 10.1210/jc.2002-020651
 48. Fukino K, Teramoto A, Adachi K, Takahashi H, Emi M. A family with hydrocephalus as a complication of cerebellar hemangioblastoma: identification of Pro157Leu mutation in the VHL gene. *J Hum Genet* (2000) 45(1):47–51. doi: 10.1007/s100380050009
 49. Hong B, Ma K, Zhou J, Zhang J, Wang J, Liu S, et al. Frequent Mutations of VHL Gene and the Clinical Phenotypes in the Largest Chinese Cohort With Von Hippel-Lindau Disease. *Front Genet* (2019) 10:867. doi: 10.3389/fgene.2019.00867
 50. Martin RL, Walpole I, Goldblatt J. Identification of two sporadically derived mutations in the Von Hippel-Lindau gene. *Hum Mutat* (1996) 7(2):185. doi: 10.1002/(SICI)1098-1004(1996)7:2<185::AID-HUMU22>3.0.CO;2-Y
 51. Crossey PA, Foster K, Richards FM, Phipps ME, Latif F, Tory K, et al. Molecular genetic investigations of the mechanism of tumorigenesis in von Hippel-Lindau disease: analysis of allele loss in VHL tumours. *Hum Genet* (1994) 93(1):53–8. doi: 10.1007/BF00218913
 52. Wang H, Shepard MJ, Zhang C, Dong L, Walker D, Guedez L, et al. Deletion of the von Hippel-Lindau Gene in Hemangioblasts Causes Hemangioblastoma-like Lesions in Murine Retina. *Cancer Res* (2018) 78(5):1266–74. doi: 10.1158/0008-5472.CAN-17-1718
 53. Lee JS, Lee JH, Lee KE, Kim JH, Hong JM, Ra EK, et al. Genotype-phenotype analysis of von Hippel-Lindau syndrome in Korean families: HIF- α binding site missense mutations elevate age-specific risk for CNS hemangioblastoma. *BMC Med Genet* (2016) 17(1):48. doi: 10.1186/s12881-016-0306-2
 54. Ong KR, Woodward ER, Killick P, Lim C, Macdonald F, Maher ER. Genotype-phenotype correlations in von Hippel-Lindau disease. *Hum Mutat* (2007) 28(2):143–9. doi: 10.1002/humu.20385
 55. Liu SJ, Wang JY, Peng SH, Li T, Ning XH, Hong BA, et al. Genotype and phenotype correlation in von Hippel-Lindau disease based on alteration of the HIF- α binding site in VHL protein. *Genet Med* (2018) 20(10):1266–73. doi: 10.1038/gim.2017.261
 56. Bishop T, Lau KW, Epstein AC, Kim SK, Jiang M, O'Rourke D, et al. Genetic analysis of pathways regulated by the von Hippel-Lindau tumor suppressor in *Caenorhabditis elegans*. *PLoS Biol* (2004) 2(10):e289. doi: 10.1371/journal.pbio.0020289
 57. Bommi-Reddy A, Almeciga I, Sawyer J, Geisen C, Li W, Harlow E, et al. Kinase requirements in human cells: III. Altered kinase requirements in VHL-/- cancer cells detected in a pilot synthetic lethal screen. *Proc Natl Acad Sci USA* (2008) 105(43):16484–9. doi: 10.1073/pnas.0806574105
 58. Ohh M, Yauch RL, Lonergan KM, Whaley JM, Stemmer-Rachamimov AO, Louis DN, et al. The von Hippel-Lindau tumor suppressor protein is required for proper assembly of an extracellular fibronectin matrix. *Mol Cell* (1998) 1(7):959–68. doi: 10.1016/S1097-2765(00)80096-9
 59. Knudson AG Jr. Mutation and cancer: statistical study of retinoblastoma. *Proc Natl Acad Sci U.S.A.* (1971) 68(4):820–3. doi: 10.1073/pnas.68.4.820
 60. Joosten SC, Smits KM, Aarts MJ, Melotte V, Koch A, Tjan-Heijnen VC, et al. Epigenetics in renal cell cancer: mechanisms and clinical applications. *Nat Rev Urol* (2018) 15(7):430–51. doi: 10.1038/s41585-018-0023-z
 61. Andreasson A, Kiss NB, Caramuta S, Sulaiman L, Svahn F, Backdahl M, et al. The VHL gene is epigenetically inactivated in pheochromocytomas and abdominal paragangliomas. *Epigenetics* (2013) 8(12):1347–54. doi: 10.4161/epi.26686
 62. Morris MR, Hughes DJ, Tian YM, Ricketts CJ, Lau KW, Gentle D, et al. Mutation analysis of hypoxia-inducible factors HIF1A and HIF2A in renal cell carcinoma. *Anticancer Res* (2009) 29(11):4337–43.
 63. Gladek I, Ferdin J, Horvat S, Calin GA, Kunej T. HIF1A gene polymorphisms and human diseases: Graphical review of 97 association studies. *Genes Chromosomes Cancer* (2017) 56(6):439–52. doi: 10.1002/gcc.22449
 64. Percy MJ, Beer PA, Campbell G, Dekker AW, Green AR, Oscier D, et al. Novel exon 12 mutations in the HIF2A gene associated with erythrocytosis. *Blood* (2008) 111(11):5400–2. doi: 10.1182/blood-2008-02-137703
 65. Percy MJ, Furlow PW, Lucas GS, Li X, Lappin TR, McMullin MF, et al. A gain-of-function mutation in the HIF2A gene in familial erythrocytosis. *N Engl J Med* (2008) 358(2):162–8. doi: 10.1056/NEJMoa073123
 66. Liu Q, Tong D, Liu G, Yi Y, Zhang D, Zhang J, et al. HIF2A germline-mutation-induced polycythemia in a patient with VHL-associated renal-cell carcinoma. *Cancer Biol Ther* (2017) 18(12):944–7. doi: 10.1080/15384047.2017.1394553
 67. Lorenzo FR, Yang C, Ng Tang Fui M, Vankayalapati H, Zhuang Z, Huynh T, et al. A novel EPAS1/HIF2A germline mutation in a congenital polycythemia with paraganglioma. *J Mol Med (Berl)* (2013) 91(4):507–12. doi: 10.1007/s00109-012-0967-z

68. Comino-Mendez I, de Cubas AA, Bernal C, Alvarez-Escola C, Sanchez-Malo C, Ramirez-Tortosa CL, et al. Tumoral EPAS1 (HIF2A) mutations explain sporadic pheochromocytoma and paraganglioma in the absence of erythrocytosis. *Hum Mol Genet* (2013) 22(11):2169–76. doi: 10.1093/hmg/ddt069
69. Zhuang Z, Yang C, Lorenzo F, Merino M, Fojo T, Kebebew E, et al. Somatic HIF2A gain-of-function mutations in paraganglioma with polycythemia. *N Engl J Med* (2012) 367(10):922–30. doi: 10.1056/NEJMoa1205119
70. Pacak K, Jochmanova I, Prodanov T, Yang C, Merino MJ, Fojo T, et al. New syndrome of paraganglioma and somatostatinoma associated with polycythemia. *J Clin Oncol* (2013) 31(13):1690–8. doi: 10.1200/JCO.2012.47.1912
71. Toledo RA, Qin Y, Srikantan S, Morales NP, Li Q, Deng Y, et al. In vivo and in vitro oncogenic effects of HIF2A mutations in pheochromocytomas and paragangliomas. *Endocr Relat Cancer* (2013) 20(3):349–59. doi: 10.1530/ERC-13-0101
72. Buffet A, Smati S, Mansuy L, Menara M, Lebras M, Heymann MF, et al. Mosaicism in HIF2A-related polycythemia-paraganglioma syndrome. *J Clin Endocrinol Metab* (2014) 99(2):E369–73. doi: 10.1210/jc.2013-2600
73. Vaidya A, Flores SK, Cheng ZM, Nicolas M, Deng Y, Opatowsky AR, et al. EPAS1 Mutations and Paragangliomas in Cyanotic Congenital Heart Disease. *N Engl J Med* (2018) 378(13):1259–61. doi: 10.1056/NEJMc1716652
74. Minamishima YA, Moslehi J, Bardeesy N, Cullen D, Bronson RT, Kaelin WJr. Somatic inactivation of the PHD2 prolyl hydroxylase causes polycythemia and congestive heart failure. *Blood* (2008) 111(6):3236–44. doi: 10.1182/blood-2007-10-117812
75. Percy MJ, Furlow PW, Beer PA, Lappin TR, McMullin MF, Lee FS. A novel erythrocytosis-associated PHD2 mutation suggests the location of a HIF binding groove. *Blood* (2007) 110(6):2193–6. doi: 10.1182/blood-2007-04-084434
76. Ladrone C, Carcenac R, Leporrier M, Gad S, Le Hello C, Galateau-Salle F, et al. PHD2 mutation and congenital erythrocytosis with paraganglioma. *N Engl J Med* (2008) 359(25):2685–92. doi: 10.1056/NEJMoa0806277
77. Yang C, Zhuang Z, Flidner SM, Shankavaram U, Sun MG, Bullova P, et al. Germ-line PHD1 and PHD2 mutations detected in patients with pheochromocytoma/paraganglioma-polycythemia. *J Mol Med (Berl)* (2015) 93(1):93–104. doi: 10.1007/s00109-014-1205-7
78. Lee S, Nakamura E, Yang H, Wei W, Linggi MS, Sajan MP, et al. Neuronal apoptosis linked to EglN3 prolyl hydroxylase and familial pheochromocytoma genes: developmental culling and cancer. *Cancer Cell* (2005) 8(2):155–67. doi: 10.1016/j.ccr.2005.06.015
79. Baysal BE, Ferrell RE, Willett-Brozick JE, Lawrence EC, Myssiorek D, Bosch A, et al. Mutations in SDHD, a mitochondrial complex II gene, in hereditary paraganglioma. *Science* (2000) 287(5454):848–51. doi: 10.1126/science.287.5454.848
80. Niemann S, Muller U. Mutations in SDHC cause autosomal dominant paraganglioma, type 3. *Nat Genet* (2000) 26(3):268–70. doi: 10.1038/81551
81. Korpershoek E, Favier J, Gaal J, Burnichon N, van Gessel B, Oudijk L, et al. SDHA immunohistochemistry detects germline SDHA gene mutations in apparently sporadic paragangliomas and pheochromocytomas. *J Clin Endocrinol Metab* (2011) 96(9):E1472–6. doi: 10.1210/jc.2011-1043
82. Burnichon N, Briere JJ, Libe R, Vescovo L, Riviere J, Tissier F, et al. SDHA is a tumor suppressor gene causing paraganglioma. *Hum Mol Genet* (2010) 19(15):3011–20. doi: 10.1093/hmg/ddq206
83. Selak MA, Armour SM, MacKenzie ED, Boulahbel H, Watson DG, Mansfield KD, et al. Succinate links TCA cycle dysfunction to oncogenesis by inhibiting HIF- α prolyl hydroxylase. *Cancer Cell* (2005) 7(1):77–85. doi: 10.1016/j.ccr.2004.11.022
84. Philip B, Ito K, Moreno-Sanchez R, Ralph SJ. HIF expression and the role of hypoxic microenvironments within primary tumours as protective sites driving cancer stem cell renewal and metastatic progression. *Carcinogenesis* (2013) 34(8):1699–707. doi: 10.1093/carcin/bgt209
85. Pan Y, Mansfield KD, Bertozzi CC, Rudenko V, Chan DA, Giaccia AJ, et al. Multiple factors affecting cellular redox status and energy metabolism modulate hypoxia-inducible factor prolyl hydroxylase activity in vivo and in vitro. *Mol Cell Biol* (2007) 27(3):912–25. doi: 10.1128/MCB.01223-06
86. Wang L, Lam G, Thummel CS. Med24 and Mdh2 are required for Drosophila larval salivary gland cell death. *Dev Dyn* (2010) 239(3):954–64. doi: 10.1002/dvdy.22213
87. Calsina B, Curras-Freixes M, Buffet A, Pons T, Contreras L, Leton R, et al. Role of MDH2 pathogenic variant in pheochromocytoma and paraganglioma patients. *Genet Med* (2018) 20(12):1652–62. doi: 10.1038/s41436-018-0068-7
88. Castro-Vega LJ, Buffet A, De Cubas AA, Cascon A, Menara M, Khalifa E, et al. Germline mutations in FH confer predisposition to malignant pheochromocytomas and paragangliomas. *Hum Mol Genet* (2014) 23(9):2440–6. doi: 10.1093/hmg/ddt639
89. Zhao S, Lin Y, Xu W, Jiang W, Zha Z, Wang P, et al. Glioma-derived mutations in IDH1 dominantly inhibit IDH1 catalytic activity and induce HIF-1 α . *Science* (2009) 324(5924):261–5. doi: 10.1126/science.1170944
90. Baba M, Hirai S, Yamada-Okabe H, Hamada K, Tabuchi H, Kobayashi K, et al. Loss of von Hippel-Lindau protein causes cell density dependent deregulation of CyclinD1 expression through hypoxia-inducible factor. *Oncogene* (2003) 22(18):2728–38. doi: 10.1038/sj.onc.1206373
91. Hudson CC, Liu M, Chiang GG, Otterness DM, Loomis DC, Kaper F, et al. Regulation of hypoxia-inducible factor 1 α expression and function by the mammalian target of rapamycin. *Mol Cell Biol* (2002) 22(20):7004–14. doi: 10.1128/mcb.22.20.7004-7014.2002
92. Mayerhofer M, Valent P, Sperr WR, Griffin JD, Sillaber C. BCR/ABL induces expression of vascular endothelial growth factor and its transcriptional activator, hypoxia inducible factor-1 α , through a pathway involving phosphoinositide 3-kinase and the mammalian target of rapamycin. *Blood* (2002) 100(10):3767–75. doi: 10.1182/blood-2002-01-0109
93. Jochmanova I, Yang C, Zhuang Z, Pacak K. Hypoxia-inducible factor signaling in pheochromocytoma: turning the rudder in the right direction. *J Natl Cancer Inst* (2013) 105(17):1270–83. doi: 10.1093/jnci/djt201
94. Vicha A, Musil Z, Pacak K. Genetics of pheochromocytoma and paraganglioma syndromes: new advances and future treatment options. *Curr Opin Endocrinol Diabetes Obes* (2013) 20(3):186–91. doi: 10.1097/MED.0b013e32835fcc45
95. Semenza GL. A compendium of proteins that interact with HIF-1 α . *Exp Cell Res* (2017) 356(2):128–35. doi: 10.1016/j.yexcr.2017.03.041
96. Ajith TA. Current insights and future perspectives of hypoxia-inducible factor-targeted therapy in cancer. *J Basic Clin Physiol Pharmacol* (2018) 30(1):11–8. doi: 10.1515/jbcp-2017-0167
97. Shen C, Kaelin WJr. The VHL/HIF axis in clear cell renal carcinoma. *Semin Cancer Biol* (2013) 23(1):18–25. doi: 10.1016/j.semcancer.2012.06.001
98. Jang M, Kim SS, Lee J. Cancer cell metabolism: implications for therapeutic targets. *Exp Mol Med* (2013) 45:e45. doi: 10.1038/emmm.2013.85
99. Zhong H, De Marzo AM, Laughner E, Lim M, Hilton DA, Zagzag D, et al. Overexpression of hypoxia-inducible factor 1 α in common human cancers and their metastases. *Cancer Res* (1999) 59(22):5830–5.
100. Maxwell PH, Dachs GU, Gleadle JM, Nicholls LG, Harris AL, Stratford IJ, et al. Hypoxia-inducible factor-1 modulates gene expression in solid tumors and influences both angiogenesis and tumor growth. *Proc Natl Acad Sci USA* (1997) 94(15):8104–9. doi: 10.1073/pnas.94.15.8104
101. Liberti MV, Locasale JW. The Warburg Effect: How Does it Benefit Cancer Cells? *Trends Biochem Sci* (2016) 41(3):211–8. doi: 10.1016/j.tibs.2015.12.001
102. Vander Heiden MG, Cantley LC, Thompson CB. Understanding the Warburg effect: the metabolic requirements of cell proliferation. *Science* (2009) 324(5930):1029–33. doi: 10.1126/science.1160809
103. Semenza GL. Regulation of cancer cell metabolism by hypoxia-inducible factor 1. *Semin Cancer Biol* (2009) 19(1):12–6. doi: 10.1016/j.semcancer.2008.11.009
104. Maxwell PH, Pugh CW, Ratcliffe PJ. Activation of the HIF pathway in cancer. *Curr Opin Genet Dev* (2001) 11(3):293–9. doi: 10.1016/s0959-437x(00)00193-3
105. Masoud GN, Li W. HIF-1 α pathway: role, regulation and intervention for cancer therapy. *Acta Pharm Sin B* (2015) 5(5):378–89. doi: 10.1016/j.apsb.2015.05.007
106. Gordan JD, Thompson CB, Simon MC. HIF and c-Myc: sibling rivals for control of cancer cell metabolism and proliferation. *Cancer Cell* (2007) 12(2):108–13. doi: 10.1016/j.ccr.2007.07.006

107. Icard P, Lincet H. A global view of the biochemical pathways involved in the regulation of the metabolism of cancer cells. *Biochim Biophys Acta* (2012) 1826(2):423–33. doi: 10.1016/j.bbcan.2012.07.001
108. Kruspig B, Zhivotovsky B, Gogvadze V. Mitochondrial substrates in cancer: drivers or passengers? *Mitochondrion* (2014) 19 Pt A:8–19. doi: 10.1016/j.mito.2014.08.007
109. Weidemann A, Johnson RS. Biology of HIF-1alpha. *Cell Death Differ* (2008) 15(4):621–7. doi: 10.1038/cdd.2008.12
110. Erlic Z, Beuschlein F. Metabolic Alterations in Patients with Pheochromocytoma. *Exp Clin Endocrinol Diabetes* (2019) 127(2-03):129–36. doi: 10.1055/a-0649-0960
111. Richter S, Gieldon L, Pang Y, Peitzsch M, Huynh T, Leton R, et al. Metabolome-guided genomics to identify pathogenic variants in isocitrate dehydrogenase, fumarate hydratase, and succinate dehydrogenase genes in pheochromocytoma and paraganglioma. *Genet Med* (2019) 21(3):705–17. doi: 10.1038/s41436-018-0106-5
112. Gottlieb E, Tomlinson IP. Mitochondrial tumour suppressors: a genetic and biochemical update. *Nat Rev Cancer* (2005) 5(11):857–66. doi: 10.1038/nrc1737
113. Richter S, Peitzsch M, Rapizzi E, Lenders JW, Qin N, de Cubas AA, et al. Krebs cycle metabolite profiling for identification and stratification of pheochromocytomas/paragangliomas due to succinate dehydrogenase deficiency. *J Clin Endocrinol Metab* (2014) 99(10):3903–11. doi: 10.1210/jc.2014-2151
114. Dang L, White DW, Gross S, Bennett BD, Bittinger MA, Driggers EM, et al. Cancer-associated IDH1 mutations produce 2-hydroxyglutarate. *Nature* (2009) 462(7274):739–44. doi: 10.1038/nature08617
115. Xiao M, Yang H, Xu W, Ma S, Lin H, Zhu H, et al. Inhibition of alpha-KG-dependent histone and DNA demethylases by fumarate and succinate that are accumulated in mutations of FH and SDH tumor suppressors. *Genes Dev* (2012) 26(12):1326–38. doi: 10.1101/gad.191056.112
116. Peng X, Gao H, Xu R, Wang H, Mei J, Liu C. The interplay between HIF-1alpha and noncoding RNAs in cancer. *J Exp Clin Cancer Res* (2020) 39(1):27. doi: 10.1186/s13046-020-1535-y
117. Huang X, Zuo J. Emerging roles of miR-210 and other non-coding RNAs in the hypoxic response. *Acta Biochim Biophys Sin (Shanghai)* (2014) 46(3):220–32. doi: 10.1093/abbs/gmt141
118. Li L, Huang K, You Y, Fu X, Hu L, Song L, et al. Hypoxia-induced miR-210 in epithelial ovarian cancer enhances cancer cell viability via promoting proliferation and inhibiting apoptosis. *Int J Oncol* (2014) 44(6):2111–20. doi: 10.3892/ijo.2014.2368
119. Ying Q, Liang L, Guo W, Zha R, Tian Q, Huang S, et al. Hypoxia-inducible microRNA-210 augments the metastatic potential of tumor cells by targeting vacuole membrane protein 1 in hepatocellular carcinoma. *Hepatology* (2011) 54(6):2064–75. doi: 10.1002/hep.24614
120. Yang W, Sun T, Cao J, Liu F, Tian Y, Zhu W. Downregulation of miR-210 expression inhibits proliferation, induces apoptosis and enhances radiosensitivity in hypoxic human hepatoma cells in vitro. *Exp Cell Res* (2012) 318(8):944–54. doi: 10.1016/j.yexcr.2012.02.010
121. Calsina B, Castro-Vega LJ, Torres-Perez R, Inglada-Perez L, Curras-Freixes M, Roldan-Romero JM, et al. Integrative multi-omics analysis identifies a prognostic miRNA signature and a targetable miR-21-3p/TSC2/mTOR axis in metastatic pheochromocytoma/paraganglioma. *Theranostics* (2019) 9(17):4946–58. doi: 10.7150/thno.35458
122. Flippot R, Beinse G, Boileve A, Vibert J, Malouf GG. Long non-coding RNAs in genitourinary malignancies: a whole new world. *Nat Rev Urol* (2019) 16(8):484–504. doi: 10.1038/s41585-019-0195-1
123. Kim HC, Lee JS, Kim SH, So HS, Woo CY, Lee JL. Sunitinib treatment for metastatic renal cell carcinoma in patients with von hippel-lindau disease. *Cancer Res Treat* (2013) 45(4):349–53. doi: 10.4143/crt.2013.45.4.349
124. Semenza GL. Defining the role of hypoxia-inducible factor 1 in cancer biology and therapeutics. *Oncogene* (2010) 29(5):625–34. doi: 10.1038/onc.2009.441
125. Melillo G. Hypoxia-inducible factor 1 inhibitors. *Methods Enzymol* (2007) 435:385–402. doi: 10.1016/S0076-6879(07)35020-9
126. Melillo G. Targeting hypoxia cell signaling for cancer therapy. *Cancer Metastasis Rev* (2007) 26(2):341–52. doi: 10.1007/s10555-007-9059-x
127. Xia Y, Choi HK, Lee K. Recent advances in hypoxia-inducible factor (HIF)-1 inhibitors. *Eur J Med Chem* (2012) 49:24–40. doi: 10.1016/j.ejmech.2012.01.033
128. Wang Y, Li Z, Zhang H, Jin H, Sun L, Dong H, et al. HIF-1alpha and HIF-2alpha correlate with migration and invasion in gastric cancer. *Cancer Biol Ther* (2010) 10(4):376–82. doi: 10.4161/cbt.10.4.12441
129. Joshi S, Singh AR, Zulcic M, Durden DL. A macrophage-dominant PI3K isoform controls hypoxia-induced HIF1alpha and HIF2alpha stability and tumor growth, angiogenesis, and metastasis. *Mol Cancer Res* (2014) 12(10):1520–31. doi: 10.1158/1541-7786.MCR-13-0682
130. Philips GK, Atkins MB. New agents and new targets for renal cell carcinoma. *Am Soc Clin Oncol Educ Book* (2014) e222–7. doi: 10.14694/EdBook_AM.2014.34.e222
131. Roskoski RJr. Properties of FDA-approved small molecule protein kinase inhibitors. *Pharmacol Res* (2019) 144:19–50. doi: 10.1016/j.phrs.2019.03.006
132. McCormack PL. Pazopanib: a review of its use in the management of advanced renal cell carcinoma. *Drugs* (2014) 74(10):1111–25. doi: 10.1007/s40265-014-0243-3
133. Faivre S, Demetri G, Sargent W, Raymond E. Molecular basis for sunitinib efficacy and future clinical development. *Nat Rev Drug Discovery* (2007) 6(9):734–45. doi: 10.1038/nrd2380
134. Saito Y, Tanaka Y, Aita Y, Ishii KA, Ikeda T, Isobe K, et al. Sunitinib induces apoptosis in pheochromocytoma tumor cells by inhibiting VEGFR2/Akt/mTOR/S6K1 pathways through modulation of Bcl-2 and BAD. *Am J Physiol Endocrinol Metab* (2012) 302(6):E615–25. doi: 10.1152/ajpendo.00035.2011
135. Aita Y, Ishii KA, Saito Y, Ikeda T, Kawakami Y, Shimano H, et al. Sunitinib inhibits catecholamine synthesis and secretion in pheochromocytoma tumor cells by blocking VEGF receptor 2 via PLC-gamma-related pathways. *Am J Physiol Endocrinol Metab* (2012) 303(8):E1006–14. doi: 10.1152/ajpendo.00156.2012
136. Joshua AM, Ezzat S, Asa SL, Evans A, Broom R, Freeman M, et al. Rationale and evidence for sunitinib in the treatment of malignant paraganglioma/pheochromocytoma. *J Clin Endocrinol Metab* (2009) 94(1):5–9. doi: 10.1210/jc.2008-1836
137. Jimenez C, Cabanillas ME, Santarpia L, Jonasch E, Kyle KL, Lano EA, et al. Use of the tyrosine kinase inhibitor sunitinib in a patient with von Hippel-Lindau disease: targeting angiogenic factors in pheochromocytoma and other von Hippel-Lindau disease-related tumors. *J Clin Endocrinol Metab* (2009) 94(2):386–91. doi: 10.1210/jc.2008-1972
138. Ayala-Ramirez M, Chougnet CN, Habra MA, Palmer JL, Leboulleux S, Cabanillas ME, et al. Treatment with sunitinib for patients with progressive metastatic pheochromocytomas and sympathetic paragangliomas. *J Clin Endocrinol Metab* (2012) 97(11):4040–50. doi: 10.1210/jc.2012-2356
139. Motzer RJ, Hutson TE, Cella D, Reeves J, Hawkins R, Guo J, et al. Pazopanib versus sunitinib in metastatic renal-cell carcinoma. *N Engl J Med* (2013) 369(8):722–31. doi: 10.1056/NEJMoa1303989
140. Rini BI, Escudier B, Tomczak P, Kaprin A, Szczylik C, Hutson TE, et al. Comparative effectiveness of axitinib versus sorafenib in advanced renal cell carcinoma (AXIS): a randomised phase 3 trial. *Lancet* (2011) 378(9807):1931–9. doi: 10.1016/S0140-6736(11)61613-9
141. Yuan G, Liu Q, Tong D, Liu G, Yi Y, Zhang J, et al. A retrospective case study of sunitinib treatment in three patients with Von Hippel-Lindau disease. *Cancer Biol Ther* (2018) 19(9):766–72. doi: 10.1080/15384047.2018.1470732
142. O'Kane GM, Ezzat S, Joshua AM, Bourdeau I, Leibowitz-Amit R, Olney HJ, et al. A phase 2 trial of sunitinib in patients with progressive paraganglioma or pheochromocytoma: the SNIPP trial. *Br J Cancer* (2019) 120(12):1113–9. doi: 10.1038/s41416-019-0474-x
143. Facchin C, Perez-Liva M, Garofalakis A, Viel T, Certain A, Balvay D, et al. Concurrent imaging of vascularization and metabolism in a mouse model of paraganglioma under anti-angiogenic treatment. *Theranostics* (2020) 10(8):3518–32. doi: 10.7150/thno.40687
144. Denorme M, Yon L, Roux C, Gonzalez BJ, Baudin E, Anouar Y, et al. Both sunitinib and sorafenib are effective treatments for pheochromocytoma in a xenograft model. *Cancer Lett* (2014) 352(2):236–44. doi: 10.1016/j.canlet.2014.07.005
145. Wallace EM, Rizzi JP, Han G, Wehn PM, Cao Z, Du X, et al. A Small-Molecule Antagonist of HIF2alpha Is Efficacious in Preclinical Models of

- Renal Cell Carcinoma. *Cancer Res* (2016) 76(18):5491–500. doi: 10.1158/0008-5472.CAN-16-0473
146. Gunaldi M, Kara IO, Duman BB, Afsar CU, Ergin M, Avci A. A new approach to the treatment of metastatic paraganglioma: sorafenib. *Cancer Res Treat* (2014) 46(4):411–4. doi: 10.4143/crt.2013.093
 147. Jimenez C, Fazeli S, Roman-Gonzalez A. Antiangiogenic therapies for pheochromocytoma and paraganglioma. *Endocr Relat Cancer* (2020) 27(7):R239–R54. doi: 10.1530/ERC-20-0043
 148. Pichun MEB, Edgerly M, Velarde M, Bates SE, Daerr R, Adams K, et al. Phase II clinical trial of axitinib in metastatic pheochromocytomas and paragangliomas (P/PG): Preliminary results. *J Clin Oncol* (2015) 33:457–. doi: 10.1200/jco.2015.33.7_suppl.457
 149. Jasim S, Suman VJ, Jimenez C, Harris P, Sideras K, Burton JK, et al. Phase II trial of pazopanib in advanced/progressive malignant pheochromocytoma and paraganglioma. *Endocrine* (2017) 57(2):220–5. doi: 10.1007/s12020-017-1359-5
 150. van Geel RM, Beijnen JH, Schellens JH. Concise drug review: pazopanib and axitinib. *Oncologist* (2012) 17(8):1081–9. doi: 10.1634/theoncologist.2012-0055
 151. Gross-Goupil M, Kwon TG, Eto M, Ye D, Miyake H, Seo SI, et al. Axitinib versus placebo as an adjuvant treatment of renal cell carcinoma: results from the phase III, randomized ATLAS trial. *Ann Oncol* (2018) 29(12):2371–8. doi: 10.1093/annonc/mdy454
 152. Erbel PJ, Card PB, Karakuzu O, Bruick RK, Gardner KH. Structural basis for PAS domain heterodimerization in the basic helix–loop–helix-PAS transcription factor hypoxia-inducible factor. *Proc Natl Acad Sci USA* (2003) 100(26):15504–9. doi: 10.1073/pnas.2533374100
 153. Cho H, Du X, Rizzi JP, Liberzon E, Chakraborty AA, Gao W, et al. On-target efficacy of a HIF-2 α antagonist in preclinical kidney cancer models. *Nature* (2016) 539:107–11. doi: 10.1038/nature19795
 154. Chen W, Hill H, Christie A, Kim MS, Holloman E, Pavia-Jimenez A, et al. Targeting renal cell carcinoma with a HIF-2 antagonist. *Nature* (2016) 539(7627):112–7. doi: 10.1038/nature19796
 155. Courtney KD, Infante JR, Lam ET, Figlin RA, Rini BI, Brugarolas J, et al. Phase I Dose-Escalation Trial of PT2385, a First-in-Class Hypoxia-Inducible Factor-2 α Antagonist in Patients With Previously Treated Advanced Clear Cell Renal Cell Carcinoma. *J Clin Oncol* (2018) 36(9):867–74. doi: 10.1200/JCO.2017.74.2627
 156. Toledo RA. New HIF2 α inhibitors: potential implications as therapeutics for advanced pheochromocytomas and paragangliomas. *Endocr Relat Cancer* (2017) 24(9):C9–C19. doi: 10.1530/ERC-16-0479
 157. Xu R, Wang K, Rizzi JP, Huang H, Grina JA, Schlachter ST, et al. 3-[(1S,2S,3R)-2,3-Difluoro-1-hydroxy-7-methylsulfonylindan-4-yl]oxy-5-fluorobenzo nitrile (PT2977), a Hypoxia-Inducible Factor 2 α (HIF-2 α) Inhibitor for the Treatment of Clear Cell Renal Cell Carcinoma. *J Med Chem* (2019) 62(15):6876–93. doi: 10.1021/acs.jmedchem.9b00719
 158. Choueiri TK, Plimack ER, Bauer TM, Merchan JR, Papadopoulos KP, McDermott DF, et al. (2019). A First-in-Human Phase 1/2 Trial of the Oral HIF-2 α Inhibitor PT2977 in Patients with Advanced RCC, in: *Presented at the 14th European International Kidney Cancer Symposium*, Dubrovnik, Croatia, March 29–30. doi: 10.1093/annonc/mdz249.010
 159. Favier J, Briere JJ, Burnichon N, Riviere J, Vescovo L, Benit P, et al. The Warburg effect is genetically determined in inherited pheochromocytomas. *PLoS One* (2009) 4(9):e7094. doi: 10.1371/journal.pone.0007094
 160. Morin A, Goncalves J, Moog S, Castro-Vega LJ, Job S, Buffet A, et al. TET-Mediated Hypermethylation Primes SDH-Deficient Cells for HIF2 α -Driven Mesenchymal Transition. *Cell Rep* (2020) 30(13):4551–66.e7. doi: 10.1016/j.celrep.2020.03.022
 161. Newman B, Liu Y, Lee HF, Sun D, Wang Y. HSP90 inhibitor 17-AAG selectively eradicates lymphoma stem cells. *Cancer Res* (2012) 72(17):4551–61. doi: 10.1158/0008-5472.CAN-11-3600
 162. Bohonowych JE, Peng S, Gopal U, Hance MW, Wing SB, Argraves KM, et al. Comparative analysis of novel and conventional Hsp90 inhibitors on HIF activity and angiogenic potential in clear cell renal cell carcinoma: implications for clinical evaluation. *BMC Cancer* (2011) 11:520. doi: 10.1186/1471-2407-11-520
 163. Ibrahim NO, Hahn T, Franke C, Stiehl DP, Wirthner R, Wenger RH, et al. Induction of the hypoxia-inducible factor system by low levels of heat shock protein 90 inhibitors. *Cancer Res* (2005) 65(23):11094–100. doi: 10.1158/0008-5472.CAN-05-1877
 164. Wigerup C, Pahlman S, Bexell D. Therapeutic targeting of hypoxia and hypoxia-inducible factors in cancer. *Pharmacol Ther* (2016) 164:152–69. doi: 10.1016/j.pharmthera.2016.04.009
 165. Hutt DM, Roth DM, Vignaud H, Cullin C, Bouchecareilh M. The histone deacetylase inhibitor, Vorinostat, represses hypoxia inducible factor 1 α expression through translational inhibition. *PLoS One* (2014) 9(8):e106224. doi: 10.1371/journal.pone.0106224
 166. Puppo M, Battaglia F, Ottaviano C, Delfino S, Ribatti D, Varesio L, et al. Topotecan inhibits vascular endothelial growth factor production and angiogenic activity induced by hypoxia in human neuroblastoma by targeting hypoxia-inducible factor-1 α and -2 α . *Mol Cancer Ther* (2008) 7(7):1974–84. doi: 10.1158/1535-7163.MCT-07-2059
 167. Rapisarda A, Uranchimeg B, Sordet O, Pommier Y, Shoemaker RH, Melillo G. Topoisomerase I-mediated inhibition of hypoxia-inducible factor 1: mechanism and therapeutic implications. *Cancer Res* (2004) 64(4):1475–82. doi: 10.1158/0008-5472.can-03-3139
 168. Bertozzi D, Marinello J, Manzo SG, Fornari F, Gramantieri L, Capranico G, et al. camptothecin, modulates HIF-1 α activity by changing miR expression patterns in human cancer cells. *Mol Cancer Ther* (2014) 13(1):239–48. doi: 10.1158/1535-7163.MCT-13-0729
 169. Lorusso D, Pietragalla A, Mainenti S, Masciullo V, Di Vagno G, Scambia G. Review role of topotecan in gynaecological cancers: current indications and perspectives. *Crit Rev Oncol Hematol* (2010) 74(3):163–74. doi: 10.1016/j.critrevonc.2009.08.001
 170. Horita N, Yamamoto M, Sato T, Tsukahara T, Nagakura H, Tashiro K, et al. Topotecan for Relapsed Small-cell Lung Cancer: Systematic Review and Meta-Analysis of 1347 Patients. *Sci Rep* (2015) 5:15437. doi: 10.1038/srep15437
 171. Musa F, Blank S, Muggia F. A pharmacokinetic evaluation of topotecan as a cervical cancer therapy. *Expert Opin Drug Metab Toxicol* (2013) 9(2):215–24. doi: 10.1517/17425255.2013.758249
 172. Lee K, Zhang H, Qian DZ, Rey S, Liu JO, Semenza GL. Acriflavine inhibits HIF-1 dimerization, tumor growth, and vascularization. *Proc Natl Acad Sci USA* (2009) 106(42):17910–5. doi: 10.1073/pnas.0909353106
 173. Ma L, Li G, Zhu H, Dong X, Zhao D, Jiang X, et al. 2-Methoxyestradiol synergizes with sorafenib to suppress hepatocellular carcinoma by simultaneously dysregulating hypoxia-inducible factor-1 and -2. *Cancer Lett* (2014) 355(1):96–105. doi: 10.1016/j.canlet.2014.09.011
 174. Zhou X, Liu C, Lu J, Zhu L, Li M. 2-Methoxyestradiol inhibits hypoxia-induced scleroderma fibroblast collagen synthesis by phosphatidylinositol 3-kinase/Akt/mTOR signalling. *Rheumatol (Oxford)* (2018) 57(9):1675–84. doi: 10.1093/rheumatology/key166
 175. Li SH, Shin DH, Chun YS, Lee MK, Kim MS, Park JW. A novel mode of action of YC-1 in HIF inhibition: stimulation of FIH-dependent p300 dissociation from HIF-1 α . *Mol Cancer Ther* (2008) 7(12):3729–38. doi: 10.1158/1535-7163.MCT-08-0074
 176. Lee K, Qian DZ, Rey S, Wei H, Liu JO, Semenza GL. Anthracycline chemotherapy inhibits HIF-1 transcriptional activity and tumor-induced mobilization of circulating angiogenic cells. *Proc Natl Acad Sci USA* (2009) 106(7):2353–8. doi: 10.1073/pnas.0812801106
 177. Pan X, Lv Y. Effects and Mechanism of Action of PX-478 in Oxygen-Induced Retinopathy in Mice. *Ophthalmic Res* (2020) 63(2):182–93. doi: 10.1159/000504023
 178. Lee K, Kim HM. A novel approach to cancer therapy using PX-478 as a HIF-1 α inhibitor. *Arch Pharm Res* (2011) 34(10):1583–5. doi: 10.1007/s12272-011-1021-3
 179. Sun K, Halberg N, Khan M, Magalang UJ, Scherer PE. Selective inhibition of hypoxia-inducible factor 1 α ameliorates adipose tissue dysfunction. *Mol Cell Biol* (2013) 33(5):904–17. doi: 10.1128/MCB.00951-12
 180. Coltella N, Valsecchi R, Ponente M, Ponzone M, Bernardi R. Synergistic Leukemia Eradication by Combined Treatment with Retinoic Acid and HIF Inhibition by EZN-2208 (PEG-SN38) in Preclinical Models of PML-RAR α and PLZF-RAR α -Driven Leukemia. *Clin Cancer Res* (2015) 21(16):3685–94. doi: 10.1158/1078-0432.CCR-14-3022
 181. Jeong W, Rapisarda A, Park SR, Kinders RJ, Chen A, Melillo G, et al. Pilot trial of EZN-2968, an antisense oligonucleotide inhibitor of hypoxia-

- inducible factor-1 alpha (HIF-1alpha), in patients with refractory solid tumors. *Cancer Chemother Pharmacol* (2014) 73(2):343–8. doi: 10.1007/s00280-013-2362-z
182. Greenberger LM, Horak ID, Filpula D, Sapra P, Westergaard M, Frydenlund HF, et al. A RNA antagonist of hypoxia-inducible factor-1alpha, EZN-2968, inhibits tumor cell growth. *Mol Cancer Ther* (2008) 7(11):3598–608. doi: 10.1158/1535-7163.MCT-08-0510
 183. Kung AL, Zabludoff SD, France DS, Freedman SJ, Tanner EA, Vieira A, et al. Small molecule blockade of transcriptional coactivation of the hypoxia-inducible factor pathway. *Cancer Cell* (2004) 6(1):33–43. doi: 10.1016/j.ccr.2004.06.009
 184. Kong D, Park EJ, Stephen AG, Calvani M, Cardellina JH, Monks A, et al. Echinomycin, a small-molecule inhibitor of hypoxia-inducible factor-1 DNA-binding activity. *Cancer Res* (2005) 65(19):9047–55. doi: 10.1158/0008-5472.CAN-05-1235
 185. Hu N, Jiang D, Huang E, Liu X, Li R, Liang X, et al. BMP9-regulated angiogenic signaling plays an important role in the osteogenic differentiation of mesenchymal progenitor cells. *J Cell Sci* (2013) 126(Pt 2):532–41. doi: 10.1242/jcs.114231
 186. Narita T, Yin S, Gelin CF, Moreno CS, Yepes M, Nicolaou KC, et al. Identification of a novel small molecule HIF-1alpha translation inhibitor. *Clin Cancer Res* (2009) 15(19):6128–36. doi: 10.1158/1078-0432.CCR-08-3180
 187. Lee SH, Jee JG, Bae JS, Liu KH, Lee YM. A group of novel HIF-1alpha inhibitors, glyceollins, blocks HIF-1alpha synthesis and decreases its stability via inhibition of the PI3K/AKT/mTOR pathway and Hsp90 binding. *J Cell Physiol* (2015) 230(4):853–62. doi: 10.1002/jcp.24813
 188. Pham TH, Lecomte S, Efsthathiou T, Ferriere F, Pakdel F. An Update on the Effects of Glyceollins on Human Health: Possible Anticancer Effects and Underlying Mechanisms. *Nutrients* (2019) 11(1):79. doi: 10.3390/nu11010079
 189. Kubo T, Maezawa N, Osada M, Katsumura S, Funae Y, Imaoka S, et al. an environmental endocrine-disrupting chemical, inhibits hypoxic response via degradation of hypoxia-inducible factor 1alpha (HIF-1alpha): structural requirement of bisphenol A for degradation of HIF-1alpha. *Biochem Biophys Res Commun* (2004) 318(4):1006–11. doi: 10.1016/j.bbrc.2004.04.125
 190. Fu B, Xue J, Li Z, Shi X, Jiang BH, Fang J. Chrysin inhibits expression of hypoxia-inducible factor-1alpha through reducing hypoxia-inducible factor-1alpha stability and inhibiting its protein synthesis. *Mol Cancer Ther* (2007) 6(1):220–6. doi: 10.1158/1535-7163.MCT-06-0526
 191. Lee K, Kang JE, Park SK, Jin Y, Chung KS, Kim HM, et al. LW6, a novel HIF-1 inhibitor, promotes proteasomal degradation of HIF-1alpha via upregulation of VHL in a colon cancer cell line. *Biochem Pharmacol* (2010) 80(7):982–9. doi: 10.1016/j.bcp.2010.06.018
 192. Kim YH, Coon A, Baker AF, Powis G. Antitumor agent PX-12 inhibits HIF-1alpha protein levels through an Nrf2/PMF-1-mediated increase in spermidine/spermine acetyl transferase. *Cancer Chemother Pharmacol* (2011) 68(2):405–13. doi: 10.1007/s00280-010-1500-0
 193. Jordan BF, Runquist M, Raghunand N, Gillies RJ, Tate WR, Powis G, et al. The thioredoxin-1 inhibitor 1-methylpropyl 2-imidazolyl disulfide (PX-12) decreases vascular permeability in tumor xenografts monitored by dynamic contrast enhanced magnetic resonance imaging. *Clin Cancer Res* (2005) 11(2 Pt 1):529–36.
 194. Zhang L, Chen C, Duanmu J, Wu Y, Tao J, Yang A, et al. Cryptotanshinone inhibits the growth and invasion of colon cancer by suppressing inflammation and tumor angiogenesis through modulating MMP/TIMP system, PI3K/Akt/mTOR signaling and HIF-1alpha nuclear translocation. *Int Immunopharmacol* (2018) 65:429–37. doi: 10.1016/j.intimp.2018.10.035
 195. Miranda E, Nordgren IK, Male AL, Lawrence CE, Hoakwie F, Cuda F, et al. A cyclic peptide inhibitor of HIF-1 heterodimerization that inhibits hypoxia signaling in cancer cells. *J Am Chem Soc* (2013) 135(28):10418–25. doi: 10.1021/ja402993u
 196. Minegishi H, Fukushima S, Ban HS, Nakamura H. Discovery of Indenopyrazoles as a New Class of Hypoxia Inducible Factor (HIF)-1 Inhibitors. *ACS Med Chem Lett* (2013) 4(2):297–301. doi: 10.1021/ml300463z

Conflict of Interest: The authors declare that the research was conducted in the absence of any commercial or financial relationships that could be construed as a potential conflict of interest.

Copyright © 2020 Peng, Zhang, Tan, Huang, Xu, Silk, Zhang, Liu and Jiang. This is an open-access article distributed under the terms of the Creative Commons Attribution License (CC BY). The use, distribution or reproduction in other forums is permitted, provided the original author(s) and the copyright owner(s) are credited and that the original publication in this journal is cited, in accordance with accepted academic practice. No use, distribution or reproduction is permitted which does not comply with these terms.



Glucose Intolerance on Pheochromocytoma and Paraganglioma—The Current Understanding and Clinical Perspectives

Ichiro Abe^{1,2}, Farhadul Islam³ and Alfred King-Yin Lam^{1*}

¹ Cancer Molecular Pathology of School of Medicine, Griffith University, Gold Coast, QLD, Australia, ² Department of Endocrinology and Diabetes Mellitus, Fukuoka University Chikushi Hospital, Chikushino, Fukuoka, Japan, ³ Department of Biochemistry and Molecular Biology, University of Rajshahi, Rajshahi, Bangladesh

OPEN ACCESS

Edited by:

Olfa Masmoudi-Kouki,
University Tunis El Manar, Tunisia

Reviewed by:

Hiroshi Ikegami,
Kindai University, Japan
Masaru Doi,
Doi Internal Medicine Clinic, Japan

*Correspondence:

Alfred King-Yin Lam
a.lam@griffith.edu.au

Specialty section:

This article was submitted to
Neuroendocrine Science,
a section of the journal
Frontiers in Endocrinology

Received: 11 August 2020

Accepted: 30 October 2020

Published: 26 November 2020

Citation:

Abe I, Islam F and Lam AK
(2020) Glucose Intolerance
on Pheochromocytoma
and Paraganglioma—The
Current Understanding and
Clinical Perspectives.
Front. Endocrinol. 11:593780.
doi: 10.3389/fendo.2020.593780

Half of the patients with pheochromocytoma have glucose intolerance which could be life-threatening as well as causing postoperative hypoglycemia. Glucose intolerance is due to impaired insulin secretion and/or increased insulin resistance. Impaired insulin secretion is caused by stimulating adrenergic α_2 receptors of pancreatic β -cells and increased insulin resistance is caused by stimulating adrenergic α_1 and β_3 receptors in adipocytes, α_1 and β_2 receptors of pancreatic α -cells and skeletal muscle. Furthermore, different affinities to respective adrenergic receptors exist between epinephrine and norepinephrine. Clinical studies revealed patients with pheochromocytoma had impaired insulin secretion as well as increased insulin resistance. Furthermore, excess of epinephrine could affect glucose intolerance mainly by impaired insulin secretion and excess of norepinephrine could affect glucose intolerance mainly by increased insulin resistance. Glucose intolerance on paraganglioma could be caused by increased insulin resistance mainly considering paraganglioma produces more norepinephrine than epinephrine. To conclude, the difference of actions between excess of epinephrine and norepinephrine could lead to improve understanding and management of glucose intolerance on pheochromocytoma.

Keywords: pheochromocytoma, glucose intolerance, insulin secretion, insulin resistance, paraganglioma

INTRODUCTION

Pheochromocytoma is a neuroendocrine tumor derived from chromaffin cells in the adrenal medulla that produces catecholamines (1, 2). There are recent advances on molecular pathogenesis as well as on the clinical perspectives in the tumor (1, 3). Common clinical complications in patients with pheochromocytoma include hypertension, glucose intolerance, and cardiovascular dysfunctions (4). Among these complications, glucose intolerance attracts attention as recent developments noted regarding the mechanisms. Commonly, glucose intolerance is known for its hyperglycemia due to impaired glucose homeostasis, which is a result of impaired insulin secretion and/or increased insulin resistance (5, 6). In patients with pheochromocytoma, Wilber and co-workers reported that insulin secretion was inhibited by

an excess of catecholamine (7). In addition, Deibert and co-workers showed that insulin resistance was increased by excess catecholamine (8). Thus, impaired insulin secretion as well as increased insulin resistance could affect glucose intolerance in patients with pheochromocytoma. Recent studies started to elucidate the mechanisms of glucose intolerance in pheochromocytoma. In this review, we aim to summarize these recent findings of glucose intolerance in patients with pheochromocytoma.

GLUCOSE INTOLERANCE ON PHAECHROMOCYTOMA: INCIDENTS AND ISSUES

Glucose intolerance is one of the complications of pheochromocytoma and often found in patients with pheochromocytoma (9, 10). Elenkova and co-workers revealed that half of the patients (93/186) with pheochromocytoma had glucose intolerance (11). Beninato and co-workers also investigated 153 patients with pheochromocytoma, showing that 23% (n=36) had diabetes mellitus. Of these, and 79% (n=33) had complete resolution of diabetes mellitus after extirpation of pheochromocytoma (12).

Elenkova and co-workers indicated that patients with glucose intolerance had increased urine metanephrine (metadrenaline; metabolite of epinephrine/adrenaline) and normetanephrine (a metabolite of norepinephrine/noradrenaline) and were older than those without glucose intolerance (11). There were no significant differences among the two groups with respect to tumor size and body mass index. On the other hand, Beninato and co-workers indicated patients with diabetes mellitus had larger tumors than those without diabetes mellitus but there was no significant difference between the two groups in patients' age and catecholamine values (12). Considering the different results of two studies, it remains controversial about the relationship between the incidence of glucose intolerance and the other clinical parameters. Thus, it is difficult to predict the risk of glucose intolerance in patients with pheochromocytoma.

Almost all of the patients treated as diabetes mellitus before diagnosed pheochromocytoma were initially diagnosed as type 2 diabetes mellitus. Glucose intolerance in patients with pheochromocytoma is often difficult to be well-controlled and insulin therapy is sometimes needed. Nevertheless, a few cases were diagnosed as type 1 diabetes mellitus because of their impaired insulin secretion and necessity of insulin therapy (13, 14). In addition, the clinical manifestations of glucose intolerance in patients with pheochromocytoma are sometimes severe. There were some cases of diabetic ketoacidosis or hyperglycemic hyperosmolar syndrome, which could be lethal without accurate therapy in patients with pheochromocytoma (15–17). These previous reports indicated glucose intolerance in patients with pheochromocytoma could exhibit severe phenotypes and must not be overlooked.

Glucose intolerance of pheochromocytoma is a problem in the perioperative period. After tumor extirpation, hypoglycemia occurs to some patients with pheochromocytoma. Akiba and

co-workers demonstrated that 13% of patients had severe hypoglycemia after extirpation of pheochromocytoma. This postoperative hypoglycemia is likely due to a sharp decrease of catecholamines by tumor extirpation (18). Recently, Araki and co-workers showed patients who had higher epinephrine and those who had glucose intolerance preoperatively were more likely to develop postoperative hypoglycemia, which indicated patients with higher epinephrine and glucose intolerance must be careful observation in the perioperative period (19).

THE MOLECULAR ADRENERGIC MECHANISMS RELATED TO GLUCOSE INTOLERANCE AND THE DIFFERENCES AMONG TYPES OF CATECHOLAMINE EXCESS IN GLUCOSE INTOLERANCE

Multifarious adrenergic receptor ($\alpha 1$, $\alpha 2$, $\beta 1$, $\beta 2$, and $\beta 3$) and their different functions were noted in various organs (20). In patients with pheochromocytoma, various adrenergic receptors were reported to be responsible for the glucose intolerance (21–26). Impaired secretion of insulin by catecholamines on pheochromocytoma is caused mainly through adrenergic $\alpha 2$ receptors of β -cells in pancreatic islets (21, 22). The $\alpha 2$ receptors are divided into 3 subtypes ($\alpha 2A$, $\alpha 2B$, and $\alpha 2C$). Among them, $\alpha 2A$ receptors were reported to suppress insulin secretion from pancreatic β -cells. Fagerholm and co-workers showed that adrenergic $\alpha 2A$ receptor knockout mice or adrenergic $\alpha 2$ receptor antagonists exhibit elevated insulin levels and reduced glucose levels (21).

On the other hand, increased insulin resistance on pheochromocytoma is caused by stimulated gluconeogenesis and glycogenolysis in the liver, which arises from an excess of glucagon and increase of free fatty acids as well as elevated glucose uptake in skeletal muscle. Stimulation of adrenergic $\beta 2$ and $\alpha 1$ receptors of the pancreatic α -cells causes an increase in glucagon secretion (21, 23–25). Two previous *in vitro* studies demonstrated stimulation of adrenergic β receptors could increase glucagon secretion through elevated intracellular cAMP and Ca^{2+} signaling (23, 24). Among the β receptors, Philipson showed adrenergic $\beta 2$ receptors could have most effects on glucagon secretion among adrenergic β receptors (25). Vieira and co-workers showed adrenergic $\alpha 1$ receptors antagonists stimulated glucagon secretion (23). In addition, they also showed adrenergic $\alpha 2$ receptor antagonists and agonists did not affect glucagon secretion although it was reported adrenergic $\alpha 2$ receptors were detected in pancreatic α -cells (21, 23).

In adipocytes, stimulation of the adrenergic $\beta 3$ and $\alpha 1$ receptors affects the production of fatty acids (26, 27). de Souza and co-workers showed stimulation of adrenergic $\beta 3$ receptors increased intracellular cAMP and elevated lipolysis, which caused increased fatty acid (26). In addition, Boschmann and co-workers showed that stimulation of adrenergic $\alpha 1$ receptors with adrenergic $\alpha 1$ receptor agonists led to promoting lipolysis and results in increased fatty acid (27).

Regarding glucose uptake in skeletal muscle, Shi and co-workers showed stimulating adrenergic $\alpha 1$ receptors increased glucose uptake in skeletal muscle with elevated leptin signaling with adrenergic $\alpha 1$ receptors deficient and transgenic mice (28). Shiuchi and co-workers also showed that adrenergic $\beta 2$ receptors in skeletal muscle could mediate induction of glucose uptake in skeletal muscle by leptin signaling investigating adrenergic β receptor-deficient mice and forced expression of adrenergic $\beta 2$ receptors (29). In addition, Mukaida and co-workers showed stimulating adrenergic $\beta 2$ receptors which promoted glucose transporter type 4 (GLUT4) translocation (a protein acts as glucose transporter found in adipose tissue and striated muscles) and glucose uptake in skeletal muscle using adrenergic $\beta 3$ receptor-deficient mice with adrenergic $\beta 2/\beta 3$ receptor agonists (30).

Epinephrine and norepinephrine were reported to have different affinities to respective adrenergic receptors. Epinephrine was reported to have a higher affinity to adrenergic $\alpha 2$ and $\beta 2$ receptors than norepinephrine. On the contrary, norepinephrine was reported to have a higher affinity to adrenergic $\alpha 1$ and $\beta 1$ receptors than epinephrine. Moreover, epinephrine and norepinephrine were reported to have a similar affinity to adrenergic $\beta 3$ receptors (31).

These molecular findings indicated an excess of catecholamine in pheochromocytoma could lead to both impaired insulin secretion and increased insulin resistance through various adrenergic receptors as well as different actions between epinephrine and norepinephrine in them (Table 1, Figure 1).

CLINICAL STUDIES: IMPAIRED INSULIN SECRETION AND INCREASED INSULIN RESISTANCE IN PATIENTS WITH PHAEOCHROMOCYTOMA

Clinical studies revealed patients with pheochromocytoma had impaired insulin secretion (32–34). Komada and co-workers demonstrated impairment of insulin secretion, particularly in an early phase of the insulin secretory response in 13 patients with pheochromocytoma/paraganglioma (extra-adrenal pheochromocytoma) (11 with pheochromocytoma and two with paraganglioma) (32). They noted that improved insulin secretion after surgical removal of pheochromocytoma/paraganglioma with hyperglycemic clamps as well as an oral glucose tolerance test. Moreover, the study investigated insulin resistance with hyperinsulinemic-euglycemic clamps and

homeostasis model assessment of insulin resistance (HOMA-IR), which is surrogate marker of insulin resistance. There were no significant changes of insulin sensitivity index on hyperinsulinemic-euglycemic clamps from pre-operation to post-operation although postoperative HOMA-IR value was significantly improved than preoperative value, which indicated increased insulin resistance in patients with pheochromocytoma was controversial in the study (32).

Petrák and co-workers demonstrated impaired insulin secretion and glucose intolerance in patients with pheochromocytoma using meal test and the homeostasis model assessment of β -cell function (HOMA- β), which is surrogate marker of insulin secretion. In the study, they indicated that impaired insulin secretion could be due to impaired glucagon-like peptide 1 (GLP-1) secretion (33) (Figure 1). Meanwhile, the study revealed significant increment of glucagon value and no changes in insulin/glucagon ratio between the preoperative and postoperative period. Commonly, GLP-1 decreases glucagon secretion (34). Considering excess of catecholamine leads to elevation of glucagon through adrenergic $\beta 2$ and $\alpha 1$ receptors together, the results of the study about glucagon secretion might indicate there exists some unknown mechanism of glucagon secretion in patients with pheochromocytoma (Figure 1).

There were clinical studies which revealed insulin resistance improved after adrenalectomy in patients with pheochromocytoma as well as those related to the improvement of insulin secretion (35–38). Blüher and co-workers demonstrated increased insulin resistance in three patients with pheochromocytoma having hyperglycemia medicated with anti-diabetic agents, which improved after surgical removal of pheochromocytoma (35). A follow-up study by the same group revealed an excess of catecholamine-induced glucose intolerance through increased insulin resistance with the hyperinsulinemic-euglycemic clamp study in 10 patients with pheochromocytoma (36). Moreover, Diamanti-Kandarakis and co-workers investigated glucose intolerance in 5 patients with pheochromocytoma using oral glucose tolerance test and hyperinsulinemic-euglycemic clamp. The results demonstrated not only the improvement of glucose intolerance but also reduced insulin resistance by tumor extirpation (37). Recently, Guclu and co-workers investigated 44 patients with pheochromocytoma using HOMA-IR and noted 65.9% of them (29 patients) had increased insulin resistance (38). Considering the results of these studies, both impaired insulin secretion and increased insulin resistance could induce glucose intolerance in patients with pheochromocytoma. However, it has

TABLE 1 | Different effects on glucose intolerance among adrenergic receptors.

Adrenergic receptors	Mechanism of effect on glucose intolerance	Affinity of epinephrine and norepinephrine
$\alpha 1$ receptors	fatty free acid \uparrow , glucagon secretion \uparrow , glucose uptake in skeletal muscle \uparrow , GLP-1 secretion \downarrow	Norepinephrine > Epinephrine
$\alpha 2$ receptors	insulin secretion \downarrow , GLP-1 secretion \downarrow	Epinephrine > Norepinephrine
$\beta 1$ receptors	GLP-1 secretion \uparrow	Norepinephrine > Epinephrine
$\beta 2$ receptors	glucagon secretion \uparrow , glucose uptake in skeletal muscle \uparrow	Epinephrine > Norepinephrine
$\beta 3$ receptors	fatty free acid \uparrow	Epinephrine = Norepinephrine

GLP-1, glucagon-like peptide-1.

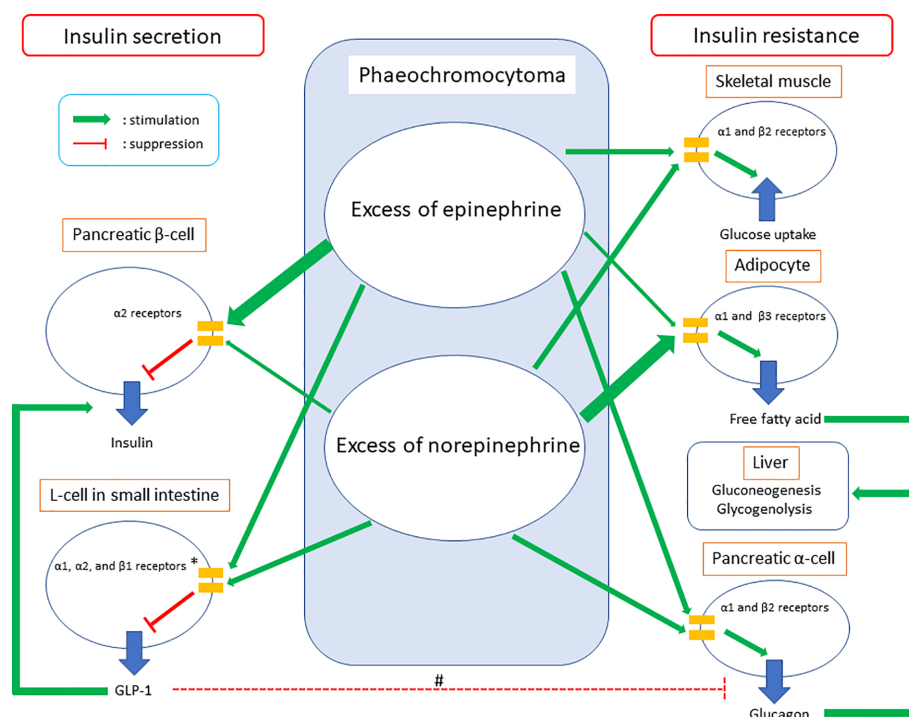


FIGURE 1 | Summary of glucose intolerance on pheochromocytoma. GLP-1, glucagon-like peptide-1. *The clinical study demonstrated GLP-1 secretion could be suppressed on pheochromocytoma. Meanwhile, *in vivo* and *in vitro* studies showed epinephrine could increase GLP-1 secretion through adrenergic α_1 , α_2 , and β_1 receptors and norepinephrine could inhibit GLP-1 secretion through adrenergic α_1 and/or α_2 receptors. #GLP-1 inhibits glucagon secretion in pancreatic α -cells commonly, while glucagon secretion was suppressed in the clinical study which investigated GLP-1 secretion on pheochromocytoma. Considering both epinephrine and norepinephrine could increase glucagon secretion in pancreatic α -cells directly together, the study did not clarify whether increased GLP-1 secretion on pheochromocytoma could inhibit glucagon secretion in pancreatic α -cells or not.

remained unclear whether the main factor of glucose intolerance is impaired insulin secretion or increased insulin resistance.

Glucose intolerance in patients with pheochromocytoma could be improved by tumor extirpation. Meanwhile, there could be cases who could not receive tumor removal because of their complications or having metastatic phenotypes. Diamanti-Kandarakis and co-workers showed administrations of non-selective adrenergic α blocker and β blockers could improve glucose intolerance in patients with pheochromocytoma, while the effects of the agents were significantly lower than those of tumor extirpation (37). This study indicated glucose intolerance in patients who could not undergo tumor removal could be difficult only by agents of adrenergic receptor antagonists.

THE NEW INSIGHT: DIFFERENCES IN THE ACTIONS ON GLUCOSE INTOLERANCE AMONG TYPES OF THE EXCESS OF CATECHOLAMINE ON PHAECHROMOCYTOMA

DiSalvo and co-workers showed epinephrine could have more effects on hyperglycemia than norepinephrine based on the

investigation of infusion epinephrine and norepinephrine into healthy humans (39). However, there was no clinical study on the differences in the mechanisms between excess of epinephrine and that of norepinephrine on glucose intolerance in patients with pheochromocytoma.

A recent study elucidated the differences in the actions between epinephrine and norepinephrine on glucose intolerance in patients with pheochromocytoma (40). The study investigated the association between the changes of urinary metanephrine/normetanephrine (metabolic product of epinephrine/norepinephrine) and those of HOMA- β /HOMA-IR from pre-operation to post-operation in 12 patients with pheochromocytoma. The study revealed that pheochromocytoma could lead to glucose intolerance by both impaired insulin secretion and increased insulin resistance. Furthermore, the study demonstrated there could be the differences in the actions on glucose intolerance between excess of epinephrine and that of norepinephrine. The results indicated an excess of epinephrine could affect glucose intolerance mainly by impaired secretion of insulin and that of norepinephrine could affect glucose intolerance mainly by increased insulin resistance. Regarding impaired insulin secretion, the results could be explained by the molecular mechanisms which epinephrine has a higher affinity to adrenergic α_2 receptors than norepinephrine. Considering increased insulin

resistance, norepinephrine could have stronger effects than epinephrine on increased fatty acids due to lipolysis in adipocytes, which were through adrenergic β_3 and α_1 receptors. Seeing the contrary affinities to adrenergic α_1 and β_2 receptors between epinephrine and norepinephrine on glucagon secretion as well as glucose uptake in skeletal muscle together, the results of the clinical study about increased insulin resistance could be consistent with the molecular mechanisms (Figure 1).

Hence, the study of different types of the excess of catecholamine should be important for understanding the mechanism of glucose intolerance in patients with pheochromocytoma. It is also possible that types of the excess of catecholamine affects GLP-1 secretion on pheochromocytoma. Regarding the association between GLP-1 secretion and excess of catecholamine, there were two previous *in vivo* and *in vitro* studies (41, 42). The *in vitro* study indicated epinephrine could increase GLP-1 secretion through adrenergic α_1 , α_2 , and β_1 receptors, whereas the *in vivo* study indicated norepinephrine could inhibit GLP-1 secretion through adrenergic α_1 and/or α_2 receptors (41, 42) (Table 1, Figure 1). These studies indicated differences in effects on GLP-1 secretion between epinephrine and norepinephrine could exist. Petrák and co-workers did not investigate the different effects on GLP-1 secretion between excess of epinephrine and that of norepinephrine (33). Hence, future studies about the association between GLP-1 and the type of excess of catecholamine might reveal further knowledge of GLP-1 secretion on pheochromocytoma. Furthermore, they might lead to clarification of the mechanism of increased glucagon secretion after extirpation of pheochromocytoma, which was seen in the study by Petrák and co-workers.

GLUCOSE INTOLERANCE ON PARAGANGLIOMA

Paragangliomas is extra-adrenal non-epithelial tumors originating from neural crest-derived paraganglion cells located in the region of autonomic nervous system ganglia and accompanying nerves with histology like pheochromocytoma (3). Regarding glucose intolerance in paraganglioma, Elenkova and co-workers noted that 44% (8/18) of patients with paraganglioma had glucose intolerance (11). However, there were no other studies investigating glucose intolerance focused on paraganglioma

including differences between glucose intolerance on pheochromocytoma and that on paraganglioma. The mechanism of glucose intolerance on paraganglioma had never been investigated in clinical studies in the English literature. di Paolo and co-workers previously reported the case of extra-adrenal pheochromocytoma (paraganglioma) with glucose intolerance due to increased insulin resistance (43). The case had also high norepinephrine secretion. Commonly, paraganglioma produces more norepinephrine than epinephrine (44). Considering the different actions on glucose intolerance between epinephrine and norepinephrine, glucose intolerance in patients with paraganglioma could be caused by increased insulin resistance mainly as the reported case.

CONCLUSION

In this article, current perspectives about glucose intolerance in patients with pheochromocytoma were presented along underlying the mechanism of glucose intolerance. The findings indicated that patients with pheochromocytoma could have both impaired insulin secretion and increased insulin resistance by an excess of catecholamine. However, the definite mechanism remains unknown, and it has been controversial whether the main factor of glucose intolerance is impaired insulin secretion or increased insulin resistance. Recent advances from the viewpoint of the difference of actions between excess of epinephrine and that of norepinephrine could clarify this controversy. A larger cohort of patients is required to investigate the mechanism and effects of hyperglycemia in pheochromocytoma and paraganglioma.

AUTHOR CONTRIBUTIONS

IA wrote the first draft of the manuscript. FI and AKL revised and edited the manuscript. All authors contributed to the article and approved the submitted version.

FUNDING

Funding from private practice funding account in Griffith University.

REFERENCES

- Lam AK. Updated on paragangliomas and pheochromocytomas. *Turk Patoloji Derg* (2015) 31:105–12. doi: 10.5146/tjpath.2015.01318
- Walther MM, Keiser HR, Linehan WM. Pheochromocytoma: evaluation, diagnosis, and treatment. *World J Urol* (1999) 17:35–9. doi: 10.1007/s003450050102
- Lam AK. Update on Adrenal Tumors in 2017 World Health Organization (WHO) of Endocrine Tumors. *Endocr Pathol* (2017) 28:213–27. doi: 10.1007/s12022-017-9484-5
- Reisch N, Peczkowska M, Januszewicz A, Neumann HP. Pheochromocytoma: presentation, diagnosis and treatment. *J Hypertens* (2006) 24:2331–9. doi: 10.1097/01.hjh.0000251887.01885.54
- Virally M, Blicklé JF, Girard J, Halimi S, Simon D, Guillausseau PJ. Type 2 diabetes mellitus: epidemiology, pathophysiology, unmet needs and therapeutic perspectives. *Diabetes Metab* (2007) 33:231–44. doi: 10.1016/j.diabet.2007.07.001
- Ferrannini E. Insulin resistance versus insulin deficiency in non-insulin-dependent diabetes mellitus: problems and prospects. *Endocr Rev* (1998) 19:477–90. doi: 10.1210/edrv.19.4.0336
- Wilber JF, Turtle JR, Crane NA. Inhibition of insulin secretion by a pheochromocytoma. *Lancet* (1966) 2:733. doi: 10.1016/s0140-6736(66)92986-2
- Deibert DC, DeFronzo RA. Epinephrine-induced insulin resistance in man. *J Clin Invest* (1980) 65:717–21. doi: 10.1172/JCI109718
- Lenders JW, Eisenhofer G, Mannelli M, Pacak K. Pheochromocytoma. *Lancet* (2005) 366:665–75. doi: 10.1016/S0140-6736(05)67139-5
- Stenstrom G, Sjostrom L, Smith U. Diabetes mellitus in pheochromocytoma. Fasting blood glucose levels before and after surgery in 60 patients with pheochromocytoma. *Acta Endocrinol (Copenh)* (1984) 106:511–5. doi: 10.1530/acta.0.1060511
- Elenkova A, Matrozkova J, Vasilev V, Robeva R, Zacharieva S. Prevalence and progression of carbohydrate disorders in patients with pheochromocytoma/

- paraganglioma: retrospective single-center study. *Ann Endocrinol (Paris)* (2020) 81:3–10. doi: 10.1016/j.ando.2020.01.001
12. Beninato T, Kluijfhout WP, Drake FT, Lim J, Kwon JS, Xiong M, et al. Resection of Pheochromocytoma Improves Diabetes Mellitus in the Majority of Patients. *Ann Surg Oncol* (2017) 24:1208–13. doi: 10.1245/s10434-016-5701-6
 13. Bole D, Simon B. Pheochromocytoma-induced hyperglycemia leading to misdiagnosis of type 1 diabetes mellitus. *AACE Clin Case Rep* (2017) 3:e83–6. doi: 10.4158/EP161210.CR
 14. Leng OM, Madathil AC. Remission of longstanding insulin-treated diabetes mellitus following surgical resection of pheochromocytoma. *AACE Clin Case Rep* (2019) 5:e62–5. doi: 10.4158/ACCR-2018-0091
 15. Isotani H, Fujimura Y, Furukawa K, Morita K. Diabetic ketoacidosis associated with the pheochromocytoma of youth. *Diabetes Res Clin Pract* (1996) 34:57–60. doi: 10.1016/s0168-8227(96)01330-7
 16. Ishii C, Inoue K, Negishi K, Tane N, Awata T, Katayama S. Diabetic ketoacidosis in a case of pheochromocytoma. *Diabetes Res Clin Pract* (2001) 54:137–42. doi: 10.1016/s0168-8227(01)00261-3
 17. Lee IS, Lee TW, Chang CJ, Chien YM, Lee TI. Pheochromocytoma presenting as hyperglycemic hyperosmolar syndrome and unusual fever. *Intern Emerg Med* (2015) 10:753–5. doi: 10.1007/s11739-015-1217-5
 18. Akiba M, Kodama T, Ito Y, Obara T, Fujimoto Y. Hypoglycemia induced by excessive rebound secretion of insulin after removal of pheochromocytoma. *World J Surg* (1990) 14:317–24. doi: 10.1007/BF01658514
 19. Araki S, Kijima T, Waseda Y, Komai Y, Nakanishi Y, Uehara S, et al. Incidence and predictive factors of hypoglycemia after pheochromocytoma resection. *Int J Urol* (2019) 26:273–7. doi: 10.1111/iju.13864
 20. Strosberg AD. Structure, function, and regulation of adrenergic receptors. *Protein Sci* (1993) 2:1198–209. doi: 10.1002/pro.5560020802
 21. Fagerholm V, Grönroos T, Marjamki P, Viljanen T, Scheinin M, Haaparanta M. Altered glucose homeostasis in alpha2A-adrenoceptor knockout mice. *Eur J Pharmacol* (2004) 505:243–52. doi: 10.1016/j.ejphar.2004.10.023
 22. Hu X, Friedman D, Hill S, Caprioli R, Nicholson W, Powers AC, et al. Proteomic exploration of pancreatic islets in mice null for the alpha2A adrenergic receptor. *J Mol Endocrinol* (2005) 35:73–88. doi: 10.1677/jme.1.01764
 23. Vieira E, Liu YJ, Gylfe E. Involvement of alpha1 and beta-adrenoceptors in adrenaline stimulation of the glucagon-secreting mouse alpha-cell. *Naunyn Schmiedeberg Arch Pharmacol* (2004) 369:179–83. doi: 10.1007/s00210-003-0858-5
 24. Hamilton A, Zhang Q, Salehi A, Willems M, Knudsen JG, Ringgaard AK, et al. Adrenaline stimulates glucagon secretion by Tpc2-dependent Ca(2+) mobilization from acidic stores in pancreatic α -cells. *Diabetes* (2018) 67(6):1128–39. doi: 10.2337/db17-1102
 25. Philipson LH. Beta-agonists and metabolism. *J Allergy Clin Immunol* (2002) 110:S313–7. doi: 10.1067/mai.2002.129702
 26. de Souza CJ, Burkey BF. Beta 3-adrenoceptor agonists as anti-diabetic and anti-obesity drugs in humans. *Curr Pharm Des* (2001) 7:1433–49. doi: 10.2174/1381612013397339
 27. Boschmann M, Krupp G, Luft FC, Klaus S, Jordan J. In vivo response to alpha (1)-adrenoreceptor stimulation in human white adipose tissue. *Obes Res* (2002) 10:555–8. doi: 10.1038/oby.2002.75
 28. Shi T, Papay RS, Perez DM. The role of α (1)-adrenergic receptors in regulating metabolism: increased glucose tolerance, leptin secretion and lipid oxidation. *J Recept Signal Transduct Res* (2017) 37:124–32. doi: 10.1080/10799893.2016.1193522
 29. Shiuchi T, Toda C, Okamoto S, Coutinho EA, Saito K, Miura S, et al. Induction of glucose uptake in skeletal muscle by central leptin is mediated by muscle β 2-adrenergic receptor but not by AMPK. *Sci Rep* (2017) 7:15141. doi: 10.1038/s41598-017-15548-6
 30. Mukaida S, Sato M, Öberg AI, Dehvari N, Olsen JM, Kocan M, et al. BRL37344 stimulates GLUT4 translocation and glucose uptake in skeletal muscle via β (2)-adrenoceptors without causing classical receptor desensitization. *Am J Physiol Regul Integr Comp Physiol* (2019) 316:R666–77. doi: 10.1152/ajpregu.00285.2018
 31. Ritter JM, Flower R, Henderson G, Loke YK, MacEwan D, Rang HP. *Rang & Dale's Pharmacology*. 9th ed. United Kingdom: Elsevier (2020).
 32. Komada H, Hirota Y, So A, Nakamura T, Okuno Y, Fukuoka H, et al. Insulin Secretion and Insulin Sensitivity Before and After Surgical Treatment of Pheochromocytoma or Paraganglioma. *J Clin Endocrinol Metab* (2017) 102:3400–5. doi: 10.1210/jc.2017-00357
 33. Petrák O, Klimová J, Mráz M, Haluzíková D, Doležalová RP, Kratochvílová H, et al. Pheochromocytoma with adrenergic biochemical phenotype shows decreased GLP-1 secretion and impaired glucose tolerance. *J Clin Endocrinol Metab* (2020) 105:dgaal54. doi: 10.1210/clinem/dgaal54
 34. Meier JJ. GLP-1 receptor agonists for individualized treatment of type 2 diabetes mellitus. *Nat Rev Endocrinol* (2012) 8:728–42. doi: 10.1038/nrendo.2012.140
 35. Blüher M, Windgassen M, Paschke R. Improvement of insulin sensitivity after adrenalectomy in patients with pheochromocytoma. *Diabetes Care* (2000) 23:1591–2. doi: 10.2337/diacare.23.10.1591
 36. Wiesner TD, Blüher M, Windgassen M, Paschke R. Improvement of insulin sensitivity after adrenalectomy in patients with pheochromocytoma. *J Clin Endocrinol Metab* (2003) 88:3632–6. doi: 10.1210/jc.2003-030000
 37. Diamanti-Kandarakis E, Zapanti E, Peridis MH, Ntavos P, and Mastorakos G. Insulin resistance in pheochromocytoma improves more by surgical rather than by medical treatment. *Hormones (Athens)* (2003) 2:61–6. doi: 10.14310/horm.2002.1184
 38. Guclu F, Taskiran E, Kaypak MA, Akmes A. Insulin resistance on pheochromocytoma. *Endocr Pract* (2017) 23:10A.
 39. DiSalvo RJ, Bloom WL, Brust AA, Ferguson RW, Ferris EB. A comparison of the metabolic and circulatory effects of epinephrine, nor-epinephrine and insulin hypoglycemia with observations on the influence of autonomic blocking agents. *J Clin Invest* (1956) 35:568–77. doi: 10.1172/JCI103310
 40. Abe I, Fujii H, Ohishi H, Sugimoto K, Minezaki M, Nakagawa M, et al. Differences in the actions of adrenaline and noradrenaline with regard to glucose intolerance in patients with pheochromocytoma. *Endocr J* (2019) 66:187–92. doi: 10.1507/endocrj.EJ18-0407
 41. Harada K, Kitaguchi T, Tsuboi T. Integrative function of adrenaline receptors for glucagon-like peptide-1 exocytosis in enteroendocrine L cell line GLUTag. *Biochem Biophys Res Commun* (2015) 460:1053–8. doi: 10.1016/j.bbrc.2015.03.151
 42. Hansen L, Lampert S, Mineo H, Holst JJ. Neural regulation of glucagon-like peptide-1 secretion in pigs. *Am J Physiol Endocrinol Metab* (2004) 287:E939–47. doi: 10.1152/ajpendo.00197.2004
 43. di Paolo S, de Pergola G, Cospite MR, Guastamacchia E, Cignarelli M, Balice A, et al. Beta-adrenoceptors desensitization may modulate catecholamine induced insulin resistance in human pheochromocytoma. *Diabetes Metab* (1989) 15:409–15.
 44. van Berkel A, Lenders JW, Timmers HJ. Diagnosis of endocrine disease: Biochemical diagnosis of pheochromocytoma and paraganglioma. *Eur J Endocrinol* (2014) 170:R109–19. doi: 10.1530/EJE-13-0882

Conflict of Interest: The authors declare that the research was conducted in the absence of any commercial or financial relationships that could be construed as a potential conflict of interest.

Copyright © 2020 Abe, Islam and Lam. This is an open-access article distributed under the terms of the Creative Commons Attribution License (CC BY). The use, distribution or reproduction in other forums is permitted, provided the original author(s) and the copyright owner(s) are credited and that the original publication in this journal is cited, in accordance with accepted academic practice. No use, distribution or reproduction is permitted which does not comply with these terms.



A Durable Response With the Combination of Nivolumab and Cabozantinib in a Patient With Metastatic Paraganglioma: A Case Report and Review of the Current Literature

Minas P. Economides¹, Amishi Y. Shah², Camilo Jimenez³, Mouhammed A. Habra³, Monica Desai⁴ and Matthew T. Campbell^{2*}

OPEN ACCESS

Edited by:

Ichiro Abe,

Fukuoka University Chikushi Hospital,
Japan

Reviewed by:

Takeshi Usui,

Shizuoka General Hospital, Japan

Ronald De Krijger,

Princess Maxima Center for Pediatric

Oncology, Netherlands

Letizia Canu,

University of Florence, Italy

*Correspondence:

Matthew T. Campbell

mcampbell3@mdanderson.org

Specialty section:

This article was submitted to
Neuroendocrine Science,
a section of the journal
Frontiers in Endocrinology

Received: 26 August 2020

Accepted: 26 October 2020

Published: 27 November 2020

Citation:

Economides MP, Shah AY, Jimenez C, Habra MA, Desai M and Campbell MT (2020) A Durable Response With the Combination of Nivolumab and Cabozantinib in a Patient With Metastatic Paraganglioma: A Case Report and Review of the Current Literature. *Front. Endocrinol.* 11:594264. doi: 10.3389/fendo.2020.594264

¹ Department of Internal Medicine, The University of Texas School of Health Sciences at Houston, Houston, TX, United States, ² Department of Genitourinary Medical Oncology, The University of Texas MD Anderson Cancer Center, Houston, TX, United States, ³ Department of Endocrine Neoplasia and Hormonal Disorders, The University of Texas MD Anderson Cancer Center, Houston, TX, United States, ⁴ Department of Oncology/Hematology, Houston Methodist Cancer Center, Houston, TX, United States

Introduction: Pheochromocytomas and sympathetic paragangliomas (PPGL) are neuroendocrine catecholamine-secreting tumors that are usually localized. Metastatic disease is rare and systemic treatment consists of conventional chemotherapy and high-specific-activity iodine-131-MIBG which was approved by the FDA in 2018. Although chemotherapy combinations still have value in specific settings, the debilitating side effects of treatment with only modest benefit have limited their use. With the introduction of a new generation of targeted therapy and immunotherapy patients with metastatic PPGL may have improved therapeutic options.

Areas Covered: The current paper presents a case of a patient with metastatic PPGL who received multiple lines of systemic treatment. Despite progression on previous single agent cabozantinib and single agent pembrolizumab on separate clinical trials, the patient has exhibited a major response to the combination of cabozantinib and nivolumab for the past 22 months. In addition, we will review the available therapies for metastatic PPGL and discuss novel agents under clinical development.

Conclusion: Newer targeted therapies and immunotherapy options are under clinical development with promising results for patients with PPGL.

Keywords: cabozantinib, immunotherapy, pheochromocytoma, paraganglioma, nivolumab

INTRODUCTION

Pheochromocytomas and sympathetic paragangliomas (PPGL) are catecholamine-secreting neuroendocrine tumors that arise from chromaffin cells of the adrenal medulla (in the case of pheochromocytomas) and the autonomic paraganglia (in the case of paragangliomas). The catecholamine excess produced by the majority of these tumors predisposes patients to cardiovascular

and gastrointestinal morbidity and mortality (1, 2). Most PPGL are localized with 10% of the pheochromocytomas and more than 25% of the sympathetic paragangliomas undergoing metastatic spread of disease (3, 4). At present, there is no combination of clinical, histopathologic or biochemical features shown to reliably predict malignant behavior. As such, the diagnosis of a metastatic PPGL can only be made by identifying tumor deposits in tissues that normally do not contain chromaffin cells (e.g., lymph nodes, skeleton and brain) (5). Most frequent metastatic sites include the lymph nodes (80%), bone (71%), liver (50%), and the lungs (50%) (6). Among metastatic tumors the survival rate depends on the primary tumor site, the sites of metastases, the speed of progression, and the synthesis of catecholamines. Patients usually succumb from complications related to tumor burden (7).

At present, systemic treatment options include the consideration of conventional chemotherapy, radioactive iodine therapy for patients with uptake on the nuclear Iodine-131 meta-iodo-benzyl-guanidine (I^{131} -MIBG) scan, and clinical studies. For patients with metastatic PPGL, the FDA approved high-specific activity Iodine-131 meta-iodo-benzyl-guanidine (I^{131} -MIBG) in 2018 (8). In patients who present with *de novo* metastatic disease at initial presentation, a cytoreductive approach involving addressing the primary tumor is often pursued. The rationale behind this multidisciplinary approach is to de-bulk the extent of systemic tumor burden and decrease the catecholamine load. A retrospective review has suggested this approach may improve patient outcomes, but has not been prospectively validated (9).

Due to the rarity of this disease entity, prospective randomized trials in this rare disease are challenging and significant toxicity remains with the most commonly prescribed chemotherapy regimens (10–12). More recently, molecularly targeted and immunotherapeutic agents have been introduced with promising results (13–18). We report a patient with metastatic paraganglioma who received multiple targeted therapies and eventually had a dramatic, durable response to combination of cabozantinib and nivolumab. We also review the literature regarding current treatment options available for this rare disease. All the active clinical trials involving treatment options for metastatic PPGL are depicted in **Table 1**.

CASE REPORT

In 2007, a 32-year-old male patient was being worked up for a potential sinus surgery and was found to have a right sided neck mass. He underwent a surgical resection with histologic confirmation of a paraganglioma. Prior to his surgery he had no clinical evidence of catecholamine excess. In 2011, the patient underwent a scheduled surgery on his ankle which was complicated by a hypertensive crisis. He was found to have elevated plasma metanephrines and urinary catecholamines. On imaging work up, he was found to have a tumor involving his aorta originating from the organ of Zuckerkandl. After being started on phenoxybenzamine, he underwent surgery with resection of this tumor. In 2012, he was evaluated by a geneticist and reported no family history of malignancy. Genetic testing for *SDHB*, *SHDC*, and *SDHD* gene mutations by aCGH (ExonArrayDx) did not detect any disease-associated mutations in exons 1–8 of the *SDHB* gene, exons 1–6 of the *SDHC* gene, exons 1–4 of the *SDHD* gene, or the c.232 G>A in exon 3 of the *SDHAF2* gene (required for flavination of the SDHA subunit). He did not have detected mutations in the von Hippel-Lindau (*VHL*) *SDHA*, and Fumarase (*FH*) genes. In 2014 he suffered a transient ischemic attack with left-sided weakness that self-resolved within 24 h. At that time, his blood pressure was minimally elevated with systolic blood pressure in the 140–150 mm Hg range. In 2015, he was diagnosed with multiple metastatic lymph nodes involving his retroperitoneum encasing his left ureter. He again underwent surgical resection with eventual ureteral stent placement. In late 2015, he was found to have a metastatic tumor involving the caudate lobe of his liver for which he underwent transcatheter arterial chemoembolization. In 2016, he underwent an octreotide nuclear scan of his abdomen. He was found to have a new metastatic lesion involving his sacrum and a left-sided skull-based lesion. In addition, a new retroperitoneal lesion was identified and the lesion involving the caudate lobe of the liver remained stable. The tumors showed I^{131} -MIBG uptake. In 2016, he had resection of his caudate lobe and resection of the pre-aortic tumor. Soon after he was found to have disease progression in a para-aortic lymph node and within multiple bony lesions including his calvarium, thoracic spine, rib cage, and sacrum. He was enrolled in a clinical trial and received cabozantinib 60 mg by mouth daily on protocol. The patient was on study for 7.5 months prior to developing progressive disease in

TABLE 1 | Current clinical trials including agents used for patients with metastatic PPGL.

Agent	Eligible Patients	Phase	NCT#	Primary Outcome
I^{131} -MIBG	Refractory neuroblastoma/metastatic PPGL	I	NCT03649438	Number of patients who receive MIBG
I^{131} -MIBG	Refractory neuroblastoma or malignant PPGL	II	NCT00107289	Response rate
Lanreotide	Metastatic PPGL	II	NCT03946527	Tumor growth measurement
Sunitinib	Metastatic PPGL	II	NCT00843037	Clinical benefit rate ¹
Cabozantinib	Metastatic PPGL	II	NCT02302833	Response rate
Axitinib	Metastatic PPGL	II	NCT03839498	Response rate
Axitinib	Metastatic PPGL	II	NCT01967576	Response rate
Lenvatinib	Metastatic/advanced unresectable PPGL	II	NCT03008369	Response rate
ONC201	Neuroendocrine tumors	II	NCT03034200	Response rate
Temozolomide +/- Olaparib	Neuroendocrine tumor	II	NCT04394858	Progression Free Survival
Pembrolizumab	Rare unresectable or metastatic tumors	II	NCT02721732	Non-progression rate ²

I^{131} -MIBG, I^{131} meta-iodo-benzyl-guanidine; PPGL, pheochromocytoma and paraganglioma. ¹Clinical benefit rate is defined as either a partial response, complete response or stable disease for more than 12 weeks using Response Evaluation Criteria in Solid Tumors. ²Defined as the proportion of subjects in the analysis population who have no progression of disease at 27 weeks.

multiple known and new bone metastases, development of a new pulmonary metastasis, and progression of his known retroperitoneal lymph nodes. In 2017, the patient enrolled on a basket clinical trial with pembrolizumab and received 200 mg intravenously every 3 weeks for 5 months prior to experiencing disease progression in retroperitoneal and pelvic lymph nodes, new soft tissue metastasis within the abdomen, additional lung metastasis, and progression of multiple bone metastases including the development of a new femoral lesion. His best response on the study was considered stable disease. He then received three cycles of cyclophosphamide, vincristine, and dacarbazine. His treatment course was complicated by severe myelosuppression. He required admission for neutropenic fever and received multiple transfusions of both packed red blood cells and platelets. With chemotherapy he had evidence of disease response with a 12.2% reduction in his measurable disease with stability in his bone metastasis. However, within 3 months of ending chemotherapy he had progressive pain in his back and was found to have progression of disease in vertebral column bone metastases. A timeline of his systemic treatment is provided in **Figure 1**. The patient was started on off label cabozantinib and nivolumab.

Cabozantinib was dosed at 40 mg by mouth daily and nivolumab was provided at 240 mg IV every 2 weeks as per the phase I study by Apolo et al. (19) **Figure 2** contrasts his baseline imaging studies with the ones obtained 18 months after treatment initiation. The patient's course was complicated by several events including ulcerations on his lower extremities shown in **Figure 3**. A biopsy of these ulcerations found evidence of mild epithelial spongiosis with focal parakeratosis. There was evidence of a superficial perivascular lymphocytic infiltrate with scattered eosinophils. The dermatopathology group at MD Anderson Cancer Center determined these findings were most consistent with a hypersensitivity reaction to an internal medication. Breaks from cabozantinib allowed these ulcerations to heal. At present the patient remains on this regimen 22 months after initiation with evidence of continued clinical benefit. He had significant tumor reduction with decrease in size of lung, abdominal, bone and retroperitoneal lesions. On treatment his plasma metanephrines decreased from a baseline level of 14 nmol/L to 3.6 nmol/L. In addition, the patient symptomatically improved without signs of catecholamine

Timeline of Systemic Treatment

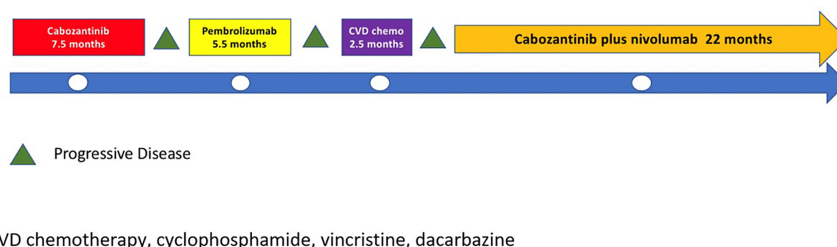


FIGURE 1 | Timeline of systematic treatment.

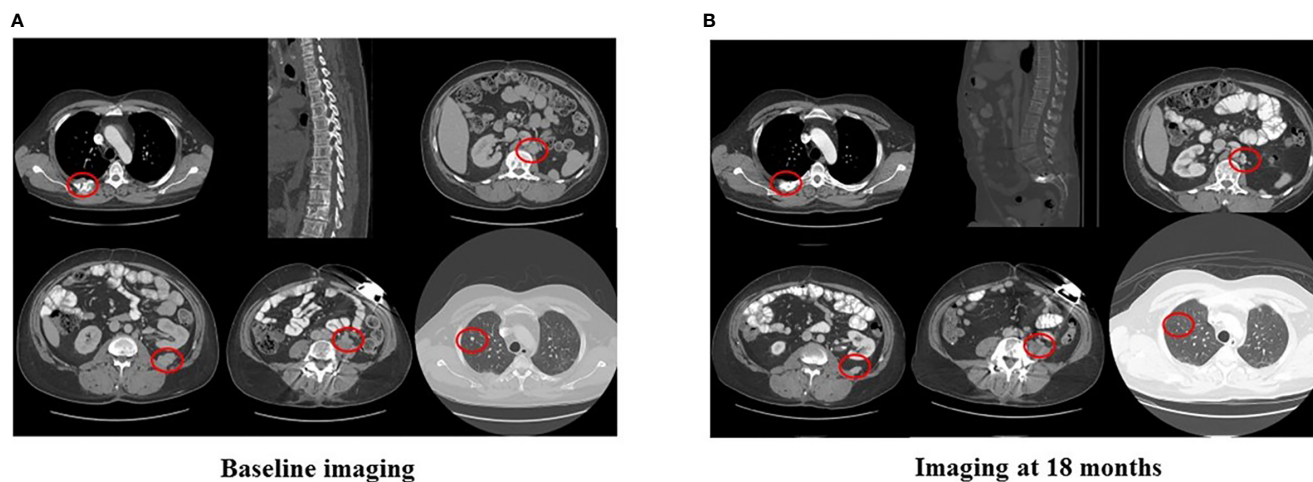


FIGURE 2 | Imaging at baseline and after 18 months of nivolumab plus cabozantinib.



FIGURE 3 | Right lower extremity shin ulcerations.

excess and his blood pressure remains very well controlled after being started on both alpha and beta blockers.

DISCUSSION

When considering this gentleman's case, several interesting observations can be rapidly gleaned. First, the patient had been heavily pre-treated prior to receiving the combination of cabozantinib and nivolumab. The second observation was the greatly enhanced activity of the combination of cabozantinib and nivolumab as compared to when he received either single agent cabozantinib or pembrolizumab on two protocols. The third and final observation are the potential challenges in toxicity that can emerge with new treatments alone or in combination. In the following discussion we will review the currently available systemic treatment options and will provide additional information in regards to both targeted therapeutics and immunotherapy that have prospective data and highlight ongoing studies.

Cytotoxic Chemotherapy

Systemic chemotherapy should be considered for patients with unresectable and rapidly progressive metastatic/unresectable PPGL and in patients with high tumor burden. The most extensively used chemotherapeutic agents include cyclophosphamide, vincristine, dacarbazine (CVD) (12, 20–22). In a retrospective study evaluating 54 patients treated with chemotherapy at MD Anderson Cancer Center, 33% of patients had a decrease in tumor size and achieved blood pressure control (12). In addition, a meta-analysis performed by Niemeijer et al. reported an objective response rate of 37% and a partial response in catecholamine excess in 40% of patients receiving CVD (10).

Radionuclide Therapy

Radionuclide therapy has been long used for treatment of metastatic PPGL and consists mainly of I^{131} -MIBG. I^{131} -MIBG was first

introduced in the 1980s as a potential therapy for PPGL that express the norepinephrine transporter (NET) in their cell membranes (23). Like norepinephrine, I^{131} -MIBG is captured by the NET. With increasing dose levels, I^{131} -MIBG emits sufficient radiation to lead to cellular damage. In an effort to improve the activity and the toxicity profile of I^{131} -MIBG, high-specific-activity (HSA I^{131} -MIBG) was introduced and the recommended phase II dose was determined (24). In the pivotal phase II study of HSA I^{131} -MIBG, the primary endpoint was the reduction in the number of anti-hypertensives and anti-hypertensive dose by greater than or equal to 50%. The primary endpoint was achieved in 25% of the population. An impressive 92% of patients had disease control as best response as defined by the proportion of patients with complete response, partial response, and stable disease as per RECIST v1.1 criteria (25). While myelosuppression was again witnessed, no patients required autologous stem cell rescue and no patients experienced a hypertensive crisis during the delivery of therapy. These findings led the FDA to approve HSA I^{131} -MIBG for patients with metastatic PPGL in 2018 and has become the de facto standard of care.

Molecularly Targeted Therapy

Small molecule TKIs targeting the vascular endothelial growth factor receptor (VEGFR) are well established in the treatment of metastatic renal cell carcinoma including sorafenib, sunitinib, pazopanib, axitinib, cabozantinib, and lenvatinib (26). In addition to VEGFR, significant activity against other important targets in malignancy including the fibroblast growth factor receptors for lenvatinib and c-Met for cabozantinib (27). Early reports suggest the utility of these agents in metastatic PPGL (13–15, 28, 29). The largest retrospective series included 17 patients with metastatic PPGL who were treated with sunitinib monotherapy (15). Of 14 evaluable patients, three (21%) had a partial response and five (36%) had stable disease. The median progression-free survival was 4.1 months. Six patients (43%) had a reduction in catecholamines. Finally, in a recent phase II trial of sunitinib in patients with PPGL,

25 patients with progressive disease were enrolled and received sunitinib at a dose of 50 mg daily 4 weeks on 2 weeks off. The median progression free survival was 13.4 months and three patients (13%) with germline mutations (SDHB) achieved partial remissions (18).

The most worrisome adverse effect of TKIs in patients with PPGL is exacerbation of pre-existing secondary hypertension. Patients with PPGL already have elevated blood pressure due to catecholamine excess. A class effect of TKIs targeting VEGFR is hypertension. Suggested management of hypertension in patients with PPGL can be found in a review by Jasim and Jimenez (30).

Sunitinib is currently being studied in an open label phase II study for patients with metastatic PPGL (NCT00843037). Axitinib is being studied in a two phase II trials in the same population (NCT03839498, NCT01967576). Cabozantinib is used as monotherapy in an active phase II clinical trial (NCT02302833). In addition, lenvatinib is being evaluated in a phase II study in patients with metastatic or advanced unresectable PPGL (NCT03008369).

Immunotherapy

The discovery of immune checkpoints and the development of antibodies targeting cytotoxic lymphocyte antigen 4 (CTLA-4), programmed death receptor 1 (PD-1), and programmed death receptor ligand 1 (PD-L1) has resulted in a paradigm shift in the treatment of both solid and liquid malignancies. In a recent phase II clinical trial of pembrolizumab (anti-PD-1) in advanced rare cancers, 11 patients with metastatic PPGL were evaluated (31). Of the 11 patients, four patients had germline mutations and seven of the patients were hormonally active. The progression free survival (PFS) at 27 weeks after initiation of therapy was 40%, the median PFS was 5.7 months. The overall response rate was 9%.

Combination of TKI and Immune Checkpoint Therapy in Other Malignancies

In metastatic renal cell carcinoma (mRCC), the combination of axitinib (targeting VEGFR 1,2,3) with both pembrolizumab (KEYNOTE 426 study) and avelumab (JAVELIN 101 study) have both received FDA approval based on pivotal phase III trials (32, 33). The combination of cabozantinib and nivolumab (anti-PD-1) with or without ipilimumab (anti-CTLA-4) has also been explored in patients with genitourinary malignancies (19). The combination was found to have activity across a variety of tumors including multiple rare genitourinary tumors including rare variants of urothelial cancer and penile cancer. Recently, the initial results of a phase III randomized study of cabozantinib plus nivolumab versus sunitinib as initial therapy for mRCC (NCT03141177) found a significant improvement in both progress survival and overall survival (Choueiri T et al). The combination of lenvatinib and pembrolizumab recently received FDA for the treatment of advanced endometrial cancer after a phase IB/II study found a 38% overall response rate in previously treated patients (34). This response rate was favorable as compared to a single agent study of lenvatinib which found an overall response rate of 14% (35) and of single agent pembrolizumab finding a response rate of 13% (36).

Significant debate has emerged if TKI plus immune checkpoint therapy leads to additive or synergistic impact. Besides the extrapolation from other malignancies, the use of TKIs and

immunotherapy might have a plausible mechanistic rationale in the treatment of PPGL. In surgically resected PPGL up to 50% of tumors express PD-L1/PD-L2 (37). TKIs inhibit multiple endothelial growth factors that prevent neo-angiogenesis. Cabozantinib is a potent antiangiogenic medication used in clinical practice targeting VEGFR2, c-MET, Axl, and Ron (36). Targeting c-Met may be particularly relevant to metastatic PPGL since activating mutations of the MET gene have recently been described (38, 39). Furthermore, cabozantinib may induce vascular normalization that facilitates the recognition of the tumor cells by the immune system (Reference: Jimenez C, Antiangiogenic therapies for pheochromocytoma and paragangliomas, Endocrine Related Cancer, 2020).

In our patient, it is impossible to know if he would have this tremendous durable response if he had received the combination initially or if chemotherapy prior to treatment potentially enhanced the benefit. However, in multiple other tumor types including renal cell carcinoma and urothelial carcinoma, response rates have been numerically less when immunotherapy is provided either post TKI (40) vs as upfront therapy (41) or post chemotherapy in urothelial cancer (42, 43). Given the activity seen in metastatic PPGL with TKI therapy and with immune checkpoint therapy in small studies, we feel a prospective combination study of cabozantinib plus immune checkpoint therapy is warranted.

CONCLUSION

The development of tyrosine kinase inhibitors and immunotherapy in common cancers has led to exploration of activity in patients with metastatic PPGL. Despite the significant improvement in our understanding of the disease and the exciting approval of HSA I¹³¹ MIBG, patients with metastatic PPGL continue to present multiple therapeutic challenges. The clinical heterogeneity of metastatic PPGL patients necessitates a deep understanding of the molecular features of the disease in order to individualize treatment and improve outcomes. While the backbone of chemotherapy will still be used in patients with rapidly progressive disease there is substantial hope that targeted therapy, immunotherapy, and combination approaches will improve the outcomes for patients with this rare disease.

DATA AVAILABILITY STATEMENT

The raw data supporting the conclusions of this article will be made available by the authors, without undue reservation.

ETHICS STATEMENT

Written informed consent was obtained from the individual(s) for the publication of any potentially identifiable images or data included in this article.

AUTHOR CONTRIBUTIONS

All authors contributed to the drafting of this manuscript and agree with the details included. All authors contributed to the article and approved the submitted version.

REFERENCES

- Lenders JW, Duh QY, Eisenhofer G, Gimenez -Roqueplo AP, Grebe SK, Murad MH, et al. Pheochromocytoma and paraganglioma: an endocrine society clinical practice guideline. *J Clin Endocrinol Metab* (2014) 99:1915–42. doi: 10.1210/jc.2014-1498
- Thosani S, Ayala-Ramirez M, Roman-Gonzalez A, Zhou S, Thosani N, Bisanz A, et al. Constipation: an overlooked, unmanaged symptom of patients with pheochromocytoma and sympathetic paraganglioma. *Eur J Endocrinol* (2015) 173:377–87. doi: 10.1530/EJE-15-0456
- Chen H, Sippel RS, O'Dorisio MS, Vinik AI, Lloyd RV, Pacak K, et al. The North American Neuroendocrine Tumor Society consensus guideline for the diagnosis and management of neuroendocrine tumors: pheochromocytoma, paraganglioma, and medullary thyroid cancer. *Pancreas* (2010) 39:775–83. doi: 10.1097/MPA.0b013e3181eb4f0
- Ayala-Ramirez M FL, Johnson MM, Ejaz S, Habra MA, Rich T, Busaidy N, et al. Clinical Risk Factors for Malignancy and Overall Survival in Patients with Pheochromocytomas and Sympathetic Paragangliomas: Primary Tumor Size and Primary Tumor Location as Prognostic Indicators. *J Clin Endocrinol Metab* (2011) 96:717–25. doi: 10.1210/jc.2010-1946
- Jimenez C, Rohren E, Habra MA, Rich T, Jimenez P, Ayala -Ramirez M, et al. Current and future treatments for malignant pheochromocytoma and sympathetic paraganglioma. *Curr Oncol Rep* (2013) 15:356–71. doi: 10.1007/s11912-013-0320-x
- Baudin E, Habra MA, Deschamps F, Cote G, Dumont F, Cabanillas M, et al. Therapy of endocrine disease: treatment of malignant pheochromocytoma and paraganglioma. *Eur J Endocrinol* (2014) 171:R111–22. doi: 10.1530/EJE-14-0113
- Jimenez P, Tatsui C, Jessop A, Thosani S, Jimenez C. Treatment for Malignant Pheochromocytomas and Paragangliomas: 5 Years of Progress. *Curr Oncol Rep* (2017) 19:83. doi: 10.1007/s11912-017-0643-0
- Pryma DA, Chin BB, Noto RB, Dillon JS, Perkins S, Solnes L, et al. Efficacy and Safety of High-Specific-Activity ¹³¹I-MIBG Therapy in Patients with Advanced Pheochromocytoma or Paraganglioma. *J Nucl Med* (2019) 60:623–30. doi: 10.2967/jnumed.118.217463
- Roman-Gonzalez A, Zhou S, Ayala-Ramirez M, Shen C, Waguespack SG, Habra MA, et al. Impact of Surgical Resection of the Primary Tumor on Overall Survival in Patients With Metastatic Pheochromocytoma or Sympathetic Paraganglioma. *Ann Surg* (2018) 268:172–8. doi: 10.1097/SLA.0000000000002195
- Niemeijer ND, Alblas G, van Hulsteijn LT, Dekkers OM, Corssmit EP. Chemotherapy with cyclophosphamide, vincristine and dacarbazine for malignant paraganglioma and pheochromocytoma: systematic review and meta-analysis. *Clin Endocrinol (Oxf)* (2014) 81:642–51. doi: 10.1111/cen.12542
- van Hulsteijn LT, Niemeijer ND, Dekkers OM, Corssmit EP. ¹³¹I-MIBG therapy for malignant paraganglioma and phaeochromocytoma: systematic review and meta-analysis. *Clin Endocrinol (Oxf)* (2014) 80:487–501. doi: 10.1111/cen.12341
- Ayala-Ramirez M, Feng L, Habra MA, Rich T, Dickson PV, Perrier N, et al. Clinical benefits of systemic chemotherapy for patients with metastatic pheochromocytomas or sympathetic extra-adrenal paragangliomas: insights from the largest single-institutional experience. *Cancer* (2012) 118:2804–12. doi: 10.1002/cncr.26577
- Joshua AM, Ezzat S, Asa SL, Evans A, Broom R, Freeman M, et al. Rationale and evidence for sunitinib in the treatment of malignant paraganglioma/pheochromocytoma. *J Clin Endocrinol Metab* (2009) 94:5–9. doi: 10.1210/jc.2008-1836
- Jimenez C, Cabanillas ME, Santarpia L, Jonasch E, Kyle KL, Lano EA, et al. Use of the tyrosine kinase inhibitor sunitinib in a patient with von Hippel-Lindau disease: targeting angiogenic factors in pheochromocytoma and other von Hippel-Lindau disease-related tumors. *J Clin Endocrinol Metab* (2009) 94:386–91. doi: 10.1210/jc.2008-1972
- Ayala-Ramirez M, Choungnet CN, Habra MA, Palmer JL, Leboulleux S, Cabanillas ME, et al. Treatment with sunitinib for patients with progressive metastatic pheochromocytomas and sympathetic paragangliomas. *J Clin Endocrinol Metab* (2012) 97:4040–50. doi: 10.1210/jc.2012-2356
- Oh DY, Kim TW, Park YS, Shin SJ, Shin SH, Song EK, et al. Phase 2 study of everolimus monotherapy in patients with nonfunctioning neuroendocrine tumors or pheochromocytomas/paragangliomas. *Cancer* (2012) 118:6162–70. doi: 10.1002/cncr.27675
- Naing A, Meric-Bernstam F, Stephen B, Karp DD, Hajjar J, Rodon Ahnert J, et al. Phase 2 study of pembrolizumab in patients with advanced rare cancers. *J Immunother Cancer* (2020) 8. doi: 10.1136/jitc-2019-000347corr1
- O'Kane GM, Ezzat S, Joshua AM, Bourdeau I, Leibowitz-Amit R, Olney HJ, et al. A phase 2 trial of sunitinib in patients with progressive paraganglioma or pheochromocytoma: the SNIPP trial. *Br J Cancer* (2019) 120:1113–9. doi: 10.1038/s41416-019-0474-x
- Apolo ABMA, Mortazavi A, Stein MN, Pal SK, Davarpranah NN, Nadal RM, et al. A phase I study of cabozantinib plus nivolumab (CaboNivo) and ipilimumab (CaboNivoIpi) in patients (pts) with refractory metastatic urothelial carcinoma (mUC) and other genitourinary (GU) tumors. *J Clin Oncol* (2017) 35(6):293. doi: 10.1200/JCO.2017.35.6_suppl.293
- Patel SR, Winchester DJ, Benjamin RS. A 15-year experience with chemotherapy of patients with paraganglioma. *Cancer* (1995) 76:1476–80. doi: 10.1002/1097-0142(19951015)76:8<1476::AID-CNCR2820760827>3.0.CO;2-9
- Huang H, Abraham J, Hung E, Averbuch S, Merino M, Steinberg SM, et al. Treatment of malignant pheochromocytoma/paraganglioma with cyclophosphamide, vincristine, and dacarbazine: recommendation from a 22-year follow-up of 18 patients. *Cancer* (2008) 113:2020–8. doi: 10.1002/cncr.23812
- Edstrom Elder E, Hjelm Skog AL, Hoog A, Hamberger B. The management of benign and malignant pheochromocytoma and abdominal paraganglioma. *Eur J Surg Oncol* (2003) 29:278–83. doi: 10.1053/ejsco.2002.1413
- Sisson J, Shapiro B, Beierwaltes WH, Nakajo M., Glowniak J, Mangner T, et al. Treatment of malignant pheochromocytoma with a new radiopharmaceutical. *Trans Assoc Am Physicians* (1983) 96:209–17.
- Agrawal A, Rangarajan V, Shah S, Puranik A, Purandare N. MIBG (metaiodobenzylguanidine) theranostics in pediatric and adult malignancies. *Br J Radiol* (2018) 91:20180103. doi: 10.1259/bjr.20180103
- Eisenhauer EA, Therasse P, Bogaerts J, Schwartz LH, Sargent D, Ford R, et al. New response evaluation criteria in solid tumours: revised RECIST guideline (version 1.1). *Eur J Cancer* (2009) 45:228–47. doi: 10.1016/j.ejca.2008.10.026
- Motzer RJ, Hutson TE, Tomczak P, Michaelson MD, Bukowski RM, Rixe O, et al. Sunitinib versus interferon alfa in metastatic renal-cell carcinoma. *N Engl J Med* (2007) 356:115–24. doi: 10.1056/NEJMoa065044
- Roskoski R Jr. Vascular endothelial growth factor (VEGF) and VEGF receptor inhibitors in the treatment of renal cell carcinomas. *Pharmacol Res* (2017) 120:116–32. doi: 10.1016/j.phrs.2017.03.010
- Hahn NM, Reckova M, Cheng L, Baldrige LA, Cummings OW, Sweeney CJ. Patient with malignant paraganglioma responding to the multikinase inhibitor sunitinib malate. *J Clin Oncol* (2009) 27:460–3. doi: 10.1200/JCO.2008.19.9380
- Park KS, Lee JL, Ahn H, Koh JM, Park I, Choi JS, et al. Sunitinib, a novel therapy for anthracycline- and cisplatin-refractory malignant pheochromocytoma. *Jpn J Clin Oncol* (2009) 39:327–31. doi: 10.1093/jcco/hyp005
- Jasim S, Jimenez C. Metastatic pheochromocytoma and paraganglioma: Management of endocrine manifestations, surgery and ablative procedures, and systemic therapies. *Best Pract Res Clin Endocrinol Metab* (2019) 101354:1–19. doi: 10.1016/j.beem.2019.101354
- Jimenez C SV, Steph B, Ma J, Milton D, Xu M, Zarifa A, et al. Phase II Clinical Trial of Pembrolizumab in Patients with Progressive Metastatic Pheochromocytomas and Paragangliomas. *Cancers* (2020) 12:2307. doi: 10.3390/cancers12082307
- Rini BI, Plimack ER, Stus V, Gafanov R, Hawkins R, Nosov D, et al. Pembrolizumab plus Axitinib versus Sunitinib for Advanced Renal-Cell Carcinoma. *N Engl J Med* (2019) 380:1116–27. doi: 10.1056/NEJMoa1816714
- Motzer RJ, Penkov K, Haanen J, Rini B, Albiges L, Campbell MT, et al. Avelumab plus Axitinib versus Sunitinib for Advanced Renal-Cell Carcinoma. *N Engl J Med* (2019) 380:1103–15. doi: 10.1056/NEJMoa1816047
- Makker V, Rasco D, Vogelzang NJ, Brose MS, Cohn AL, Mier J, et al. Lenvatinib plus pembrolizumab in patients with advanced endometrial cancer: an interim analysis of a multicentre, open-label, single-arm, phase 2 trial. *Lancet Oncol* (2019) 20:711–8. doi: 10.1016/S1470-2045(19)30020-8

35. Vergote I, Teneriello M, Powell MA, Miller DS, Garcia AA, Mikheeva Tamas Pinter ON, et al. A phase II trial of lenvatinib in patients with advanced or recurrent endometrial cancer: Angiopoietin-2 as a predictive marker for clinical outcomes. *J Clin Oncol* (2013) 31:5520–. doi: 10.1200/jco.2013.31.15_suppl.5520
36. Ott PA, Bang YJ, Berton-Rigaud D, Elez E, Pishvaian MJ, Rugo HS, et al. Safety and Antitumor Activity of Pembrolizumab in Advanced Programmed Death Ligand 1-Positive Endometrial Cancer: Results From the KEYNOTE-028 Study. *J Clin Oncol* (2017) 35:2535–41. doi: 10.1200/JCO.2017.72.5952
37. Pinato DJ, Black JR, Trousil S, Dina RE, Trivedi P, Mauri FA, et al. Programmed cell death ligands expression in pheochromocytomas and paragangliomas: Relationship with the hypoxic response, immune evasion and malignant behavior. *Oncoimmunology* (2017) 6:e1358332. doi: 10.1080/2162402X.2017.1358332
38. Toledo RA, Qin Y, Cheng ZM, Gao Q, Iwata S, Silva GM, et al. Recurrent Mutations of Chromatin-Remodeling Genes and Kinase Receptors in Pheochromocytomas and Paragangliomas. *Clin Cancer Res* (2016) 22:2301–10. doi: 10.1158/1078-0432.CCR-15-1841
39. Jimenez C. Treatment for Patients With Malignant Pheochromocytomas and Paragangliomas: A Perspective From the Hallmarks of Cancer. *Front Endocrinol (Lausanne)* (2018) 9:277. doi: 10.3389/fendo.2018.00277
40. Motzer RJ, Escudier B, Choueiri TK. Treatment of Advanced Renal-Cell Carcinoma. *N Engl J Med* (2016) 374:889–90. doi: 10.1056/NEJMc1515613
41. McDermott DF, Lee JL, Ziobro M, Gafanov RA, Matveev VB, et al. First-line pembrolizumab (pembro) monotherapy for advanced non-clear cell renal cell carcinoma (nccRCC): Results from KEYNOTE-427 cohort B. *J Clin Oncol* (2019) 37:546–. doi: 10.1200/JCO.2019.37.7_suppl.546
42. Bellmunt J, de Wit R, Vaughn DJ, Fradet Y, Lee JL, Fong L, et al. Pembrolizumab as Second-Line Therapy for Advanced Urothelial Carcinoma. *N Engl J Med* (2017) 376:1015–26. doi: 10.1056/NEJMoa1613683
43. Balar AV, Castellano D, O'Donnell PH, Grivas P, Vuky J, Powles T, et al. First-line pembrolizumab in cisplatin-ineligible patients with locally advanced and unresectable or metastatic urothelial cancer (KEYNOTE-052): a multicentre, single-arm, phase 2 study. *Lancet Oncol* (2017) 18:1483–92. doi: 10.1016/S1470-2045(17)30616-2

Conflict of Interest: AS: Research grant support from Exelixis, Bristol Myers Squibb, Merck. CJ, MH, MC: Research grant from Exelixis.

The remaining authors declare that the research was conducted in the absence of any commercial or financial relationships that could be construed as a potential conflict of interest.

The reviewer LC declared a past co-authorship with one of the authors CJ to the handling editor.

Copyright © 2020 Economides, Shah, Jimenez, Habra, Desai and Campbell. This is an open-access article distributed under the terms of the Creative Commons Attribution License (CC BY). The use, distribution or reproduction in other forums is permitted, provided the original author(s) and the copyright owner(s) are credited and that the original publication in this journal is cited, in accordance with accepted academic practice. No use, distribution or reproduction is permitted which does not comply with these terms.



Genetic and Clinical Profiles of Pheochromocytoma and Paraganglioma: A Single Center Study

Xiaosen Ma^{1†}, Ming Li^{2†}, Anli Tong^{1*}, Fen Wang³, Yunying Cui¹, Xuebin Zhang⁴, Yushi Zhang⁴, Shi Chen¹ and Yuxiu Li¹

¹ Department of Endocrinology, Key Laboratory of Endocrinology, National Health Commission of the People's Republic of China, Peking Union Medical College Hospital, Peking Union Medical College, Chinese Academy of Medical Sciences, Beijing, China, ² Department of Clinical Laboratory, Peking Union Medical College Hospital, Peking Union Medical College, Chinese Academy of Medical Sciences, Beijing, China, ³ Department of Endocrinology, Tongji Hospital, Tongji Medical College, Huazhong University of Science and Technology, Wuhan, China, ⁴ Department of Urology, Peking Union Medical College Hospital, Peking Union Medical College, Chinese Academy of Medical Sciences, Beijing, China

OPEN ACCESS

Edited by:

Lee E. Eiden,
National Institutes of Health (NIH),
United States

Reviewed by:

Stephanie Fliedner,
University Medical Center Schleswig-
Holstein, Germany
Anne-Paule Gimenez-Roqueplo,
Assistance Publique Hopitaux De
Paris, France

*Correspondence:

Anli Tong
tonganli@hotmail.com

[†]These authors have contributed
equally to this work and share
first authorship

Specialty section:

This article was submitted to
Neuroendocrine Science,
a section of the journal
Frontiers in Endocrinology

Received: 20 June 2020

Accepted: 03 November 2020

Published: 11 December 2020

Citation:

Ma X, Li M, Tong A, Wang F, Cui Y,
Zhang X, Zhang Y, Chen S and Li Y
(2020) Genetic and Clinical
Profiles of Pheochromocytoma
and Paraganglioma:
A Single Center Study.
Front. Endocrinol. 11:574662.
doi: 10.3389/fendo.2020.574662

Pheochromocytoma/paraganglioma (PPGL) has a high genetic heterogeneity with 40% germline variants in known pathogenic genes. Data in Chinese on this aspect are scanty. To detect the genetic and clinical profile of Chinese PPGL patients, we examined the variants of 12 known germline pathogenic genes (*SDHA*, *SDHB*, *SDHC*, *SDHD*, *SDHAF2*, *FH*, *VHL*, *RET*, *NF1*, *MAX*, *TMEM127*, and *KIF1B*) by next-generation sequencing and Sanger sequencing in 314 Chinese PPGL subjects. Twenty nine percent of Chinese PPGL patients had germline variants and *SDHB* was the most frequently mutated (14.6%). The most frequent *SDHB* variants were in exon 2, exon 7, and IVS 7. Pathogenic variants were more likely to occur in metastatic PPGL patients, paragangliomas, and patients under 30, with the ratio being 50.7% (35/69), 35.9% (56/156), and 49.5% (52/105), respectively. Our cohort included 314 patients from a single setting. The genetic and clinical features of Chinese PPGL patients were unique in some aspects compared to their non-Chinese counterparts. Identification of genotype-phenotype relation can serve as an effective tool for genetic prioritization and clinical decision-making.

Keywords: pheochromocytoma, paraganglioma, Chinese, genetics, genotype-phenotype relation

INTRODUCTION

Pheochromocytoma (PCC) and paraganglioma (PGL) are tumors that originate from adrenal medulla, sympathetic ganglia and parasympathetic ganglia. With the development of the next-generation sequencing (1), about 40% of PCC and PGL (PPGL) bear a relationship with the germline variants of known pathogenic genes and the germline variants are genetically highly heterogeneous (2, 3). Over the last two decades, more than 20 genes have been found to be associated with the development of hereditary PPGL. Of them, *VHL*, *SDHB*, *SDHD*, *SDHA*, and *RET* are the most common pathogenic genes, while several novel pathogenic genes mutated with extremely low frequency, which were only found in one or several families (4–7). At present, the

variants have been profiled in different races. In 2006, a review from the European Network for the Study of Adrenal Tumors (ENS@T) summarized germline variants (*VHL*, *SDHB*, *SDHD*, *RET*, and *NF1*) in 166 (25.9%) of 642 PPGL patients and *VHL* was reportedly the most frequently mutated gene (56/642, 8.7%) (8). Recently, a research conducted in Saudi Arabia exhibited that the variant rate was 36.6% in PPGL subjects and *SDHB* was the most common variant (9). Collectively, these studies showed that the variant rate and underlying genetic profile, to some extent, varied with different ethnic populations. Germline profiling of Chinese PPGLs from two centers found that the variant rate was 21.7% (55/261) and *VHL* was the most frequently mutated gene (10). To know the profile of germline variants and genotype-phenotype correlation in Chinese PPGLs from a single center, we examined the variants in 12 known germline pathogenic genes (*SDHA*, *SDHB*, *SDHC*, *SDHD*, *SDHAF2*, *FH*, *VHL*, *RET*, *NF1*, *MAX*, *TMEM127*, and *KIF1B*) in 314 Chinese PPGLs from a single center. Our study shows that twenty nine percent of Chinese PPGLs had germline variants and *SDHB* was the most frequently mutated (14.6%). We also found the mutation hotspots are different with Chinese and Western populations.

MATERIALS AND METHODS

Patients and Sample Collection

Our study included 314 PPGL patients from the Peking Union Medical College Hospital, Beijing, China. Most patients had undergone surgery and were histopathologically diagnosed with PPGL. For the patients with unresectable or metastatic tumor, PPGL diagnosis was established on the basis of clinical features (headache, palpitations and sweating), increased 24-h urinary catecholamine excretion or plasma metanephrines and imaging tests. 99mTc-hydrazinonicotinyl-Tyr3-Octreotide (99mTc-HYNIC-TOC) scintigraphy, Iodine-131 metaiodobenzylguanidine scintigraphy and contrast-enhanced thoracoabdominal-pelvic computed tomography (CT) were performed for almost all PPGLs. Some patients underwent head and neck enhanced CT or head and neck enhanced MRI examination. 18F-FDG-PET/CT or 68Ga-DOATATATE-PET/CT were performed to patients suspected of metastasis or PPGLs with multiple lesions. Blood samples of the patients were collected, with informed consents obtained from the patients and approval from the medical ethics committee of the hospital.

Genomic DNA Preparation and Sanger Sequencing

Genomic DNA was extracted from the peripheral blood of PPGL patients by using blood DNA Midi Kit (Omega Bio-Tek, Norcross, Georgia, USA). For patients with metastatic PPGL, all the coding sequences and the intro-exon junctions of *SDHB* (NM_003000.3) were amplified and sequenced on an ABI3730 DNA analyzer (Applied Biosystems, CA, USA). For patients with head or neck PPGL, all the coding sequences and the intron-exon junctions of *SDHB* and *SDHD* (NM_003002.4) were amplified and sequenced. As for patients with clinically-diagnosed

hereditary syndromes, such as multiple endocrine neoplasia Type 2 (MEN2) and Von Hippel-Lindau (VHL) disease, hot spots (10, 11, 16 exons) of *RET* (NM_020630.4) and all exons, including intro-exon junctions of *VHL* (NM_000551.3), were amplified and sequenced, respectively. The primers used for the PCR amplification were listed in **Supplementary Table 1**.

Next-Generation Sequencing

For all the patients except those whose variants were detected by the aforementioned Sanger sequencing, next-generation sequencing covering *SDHA* (NM_004168.4), *SDHB* (NM_003000.3), *SDHC* (NM_003001.5), *SDHD* (NM_003002.4), *SDHAF2* (NM_017841.4), *VHL* (NM_000551.3), *RET* (NM_020630.4), *MAX* (NM_002382.5), *TMEM127* (NM_017849.4), *FH* (NM_000143.4), *NF1* (NM_001042492.3), and *KIF1B* (NM_015074.3) was performed to examine the potential pathogenic germline variations.

The probes of target regions for relevant genes were designed against Agilent available online (<http://www.agilent.com>). Agilent SureSelectXT custom kit (Agilent Technologies, Palo Alto, CA) was used to generate sequence library according to instructions. Briefly, fragments of 180-280bp were produced by using a hydrodynamic shearing system (Covaris, Massachusetts, USA). The DNA fragments were end-repaired, A-tailed and adapter-ligated for Illumina sequencing. Then, size selection, PCR amplification and library hybridization were performed. Each captured library with an index was loaded onto the Illumina HiSeq X platform (Illumina Inc., San Diego, CA), and 150-bp paired-end reads were generated.

The fastq files were subjected to quality control to exclude unwanted sequences, including adapter-contaminated or low quality or unrecognizable nucleotides. The fastq files were aligned against the Human Reference Genome (UCSC hg19) by using the Burrows-Wheeler Aligner (BWA). Then, the SAM tools (11) were used to generate the final BAM file (12) to calculate the sequence coverage and depth by sorting the BAM files and performing repeated marking, partial realignment and base quality recalibration. At last, the Variant Call Format files obtained in the previous step were annotated by ANNOVAR (13).

Annotated variants with coverage over 10×, mutant allele frequency (MAF) < 0.01 in the 1,000 Genomes databases and in the exonic or splicing region (10 bp upstream and downstream of splicing sites) were retained (14). The synonymous variants were excluded. Non-synonymous SNVs were retained if at least two of the functional predictions by PolyPhen-2, SIFT, MutationTaster and CADD showed the SNV was damaging. “Benign” or “likely benign” variants in ClinVar were eliminated (15–18). American College of Genomic Medicine (ACMG) guidelines were used for the classification of variant pathogenicity (19). All the variants were confirmed by Sanger sequencing.

SDHB Immunohistochemistry

Immunohistochemical procedures of *SDHB* (ZM-0162, Beijing Zhongshan Golden Bridge Biotechnology Co., Ltd., Beijing, China) were performed on formalin-fixed, paraffin-embedded (FFPE) tissue sections of PPGL according to the manufacturer's recommendations (1:50 dilution). Positive *SDHB* staining was

defined as strong granular staining in cytoplasm; negative SDHB as cytoplasm showing no staining with positive staining for the internal control.

Multiplex Ligation Dependent Probe Amplification

Screening for large deletions of *SDHx* was carried out using the P226-D1 Multiplex Ligation dependent Probe Amplification (MLPA) kit, following the manufacturer's protocol (MRC-Holland, Amsterdam, Netherlands). This P226-D1 probemix contains probes for all exons of the SDHB, SDHC, SDHD, SDHAF2, and SDHAF1 genes. In addition, 13 reference probes are included in this probemix, detecting several different autosomal chromosomal locations.

Large deletions of VHL was detected using MLPA kit (P016-C2 VHL obtained from MRC-Holland, Netherlands), following the protocols described by the manufacturer. This P016-C2 probemix contains 9 probes for VHL, 6 probes for genes located close to VHL, 2 probes on 3p which are further telomeric or centromeric from VHL, and 12 reference probes detecting sequences on other chromosomes.

Final products were separated using ABI 3730xl capillary electrophoresis (Life technologies, CA USA) and the electropherogram was evaluated using Coffalyser.Net.

Statistical Analysis

Continuous variables with non-normal distribution were expressed as median (25%, 75%). Two independent samples were compared by using Mann-Whitney test. Categorical variables were presented as frequency counts and percentages.

Association between two categorical variables was determined by Chi-square test. Kaplan-Meier survival analysis was employed as appropriate. A $P < 0.05$ was considered to be statistically significant. SPSS version 23.0 for Windows was used for all statistical analysis. All unverified VUS were not included in the genotype-phenotypic analysis.

RESULTS

Patient Characteristics

Our study included 314 PPGL patients (165 females and 149 males), with a median age of 38 at diagnosis, ranging from 5 to 68. The clinical and genetic features of the patients are shown in **Figure 1** and **Tables 1** and **2**. In all, 314 patients, 69 (22.0%) had metastatic diseases. In addition, 156 (49.7%) patients had PGL in head and neck, thoracic, retroperitoneal, and pelvic locations; and 158 (50.3%) had PCC which contained 20 bilateral PCC; and 17 patients had tumors in both adrenal and extra-adrenal glands.

The Profile of Gene Variants

We found 107 variants in 314 cases (34.1%) (**Table 1**). Among them, 76/107 variants (65.4%) were previously reported as pathogenic or likely pathogenic, 8/107 variants were uncertainly significant, and 23/107 variants (21.5%) were novel. According to the guidelines of ACMG, 13/23 (56.5%) novel variations were classified as pathogenic or likely pathogenic, 10 variants remained of uncertain significance. SDHB immunohistochemistry was performed on available FFEP tissue sections with VUS of *SDHx*. Negative

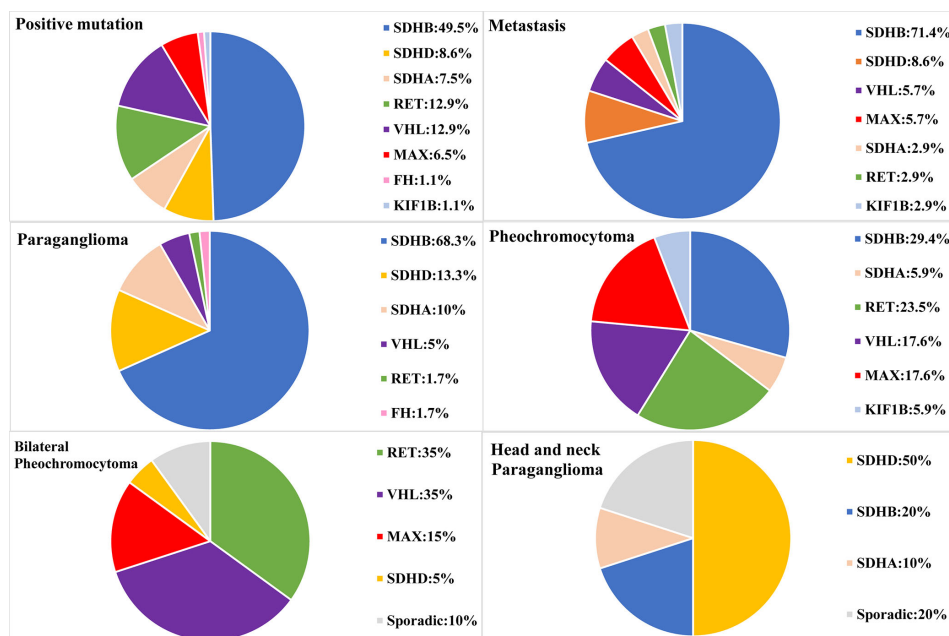


FIGURE 1 | Genetic characteristics of PPGL patients with different phenotypes. Circular statistical graphic was used to illustrate the proportion of mutated gene in different clinical characteristic of PPGL.

TABLE 1 | Clinical and genetic characteristics of variant-positive patients.

No.	Gene	Exon	DNA mutation	Protein change	ACMG	Adjusted ACMG	Novel/ PMID/RS/	Gender	Age on set (year)	Age at dia. (year)	Delay (year)	Duration (month)	Metastasis	Age at meta.(y)	Tumor Location	Tumor Size (cm)	Family History
1	SDHB	E2	c.79C>T	p.R27X	P	P	12000816	F	15	15	36	8	Yes	37	R- PGL	6	No
2	SDHB	E2	c.79C>T	p.R27X	P	P	12000816	M	36	37	1	12	Yes	37	R- PGL,P- PGL		No
3	SDHB	E2	c.137G>A	p.R46Q	P	P	12364472	F	37	41	4	48	No		R- PGL	15	No
4	SDHB	E2	c.137G>A	p.R46Q	P	P	12364472	M	10	10	4	–	Yes	14	R- PGL		No
5	SDHB	E2	c.136C>T	p.R46X	P	P	12618761	F	16	16	1		Yes	17	R- PGL		No
6	SDHB	E2	c.136C>T	p.R46X	P	P	12618761	F	25	31	0	72	Yes	30	P- PGL	8	No
7	SDHB	E2	c.136C>T	p.R46X	P	P	12618761	F	17	18	9	12	No		R- PGL	4	No
8	SDHB	E2	c.136C>T	p.R46X	P	P	12618761	F	20	21	0	5	Yes	21	R- PGL		No
9	SDHB	E2	c.136C>T	p.R46X	P	P	12618761	M	18	18	21	6	Yes	34	PCC	20	No
10	SDHB	E2	c.136C>T	p.R46X	P	P	12618761	F	25	26	6	12	Yes	29	R- PGL	4.7	No
11	SDHB	E2	c.142delG	p.D48fs	P	P	novel	M	15	15	4	1	No		PCC	8.2	No
															R-PGL		
12	SDHB	E2	c.170A>C	p.H57P	LP	LP	novel	M	49	49		6	Yes	51	R- PGL	13	No
13	SDHB	E2	c.170delA	p.H57fs	P	P	novel	M	36	40	16	48	No		T- PGL	7	No
14	SDHB	E2	c.172dup	p.M58fs	P	P	novel	F	13	19	0	72	Yes	19	R- PGL	5	No
15	SDHB	E2	c.194T>G	p.L65R	P	P	23175444	M	32	32	1	1	No		R- PGL	8.1	No
16	SDHB	E3	c.229dup	p.I77fs	P	P	novel	M	53	60	0	84	Yes	60	R- PGL	7	No
17	SDHB	E3	c.277T>C	p.C93R	P	P	17848412	F	48	54	0	72	No		R- PGL	9	No
18	SDHB	E4	c.331_332del	p.L111fs	P	P	19454582	M	26	26	7	8	No		R- PGL	5.3	No
19	SDHB	E4	c.343C>G	p.R115G	P	P	rs751000085	M	61	62	7	6	No		PCC	3.3	No
20	SDHB	E4	c.386C>G	p.P129R	LP	LP	rs587781735	M	14	14	1	3	Yes	14	R- PGL	1.8	No
21	SDHB	E4	c.416T>G	p.L139R	P	P	27279923	F	42	47	1	60	No		R- PGL	4.2	No
22	SDHB	E6	c.552C>G	p.Y184X	P	P	29386252	F	9	10	2	12	Yes	12	R- PGL	6	No
23	SDHB	E6	c.574T>G	p.C192G	P	P	12000816	F	15	15	15	5	Yes	24	Multiple	4.4	No
															R- PGL		
24	SDHB	E7	c.662A>G	p.D221G	LP	LP	novel	M	17	17	11	5	Yes	22	PCC	8	No
25	SDHB	E7	c.662A>G	p.D221G	LP	LP	novel	F	16	16	1	3	Yes	16	R- PGL		No
26	SDHB	E7	c.688C>T	p.R230C	P	P	22517557	M	51	56	0	60	No		R- PGL	8.7	Yes
27	SDHB	E7	c.688C>T	p.R230C	P	P	22517557	F	–	37		–	No		R- PGL		Yes
28	SDHB	E7	c.689G>A	p.R230H	P	P	16314641	F	18	28	5	120	No		R- PGL	6.5	No
29	SDHB	E7	c.689G>A	p.R230H	P	P	16314641	M	26	26	2	10	No		R- PGL	4.1	No
30	SDHB	E7	c.689G>A	p.R230H	P	P	16314641	F	17	19	1	24	No		R- PGL	4.8	No
31	SDHB	E7	c.725G>A	p.R242H	P	P	12000816	M	54	57	10	36	Yes	58	R- PGL	6.2	No
32	SDHB	E7	c.725G>A	p.R242H	P	P	12000816	M	59	59	1	5	Yes	60	R- PGL		No
33	SDHB	E7	c.725G>A	p.R242H	P	P	12000816	F	24	25	1	13	No		HN PGL	4.2	No
34	SDHB	E7	c.725G>A	p.R242H	P	P	12000816	M	10	10	0	1	Yes	13	R- PGL		No
35	SDHB		c.72+1G>T		P	P	16317055	M	39	45	1	72	No		R- PGL	5.1	No
36	SDHB		c.72+1G>T		P	P	16317055	M	13	13	3	6	Yes	16	R- PGL	8	Yes
37	SDHB		c.200+1G>C		P	P	19454582	M	10	10	4	1	No		PCC	3.2	No
															R-PGL		
38	SDHB		c.423+1G>A		P	P	16405730	F	42	48	6	72	No		R- PGL	7.5	Yes
39	SDHB		c.423+1G>C		P	P	16314641	M	25	25	2	1	Yes	25	R- PGL	7.5	No
40	SDHB		c.765+1G>A		P	P	15328326	M	48	50	6	24	Yes	50	R- PGL	6.7	No
41	SDHB		c.765+1G>A		P	P	15328326	M	10	11	0	12	Yes	11	R- PGL	7	No
42	SDHB		c.765+1G>A		P	P	15328326	M	16	20	3	48	Yes	22	PCC	8.5	No
43	SDHB		c.766-1G>A		P	P	novel	M	6	16	4	120	Yes	19	R- PGL	5.3	Yes
44	SDHB		c.766-1G>A		P	P	novel	M	29	32	5	36	No		PCC	3.3	No

(Continued)

TABLE 1 | Continued

No.	Gene	Exon	DNA mutation	Protein change	ACMG	Adjusted ACMG	Novel/ PMID/RS/	Gender	Age on set (year)	Age at dia. (year)	Delay (year)	Duration (month)	Metastasis	Age at meta.(y)	Tumor Location	Tumor Size (cm)	Family History
45	SDHB		c.766-1G>A		P	P	novel	F	27	27	2	1	No		R- PGL	14.4	No
46	SDHB	E1	Large deletions		P	P		M	25	28	2	36	No		R-PGL, HN-PGL	2.6	No
47	SDHA	E3	c.163T>C	p.Y55H	VUS ⁺	VUS		M	58	62	2	48	No		R-PGL	5.0	No
48	SDHA	E3	c.163T>C	p.Y55H	VUS ⁺	VUS		F	64	66	2	24	No		HN-PGL	1.9	No
49	SDHA	E4	c.323A>G	p.N108S	VUS ⁺	VUS	rs758086385	M	61	61	12	3	No		PCC	7	No
50	SDHA	E5	c.460G>T	p.E154X	P	P	novel	F	61	61	1	1	No		R- PGL	4.4	No
51	SDHA	E5	c.508C>A	p.Q170K	VUS ⁻	P	novel	F	30	40	2	120	No		P- PGL	2.9	No
52	SDHA	E5	c.562C>T	p.R188W	P	P	23282968	M	36	46	5	120	No		P- PGL	3	No
53	SDHA	E7	c.773G>T	p.G258V	VUS ⁻	P	novel	F	12	13	7	6	No		R- PGL	12	No
54	SDHA	E8	c.935G>A	p.R312H	VUS ⁺	VUS	novel	F	53	63	1	120	Yes	64	R-PGL	9.8	No
55	SDHA	E8	c.1054C>T	p.R352X	P	P	novel	M	61	63	1	24	No		R- PGL	4.5	No
56	SDHA	E8	c.1058A>G	p.E353G	VUS ⁺	VUS	novel	M	39	41	5	18	No		R-PGL HN-PGL	7.2	No
57	SDHA	E9	c.1135C>T	p.R379C	VUS ⁺	VUS	rs749309213	F	55	55	0	3	No		PCC	4.6	No
58	SDHA	E10	c.1334C>T	p.S445L	P	P	28384794	M	58	58	1	1	Yes	58	PCC	9	No
59	SDHA	E14	c.1865G>A	p.W622X	VUS ⁻	P	23633203	F	21	33	1	144	No		R- PGL	4	No
60	RET	E10	c.1832G>A	p.C611Y	P	P	8557249	F	19	19	6	8	No		bil-PCC	9	No
61	RET	E11	c.1891G>T	p.D631Y	P	P	11149622	F	19	24	3	60	No		PCC	7	No
62	RET	E11	c.1892A>G	p.D631G	LP	LP	rs121913308	F		32	2		No		P- PGL		No
63	RET	E11	c.1900T>A	p.C634S	P	P	8099202	M	39	39	0	1	No		bil-PCC	4.1	Yes
64	RET	E11	c.1900T>C	p.C634R	P	P	8103403	F	30	33	3	36	No		bil-PCC	4.5	No
65	RET	E11	c.1900T>C	p.C634R	P	P	8103403	F	40	42	4	18	No		bil-PCC	5	No
66	RET	E11	c.1900T>C	p.C634R	P	P	8103403	F	31	31	1	2	No		PCC	4.6	Yes
67	RET	E11	c.1900T>G	p.C634G	P	P	8099202	F	21	21	4	7	Yes	25	bil-PCC	8	Yes
68	RET	E11	c.1900T>G	p.C634G	P	P	8099202	F	20	22	3	24	No		bil-PCC	4	Yes
69	RET	E11	c.1901G>A	p.C634Y	P	P	8099202	M	24	25	1	12	No		PCC	6	No
70	RET	E11	c.1901G>A	p.C634Y	P	P	8099202	F	39	39	16	6	No		bil-PCC	7.9	Yes
71	RET	E14	c.2410G>T	p.V804L	P	P	14718397	M	38	38	1	2	No		PCC	6.4	No
72	SDHD	E1	c.19C>G	p.L7V	VUS ⁺	VUS	novel	F	29	59	0	360	No		R-PGL	9.6	No
73	SDHD	E1	c.24T>G	p.S8R	VUS ⁻	LP	rs11550094	F	50	50	1	3	No		R- PGL	6.2	No
74	SDHD	E1	c.49C>T	p.R17X	P	P	18213727	M	26	26	2	2	Yes	28	HN PGL	4.6	No
75	SDHD	E2	c.64C>T	p.R22X	P	P	11391798	M	25	26	0	12	Yes	26	HN PGL	4.7	No
76	SDHD	E3	c.177_181del	p.S59fs	P	P	novel	M	23	23	32		No		PCC,R- PGL,HN PGL,T- PGL, Multiple-HN PGL	3.6	Yes
77	SDHD	E3	c.188_198del	p.S63fs	P	P	30484866	F	53	57	1	48	No		R-PGL	3	No
78	SDHD	E3	c.217A>G	p.S73G	VUS ⁺	VUS	rs748545223	F	43	43	1	2	Yes	52	PCC	5	No
79	SDHD	E3	c.217A>G	p.S73G	VUS ⁺	VUS	rs748545223	M	23	29	0	72	No		HN PGL	6.5	No
80	SDHD	E3	c.305A>C	p.H102P	P	P	19454582	F		48	7		Yes	53	R- PGL	5.3	No
81	SDHD	E4	c.338A>T	p.D113V	LP	LP	rs786202513	F	24	26	6	24	No		bil-PCC,R- PGL,HN PGL		Yes
82	SDHD		c.315-1G>T		P	P	novel	F	25	28	4	36	No				No
83	VHL	E1	c.250G>A	p.V84M	P	P	17688370	F	24	30	0	72	No		R- PGL	4.1	No
84	VHL	E1	c.260T>A	p.V87E	P	P	28388566	M		12			No		bil-PCC		No
85	VHL	E1	c.314C>T	p.T105M	LP	LP	rs761240835	M	9	13	10	48	No		bil-PCC, R- PGL		No
86	VHL	E2	c.414A>G	p.P138P	P	P	30946460	M	15	15	2	3	No		bil-PCC	6.8	Yes

(Continued)

TABLE 1 | Continued

No.	Gene	Exon	DNA mutation	Protein change	ACMG	Adjusted ACMG	Novel/ PMID/RS/	Gender	Age on set (year)	Age at dia. (year)	Delay (year)	Duration (month)	Metastasis	Age at meta.(y)	Tumor Location	Tumor Size (cm)	Family History
87	VHL	E2	c.414A>G	p.P138P	P	P	30946460	M	36	36	2	2	No		PCC	2.3	No
88	VHL	E2	c.458T>A	p.L153Q	P	P	24466223	M	13	22	0	156	No		bil-PCC	8	Yes
89	VHL	E2	c.460C>T	p.P154S	P	P	16595991	F		39	0		Yes	39	R- PGL	6.8	No
90	VHL	E3	c.482G>A	p.R161Q	P	P	7728151	M	19	19	4	6	No		bil-PCC, R- PGL	6.6	Yes
91	VHL	E3	c.482G>A	p.R161Q	P	P	7728151	F	10	10	18	6	Yes	28	bil-PCC, R- PGL	7	No
92	VHL	E3	c.499C>T	p.R167W	P	P	7987306	M	9	9	22		No		bil-PCC, R- PGL	5	No
93	VHL	E3	c.500G>A	p.R167Q	P	P	7987306	M	10	13	9	36	No		PCC	6.5	Yes
94	VHL	E3	c.500G>A	p.R167Q	P	P	7987306	M	14	14	31		No		PCC		No
95	FH	E2	c.193G>A	p.D65N	VUS*	VUS	rs769956664	M	57	57	5	6	No		PCC	6.1	No
96	FH	E2	c.206G>A	p.G69D	VUS*	VUS	novel	F	26	27	6	12	No		R-PGL	4.5	No
97	FH	E6	c.799C>G	p.P267A	VUS*	VUS	novel	F	46	48	2	24	No		PCC	3.5	No
98	FH	E6	c.817G>A	p.A273T	P	P	&	F	30	36	2	72	No		P- PGL	2.5	Yes
99	FH	E9	c.1373C>T	p.A458V	VUS*	VUS	novel	M	46	61	0	180	No		PCC	6.3	No
100	FH	E10	c.1516A>G	p.M506V	VUS*	VUS	rs762413315	F	49	56	1	84	Yes	56	P-PGL		No
101	MAX	E1	c.1A>G	p.M1V	P	P	21685915	M	36	37	3	12	No		bil-PCC	5.9	No
102	MAX	E3	c.97C>T	p.R33X	P	P	21685915	M	16	18	8	24	No		PCC	4	Yes
103	MAX	E3	c.97C>T	p.R33X	P	P	21685915	F	31	31	17	3	Yes	48	PCC	10	No
104	MAX	E3	c.97C>T	p.R33X	P	P	21685915	F	39	43	2	48	No		bil-PCC	3.5	No
105	MAX	E3	c.97C>T	p.R33X	P	P	21685915	F	18	18	14		Yes	22	PCC	7	No
106	MAX	E4	c.223C>T	p.R75X	P	P	21685915	M	24	25	14	12	No		bil-PCC	3.5	No
107	TMEM127	E2	c.133T>C	p.C45R	VUS*	VUS	novel	M	27	27	2	3	No		PCC	5	No
108	KIF1B	E33	c.3649C>T	p.P1217S	P	P	18334619	F		36	0		Yes	36	PCC		No

&<https://doi.org/10.1101/663609>.

P represents for Pathogenic; LP represents for Likely Pathogenic; VUS represents for Variant of Uncertain Significance; F represents for female; M represents for male.

Age at dia. represents for Age at diagnosis; Age at meta. represents for Age at metastasis; Delay represents for delay between the PPGL diagnosis and the PPGL genetic testing; R represents for Retroperitoneal; P represents for Pelvic; T represents for Thoracic; HN represents for Head and neck; bil-PCC represents for bilateral pheochromocytoma.

~represents for SDHB immunohistochemical negative.

*represents for SDHB immunohistochemical positive.

*represents for FFPE unavailable.

TABLE 2 | Clinical characteristics of different pathogenic genes in PPGL patients.

	SDHB (n = 46)	SDHD (n = 8)	SDHA (n = 7)	RET (n = 12)	VHL (n = 12)	MAX (n = 6)	FH (n = 1)	KIF1B (n = 1)
Sex(M/F)	27/19	3/5	3/4	3/9	9/3	3/3	0/1	0/1
Age (year)	26 (16, 41)	27 (26, 49)	46 (37, 60)	32 (23, 28)	15 (13, 24)	28 (20, 36)	36	36
Duration (month)	12 (5, 48)	18 (5, 33)	24 (4, 120)	8 (6, 21)	7 (5, 45)	12 (12, 24)	72	3
Delay (year)	2 (1, 6)	3 (1, 6)	1 (1, 4)	3 (2, 4)	4 (1, 14)	11 (4, 14)	2	0
Multiple	5/46 (10.9%)	3/8 (37.5%)	0	7/12 (58.3%)	7/12 (58.3%)	3/6 (50.0%)	0	0
Metastasis	25/46 (54.3%)	3/8 (37.5%)	1/7 (14.3%)	1/12 (8.3%)	2/12 (16.7%)	2/6 (33.3%)	0	1
Location								
PCC	6/46 (13.0%)	0	1/7 (14.3%)	4/12 (33.3%)	3/12 (25.0%)	3/6 (50.0%)	0	1
Bil-PCC	0	1/8(12.5%)	0	7/12 (58.3%)	7/12 (58.3%)	3/6 (50.0%)	0	0
PGL	41/46 (89.1%)	8/8(100.0%)	6/7 (85.7%)	1/12 (8.3%)	3/12 (25.0%)		1	0
HN-PGL	2/46 (4.3%)	6/8(75.0%)	0	0	0	0	0	0
T-PGL	1/46 (2.1%)	1/8(12.5%)	0	0	0	0	0	0
R-PGL	38/46 (82.6%)	4/8(50.0%)	4/7 (57.1%)	0	3/12 (25.0%)	0	0	0
P-PGL	2/46 (4.3%)	0	2/7 (28.6%)	1/12 (8.3%)	0	0	1	0
PCC+PGL	1/46 (2.1%)	2/8(25.0%)	0		2/12 (16.7%)	0	0	0
Family History	5/46 (10.9%)	2/8(25.0%)	0	5/12 (41.7%)	0	1/6(16.7%)	1	0
Catecholamine								
NE	271.3 (126.0, 967.5)	148.0 (81.7, 211.0)	135.0 (51.9, 246.7)	77.6 (38.6, 364.8)	502.6 (300.7, 786.4)	343.4 (303.1, 399.8)	31.4	256.9
E	3.5 (2.6, 4.6)	3.0 (2, 3.7.0)	4.0 (3, 4.3)	6.1 (3.4, 36.7)	3.6 (2.9, 4.7)	4.7 (4.0, 7.3)	4.4	105.8
DA	274.5 (220.9, 462.1)	171 (127.1, 212.5)	258.4 (176, 295.4)	287.7 (187.6, 326.8)	253.3 (217.3, 302.6)	389.8 (211, 617.1)	326	284.2
Tumor size(cm)	6.4(4.5, 8.0)	4.7 (3.9, 5.2)	4.4 (3.5, 6.8)	6.0 (4.5, 7.5)	6.6 (5.0, 6.8)	5.0 (3.6, 6.7)	2.5	NA

Data are medians and interquartile ranges.

PCC represents for pheochromocytoma; PGL represents for paraganglioma; R represents for Retroperitoneal; P represents for Pelvic; T represents for Thoracic; HN represents for Head and neck; bil-PCC represents for bilateral pheochromocytoma.

NE represents for 24-h urinary Norepinephrine (normal range:16.7–40.7 µg/24 h); E represents for 24-h urinary Epinephrine (normal range: 1.7–6.4 µg/24 h); DA represents for 24-h urinary Dopamine (normal range: 120.9–330.6 µg/24 h).

NA represents for unavailable.

immunostaining of SDHB was presented in 3 VUS of SDHA and one VUS of SDHD (**Figure 2**). Positive immunostaining of SDHB was presented in 2 VUS of SDHA and 2 VUS of SDHD, which suggests variants may not be pathogenic (**Supplementary Figure S1**).

In 207 cases without variants in 12 common pathogenic genes. SDHB immunohistochemistry was performed in 96/207 FFPE tissue sections, only one sample presented negative immunostaining of SDHB. MLPA analysis of the SDHx was then used in the immunohistochemistry negative sample and another 43 samples which contain multiple, metastatic PPGL. MLPA analysis of the VHL was used in early onset (under 20 years old) (n = 19), bilateral PCC (n = 2) or PCC and PGL (n = 6) in succession. We did not detect any deletions and duplications of VHL. Deletions of SDHB gene were detected in the negative immunostaining sample, affecting exon 1.

Altogether, 93/314(29.6%) of PPGLs had germline mutations in 12 known pathogenic genes. SDHB was the most frequently mutated gene (46/314, 14.6%), followed by RET (12/314, 3.8%), VHL (12/314, 3.8%), SDHD (8/314, 2.5%), SDHA (7/314, 2.2%), MAX (6/314, 1.9%), FH (1/314, 0.3%), and KIF1B (1/314, 0.3%).

SDHB Variants

SDHB was the most commonly mutated gene in our series (46/93 variants, 49.5%) with a median age at diagnosis of 26. Compared to sporadic PPGL, PPGL with SDHB variants were more likely to

develop distant metastases or PGL (**Table 3**). 25/46(54.3%) of cases developed metastasis with the median duration of 12 (5, 51) months. Eighty-five percent (39/46) of the cases were PGL, 5/46 of the cases were PCC and 2/46 of the cases had both PCC and PGL (**Table 2**). In our cohort, SDHB variants were mainly located in exon 2 and exon 7, which accounted for 26/46 (56.5%) of all SDHB variants. Among them, codon 46 in exon 2 and codons 230 and 242 in exon 7 were hot variant sites, and were found in 8, 5, and 4 patients, respectively. Besides, variants in IVS7 (c.765+1G>A and c.766–1G>A) were also common in our study and the rate was 6/46 (13.0%). Four unrelated individuals had a family history of PPGL. Two PPGL complicated with pancreatic neuroendocrine tumor and renal clear cell carcinoma, respectively.

The risk of metastasis in SDHB-mutated and sporadic PPGL patients was shown in **Figure 3**. There was a statistically significant difference in the risk of development into distant metastasis between patients with SDHB variants and sporadic PPGLs ($P < .001$). For PPGLs with SDHB variants, the risk of metastasis by the age of 60 was close to 60%, while in patients with sporadic PPGL, the risk was roughly 20% ($P < .001$) (**Figure 3**).

SDHA Variants

There were 13 cases with SDHA variants. Seven patients with pathogenic SDHA variants were diagnosed at a median age of 46 (range: from 13 to 63 years). Most of the patients had PGL (6/7,

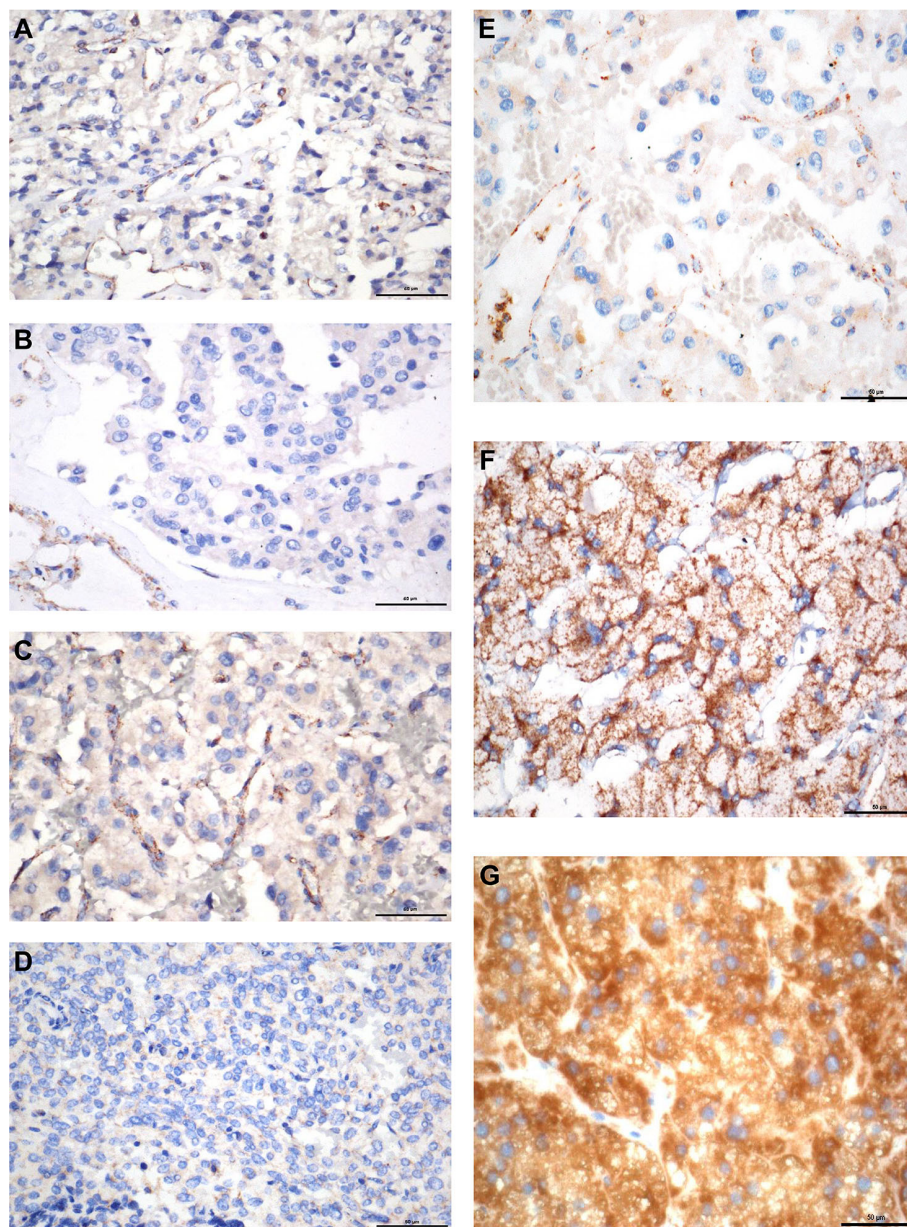


FIGURE 2 | SDHB immunohistochemistry. **(A)** PPGL with *SDHA* mutation (c.C508A). **(B)** PPGL with *SDHA* mutation (c.G773T). **(C)** PPGL with *SDHA* mutation (c.G1865A). **(D)** PPGL with *SDHD* mutation (c.T24G). **(E)** PPGL with an exon 1 large deletion of *SDHB*. **(F)** PPGL with *RET* mutation. **(G)** Normal adrenal medulla. Note: Absence of SDHB immunostaining in the tumour cells **(A–E)**, with positive staining in the normal cells of the intratumoral fibrovascular network. Strong granular staining in PPGL with *RET* mutation and normal adrenal medulla **(F, G)**.

85.7%), and of them, 4 had retroperitoneal PGL and 2 had pelvic PGL. One cases developed metastasis (**Table 2**). Exon 5 tended to have recurrent variants. There was no family history or syndrome in PPGLs with *SDHA* variants.

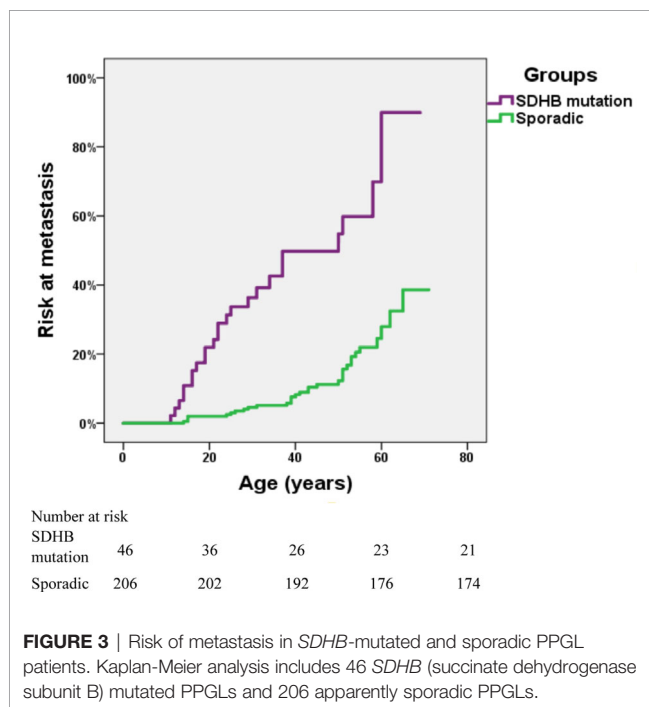
***SDHD* Variants**

There were 11 cases with *SDHD* variants while 8 variants were verified as pathogenic and 3 remained VUS. Cases carrying

pathogenic *SDHD* mutation were diagnosed at a median age of 27 (range: from 23 to 57 years), and 99mTc-HYNIC-TOC scintigraphy was used for the detection of head and neck PGL or multiple PGL in *SDHD* mutation carriers. All cases had PGL. PGL was in head and neck in 4 and in retroperitoneal cavity in 2. Thirty seven percent (3/8) of cases had multiple PPGL. The mutation type of 3 cases with multiple PPGL were frameshifts or splicing. Three cases with single nucleotide variants, mostly (2/3,

TABLE 3 | Genotype-phenotype correlation in patients with PPGL.

	Metastasis		Location			Age(years)		Family History	
	Yes n = (69)	No n = (245)	PCC n = (141)	PGL n = (156)	Multiple (PCC and PGL) n = (17)	<30 n = (105)	>30 n = (209)	Yes n = (18)	No n = (296)
SDHB (n = 46)	25/69 (36.2%)	21/245 (8.6%)	5/141 (3.5%)	39/156 (25.0%)	2/17 (11.8%)	28/105 (26.7%)*	18/209 (8.6%)	5/18 (27.8%)	40/296 (13.5%)
SDHD (n = 8)	3/69 (4.3%)	5/245 (2.0%)	0	6/156 (3.8%)	2/17 (11.8%)	5/105 (4.8%)	2/209 (1.0%)	2/18 (11.1%)	6/296 (2.0%)
SDHA (n = 7)	1/69 (1.4%)	6/245 (2.4%)	1/141 (0.7%)	6/156 (3.8%)	0	1/105 (1.0%)	6/209 (2.9%)	0	7/296 (2.4%)
RET (n = 12)	1/69 (1.4%)	11/245 (4.5%)	11/141 (7.8%)	1/156 (0.6%)	0	5/105 (4.8%)	7/209 (3.3%)	5/18 (27.8%)	7/296 (2.4%)
VHL (n = 12)	2/69 (2.9%)	10/245 (4.1%)	6/141 (5.0%)	3/156 (1.9%)	2/17 (11.8%)	10/105 (9.5%)*	2/209 (1.0%)	4/18 (22.2%)	8/296 (2.7%)
MAX (n = 6)	2/69 (2.9%)	4/245 (1.6%)	6/141 (4.3%)	0	0	3/105 (2.9%)	6/209 (2.9%)	1/18 (5.6%)	5/296 (1.7%)
FH (n = 1)	0	1/245 (0.4%)	0	1/156 (0.6%)	0	0	1/209 (0.5%)	1/18 (5.6%)	0
KIF1B (n = 1)	1/69 (1.4%)	0	1/141 (0.7%)	0	0	0	1/209 (0.5%)	0	1/296 (0.3%)
12 pathogenic genes (n = 93)	35/69 (50.7%)*	58/245 (23.7%)	30/141 (21.3%)	56/156 (35.9%)*	6/17 (35.3%)	52/105 (49.5%)*	43/209 (20.6%)	18*	75/296 (25.3%)
Sporadic(n = 206)	31/69 (44.9%)	175/245 (71.4%)	105/141 (74.5%)	93/156 (59.6%)	8/17 (47.1%)	50/105 (47.6%)	156/209 (74.6%)	0	206/296 (69.6%)

P* < 0.001 vs. sporadic group.#*P* < 0.05 vs. sporadic group.FIGURE 3 |** Risk of metastasis in *SDHB*-mutated and sporadic PPGL patients. Kaplan-Meier analysis includes 46 *SDHB* (succinate dehydrogenase subunit B) mutated PPGLs and 206 apparently sporadic PPGLs.

66.7%) nonsense mutation, tend to develop into single head and neck PGL and metastasis. Two patients had both PCC and PGL. The variant scattered across the 4 exons of *SDHD*. Two cases had a family history of PPGL, and one case had pituitary growth hormone adenoma in addition to PPGL.

RET Variants

RET variants were found in 12 patients. Ninety one percent (11/12) of patients had PCC, among which, 7 had bilateral PCC. Variants in codon 631 and codon 634 in exon 11 of *RET*, were found in 10/12 (83.3%) cases. Forty one percent (5/12) had PPGL family history. In addition to PPGL, 6 patients also had clinical manifestations of medullary thyroid carcinoma. One patient had both PCC and primary hyperparathyroidism.

VHL Variants

VHL variants were detected in 12 patients. Six cases had PCC, including 3 bilateral PCC. Two patients had retroperitoneal PGL, and 4 patients had both bilateral PCC and retroperitoneal PGL (Table 1). Two metastatic PPGL which had no proof of renal cell carcinoma were also found in *VHL* mutated patients. Variants in codon 161 and 167, the most frequently reported mutant sites, were detected in 5/12 (41.7%) patients. Four patients had family history of PPGL. And two cases had other clinical manifestations of *VHL* disease, such as bilateral retinoblastoma, cerebellar hemangioblastoma, renal clear cell carcinoma, and pancreatic neuroendocrine tumor in addition to PPGL.

Compared to sporadic PPGLs, pathogenic germline variants, especially *SDHB* and *VHL*, were more likely to be detected in patients under 30 (*P* < .001).

Other Gene Variants

Six cases had *MAX* variants, and all of them were PCC and half of the PCC were bilateral. Five variants were nonsense and one disrupted the *MAX* protein by affecting the initial methionine (c.1A>G). The most frequent variant was c.97C>T, p.Arg33Ter (4/6, 66.7%), and 2 of the 4 patients with such variant had

metastatic PPGL. One of the patients with *MAX* variants had family history. In addition to PCC, two patients had pituitary growth hormone/prolactin adenoma and thyroid papillary carcinoma, respectively. One case with a family history of PPGL carried a *FH* pathogenic variant. A patient with *KIF1B* variant had metastatic PCC.

Comparison Between Apparently Sporadic PPGLs and Their Counterparts

In our cohort, further analysis was conducted in 206 patients with apparently sporadic PPGL (i.e., patients without variants in 12 known pathogenic genes) and 25 cases with family history or syndromic presentation (Table 4). Compared to apparently sporadic PPGLs, patients with family history or syndromic presentation had an earlier age of onset ($P < .000$), a higher level of norepinephrine ($P < .038$) and were more likely to develop multiple PPGL ($P < .000$). Besides, PCC was more common in apparently sporadic PPGLs ($P = 0.014$).

Variants in PCC and PGL

There were 141 PCC in 314 PPGLs. The 141 PCC patients included 15 bilateral PCC and 21 metastatic PCC patients. Thirty PCC patients (30/141, 21.3%) had germline variants (Figure 1 and Table 3). The top two most frequently mutated genes were *RET* (11/141, 7.8%) and *VHL* (6/141, 4.3%), followed by *MAX* (6/141, 4.3%), *SDHB* (5/141, 3.5%), *SDHA* (1/141, 0.7%), and *KIF1B* (1/141, 0.7%).

Twenty bilateral PCC were included in our cohort (Figure 1), 5 were complicated with PGL. 7/20 (35%) had *RET* variants, 7/20 (35%) had *VHL* variants, 3/20 (15%) had *MAX* variants, 1/20 (5%) had *SDHD* variant, and 2/20 (10%) had no known germline variants (Table 2).

One hundred and fifty six PGL patients were included in our research, involving 129 retroperitoneal PGL, 18 pelvic PGL, 9

head and neck PGL, and 4 thoracic PGL (Table 2). Thirty six percent (56/156) of the PGLs had known pathogenic gene variants (Table 3). In 129 retroperitoneal PGL (Table 2), 34.1% of them had germline mutations. The most frequently mutated gene was *SDHB* (36/129, 27.9%), followed by *SDHA* (4/129, 3.1%), *VHL* (2/129, 1.6%), *SDHD* (1/129, 0.8%), and *RET* (1/129, 0.8%). In 18 pelvic PGL patients, 33.3% of them had germline variants, including *SDHB* (2/18, 11.1%), *SDHA* (2/18, 11.1%), *RET* (1/18, 5.6%), and *FH* (1/18, 5.6%). In 9 patients with head and neck PGL (Figure 1), 66.7% of the patients had germline variants, including *SDHD* (4/9, 44.4%) and *SDHB* (2/9, 22.2%). Thoracic PGL were related to *SDHB* (1/4, 25%) and sporadic PPGL (3/4, 75%). Five patients had both bilateral PCC and PGL. All of them had pathogenic variants, of which 4 carried *VHL* mutation and 1 carried *SDHD* mutation.

Compared to sporadic PPGLs, PPGLs with variants in known pathogenic genes were more likely to develop PGL ($P < .001$).

Genetic Alterations in Metastatic PPGLs

Pathogenic germline variants were more likely to occur in metastatic PPGL than in their non-metastatic counterparts [35/69 (50.7%) vs. 58/245 (23.7%), $P < .001$]. Moreover, distant metastasis occurred more often in PGL than in PCC [45/156 (28.8%) in PGL vs. 21/141 (14.9%) in PCC, $P = 0.004$]. In metastatic PPGL, *SDHB* (25/69, 36.2%) was the most commonly mutated gene (Figure 1 and Table 3). *SDHD* (3/69, 4.3%), *MAX* (2/69, 2.9%), and *VHL* (2/69, 2.9%) had relatively higher frequency of variants. *SDHA*, *RET*, and *KIF1B* were also found to have variants, with a rate of 1.4% (1/69), while we did not find mutations in *FH* in metastatic PPGLs. Of note, 31/69 (44.9%) metastatic PPGL did not possess 12 known pathogenic genes (Figure 1 and Table 3).

Catecholamine Phenotype in PPGLs

Twenty four-hour urinary catecholamine excretion characterized elevated NE or elevated NE and DA in *SDHB* mutated PPGLs. Most patients carrying mutations in *SDHD*, *SDHA*, or *MAX* had elevated NE.

DISCUSSION

In this cohort of Chinese PPGL patients, we profiled the genetic variants and demonstrated genotype-phenotype correlation in Chinese PPGL patients. We found that germline variant rate in PPGL patients was up to 29.6%, and *SDHB* was the most frequently mutated gene. The genetic and clinical features of Chinese PPGL patients were unique in some aspects compared to their non-Chinese counterparts.

The overall variant rates of pathogenic genes in PPGLs in our cohort were similar to those reported previously, standing somewhere between 11% to over 40% (7, 20, 21). A study conducted in Italy examined 10 genes in 501 PPGL patients and found that germline variant rate was 32.1%, and *VHL* was the most frequently mutated gene (22). A recent study from Saudi Arabia reveals that the variant rate was 36.6%, and *SDHB* was the most common variant (9). Jiang J et al. recently reported

TABLE 4 | Comparison of the clinical characteristics between PPGLs with family history or syndromic presentation and apparently sporadic PPGLs.

	PPGLs with family history or syndromic presentation (n = 25)	PPGLs with apparently sporadic presentation (n = 206)	P-value
Age at onset (year)	24 (16, 38)	38 (30, 47)	0.000
Age at diagnosis (year)	25 (18, 37)	42 (31, 52)	0.000
Duration (month)	24 (8, 54)	24 (4, 60)	0.297
Metastasis	4/25 (16%)	32/206 (16%)	1.000
PCC	6/25 (24%)	103/206 (50%)	0.014
PGL	7/25 (28%)	89/206 (43%)	0.145
Multiple PPGL	12/25 (48%)	14/206 (7%)	0.000
Tumor size (cm)	6.0 (4.8, 8.0)	5.4 (4.0, 7.2)	0.260
NE	348.8 (141.0, 542.8)	113.7 (39.4, 440.3)	0.038
E	4.4 (2.9, 7.4)	4.0 (2.7, 6.7)	0.700
DA	285.1 (204.8, 350.0)	230.1 (172.2, 329.1)	0.300

Data are medians and interquartile ranges.

PCC represents for pheochromocytoma; PGL represents for paraganglioma; PPGL represents for pheochromocytoma and paraganglioma; NE represents for 24-h urinary Norepinephrine (normal range: 16.7–40.7 $\mu\text{g}/24\text{ h}$); E represents for 24-h urinary Epinephrine (normal range: 1.7–6.4 $\mu\text{g}/24\text{ h}$); DA represents for 24-h urinary Dopamine (normal range: 120.9–330.6 $\mu\text{g}/24\text{ h}$).

719 PPGLs from two centers in China, of the 719 PPGLs, 266 cases were included in the analysis of germline mutations. Almost twenty one percent of PPGL had pathogenic germline mutations and *VHL* was mostly mutated in PPGL at a rate of 23/261 (8.8%) in germline level (10). Compared to the research of Jiang J et al., our single center had a higher mutation rate of 29.6% and *SDHB* was the most commonly mutated gene in our center. The difference may come from that patients were referred to our hospital from all over the country mostly for their relative complicated or hard-treated diseases. Moreover, the proportion of metastatic PPGL and extra-adrenal PGL in a cohort might also affect the profile of genetic variants.

It is noteworthy that the variant hotspots of *SDHB* varied with different cohorts. According to TCGA data from 173 PPGL patients (23), the detection rate of *SDHB* germline variant was 9.8% (17/173). Among the 17 *SDHB* mutated PPGLs, p.Arg46Ter variant, which was the most frequently mutated one in our *SDHB* mutated PPGLs (6/45, 13.3%), occurred in only one patient (1/17, 5.9%). And the most frequent *SDHB* variant in TCGA data was p.Ile127Ser [29.4% (5/17)], which was not detected in our cohort. In a research conducted in Saudi Arabia, the most common *SDHB* variant was p.Arg90Ter, occurring in 57% of all the *SDHB* mutated cases, while in our series, no case had such variant (9). A national study from the Netherlands revealed that IVS4 (c.423+1G>A) was the most common variant site and was detected in 16/83 (19%) *SDHB* mutated patients, while the variant was found in 2/45 (4.4%) *SDHB* mutated patient in our cohort (24). In addition, in our study, novel variants c.765-1G>A and p.Asp221Gly in *SDHB* were recurrent. Exon 2, exon 7, and the splicing of IVS7 (c.765+1G>A and c.766-1G>A) were the most commonly mutated domains in our cohorts, and the finding was different from the results of other large sample researches (24–27). All the aforementioned studies, including ours, strongly suggest that the hotspots of *SDHB* variant vary in different races or countries, and it may be feasible to preferentially detect some specific sites of *SDHB* gene for metastatic PPGL patients according to the variant hotspots to achieve better cost-effectiveness and efficiency. The clinical features of patients with *SDHB* variants in our series mimicked those in other studies, and *SDHB* variant is associated with development of metastasis and extra-adrenal tumors.

Our results revealed that patients under 30 had a high germline variant rate (52.6%), suggesting that it is necessary to screen the genes in young patients. On the other hand, with *SDHA* and *SDHD* variants, corresponding tumors tend to affect elderly patients (23). It has been reported that the *SDHD* variant carrier had a penetrance rate of 86% at the age of 50 (22, 24, 25). In our study, only 2/8 (25%) *SDHD*-mutated patients had family history of PPGL. Family history may be underestimated because it was obtained by enquiring rather than systematic examination and gene detection in family members.

In our cohort, the hotspot variants of *RET* and *VHL* genes were similar to those reported previously, and were at codons 631 and 634 in exon 11 of *RET* gene and at codons 161 and 167 in exon 3 of *VHL* gene (26, 27). Of note, a synonymous variant recently reported in *VHL* was found in two patients in our study (28). *RET* and *VHL* gene variants mainly cause PCC, and they

are principally responsible for development of bilateral PCC, accounting for 70% in all bilateral PCC in our study. Previous studies also found PGL in *RET*- and *VHL*-mutated patients (26, 27). In our series, only one patient (1/12, 8.3%) with *RET* variant developed PGL. But in *VHL*-mutated patients, 50% (6/12 cases) had retroperitoneal PGL. The rate was higher than that of previous research (10%–20%) (26). Our study suggested that although *VHL* and *RET* gene variants mainly lead to adrenal PCC, they may also result in extra-adrenal PGL. This is especially true of *VHL* variant, which needs to be screened carefully in clinical practice.

Up to now, only 12 PPGL patients with *FH* gene variants have been reported (29–31). In our cohort, we identified six *FH* variants in 314 individuals with PPGL. Only one of the *FH* variants was identified to be pathogenic variants against ACMG. The first published report showed that metastatic PPGLs accounted for 60% (3/5 cases) in *FH*-mutated PPGLs. Nonetheless, no evidence of metastasis of the PPGL with *FH* mutation in our cohort has been found till now.

MAX has been recently described at a total of ~40 PPGLs (9, 32–34). In our study, 6 patients had *MAX* variant, with the ratio being 1.9% in all PPGL patients. All *MAX*-mutated patients developed PCC in our cohort, which was coincident with previous studies (35). The frequent variant c.97C>T was also common in European and American populations (8/23 vs. 4/6 in our study) (35). Interestingly, of all the 4 PPGL cases carrying the same variant site c.97C>T, two were metastatic cases, while previous studies (26, 35) showed that patients carrying c.97C>T did not develop metastasis. This might be a unique genotype-phenotype correlation in Chinese.

KIF1B gene variant had been reported previously in a familial PCC patient. Both the proband and his grandfather had bilateral PCC without distant metastasis. Besides, the proband was also diagnosed with a neuroblastoma and a large well-differentiated leiomyosarcoma successively (36). Our research found a case of *KIF1B* variant who had a unilateral PCC with a metastatic lesion. Of note, the variant site had been previously reported in a patient with neuroblastoma (37). Our case suggested that the germline variants of the *KIF1B* gene could also pose risk of metastatic PCC.

Metastatic PPGL was reported to make up 2% to 13% (vs. 21/141, 14.9% in our study) in PCC and 2.4% to 50% (vs. 45/156, 28.8% in our study) in PGL (38). In our cohort, 50.7% (35/69) of metastatic PPGLs had hereditary germline variants, and were mostly caused by *SDHB* variant, followed by *SDHD*, *VHL*, *MAX*, *SDHA*, *RET*, and *KIF1B*. The results were in line with previous reports (26). The median age at diagnose in metastatic PPGLs was 7 years older (32 years vs. 39 years in our study) than the previously reported age (38, 39). PPGLs with *SDHB* variants need more attention since they are highly predisposed to distant metastasis.

Our study had several limitations. The research focused on the most common 12 pathogenic genes of PPGL and registered a variant detection rate of 29.6%. Our study did not include rare pathogenic genes such as *DLST*, *SLC25A11* and *DNMT3A*, etc., which might lower the detection rate of pathogenic mutations. Furthermore, next-generation sequencing used in this study could

not detect large deletions of some pathogenic genes, such as *SDHx* and *VHL*. Nevertheless, we added *SDHB* immunohistochemistry technique and MLPA detection to all samples with multiple PPGL or metastasis or early onset that are most likely to have large deletions. The proportion of large deletions in *SDHx* was 1.6% (1/61), lower than previously reported.

CONCLUSIONS

In conclusion, our study profiled the genetic variants and identified the corresponding clinical characteristics of PPGL in Chinese subjects. *SDHB* mutation hotspots are different between Chinese and other races. The genotype-phenotype relationship in Chinese is helpful in the prioritization of genetic tests and clinical decision-making.

DATA AVAILABILITY STATEMENT

The raw sequence data reported in the manuscript have been deposited in the Genome Sequence Archive in National Genomics Data Center, Beijing Institute of Genomics (China National Center for Bioinformation), Chinese Academy of Sciences, under accession number HRA000415 that are accessible at <https://bigd.big.ac.cn/gsa-human/s/sKCKPT0A>.

ETHICS STATEMENT

The studies involving human participants were reviewed and approved by Medical Ethics Committee at Peking Union Medical College Hospital and written informed consent to participate in the study was provided by participants or their legal guardians/

next of kin. Written informed consent to participate in this study was provided by the participants' legal guardian/next of kin.

AUTHOR CONTRIBUTIONS

XM conducted the experiments and drafted the manuscript. ML conducted the experiments and analyzed the data. FW, YC, SC, XZ, and YZ collected the specimens. YL and AT reviewed the manuscript. All authors contributed to the article and approved the submitted version.

FUNDING

This research was funded by CAMS Innovation Fund for Medical Sciences (CIFMS), grant number 2017-I2M-1-001.

ACKNOWLEDGMENTS

The authors are indebted to Dr. Zhengpei Zeng in Department of Endocrinology and Dr. Hanzhong Li in Department of Urology for providing expert advice in treating the patients.

SUPPLEMENTARY MATERIAL

The Supplementary Material for this article can be found online at: <https://www.frontiersin.org/articles/10.3389/fendo.2020.574662/full#supplementary-material>. The Supplementary Material (Table_1.xlsx) for this article can be found online at: <https://doi.org/10.6084/m9.figshare.12034230.v1>

REFERENCES

- Ben Aim L, Pigny P, Castro-Vega LJ, Buffet A, Amar L, Bertherat J, et al. Targeted next-generation sequencing detects rare genetic events in pheochromocytoma and paraganglioma. *J Med Genet* (2019) 56(8):513–20. doi: 10.1136/jmedgenet-2018-105714
- Toledo RA, Burnichon N, Cascon A, Benn DE, Bayley JP, Welander J, et al. Consensus Statement on next-generation-sequencing-based diagnostic testing of hereditary pheochromocytomas and paragangliomas. *Nat Rev Endocrinol* (2017) 13(4):233–47. doi: 10.1038/nrendo.2016.185
- Toledo RA, Dahia PL. Next-generation sequencing for the diagnosis of hereditary pheochromocytoma and paraganglioma syndromes. *Curr Opin Endocrinol Diabetes Obes* (2015) 22(3):169–79. doi: 10.1097/med.0000000000000150
- Remacha L, Curras-Freixes M, Torres-Ruiz R, Schiavi F, Torres-Perez R, Calsina B, et al. Gain-of-function mutations in DNMT3A in patients with paraganglioma. *Genet Med* (2018) 20(12):1644–51. doi: 10.1038/s41436-018-0003-y
- Remacha L, Pirman D, Mahoney CE, Coloma J, Calsina B, Curras-Freixes M, et al. Recurrent Germline DLST Mutations in Individuals with Multiple Pheochromocytomas and Paragangliomas. *Am J Hum Genet* (2019) 104(5):1008–10. doi: 10.1016/j.ajhg.2019.04.010
- Buffet A, Morin A, Castro-Vega LJ, Habarou F, Lussey-Lepoutre C, Letouze E, et al. Germline Mutations in the Mitochondrial 2-Oxoglutarate/Malate Carrier SLC25A11 Gene Confer a Predisposition to Metastatic Paragangliomas. *Cancer Res* (2018) 78(8):1914–22. doi: 10.1158/0008-5472.Can-17-2463
- Dahia PL. Pheochromocytoma and paraganglioma pathogenesis: learning from genetic heterogeneity. *Nat Rev Cancer* (2014) 14(2):108–19. doi: 10.1038/nrc3648
- Gimenez-Roqueplo AP, Lehnert H, Mannelli M, Neumann H, Opocher G, Maher ER, et al. Pheochromocytoma, new genes and screening strategies. *Clin Endocrinol (Oxf)* (2006) 65(6):699–705. doi: 10.1111/j.1365-2265.2006.02714.x
- Albattal S, Alswailem M, Moria Y, Al-Hindi H, Dasouki M, Abouelhoda M, et al. Mutational profile and genotype/phenotype correlation of non-familial pheochromocytoma and paraganglioma. *Oncotarget* (2019) 10(57):5919–31. doi: 10.18632/oncotarget.27194
- Jiang J, Zhang J, Pang Y, Bechmann N, Li M, Monteagudo M, et al. Sino-European Differences in the Genetic Landscape and Clinical Presentation of Pheochromocytoma and Paraganglioma. *J Clin Endocrinol Metab* (2020) 105(10):3295–307. doi: 10.1210/clinem/dgaa502
- Li H, Handsaker B, Wysoker A, Fennell T, Ruan J, Homer N, et al. The Sequence Alignment/Map format and SAMtools. *Bioinformatics* (2009) 25(16):2078–9. doi: 10.1093/bioinformatics/btp352
- Li H, Durbin R. Fast and accurate short read alignment with Burrows-Wheeler transform. *Bioinformatics* (2009) 25(14):1754–60. doi: 10.1093/bioinformatics/btp324
- Wang K, Li M, Hakonarson H. ANNOVAR: functional annotation of genetic variants from high-throughput sequencing data. *Nucleic Acids Res* (2010) 38(16):e164. doi: 10.1093/nar/gkq603

14. Sherry ST, Ward MH, Kholodov M, Baker J, Phan L, Smigielski EM, et al. dbSNP: the NCBI database of genetic variation. *Nucleic Acids Res* (2001) 29 (1):308–11. doi: 10.1093/nar/29.1.308
15. Adzhubei I, Jordan DM, Sunyaev SR. Predicting functional effect of human missense mutations using PolyPhen-2. *Curr Protoc Hum Genet* (2013) 76 (7):20. doi: 10.1002/0471142905.hg0720s76
16. Ng PC, Henikoff S. SIFT: Predicting amino acid changes that affect protein function. *Nucleic Acids Res* (2003) 31(13):3812–4. doi: 10.1093/nar/gkg509
17. Schwarz JM, Rodelsperger C, Schuelke M, Seelow D. MutationTaster evaluates disease-causing potential of sequence alterations. *Nat Methods* (2010) 7 (8):575–6. doi: 10.1038/nmeth0810-575
18. Kircher M, Witten DM, Jain P, O'Roak BJ, Cooper GM, Shendure J. A general framework for estimating the relative pathogenicity of human genetic variants. *Nat Genet* (2014) 46(3):310–5. doi: 10.1038/ng.2892
19. Bahcall OG. Genetic testing. ACMG guides on the interpretation of sequence variants. *Nat Rev Genet* (2015) 16(5):256–7. doi: 10.1038/nrg3940
20. Brito JP, Asi N, Bancos I, Gionfriddo MR, Zeballos-Palacios CL, Leppin AL, et al. Testing for germline mutations in sporadic pheochromocytoma/paraganglioma: a systematic review. *Clin Endocrinol (Oxf)* (2015) 82 (3):338–45. doi: 10.1111/cen.12530
21. Crona J, Lamarca A, Ghosal S, Welin S, Skogseid B, Pacak K. Genotype-phenotype correlations in pheochromocytoma and paraganglioma: a systematic review and individual patient meta-analysis. *Endocr Relat Cancer* (2019) 26(5):539–50. doi: 10.1530/erc-19-0024
22. Mannelli M, Castellano M, Schiavi F, Filetti S, Giacche M, Mori L, et al. Clinically guided genetic screening in a large cohort of Italian patients with pheochromocytomas and/or functional or nonfunctional paragangliomas. *J Clin Endocrinol Metab* (2009) 94(5):1541–7. doi: 10.1210/jc.2008-2419
23. Cascon A, Remacha L, Calsina B, Robledo M. Pheochromocytomas and Paragangliomas: Bypassing Cellular Respiration. *Cancers (Basel)* (2019) 11 (5):683. doi: 10.3390/cancers11050683
24. Ricketts CJ, Forman JR, Rattenberry E, Bradshaw N, Lalloo F, Izatt L, et al. Tumor risks and genotype-phenotype-proteotype analysis in 358 patients with germline mutations in SDHB and SDHD. *Hum Mutat* (2010) 31(1):41–51. doi: 10.1002/humu.21136
25. Neumann HP, Pawlu C, Peczkowska M, Bausch B, McWhinney SR, Muresan M, et al. Distinct clinical features of paraganglioma syndromes associated with SDHB and SDHD gene mutations. *Jama* (2004) 292(8):943–51. doi: 10.1001/jama.292.8.943
26. Neumann HPH, Young WF Jr., Eng C. Pheochromocytoma and Paraganglioma. *N Engl J Med* (2019) 381(6):552–65. doi: 10.1056/NEJMra1806651
27. Castinetti F, Qi XP, Walz MK, Maia AL, Sanso G, Peczkowska M, et al. Outcomes of adrenal-sparing surgery or total adrenalectomy in pheochromocytoma associated with multiple endocrine neoplasia type 2: an international retrospective population-based study. *Lancet Oncol* (2014) 15 (6):648–55. doi: 10.1016/s1470-2045(14)70154-8
28. Flores SK, Cheng Z, Jasper AM, Natori K, Okamoto T, Tanabe A, et al. A synonymous VHL variant in exon 2 confers susceptibility to familial pheochromocytoma and von Hippel-Lindau disease. *J Clin Endocrinol Metab* (2019) 104(9):3826–34. doi: 10.1210/jc.2019-00235
29. Richter S, Gieldon L, Pang Y, Peitzsch M, Huynh T, Leton R, et al. Metabolome-guided genomics to identify pathogenic variants in isocitrate dehydrogenase, fumarate hydratase, and succinate dehydrogenase genes in pheochromocytoma and paraganglioma. *Genet Med* (2019) 21(3):705–17. doi: 10.1038/s41436-018-0106-5
30. Clark GR, Sciacovelli M, Gaudé E, Walsh DM, Kirby G, Simpson MA, et al. Germline FH mutations presenting with pheochromocytoma. *J Clin Endocrinol Metab* (2014) 99(10):E2046–50. doi: 10.1210/jc.2014-1659
31. Muller M, Ferlicot S, Guillaud-Bataille M, Le Teuff G, Genestie C, Deveaux S, et al. Reassessing the clinical spectrum associated with hereditary leiomyomatosis and renal cell carcinoma syndrome in French FH mutation carriers. *Clin Genet* (2017) 92(6):606–15. doi: 10.1111/cge.13014
32. Taieb D, Jha A, Guerin C, Pang Y, Adams KT, Chen CC, et al. 18F-FDOPA PET/CT Imaging of MAX-Related Pheochromocytoma. *J Clin Endocrinol Metab* (2018) 103(4):1574–82. doi: 10.1210/jc.2017-02324
33. Daly AF, Castermans E, Oudijk L, Guitelman MA, Beckers P, Potorac I, et al. Pheochromocytomas and pituitary adenomas in three patients with MAX exon deletions. *Endocr Relat Cancer* (2018) 25(5):L37–L42. doi: 10.1530/erc-18-0065
34. Chang X, Li Z, Ma X, Cui Y, Chen S, Tong A. A Novel Phenotype of Germline Pathogenic Variants in MAX: Concurrence of Pheochromocytoma and Ganglioneuroma in a Chinese Family and Literature Review. *Front Endocrinol (Lausanne)* (2020) 11:558. doi: 10.3389/fendo.2020.00558
35. Burnichon N, Cascon A, Schiavi F, Morales NP, Comino-Mendez I, Abermil N, et al. MAX mutations cause hereditary and sporadic pheochromocytoma and paraganglioma. *Clin Cancer Res* (2012) 18(10):2828–37. doi: 10.1158/1078-0432.Ccr-12-0160
36. Yeh IT, Lenci RE, Qin Y, Buddavarapu K, Ligon AH, Leteurtre E, et al. A germline mutation of the KIF1B beta gene on 1p36 in a family with neural and nonneural tumors. *Hum Genet* (2008) 124(3):279–85. doi: 10.1007/s00439-008-0553-1
37. Schlisio S, Kenchappa RS, Vredeveld LC, George RE, Stewart R, Greulich H, et al. The kinesin KIF1Bbeta acts downstream from EglN3 to induce apoptosis and is a potential 1p36 tumor suppressor. *Genes Dev* (2008) 22(7):884–93. doi: 10.1101/gad.1648608
38. Hamidi O, Young WF Jr., Iniguez-Ariza NM, Kittah NE, Gruber L, Bancos C, et al. Malignant Pheochromocytoma and Paraganglioma: 272 Patients Over 55 Years. *J Clin Endocrinol Metab* (2017) 102(9):3296–305. doi: 10.1210/jc.2017-00992
39. Benn DE, Gimenez-Roqueplo AP, Reilly JR, Bertherat J, Burgess J, Byth K, et al. Clinical presentation and penetrance of pheochromocytoma/paraganglioma syndromes. *J Clin Endocrinol Metab* (2006) 91(3):827–36. doi: 10.1210/jc.2005-1862

Conflict of Interest: The authors declare that the research was conducted in the absence of any commercial or financial relationships that could be construed as a potential conflict of interest.

Copyright © 2020 Ma, Li, Tong, Wang, Cui, Zhang, Zhang, Chen and Li. This is an open-access article distributed under the terms of the Creative Commons Attribution License (CC BY). The use, distribution or reproduction in other forums is permitted, provided the original author(s) and the copyright owner(s) are credited and that the original publication in this journal is cited, in accordance with accepted academic practice. No use, distribution or reproduction is permitted which does not comply with these terms.



A Predictive Nomogram for Red Blood Cell Transfusion in Pheochromocytoma Surgery: A Study on Improving the Preoperative Management of Pheochromocytoma

Ying Guo^{1†}, Lili You^{1†}, Huijun Hu², Anli Tong³, Xiaoyun Zhang¹, Li Yan¹ and Shaoling Zhang^{1*}

OPEN ACCESS

Edited by:

Ichiro Abe,
Fukuoka University Chikushi Hospital,
Japan

Reviewed by:

Xin Gao,
Tohoku University, Japan
Nils Lambrecht,
VA Long Beach Healthcare System,
United States

*Correspondence:

Shaoling Zhang
zhshaol@mail.sysu.edu.cn;
413744863@qq.com

[†]These authors have contributed
equally to this work

Specialty section:

This article was submitted to
Neuroendocrine Science,
a section of the journal
Frontiers in Endocrinology

Received: 30 December 2020

Accepted: 15 February 2021

Published: 11 March 2021

Citation:

Guo Y, You L, Hu H, Tong A,
Zhang X, Yan L and Zhang S (2021)
A Predictive Nomogram for
Red Blood Cell Transfusion in
Pheochromocytoma Surgery: A Study
on Improving the Preoperative
Management of Pheochromocytoma.
Front. Endocrinol. 12:647610.
doi: 10.3389/fendo.2021.647610

¹ Department of Endocrinology, Sun Yat-sen Memorial Hospital, Sun Yat-sen University, Guangzhou, China, ² Department of Radiology, Sun Yat-sen Memorial Hospital, Sun Yat-sen University, Guangzhou, China, ³ Department of Endocrinology, Peking Union Medical College Hospital, Beijing, China

Purpose: Surgery is the major treatment option for pheochromocytoma but carries potential risks, including hemorrhage and hemodynamic instability. Even with laparoscopic adrenalectomy, intraoperative blood transfusion happens from time to time, but few studies have investigated risk factors. For the first time we develop and validate a nomogram for prediction of red blood cell transfusion in pheochromocytoma surgery.

Methods: There were 246 patients in our center and 56 patients in Peking Union Medical College Hospital, who underwent pheochromocytoma surgery, enrolled in the study. We incorporated clinical and radiological risk factors, and presented this with a nomogram. Lasso regression model was used for feature selection. Logistic regression analysis was performed to identify the odd ratios. The performance of the nomogram was assessed with respect to its discrimination, calibration and clinical usefulness.

Results: Thirty-two features were reduced to five, which were phenoxybenzamine use, phenoxybenzamine treatment duration, preinduction heart rate, tumor diameter and surgical procedure. The model showed good discrimination (C-index, 0.857; 95% CI, 0.781–0.836) and application in the validation sets also gave good discrimination (internal validation: C-index, 0.831; 95% CI, 0.750–0.822; external validation: C-index, 0.924; 95% CI, 0.766–1.000). Calibration tested with the Hosmer-Lemeshow test yielded a good agreement between prediction and observation (training $P=0.358$; internal validation $P=0.205$; external validation $P=0.395$). Odd ratios of phenoxybenzamine use, phenoxybenzamine treatment duration, preinduction HR, tumor diameter and open surgery were 13.32 (95% CI, 1.48–197.38; $P=0.034$), 1.04 (95% CI, 0.99–1.08; $P=0.092$), 1.04 (95% CI, 1.01–1.08; $P=0.006$), 1.03 (95% CI, 1.02–1.06; $P<0.001$), 17.13 (95% CI, 5.18–78.79; $P<0.001$), respectively. Decision curve analysis demonstrated the clinical usefulness of the nomogram.

Conclusions: This study presents a nomogram that may be used to facilitate the prediction of red blood cell transfusion in pheochromocytoma surgery and help to do the preoperative management more efficiently.

Keywords: pheochromocytoma, blood transfusion, nomogram, prediction model, surgery

INTRODUCTION

Pheochromocytoma (PCC) is a catecholamine secreting tumor arising from chromaffin cells of the adrenal medulla. Circulating catecholamines cause a series of clinical symptoms such as elevated blood pressure, palpitation, headache, as well as heart, brain, kidney and other organ complications (1).

Surgery is the major treatment option but carries potential risks, including hemorrhage and hemodynamic instability, due to the tumoral release of catecholamines during anesthetic induction and tumor manipulation. The mortality associated with surgical resection has significantly improved from 20–45% to 2.9% (2), largely due to the wide use of adrenergic blockade and advances in surgical and anesthetic practice during the past three decades (3). However, surgical resection of PCC still poses significant clinical management challenges. Preoperative management is the key to safe surgery (4, 5).

There is currently no standardized method to assess operative risk for PCC surgery. Based on the available literature, clinicians take age, tumor size, preoperative blood pressure (BP), orthostatic hypotension, body weight change, hematocrit (HCT) and heart rate (HR) as the predictors of hemodynamic stability (6, 7), which is crucial for intraoperative safety. Meanwhile, due to the rich vascularity of PCC, even with laparoscopic adrenalectomy, hemorrhage stays a challenge to surgeons. Therefore intraoperative blood transfusion still happens from time to time, and the global blood product shortage increases the difficulty of such operations to a certain extent. But few studies have investigated risk factors of blood transfusion during PCC surgery to date. Here, we address the question: Is there a way to predict the intraoperative red blood cell (RBC) transfusion before surgery? To answer the question, we develop and validate a nomogram that incorporated both the radiological and clinical risk factors, which may give us some ideas about an individualized prediction of intraoperative RBC transfusion in PCC surgery and help to do the preoperative management more efficiently.

MATERIALS AND METHODS

Ethics Statement

This study was approved by the Institutional Review Board at Sun Yat-sen Memorial Hospital, Sun Yat-sen University. All the data were collected and analyzed after obtaining informed consent by participants.

Subjects

Patients who underwent surgery for PCC, of which the diagnoses were confirmed by postoperative pathological examination (8),

from January 2000 to October 2020 in Sun Yat-sen Memorial Hospital, Sun Yat-sen University and from January 2018 to October 2020 in Peking Union Medical College Hospital, were enrolled. Patients from Peking Union Medical College Hospital served as the external validation group. Patients who met any of the following criteria were excluded: (1) diagnosed metastatic PCCs; (2) extensive resection involving adjacent non-tumor organs; (3) surgery for recurrent or bilateral PCCs; (4) with incomplete medical records.

Surgical Quality Control

All surgeries were conducted under general anesthesia. Furthermore, all operations were performed by the same surgical team with experience in the treatment of PCC. Two chief surgeons were involved in the surgery.

Data Collection

We collected demographic and preoperative clinical data, pharmacological and family history, hemodynamics, biochemical and radiographic results, operation and anesthesia records. Catecholamines and their metabolites in plasma and urine were measured by radioimmunoassay methods (ALPCO, Salem, NH, US). Blood parameters were measured using a Sysmex automated blood cell counter (Sysmex XE-2100). Plasma albumin and glucose level were measured using a Mindray automatic biochemical analyzer (Mindray BC-31s). Pathoglycemia, including impaired fasting glucose (IFG), impaired glucose tolerance (IGT) and diabetes, was defined according to American Diabetes Association (ADA) guidelines updated in 2020 (9). Tumor size was derived from the maximum measurement in millimeter (mm). From 72 h before the operation, preoperative systolic blood pressure (SBP) and diastolic blood pressure (DBP) were measured and recorded every 6 h. The BP and HR were measured while seated, having the patient sit quietly for more than 15 min before measurement and avoid caffeine, exercise, eating and smoking for at least 60 min before measurement. The BP fluctuation was defined as the maximum BP minus the minimum BP. The preinduction BP and HR were defined as the BP and HR value measured in the morning of the surgery.

Preoperative Preparation

A non-selective adrenergic blockade, phenoxybenzamine, was started before surgery to control BP and was titrated according to BP level and tolerability. A beta-adrenoceptor blockade was added in patients with tachycardia after administration of phenoxybenzamine. A calcium channel blockade (CCB) was added if the use of phenoxybenzamine in a sufficient/tolerable dose did not achieve normotension. A high-sodium diet and fluid intake were encouraged to reverse catecholamine-induced blood volume contraction (8).

Statistics

Statistical analyses were performed using RStudio software. All tests were two-tailed, and a two-sided value of $P < 0.05$ was considered statistically significant. Continuous variables were presented as the means \pm standard deviation for normally distributed data and Student's *t*-test was used to compare the differences in characteristics of the patients, whereas variables with a skewed distribution were presented as the median (interquartile range, IQR) and differences between groups were tested with Mann-Whitney *U* test. For the categorical variables, the data were presented as frequencies (percentage) and was compared using the Chi-square test. The least absolute shrinkage and selection operator (LASSO) regression analysis, a method that could minimize the impact of human factors on feature selection, was used to identify the important features associated with intraoperative RBC transfusion in the training set. The glmnet package in R was used for LASSO regression analysis. Odds ratios (ORs), 95% confidence interval (CI) and probability values were calculated by logistic regression analysis.

To evaluate the predictive abilities of this model, an index of the probability of concordance (C-index) was calculated among predicted and actual outcomes. The area under the curve (AUC) in receiver operating characteristic (ROC) analysis was used to evaluate the predictive accuracy of RBC transfusion. Hosmer-Lemeshow tests were used to assess the calibration of the nomogram. Decision curve analysis (DCA) was performed to assess the clinical usefulness of nomogram by evaluating net benefits at various threshold probabilities in training and validation sets.

RESULTS

Characteristics of the Subjects

A total of 246 patients from our center and 56 patients from Peking Union Medical College Hospital were finally included in

the study. We randomly split the patients from our center into training (189 subjects, 76.83%) and internal validation (57 subjects, 23.17%) subsets in a 7:3 ratio using simple random sampling method. There was no significant difference in the demographic, clinical, biochemical or radiological parameters between the training and internal validation sets (see **Supplementary Table 1**, which shows characteristics of patients underwent PCC surgery).

The median age was 46.50 (33.25, 56.00) years old. Hypertension was the most common comorbidity (201 cases, 81.71%). The prevalence of clinical symptoms, such as headache, palpitation and sweating was 71.14%. There were 51.63% cases suffered from diabetes, IFG or IGT during disease. The mean diameter of tumor was 52.06 ± 26.31 mm. Elevated catecholamines/metabolites levels were found in 205 (83.33%) cases.

Non-selective adrenergic blockade, phenoxybenzamine, was commonly used as the preoperative preparation, while 15 patients did not have preoperative adrenergic blockade treatment. Phenoxybenzamine treatment duration was 18.46 ± 11.79 days. 112 patients (45.53%) were given beta-adrenoceptor blockades, while 57 patients (23.17%) were given CCBs. The preinduction heart rate was 80 (76, 90) bpm, which was still higher than the level recommended by current guidelines (8, 10).

The majority of patients (183 cases, 74.39%) were American Society of Anesthesiologists (ASA) physical status III. There were 201 patients (81.71%) underwent laparoscopic adrenalectomy. RBC transfusion was performed in 73 cases (29.67%), of which 41 underwent laparoscopic adrenalectomy and 32 underwent open surgery (**Table 1**).

Compared with non-transfusion group, patients in transfusion group had larger tumor volume, longer preoperative use of phenoxybenzamine, larger preoperative SBP fluctuation and faster preinduction HR, but there was no difference in gender, age, family history, prevalence of hypertension, additional medical history and medications, incidence of positive symptom, BMI, preoperative

TABLE 1 | Comparison between RBC transfusion and non-RBC transfusion groups.

Variables	Training data set (n = 189)			Validation data set (n = 57)		
	Transfusion (n = 61)	Non-transfusion (n = 128)	P-value	Transfusion (n = 12)	Non-transfusion (n = 45)	P-value
Male	27 (44.26%)	59 (46.09%)	0.936	8 (66.67%)	19 (42.22%)	0.237
Age, years	43.0 (33.0, 52.0)	49.0 (33.0, 57.5)	0.131	44.0 (39.0, 57.5)	50.0 (37.0, 56.0)	0.652
Family history	3 (4.92%)	3 (2.34%)	0.345	1 (8.33%)	2 (4.44%)	0.529
Hypertension	51 (83.61%)	103 (80.47%)	0.604	11 (91.67%)	36 (80.00%)	0.345
Elevated catecholamines	53 (86.89%)	107 (83.59%)	0.821	11 (91.67%)	34 (75.56%)	0.224
Tumor diameter, mm	67.53 ± 32.39	44.60 ± 18.00	<0.001	69.67 ± 38.89	47.57 ± 22.63	0.082
PBZ use	59 (96.72%)	119 (92.97%)	0.303	12 (100%)	41 (91.11%)	0.284
PBZ duration, day	20.36 ± 8.64	17.09 ± 10.33	0.024	16.00 ± 3.52	20.44 ± 18.58	0.138
Preoperative SBP fluctuation, mm Hg	35.93 ± 16.72	30.96 ± 13.26	0.044	33.83 ± 19.31	29.04 ± 12.65	0.43
Preoperative DBP fluctuation, mm Hg	22.03 ± 10.10	20.87 ± 8.41	0.436	21.75 ± 11.41	21.07 ± 10.19	0.853
Preinduction SBP, mm Hg	130.00 (118.00, 142.00)	132.00 (115.00, 141.00)	0.786	126.00 (118.00, 146.25)	127.00 (115.00, 141.00)	0.695
Preinduction DBP, mm Hg	80.00 (72.00, 92.00)	77.50 (70.00, 87.00)	0.190	80.00 (76.00, 87.75)	79.00 (72.00, 87.00)	0.557
Preinduction HR, bpm	88.00 (80.00, 93.00)	80.00 (73.00, 88.00)	<0.001	90.50 (81.50, 96.00)	80.00 (74.00, 84.00)	0.011
Laparoscope adrenalectomy	35 (57.38%)	120 (93.75%)	<0.001	6 (50%)	40 (88.89%)	0.002
Open Surgery	26 (42.62%)	8 (6.25%)		6 (50%)	5 (11.11%)	

RBC, red blood cell; PBZ, phenoxybenzamine; SBP, systolic blood pressure; DBP, diastolic blood pressure; HR, heart rate.

DBP fluctuation, preinduction BP or biochemical parameters between the two groups (Table 1 and Supplementary Table 2). Meanwhile, more patients in transfusion group were performed open surgery (42.62% vs. 6.25%, as shown in Table 1).

Feature Selection and Risk Factor Analysis of Intraoperative RBC Transfusion

A λ value of 0.056 with $\log(\lambda)$, -2.878 , was chosen (1 standard deviation) by LASSO regression analysis according to 10-fold cross-validation based on the minimum criteria. Features with non-zero coefficients were selected as the risk factors of intraoperative RBC transfusion (Figures 1A, B), while features excluded by LASSO analysis were more inclined to no difference between groups. Thirty-two texture features (see Supplementary Table 3 for all contents) were reduced to five (Figures 1A, B), which were phenoxybenzamine use, phenoxybenzamine treatment duration, preinduction HR, tumor diameter and surgical procedure (Table 2).

Multivariate logistic regression analysis was also performed to identify the OR values as shown in Table 2 (OR values of phenoxybenzamine use, phenoxybenzamine treatment duration, preinduction HR, tumor diameter and open surgery were 13.32 (95% CI, 1.48–197.38; $P = 0.034$), 1.04 (95% CI, 0.99–1.08; $P = 0.092$), 1.04 (95% CI, 1.01–1.08; $P = 0.006$), 1.03 (95% CI, 1.02–1.06; $P < 0.001$), 17.13 (95% CI, 5.18–78.79; $P < 0.001$), respectively.

Development and Validation of an Individualized Prediction Model for RBC Transfusion

The model for individualized prediction of intraoperative RBC transfusion, which incorporated phenoxybenzamine use, phenoxybenzamine treatment duration, preinduction HR, tumor diameter and surgical procedure, was presented as a nomogram (Figure 2). We constructed ROC curves to evaluate the predictive ability of the nomogram model to predict the prevalence of intraoperative RBC transfusion in both training set (Figure 3A) and internal validation set (Figure 3B). The AUC of ROC curve in training and internal validation were 0.857 (95% CI, 0.781–0.836)

TABLE 2 | Risk factor analysis of intraoperative RBC transfusion.

Intercept and variable	Model in training dataset		
	β	OR(95%CI)	P-value
Intercept	-9.918		<0.001
PBZ Use	2.590	13.32 (1.48–197.38)	0.034
PBZ Treatment Duration	0.035	1.04 (0.99–1.08)	0.092
Preinduction HR	0.044	1.04 (1.01–1.08)	0.006
Tumor Diameter	0.034	1.03 (1.02–1.06)	<0.001
Surgical Procedure (Open vs. Laparoscope)	2.841	17.13 (5.18–78.79)	<0.001

β is the regression coefficient.

RBC, red blood cell; OR, odd ratio; PBZ, phenoxybenzamine; HR, heart rate.

and 0.831 (95% CI, 0.750–0.822), respectively. Besides, external validation was conducted (see Supplementary Table 4) and the AUC of ROC curve was 0.924 (95% CI, 0.766–1.000) (Figure 3C). The calibration of the nomogram demonstrated good agreement between prediction and observation, while the Hosmer-Lemeshow test yielded a nonsignificant statistic in training ($P=0.358$), internal validation ($P=0.205$) and external validation ($P=0.395$) sets.

Clinical Use

DCA for the nomogram was presented in Figure 4, which showed that using the nomogram model to predict intraoperative RBC transfusion added more benefit than either the treat-all-patients scheme or the treat-none scheme in both training and validation sets. Within this range, the net benefit was comparable on the basis of the nomogram.

DISCUSSION

Currently, there is little study on blood transfusion in PCC surgery. For the first time, we developed and validated a clinical- and radiological- based nomogram for the preoperative individualized prediction of RBC transfusion in PCC surgery. The nomogram

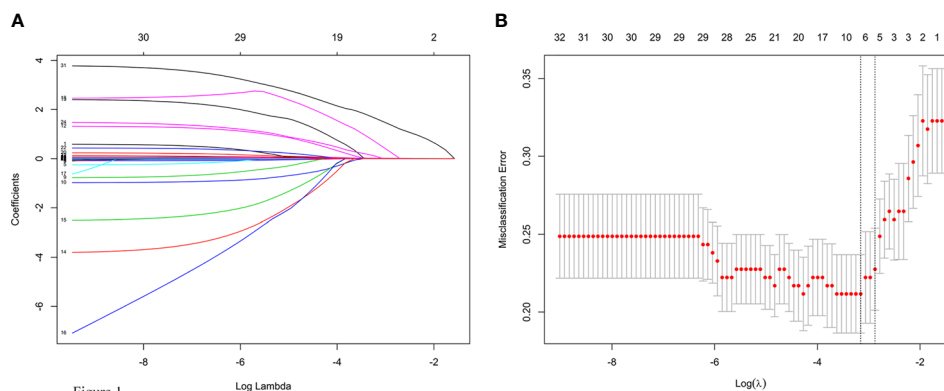


FIGURE 1 | Texture feature selection using the least absolute shrinkage and selection operator (LASSO) logistic regression model. (A) LASSO coefficient profiles of the 32 texture features. (B) Tuning parameter (lambda) selection in the LASSO model used 10-fold cross-validation via minimum criteria for risk of intraoperative RBC transfusion.

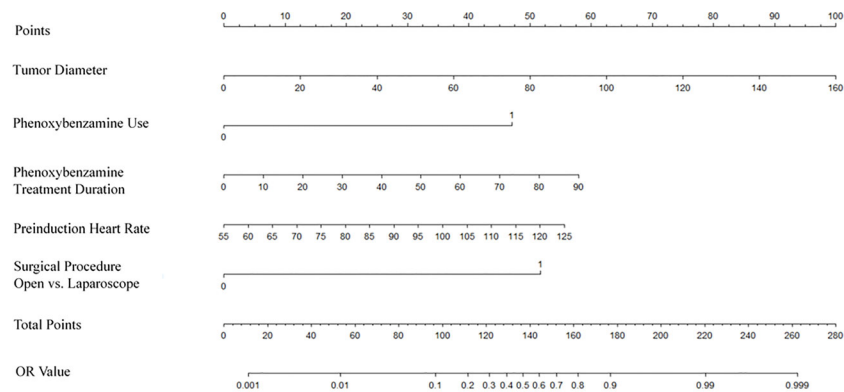


Figure 2

FIGURE 2 | Nomogram for predicting intraoperative RBC transfusion. The nomogram was developed in the training set, with the phenoxylbenzamine use, phenoxylbenzamine treatment duration, preinduction heart rate, tumor diameter and surgical procedure incorporated.

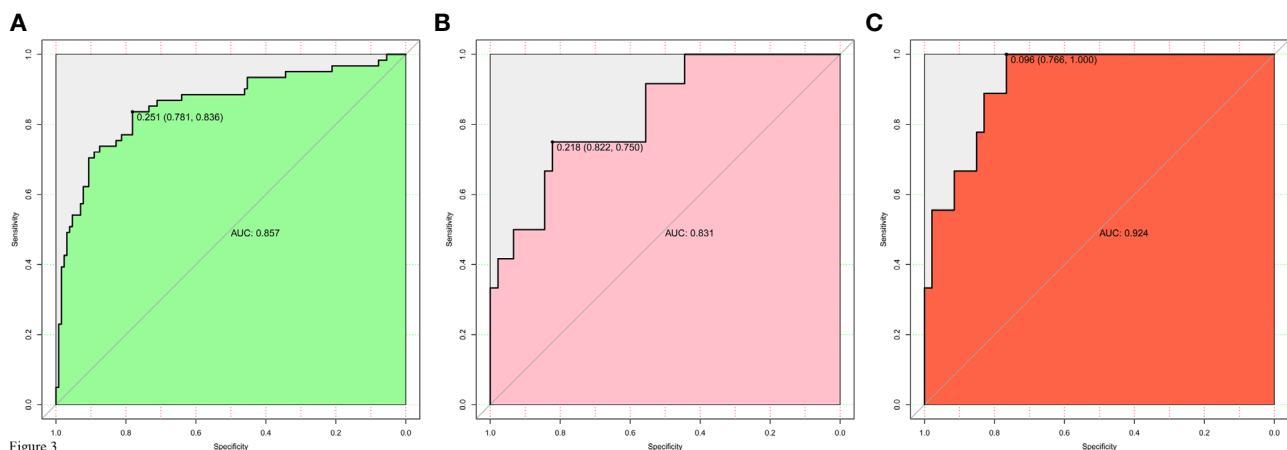


Figure 3

FIGURE 3 | Receiver operating characteristic (ROC) curves for evaluating the nomogram model's discrimination performance in both training and validation sets. **(A)** ROC curve of the nomogram in the training set. **(B)** ROC curve of the nomogram in the internal validation set. **(C)** ROC curve of the nomogram in the external validation set. The AUC of ROC curves plot sensitivity against 1-specificity of the nomogram.

integrates phenoxylbenzamine use, phenoxylbenzamine treatment duration, preinduction HR, tumor diameter and surgical procedure with satisfactory discrimination achieved.

For the construction of the nomogram, 32 texture features were reduced to 5 risk factors by examining the predictor-outcome association by shrinking the regression coefficients with the LASSO method. This method surpasses the method of choosing predictors on the basis of the strength of their univariable association with outcome and minimizes the impact of human factors (11, 12).

The data presented here demonstrate that the nomogram applies well to patients undergoing surgery for PCC. As a nomogram constructed based on data from a single institution and validated by other additional institution, this nomogram has broader applicability. But since the data are based on unilateral

PCC, this nomogram is not applicable to patients who undergo surgical resection for recurrent or bilateral disease.

In our study, preoperative phenoxylbenzamine treatment and a longer duration showed obvious predictive power of increased RBC transfusion. There was no evident reason that could account for this finding, and we speculated that the observed effect might be the impact of phenoxylbenzamine on vascular elasticity.

Current guidelines suggest that in order to normalize BP of PCC patients, the preoperative medication should be initiated 7 to 14 days before surgery, and adrenergic blockade is recommended as the first choice mostly (1, 8). Liu et al. (13) reported that preoperative adrenergic blockade treatment duration ≤ 14 days was a risk factor of massive hemorrhage in PCC surgery and increased RBC transfusion rate. Recent studies had provided different viewpoints and questioned the routine preoperative use

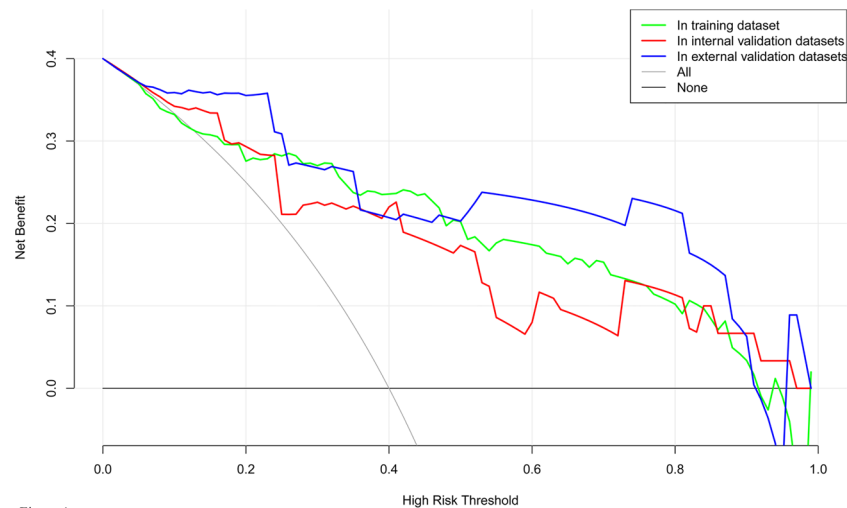


Figure 4

FIGURE 4 | Decision curve analysis for the nomogram model of intraoperative RBC transfusion in training set, internal validation set and external validation set. The y-axis measures the net benefit. The x-axis indicates the threshold probability of the risk of intraoperative RBC transfusion. The green line represents the nomogram in training set, while the red one represents the nomogram in internal validation set and the blue one represents that in external validation set. The grey line represents the assumption that all patients have intraoperative RBC transfusion. Thin black line represents the assumption that no patient has intraoperative RBC transfusion.

of adrenergic blockade. Groeben et al. (14, 15) revealed that intraoperative hypotension occurred more with a preoperative adrenergic blockade, which was closely related to the pharmacological effect of phenoxybenzamine on vasodilation. Furthermore, Li et al.'s study (16) found that intraoperative hypotension was an independent risk factor of complications, including RBC transfusion, in patients who underwent PCC surgery. Compared to Liu et al.'s study (13), the average phenoxybenzamine treatment duration in our study was longer than 14 days to meet the control criteria recommended by the guideline (10). Combined with previous studies (14–16), the influence of phenoxybenzamine use on intraoperative RBC transfusion in our study might be due to the decrease of vasoconstriction then affected hemostasis. So far the potential benefit of preoperative adrenergic blockade treatment in controlling preoperative BP and BP fluctuation in PCC surgery remains convinced (7, 17–22). To the authors' knowledge, there is no randomized controlled trial to determine the ideal application standard of the adrenergic blockade and the existing studies have failed to discuss the influence of treatment duration on perioperative safety. According to our results, the duration of adrenergic blockade treatment is not the longer the better but should be individualized.

Our study observed that faster preinduction HR was associated with more frequent intraoperative RBC transfusion. HR is an important index for evaluating hemodynamics (23, 24) as well as BP and BP fluctuation. A higher preoperative SBP variability in the RBC transfusion group was also proved as shown in **Table 1**. Our results indicated that preoperative hemodynamic instability was closely related to not only intraoperative hemodynamics but also RBC transfusion. Previous studies have proved that preoperative adrenergic blockade treatment served as a major factor affecting the

stability of preoperative hemodynamic (7, 17–20), which suggests that hemodynamics might be used as an assessment of the efficacy of preoperative medication in the future.

Our study also showed that larger tumor diameter and open surgery were identified as risk factors of RBC transfusion. In existing studies, tumor size ≥ 5 cm and open surgery were proposed to be independent risk factors for hemorrhage in PCC surgery (13, 25). Yet, studies on the impact of adrenal tumor size on intraoperative hemorrhage have yielded inconsistent results, when assessing adrenal tumors in general (26–30). However, it should be noted that PCCs have a more prominent vascular network than other types of adrenal tumors. Generally, PCCs larger than 5 cm are considered to be at the risk of metastasis (31, 32), and activated angiogenesis is indispensable and critical for establishing metastasis and growth (31, 33). Our study showed a risk of RBC transfusion increased by 3% per unit of tumor diameter (OR, 1.03; 95% CI, 1.02–1.06; **Table 2**). From the current perspective, all PCCs are believed to exhibit malignant potential though only subsets of cases will display full blown malignant properties (34). Our result allowed the possibility that activated angiogenesis was already present even in PCCs smaller than 5 cm. For further growth, activated angiogenesis promoted more vascular network formation. Therefore it was not surprising that larger tumors required more blood vessel manipulations during surgery, which resulted in more bleeding and RBC transfusion. The superiority of the laparoscopic approach over the open approach had been established by numerous studies, including shorter hospital stay, decreased need for intensive care, lower mean operative time and less hemorrhage (35, 36). The collated results of studies showed a mean hemorrhage of 48 to 150 ml in laparoscopic adrenalectomy for PCC while a mean hemorrhage of 164 to 500 ml in open surgery (37).

Laparoscopic surgery is the recommended operative approach for most PCC, which can be done *via* a transabdominal or retroperitoneal route, while open resection is only recommended for large (eg, 6 cm) or invasive PCC to ensure complete tumor resection (8). Recently with more and more practices, the size of a tumor is no longer a limitation of laparoscopic surgery (26–28). In a word, laparoscopic surgery can significantly reduce the probability of intraoperative RBC transfusion if possible.

A preoperative estimate of intraoperative RBC transfusion in PCC surgery will help to optimize blood conservation and fully prepare allogeneic blood products to ensure patient safety. Thus the most important and final argument for the usefulness of the nomogram is based on the need to interpret individual needs for additional treatment or care. However, the risk-prediction performance, discrimination and calibration, could not capture the clinical consequences of a particular level of discrimination or degree of miscalibration (12, 38, 39). Therefore, to justify the clinical usefulness, DCA was applied in this study. This method offers insight into clinical consequences on the basis of threshold probability, from which the net benefit could be derived (12, 40, 41). The decision curve showed that using the nomogram in the current study to predict RBC transfusion adds more benefit than either the treat-all-patients scheme or the treat-none scheme.

The limitation of the study is its retrospective design. This study includes patients from a 20-year interval. It is likely that increased experience of the surgical team has impacted RBC transfusion rate over the last 20 years. This effect is hard to quantify and should be considered when interpreting the results of this study. At the same time, methods of catecholamine detection had changed greatly in the past two decades so the effect of catecholamine levels in this study were unable to analyze. Besides, very few patients underwent the surgery without preoperative adrenergic blockade treatment, which could have masked some of the artificial influences. In addition, in our center retroperitoneal laparoscopic adrenalectomy is preferable, it is unknown whether transperitoneal laparoscopic adrenalectomy will give different results (42). On all these counts, further randomized controlled prospective multi-center studies are needed to improve the accuracy of this nomogram.

CONCLUSIONS

In conclusion, our study presents a nomogram that incorporates phenoxybenzamine use, phenoxybenzamine treatment duration, preinduction HR, tumor diameter and surgical procedure, which may be used to facilitate the preoperative individualized prediction of RBC transfusion in PCC surgery and help to do

the preoperative management more efficiently. This finding may also support the idea that taking into account factors that span different aspects is the most promising approach to change clinical management.

DATA AVAILABILITY STATEMENT

The original contributions presented in the study are included in the article/**Supplementary Material**. Further inquiries can be directed to the corresponding author.

ETHICS STATEMENT

The studies involving human participants were reviewed and approved by Institutional Review Board at Sun Yat-sen Memorial Hospital, Sun Yat-sen University. The patients/participants provided their written informed consent to participate in this study.

AUTHOR CONTRIBUTIONS

YG, LLY, and SZ conceived and designed the study. YG, HH, AT, and XZ collected and managed the data. YG and LLY analyzed the data and wrote the manuscript. LY and SZ reviewed and edited the manuscript. All authors contributed to the article and approved the submitted version.

FUNDING

This work was supported by the Natural Science Foundation of Guangdong Province (2018A030313596) to YG, and the National Natural Science Foundation of China (81970683) and the Natural Science Foundation of Guangdong Province (2020A1515010245) to SZ.

SUPPLEMENTARY MATERIAL

The Supplementary Material for this article can be found online at: <https://www.frontiersin.org/articles/10.3389/fendo.2021.647610/full#supplementary-material>

REFERENCES

- Berends AMA, Kerstens MN, Lenders JWM, Timmers HJLM. Approach to the Patient: Perioperative Management of the Patient with Pheochromocytoma or Sympathetic Paraganglioma. *J Clin Endocrinol Metab* (2020) 105(9):3088–102. doi: 10.1210/clinem/dgaa441
- Challis BG, Casey RT, Simpson HL, Gurnell M. Is there an optimal preoperative management strategy for pheochromocytoma/paraganglioma? *Clin Endocrinol (Oxf)* (2017) 86(2):163–7. doi: 10.1111/cen
- Tanabe A, Naruse M. Recent advances in the management of pheochromocytoma and paraganglioma. *Hypertens Res* (2020) 43:1141–51. doi: 10.1038/s41440-020-0531-0
- Pacak K, Eisenhofer G, Tischler AS. Pheochromocytoma - advances through science, collaboration and spreading the word. *Nat Rev Endocrinol* (2020) 16(11):621–2. doi: 10.1038/s41574-020-00413-w
- Lim ES, Akker SA. Haemodynamic instability of the pheochromocytoma. *Gland Surg* (2020) 9(4):869–71. doi: 10.21037/gs-20-524
- Lafont M, Fagour C, Haissaguerre M, Darancette G, Wagner T, Corcuff JB, et al. Per-operative hemodynamic instability in normotensive patients with

- incidentally discovered pheochromocytomas. *J Clin Endocrinol Metab* (2015) 100(2):417–21. doi: 10.1210/jc.2014-2998
7. Jiang M, Ding H, Liang Y, Tang J, Lin Y, Xiang K, et al. Preoperative risk factors for haemodynamic instability during pheochromocytoma surgery in Chinese patients. *Clin Endocrinol (Oxf)* (2018) 88(3):498–505. doi: 10.1111/cen.13544
 8. Lenders JW, Duh QY, Eisenhofer G, Gimenez-Roqueplo AP, Grebe SK, Murad MH, et al. Endocrine Society. Pheochromocytoma and paraganglioma: an endocrine society clinical practice guideline. *J Clin Endocrinol Metab* (2014) 99(6):1915–42. doi: 10.1210/jc.2014-1498
 9. Association AD. Standards of Medical Care in Diabetes-2020. *Diabetes Care* (2020) 43(Suppl 1):S14–31. doi: 10.2337/dc20-S001
 10. Roizen MF, Horrigan RW, Koike M, Eger IE2nd, Mulroy MF, Frazer B, et al. A prospective randomized trial of four anesthetic techniques for resection of pheochromocytoma. *Anesthesiology* (1982) 57(3A):A43. doi: 10.1097/0000542-198209001-00043
 11. Harrell FEJr. *Regression Modeling Strategies: With Applications to Linear Models, Logistic Regression, and Survival Analysis*. New York, NY: Springer (2015).
 12. Zamanipour Najafabadi AH, Ramspek CL, Dekker FW, Heus P, Hooft L, Moons KGM, et al. TRIPOD statement: a preliminary pre-post analysis of reporting and methods of prediction models. *BMJ Open* (2020) 10(9):e041537. doi: 10.1136/bmjopen-2020-041537
 13. Liu H, Li B, Yu X, Huang Y. Preoperative risk factors for massive blood loss in adrenalectomy for pheochromocytoma. *Oncotarget* (2017) 8(45):79964–70. doi: 10.18632/oncotarget.20396
 14. Groeben H, Walz MK, Nottebaum BJ, Alesina PF, Greenwald A, Schumann R, et al. International multicentre review of perioperative management and outcome for catecholamine-producing tumours. *Br J Surg* (2020) 107(2):e170–8. doi: 10.1002/bjs.11378
 15. Groeben H, Nottebaum BJ, Alesina PF, Traut A, Neumann HP, Walz MK. Perioperative α -receptor blockade in phaeochromocytoma surgery: an observational case series. *Br J Anaesth* (2017) 118(2):182–9. doi: 10.1093/bja/aew392
 16. Li N, Kong H, Li SL, Zhu SN, Zhang Z, Wang DX. Intraoperative hypotension is associated with increased postoperative complications in patients undergoing surgery for pheochromocytoma-paraganglioma: a retrospective cohort study. *BMC Anesthesiol* (2020) 20(1):147. doi: 10.1186/s12871-020-01066-y
 17. Liu Y, Wang B. The relationship between preoperative preparation and intraoperative hypotension of patients undergoing laparoscopic pheochromocytoma resection: A retrospective study. *J Clin Anesth* (2020) 64:109794. doi: 10.1016/j.jclinane.2020.109794
 18. Naranjo J, Dodd S, Martin YN. Perioperative Management of Pheochromocytoma. *J Cardiothorac Vasc Anesth* (2017) 31(4):1427–39. doi: 10.1053/j.jvca.2017.02.023
 19. Namekawa T, Utsumi T, Kawamura K, Kamiya N, Imamoto T, Takiguchi T, et al. Clinical predictors of prolonged postresection hypotension after laparoscopic adrenalectomy for pheochromocytoma. *Surgery* (2016) 159(3):763–70. doi: 10.1016/j.surg.2015.09.016
 20. Weingarten TN, Welch TL, Moore TL, Walters GF, Whipple JL, Cavalcante A, et al. Preoperative Levels of Catecholamines and Metanephrines and Intraoperative Hemodynamics of Patients Undergoing Pheochromocytoma and Paraganglioma Resection. *Urology* (2017) 100:131–8. doi: 10.1016/j.urol.2016.10.012
 21. Isaacs M, Lee P. Preoperative alpha-blockade in phaeochromocytoma and paraganglioma: is it always necessary? *Clin Endocrinol (Oxf)* (2017) 86(3):309–14. doi: 10.1111/cen.13284
 22. Livingstone M, Duttchen K, Thompson J, Sunderani Z, Hawboldt G, Sarah Rose M, et al. Hemodynamic Stability During Pheochromocytoma Resection: Lessons Learned Over the Last Two Decades. *Ann Surg Oncol* (2015) 22(13):4175–80. doi: 10.1245/s10434-015-4519-y
 23. Wachtel H, Kennedy EH, Zaheer S, Bartlett EK, Fishbein L, Roses RE, et al. Preoperative Metoprolol Improves Cardiovascular Outcomes for Patients Undergoing Surgery for Pheochromocytoma and Paraganglioma. *Ann Surg Oncol* (2015) 22(Suppl 3):S646–654. doi: 10.1245/s10434-015-4862-z
 24. Lafont M, Fagour C, Haissaguerre M, Darancette G, Wagner T, Corcuff JB, et al. Per-operative hemodynamic instability in normotensive patients with incidentally discovered pheochromocytomas. *J Clin Endocrinol Metab* (2015) 100(2):417–21. doi: 10.1210/jc.2014-2998
 25. Liu H, Li B, Yu X, Huang Y. Perioperative management during laparoscopic resection of large pheochromocytomas: A single-institution retrospective study. *J Surg Oncol* (2018) 118(4):709–15. doi: 10.1002/jso.25205
 26. Natkaniec M, Pędziwiatr M, Wierdak M, Major P, Migaczewski M, Matłok M, et al. Laparoscopic Transperitoneal Lateral Adrenalectomy for Large Adrenal Tumors. *Urol Int* (2016) 97(2):165–72. doi: 10.1159/000444146
 27. Agrusa A, Romano G, Frazzetta G, Chianetta D, Sorce V, Di Buono G, et al. Laparoscopic adrenalectomy for large adrenal masses: single team experience. *Int J Surg* (2014) 12 Suppl 1:S72–74. doi: 10.1016/j.ijss.2014.05.050
 28. Carter YM, Mazeh H, Sippel RS, Chen H. Safety and feasibility of laparoscopic resection for large (≥ 6 CM) pheochromocytomas without suspected malignancy. *Endocr Pract* (2012) 18(5):720–6. doi: 10.4158/EP12014.OR
 29. Zhao Y, Fang L, Cui L, Bai S. Application of data mining for predicting hemodynamics instability during pheochromocytoma surgery. *BMC Med Inform Decis Mak* (2020) 20(1):165. doi: 10.1186/s12911-020-01180-4
 30. Pędziwiatr M, Natkaniec M, Kisilewski M, Major P, Matłok M, Kołodziej D, et al. Adrenal incidentalomas: should we operate on small tumors in the era of laparoscopy? *Int J Endocrinol* (2014) 2014:658483. doi: 10.1155/2014/658483
 31. Gao X, Yamazaki Y, Pecori A, Tezuka Y, Ono Y, Omata K, et al. Histopathological Analysis of Tumor Microenvironment and Angiogenesis in Pheochromocytoma. *Front Endocrinol (Lausanne)* (2020) 11:587779. doi: 10.3389/fendo.2020.587779
 32. Fassnacht M, Assie G, Baudin E, Eisenhofer G, de la Fouchardiere C, Haak HR, et al. ESMO Guidelines Committee. Adrenocortical carcinomas and malignant phaeochromocytomas: ESMO-EURACAN Clinical Practice Guidelines for diagnosis, treatment and follow-up. *Ann Oncol* (2020) 31(11):1476–90. doi: 10.1016/j.annonc.2020.08.2099
 33. Sasano H, Suzuki T. Pathological evaluation of angiogenesis in human tumor. *BioMed Pharmacother* (2005) 59 Suppl 2:S334–336. doi: 10.1016/s0753-3322(05)80068-x
 34. Pacak K, Eisenhofer G, Tischler AS. Phaeochromocytoma - advances through science, collaboration and spreading the word. *Nat Rev Endocrinol* (2020) 16(11):621–2. doi: 10.1038/s41574-020-00413-w
 35. Galati SJ, Said M, Gospin R, Babic N, Brown K, Geer EB, et al. The Mount Sinai clinical pathway for the management of pheochromocytoma. *Endocr Pract* (2015) 21(4):368–82. doi: 10.4158/EP14036.RA
 36. Zhu W, Wang S, Du G, Liu H, Lu J, Yang W. Comparison of retroperitoneal laparoscopic versus open adrenalectomy for large pheochromocytoma: a single-center retrospective study. *World J Surg Oncol* (2019) 17(1):111. doi: 10.1186/s12957-019-1649-x
 37. Li J, Wang Y, Chang X, Han Z. Laparoscopic adrenalectomy (LA) vs open adrenalectomy (OA) for pheochromocytoma (PHEO): A systematic review and meta-analysis. *Eur J Surg Oncol* (2020) 46(6):991–8. doi: 10.1016/j.ejso.2020.02.009
 38. Localio AR, Goodman S. Beyond the usual prediction accuracy metrics: reporting results for clinical decision making. *Ann Intern Med* (2012) 157(4):294–5. doi: 10.7326/0003-4819-157-4-201208210-00014
 39. Van Calster B, Vickers AJ. Calibration of risk prediction models: impact on decision-analytic performance. *Med Decis Making* (2015) 35(2):162–9. doi: 10.1177/0272989X14547233
 40. Huang YQ, Liang CH, He L, Tian J, Liang CS, Chen X, et al. Development and Validation of a Radiomics Nomogram for Preoperative Prediction of Lymph Node Metastasis in Colorectal Cancer. *J Clin Oncol* (2016) 34(18):2157–64. doi: 10.1200/JCO.2015.65.9128
 41. Balachandran VP, Gonen M, Smith JJ, DeMatteo RP. Nomograms in oncology: more than meets the eye. *Lancet Oncol* (2015) 16(4):e173–180. doi: 10.1016/S1470-2045(14)71116-7
 42. Shiraishi K, Kitahara S, Ito H, Oba K, Ohmi C, Matsuyama H. Transperitoneal versus retroperitoneal laparoscopic adrenalectomy for large pheochromocytoma: Comparative outcomes. *Int J Urol* (2019) 26(2):212–6. doi: 10.1111/iju.13838

Conflict of Interest: The authors declare that the research was conducted in the absence of any commercial or financial relationships that could be construed as a potential conflict of interest.

Copyright © 2021 Guo, You, Hu, Tong, Zhang, Yan and Zhang. This is an open-access article distributed under the terms of the Creative Commons Attribution License (CC BY). The use, distribution or reproduction in other forums is permitted, provided the original author(s) and the copyright owner(s) are credited and that the original publication in this journal is cited, in accordance with accepted academic practice. No use, distribution or reproduction is permitted which does not comply with these terms.



Succinate Mediates Tumorigenic Effects *via* Succinate Receptor 1: Potential for New Targeted Treatment Strategies in Succinate Dehydrogenase Deficient Paragangliomas

OPEN ACCESS

Edited by:

Suja Pillai,
The University of Queensland,
Australia

Reviewed by:

Nils Lambrecht,
VA Long Beach Healthcare System,
United States
David Taieb,
Hôpital de la Timone, France

*Correspondence:

Stephanie M. J. Fliedner
stephanie.fliedner@uksh.de

[†]Retired

Specialty section:

This article was submitted to
Neuroendocrine Science,
a section of the journal
Frontiers in Endocrinology

Received: 30 July 2020

Accepted: 29 January 2021

Published: 12 March 2021

Citation:

Matlac DM, Hadrava Vanova K, Bechmann N, Richter S, Folberth J, Ghayee HK, Ge G-B, Abunimer L, Wesley R, Aherrahrou R, Dona M, Martínez-Montes ÁM, Calsina B, Merino MJ, Schwaninger M, Deen PMT, Zhuang Z, Neuzil J, Pacak K, Lehnert H and Fliedner SMJ (2021) Succinate Mediates Tumorigenic Effects *via* Succinate Receptor 1: Potential for New Targeted Treatment Strategies in Succinate Dehydrogenase Deficient Paragangliomas. *Front. Endocrinol.* 12:589451. doi: 10.3389/fendo.2021.589451

Dieter M. Matlac¹, Katerina Hadrava Vanova^{2,3}, Nicole Bechmann⁴, Susan Richter⁴, Julica Folberth⁵, Hans K. Ghayee⁶, Guang-Bo Ge⁷, Luma Abunimer³, Robert Wesley[†], Redouane Aherrahrou^{8,9}, Margo Dona¹⁰, Ángel M. Martínez-Montes¹¹, Bruna Calsina¹¹, Maria J. Merino¹², Markus Schwaninger⁵, Peter M. T. Deen¹³, Zhengping Zhuang¹⁴, Jiri Neuzil^{2,15}, Karel Pacak³, Hendrik Lehnert¹ and Stephanie M. J. Fliedner^{1*}

¹ Neuroendocrine Oncology and Metabolism, Medical Department I, Center of Brain, Behavior, and Metabolism, University Medical Center Schleswig-Holstein Lübeck, Lübeck, Germany, ² Institute of Biotechnology, Czech Academy of Sciences, Prague-West, Czechia, ³ Section on Medical Neuroendocrinology, Eunice Kennedy Shriver National Institute of Child Health and Human Development, National Institutes of Health, Bethesda, MD, United States, ⁴ Institute of Clinical Chemistry and Laboratory Medicine, University Hospital Carl Gustav Carus, Medical Faculty Carl Gustav Carus, Technische Universität Dresden, Dresden, Germany, ⁵ Institute for Experimental and Clinical Pharmacology and Toxicology, University of Lübeck, Lübeck, Germany, ⁶ Department of Medicine, Division of Endocrinology, University of Florida and Malcom Randall VA Medical Center, Gainesville, FL, United States, ⁷ Institute of Interdisciplinary Integrative Medicine Research, Shanghai University of Traditional Chinese Medicine, Shanghai, China, ⁸ Institute for Cardiogenetics, University of Lübeck, Lübeck, Germany, ⁹ Department of Biomedical Engineering, Centre for Public Health Genomics, University of Virginia, Charlottesville, VA, United States, ¹⁰ Division of Endocrinology 471, Department of Internal Medicine, Radboud University Medical Center, Nijmegen, Netherlands, ¹¹ Hereditary Endocrine Cancer Group, Human Cancer Genetics Program, Spanish National Cancer Research Centre (CNIO), Madrid, Spain, ¹² Laboratory of Surgical Pathology, National Cancer Institute, National Institutes of Health, Bethesda, MD, United States, ¹³ Radboud University, Nijmegen, Netherlands, ¹⁴ Surgical Neurology Branch, National Institute of Neurological Disorders and Stroke, National Institutes of Health, Bethesda, MD, United States, ¹⁵ School of Medical Science, Griffith University, Southport, QLD, Australia

Paragangliomas and pheochromocytomas (PPGLs) are chromaffin tumors associated with severe catecholamine-induced morbidities. Surgical removal is often curative. However, complete resection may not be an option for patients with succinate dehydrogenase subunit A-D (*SDHx*) mutations. *SDHx* mutations are associated with a high risk for multiple recurrent, and metastatic PPGLs. Treatment options in these cases are limited and prognosis is dismal once metastases are present. Identification of new therapeutic targets and candidate drugs is thus urgently needed. Previously, we showed elevated expression of succinate receptor 1 (*SUCNR1*) in *SDHB* PPGLs and *SDHD* head and neck paragangliomas. Its ligand succinate has been reported to accumulate due to *SDHx* mutations. We thus hypothesize that autocrine stimulation of *SUCNR1* plays a role in the pathogenesis of *SDHx* mutation-derived PPGLs. We confirmed elevated *SUCNR1* expression in *SDHx* PPGLs and after *SDHB* knockout in progenitor cells derived from a

human pheochromocytoma (hPheo1). Succinate significantly increased viability of *SUCNR1*-transfected PC12 and ERK pathway signaling compared to control cells. Candidate *SUCNR1* inhibitors successfully reversed proliferative effects of succinate. Our data reveal an unrecognized oncometabolic function of succinate in *SDHx* PPGLs, providing a growth advantage via *SUCNR1*.

Keywords: succinate receptor 1, *SUCNR1* (GPR91), paraganglioma, succinate, *SDHB* gene

INTRODUCTION

Paragangliomas (PGLs) are catecholamine-producing chromaffin tumors of the autonomic nervous system, including adrenal-derived pheochromocytomas (together PPGLs). While curative in the majority of cases, resection is not an option for many paragangliomas with loss-of-function mutations of succinate dehydrogenase (*SDH*) subunits *A-D* (summarized as *SDHx*). Particularly mutations in the *SDHB* gene predispose to metastases (34–69%) (1–4), usually making complete resection impossible. Mutations in *SDHA*, *SDHC*, and *SDHD* subunits predominantly cause head and neck PGLs (HNPs) (5–7), which can be inoperable due to proximity to vital structures such as vessels or nerves. In addition, surgical complication rate is high, particularly for carotid body location, causing nerve damage in 48% of cases, including 17% with permanent damage (8). Also for *SDHA*, *SDHC*, and *SDHD* mutations, metastatic disease has been reported (9). Treatment options for inoperable cases are extremely limited and prognosis is dismal once metastases are present. Thus, identification of new therapeutic targets and candidate drugs is urgently needed.

SDHx-PGLs are characterized by dysfunction of the *SDH* enzyme. The conversion of succinate to fumarate is impaired, causing substantial succinate accumulation (10–13). Similarly, reduced *SDH* activity and succinate accumulation has been associated with progressive disease or poor outcome in endometrial cancer (14) and hepatocellular carcinoma (15). Accumulated succinate can cross both the inner and outer mitochondrial membrane via the dicarboxylic acid transporter and the voltage-dependent anion channel (VDAC) [summarized in (12, 16)] to reach the cytosol. There, excess succinate mediates oncogenic effects by inhibition of 2-oxoglutarate-dependent prolyl hydroxylases and demethylases (17). Obstruction of prolyl hydroxylation of hypoxia inducible transcription factors (HIFs) prevents their degradation and induces expression of tumor promoting HIF-target genes. Moreover, inhibition of DNA and histone demethylases causes hypermethylation, which represses transcription of affected genes. Despite knowledge of the underlying mechanisms, targeted treatment approaches for mostly inoperable *SDHx*-PPGL are still lacking.

In addition to its established role as an oncometabolite, succinate has also been recognized to act as a ligand for the G-protein-coupled receptor succinate receptor 1 (*SUCNR1*/GPR91) (18). Elevations in succinate levels arise during hypoxia/ischemia, hyperglycemia, due to tissue damage, or at sites of inflammation [summarized in (19)]. More recently, pH dependent transport of succinate from intact cells via monocarboxylate transporter 1 has been shown in an ischemia

reperfusion model of the heart and following exercise under acidic conditions (20, 21). An apparent function of *SUCNR1* is the activation of coping mechanisms upon adverse conditions, including stimulation of proliferation of different cell types, migration, and angiogenesis (22–29).

Cancer promoting effects of succinate-*SUCNR1* signaling have recently been recognized, and include induction of epithelial to mesenchymal transition, migration, and metastatic spread of lung cancer cells as well as immunosuppressive effects (30). Involvement of *SUCNR1* in tumor angiogenesis has also been proposed (31).

Depending on cell type, the effects of *SUCNR1* stimulation are conveyed by different mechanisms, at least in part related to G-protein coupling. In kidney cells, coupling to $G\alpha_q$ - and/or $G\alpha_i$ -proteins has been proposed, leading to activation of extracellular-signal-regulated-kinases (ERK), generation of inositol triphosphate, augmentation of intracellular calcium, and decrease of cyclic adenosine monophosphate (cAMP) (25). Some authors suggested that calcium mobilization is rather mediated by the $\beta\gamma$ dimers than coupling to $G\alpha_q$ (26). In cardiomyocytes, *SUCNR1* stimulation has been shown to increase cAMP concentration, thus coupling to $G\alpha_s$ is also possible (25).

Among a range of different tissues (32) *Sucnr1* has also been observed in the mouse adrenal (33) and chromaffin cells of the carotid body (34). Its role in chromaffin cells and chromaffin cell-derived PPGLs however is not yet clear.

Succinate treatment as well as *SDHB*-silencing has been shown to induce *SUCNR1* mRNA and protein expression in human hepatoma cells (35), suggesting a positive feedback of inappropriate succinate accumulation on expression of its receptor. Consistently, we detected elevated *SUCNR1* expression in *SDHB* PPGLs and *SDHD* HNPs (36). We thus hypothesized that a combination of abundant succinate and its receptor *SUCNR1* is a unique characteristic of *SDHx*-mutated tumors, which highly likely contributes to tumor formation, growth, or spread. Potent and selective small molecule inhibitors for *SUCNR1* have been previously described (37). Targeting *SUCNR1* thus represents a promising new therapeutic strategy for *SDHx* PPGLs.

MATERIAL AND METHODS

Human Tissue

Fresh PPGL tissue was collected at the National Institutes of Health in Bethesda, MD, USA, under a protocol approved by the

Eunice Kennedy Shriver National Institute of Child Health and Human Development's Institutional Review Board. Previous to tissue collection, patients gave informed written consent in accordance with the protocol. Tumor tissue was partially fixed in 4% formalin for subsequent paraffin embedding.

Immunohistochemistry

Paraffin was removed from the tissues after warming slides to 60°C with xylene. Tissue was rehydrated stepwise in decreasing ethanol concentrations and epitopes were retrieved in heated citrate buffer (10 mM sodium citrate, 1 mM citric acid, pH 6). Tris-buffered saline with 0.1% tween 20 was used for wash steps. Endogenous peroxidases were inhibited with 3% H₂O₂ followed by DAKO protein block serum-free (Dako, Glostrup, Denmark). Slides were incubated with rabbit anti-SUCNR1 antibody (ab140795 Abcam, Cambridge, UK) in blocking solution in a humidified chamber for 1 h at 37°C. Peroxidase-labeled polymer conjugated with secondary goat anti-rabbit antibody (Dako EnVision) was applied. Visualization was based on the peroxidase reaction with 3,3'-diaminobenzidine solution (Dako). Tissue was counterstained with hematoxylin. Dehydration was performed by stepwise immersion in increasing ethanol concentrations followed by xylene before mounting.

SUCNR1 Expression Analysis

mRNA data from 227 tumors was extracted from gene expression array (38–40) and RNAseq datasets (41) using a data analysis pipeline as detailed elsewhere (42). One-tailed Mann-Whitney test was applied to test for differences in *SUCNR1* expression between *SDHx* and cluster 2 PPGLs (*RET*, *MAX*, *NF1*, *TMEM127*, *FGFR1*, and *HRAS*) in the different series.

Cell Culture

Rat pheochromocytoma cells (PC12) and mouse tumor tissue cells silenced for *Sdhb* (MTTctr, MTTsh*Sdhb*63, MTTsh*Sdhb*64) (43) were cultured at 37°C with 5% CO₂ in DMEM with 4.5 g/L glucose, 4.5 g/L L-glutamine without pyruvate (Gibco, Grand Island, NY, USA) supplemented with 10% heat-inactivated horse serum (Biowest, Nuaillé, France), 5% fetal bovine serum (BioWhittaker, Lonza, Basel, Switzerland). For PC12 1% penicillin/streptomycin (Merck, Darmstadt, Germany) was added to the media, while MTTctr, MTTsh*Sdhb*63, MTTsh*Sdhb*64 were grown in presence of 1 µg/ml puromycin (InvivoGen Euorpe, Toulouse, France) to suppress untransfected cells. Oxygen deprivation experiments and collection of cells were performed in an InvivoO₂ workstation (Baker, Sanford, ME, USA) at the indicated oxygen concentrations.

hPheo1 SDHB Knockout

Progenitor cells derived from a human pheochromocytoma (hPheo1) were used. Genomic deletion of *SDHB* in hPheo1 cells was performed by the CRISPR/AsCPF1 system (44) using the pX AsCpf1-Venus-NLS crRNA entry plasmid. Suitable guide

RNAs were identified using the Crispor software. An oligo was designed containing an overhang for plasmid insertion, followed by an array of three guide RNAs targeting before (TATCCAGCGTTACATCTGTTGTG), inside (CCATCTATC GATGGGACCCAGAC), and after (GCTTTTCACATCC TTGGAAGGCT) exon 2 of human *SDHB*, separated by the AsCpf1 direct repeat sequences: AGATTATCCAGCG TTACATCTGTTGTGAATTTCTACTCTTGATAGATCCAT CTATCGATGGGACCCAGACAATTTCTACTCTTGATAG ATGCTTTTCACATCCTTGGAAGGCT. The oligo was cloned into the plasmid cleaved by FastDigest BpiI (Thermo Fisher) and the correct insertion was confirmed by colony PCR and DNA sequencing. hPheo1 cells were transfected with the verified CPF1 construct using Lipfectamine3000 (Thermo Fisher), followed by single cell sorting for Venus-positive cells into a 96-well culture plate. Clones were collected and deletion of the targeted locus was confirmed by genomic PCR using primers ACTTCCCAACAGTATCGCTCTT and TCAAGGCAA GTTCTGGCGGT. *SDHB* knockout clones were confirmed by western blotting for *SDHB* and DNA sequencing. Human *SDHB* was re-expressed in *SDHB* KO cells from the pLYS5-*SDHB*-Flag plasmid (Addgene # 50055, a kind gift of Vamsi Mootha) using lentiviral transduction. Lentivirus particles were produced in Hek293T cells using second generation psPAX and pMD.2G plasmids and Lipofectamine3000. Virus-containing media were collected after 48 h, centrifuged at 3,000 × g for 15 min and stored at –80°C.

hPheo1 parental cells (Ctr) and *SDHB* KO (*SDHB*^{KO23}) or re-expressing cells (*SDHB*^{KO23Rec}) were kept in RPMI (Life technologies, Darmstadt, Germany) with 10% FBS (BioWhittaker), 1% penicillin/streptomycin (Merck, Darmstadt, Germany), 4.5 g/L glucose, 2mM sodium pyruvate, and 50 µg/ml uridine (Sigma-Aldrich, Saint Louis, MO, USA). *SDHB*^{KO23Rec} received 50 µg/ml hygromycin B (Th. Geyer, Hamburg, Germany).

Evaluation of Oxygen Consumption Rate

The Seahorse XF96 Extracellular Flux Analyzer was used for assessment of cellular oxygen consumption rate (OCR) following the manufacturer's instructions. Briefly, all hPheo1 cells were seeded in poly-L-lysine coated XF96 cell culture microplates at 5 × 10³ per well in standard culture media. After 24 h, the medium was replaced by serum-free DMEM containing 10 mM glucose, 2mM L-glutamine, 1 mM pyruvate, and 5 mM HEPES, pH 7.4. After equilibration of temperature and pH for 30 min at 37°C mitochondrial respiration was determined in consecutive injection steps [1 µM oligomycin (OMY), 1.5 µM CCCP, and a combination of 0.5 µM rotenone (ROT) and 0.5 µM antimycin A (AMA)]. OCR measurements were made using the manufacturer's setting. As last injection, Hoechst 33432 was added (2 µg/ml) and the number of cells was evaluated by MD ImageXpress Micro XLS. Results were analyzed by the XF Stress Test Report Generators (Agilent Technologies) and normalized to cell count.

Mass Spectrometric Analysis of Krebs Cycle Metabolites

hPheo1-Ctr, -SDHB^{KO23} and -SDHB^{KO23Rec} (300,000 cells/well) or MTTctr, MTTshSdhb63, MTTshSdhb64 (500,000 cells/well) were seeded into rat tail collagen-coated six-well plates. MTTctr, MTTshSdhb63, MTTshSdhb64 were grown under hypoxic conditions (1 and 10% O₂) and cells from the same passage were kept at normoxia (N1 and N10). Cells were harvested in ice-cold methanol. Extracts were centrifuged, dried down using a SpeedVac concentrator (Thermo Scientific) and MTTctr, MTTshSdhb63, MTTshSdhb64 metabolites were resuspended in mobile phase for subsequent quantification by ultra high-pressure liquid chromatography tandem mass spectrometry (LC-MS/MS) as described previously (11).

Conditioned media from hPheo1-Ctr, -SDHB^{KO23} and -SDHB^{KO23Rec} were collected previous to cell lysis in methanol. Extracts and media were dried down using a SpeedVac concentrator (Thermo Scientific) and metabolites were resuspended in methanol at 10-fold concentration, agitated at 600 rpm and 4°C for 10 min, followed by centrifugation at 20,000 × g for 10 min at 4°C. Relative quantification of metabolites in the supernatant was performed on a LC-MS/MS system, consisting of a Dionex Ultimate 3000 RS LC-system coupled to an Orbitrap mass spectrometer (QExactive, ThermoFisher Scientific, Bremen, Germany) equipped with a heated-electrospray ionization (HESI-II) probe. A Waters Acquity UPLC BEH Amide column (2.1 × 100 mm, 2.5 μm), maintained at 40°C, was used for chromatographic separation. Mobile phases consisted of (A) 0.1% formic acid in water and (B) 0.1% formic acid in acetonitrile with a flow rate of 0.2 ml/min. Following gradient was applied: 75% B to 70% B in 0.5 min and to 65% B in 1.0 min. Final step to 60% B in another 0.5 min, held for 1.0 min and back to 75% B in 0.1 min. Equilibration time was 1.9 min. A parallel reaction monitoring (PRM) experiment in the negative ionization mode was used for the targeted analysis of succinate and fumarate. Mass resolution was 70,000, the isolation window was set to 1.5 m/z. PRM transitions and scan parameters are shown in **Table S1**.

PC12 Cell Transfection

PC12 cells were seeded into collagen-1-coated 96-well plates (Corning Biocoat, Kaiserslautern, Germany). Lipofectamine3000 was used to transfect PC12 cells with a pmCherry-N1 vector encoding a fusion protein of mCherry and human SUCNR1 or enhanced green fluorescent protein (EGFP) following manufacturer recommendations. Plasmids were generously provided by Prof. Deen. Geneticin resistance allowed selection of stable clones in presence of 1 mg/ml geneticin (Roth, Karlsruhe, Germany). Since propagation of PC12 from single clones was not possible, multiclonal cultures were used.

Quantitative Real-Time Polymerase Chain Reaction

Cells were collected in NucleoSpin RNA mini kit lysis buffer and RNA extraction was performed according to the manufacturer's manual (Macherey-Nagel, Düren, Germany). For cDNA

synthesis the SuperScriptTM III First-Strand Synthesis SuperMix has been used (Thermo Fisher). Quantitative RT-PCR was performed on a Quant studio 5 instrument (Thermo Fisher) using SYBR green PCR Master mix (Thermo Fisher), following the recommended cycling conditions. Used primers are listed in **Table S2**.

Western Blot

Stably SUCNR1- and EGFP-expressing cells were seeded into 10 cm collagen-1-coated cell culture dishes at 10⁵ cells/ml in 10 ml DMEM supplemented as described above. Cells were treated with 0, 2, or 10 mM succinate for 5 min. Cell collection, protein estimation, separation, and transfer were done as previously reported (45). Antibodies were rabbit anti-phosphoERK (#4370 Cell Signaling, Danvers, MA, USA), rabbit anti-ERK antibody (AF1576 R&D Systems, Minneapolis, USA), goat anti-GFP (AB0020 Sicgen-Research and Development in Biotechnologia Ltd, Carcavelos, Portugal), goat anti-mCherry (AB0040 Sicgen), or mouse anti-β-actin (A1978 Sigma-Aldrich). Appropriate peroxidase-labeled secondary antibodies (Dako) were used. Visualization was achieved by chemiluminescence detection using Amersham ECL Prime Western Blotting Detection Reagent (GE Healthcare, Freiburg, Germany) in a Fusion SL imaging system (Vilber Lourmat, Eberhardzell, Germany). Band intensity was determined by optical density analysis using image J (Rasband, W.S., ImageJ, U. S. National Institutes of Health, Bethesda, MD, USA, <https://imagej.nih.gov/ij/>, 1997-2016).

Proteins of hPheo1-Ctr, -SDHB^{KO23}, and -SDHB^{KO23Rec} were harvested and blotted as previously described (46). The following primary antibodies were used: anti-GAPDH (Cell Signaling, #5174), anti-SDHA (Abcam, ab14715), anti-SDHB (Abcam, ab14714). HRP-conjugated secondary antibodies were used in TBS/tween with 5% non-fat dried milk for 1 h at room temperature. Protein bands were quantified using AzureSpot 2.0 software (Azure Biosystems).

Confocal Microscopy

Cells were grown in Lab-Tek II chamber slides (Thermo Fisher Scientific, coated with rat tail collagen (Sigma-Aldrich, Taufkirchen, Germany), as previously described (47) and fixed in 4% paraformaldehyde (Electron Microscopy Sciences, Hatfield, PA, USA) after washing in PBS (Gibco). Cells were incubated in 300 nM DAPI solution to visualize cell nuclei (Invitrogen, Thermo Fischer Scientific). After washing cells were coverslipped in a solution containing 12% mowiol 4-88 (Calbiochem, EMD Chemicals, Inc., Gibbstown, NJ, USA), 30% glycerol, 2.5% 1,4- diazobicyclo-[2.2.2]-octane (DABCO) (Sigma- Aldrich), in 0.12 M tris, pH 6.8. A TCS SP5 confocal microscope (Leica, Wetzlar, Germany) with HCX PL APO CS 63× oil UV corrected objective, aperture 1.4, scanning frequency 100 Hz, average 4× and pinhole 1 AU was used to take representative images.

Cell Viability

Stably transfected PC12 cells were seeded at 10,000 cells/well into collagen-1-coated 96-well plates in 100 μl supplemented DMEM

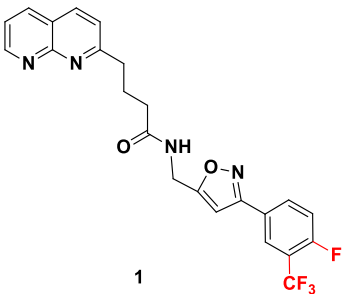
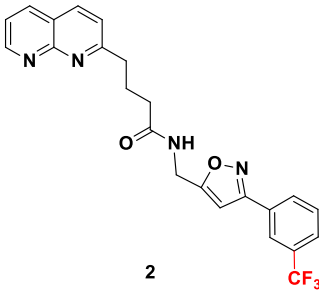
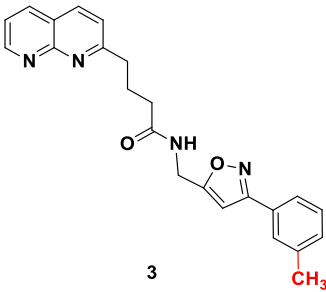
media. The following day, cells were treated with sodium succinate (Sigma-Aldrich) at 0.5, 1, 2, 10, or 20 mM in supplemented media or supplemented media alone as control. Media pH was unaffected by succinate at the indicated concentrations. Cell viability was measured after 24 h and 48 h using an XTT-based cell proliferation kit (PromoKine, PromoCell, Heidelberg, Germany). Signal was detected with a microplate reader (Spectrostar Nano, BMG Labtech, Ortenberg, Germany) at 450 nm and 630 nm 4 h after addition of 25 μ l reaction solution per well.

Candidate SUCNR1 inhibitors were kindly provided by Prof. Guang-Bo Ge (**Table 1**). Cells were treated with the inhibitors for 48 h in the presence or absence of 10 mM succinate, after which cell viability was determined.

SUCNR1 Inhibitors

SUCNR1 inhibitors have been synthesized following previously published protocols (37). Compound 1 corresponds to compound 5 g from the cited reference. Structures and purities are listed in **Table 1**.

TABLE 1 | Structure and purity of SUCNR1 inhibitors.

No.	MW	Structure	Purity
1	458.40		98.3%
2	440.42		98.4%
3	386.45		98.1%

Statistics

Statistic evaluation was performed using SPSS, Stata, or Prism. ANOVA, or multivariate ANOVA was performed with Dunnett's or LDS post-hoc analysis, as indicated.

RESULTS

SUCNR1 Expression in Human PPGLs

In a previous microarray study, we detected elevated mRNA expression of *SUCNR1* in *SDHB* PPGLs and *SDHD* HNP compared to normal adrenal medulla (36). Here we show that *SUCNR1* displays higher expression in *SDHx* PPGLs compared to cluster 2 tumors (**Figures 1A–C**). Cluster 2 PPGLs have a far lower risk of metastatic disease and are characterized by activation of kinase-signaling. Immunohistochemical staining of human PPGL tissues with different hereditary backgrounds confirmed elevated SUCNR1 protein expression in *SDHB* PPGLs and *SDHD* HNPs, compared to *VHL* pheochromocytomas. Normal adrenal medulla barely showed a *SUCNR1* signal (**Figure 1D**).

SUCNR1 in Chromaffin Cells

Sucnr1 expression was evaluated in established chromaffin cell models. However, qRT-PCR revealed very low mRNA levels in MPC, MTT, PC12, and hPheo1 (Ct >30 at 30–50 ng template load).

In HepG2 cells, *SDHB* silencing and succinate treatment have been shown to induce *SUCNR1* expression (35). We thus evaluated succinate levels and *Sucnr1* expression in previously prepared MTT cells silenced for *Sdhb* (43). The succinate to fumarate and succinate to citrate levels were increased by 1.6–2.4-fold in sh*Sdhb* cells compared to control cells, while the fumarate levels were mainly similar in all cell types (**Supplementary Figure S1A**). No significant difference was observed in *Sucnr1* expression level (**Supplementary Figure S1B**). To better model the situation observed in human PPGL tissue of 25-fold elevated succinate and 80% decreased fumarate (11), we exposed the cells to hypoxia for 24 h (1 and 10% O₂), as has been previously effectively performed (48). As hypothesized (49), hypoxia augmented succinate accumulation and fumarate depletion particularly in the sh*Sdhb* cells, leading to an increase of the succinate to fumarate ratio (**Supplementary Figure S1A**). Nevertheless, the still mild succinate accumulation did not significantly induce *Sucnr1* mRNA expression (**Supplementary Figure S1B**).

Interestingly, treatment of hPheo1 with external succinate at 10 mM or exposure to 3% oxygen for 24 h significantly increased *SUCNR1* expression (**Figure 2A**). A three-way ANOVA revealed no interaction for succinate and oxygen. Replicate and oxygen factors were coded as categorical, while the succinate level was coded with continuous values of 1/2/3, to reflect the expected ordered impact of increasing succinate dose, showing significant differences for oxygen ($p = 0.033$) and treatment ($p = 0.014$). Dunnett's *post-hoc* test on treatment main effect showed that the 0 and 10 mM succinate levels differed with $p = 0.022$.

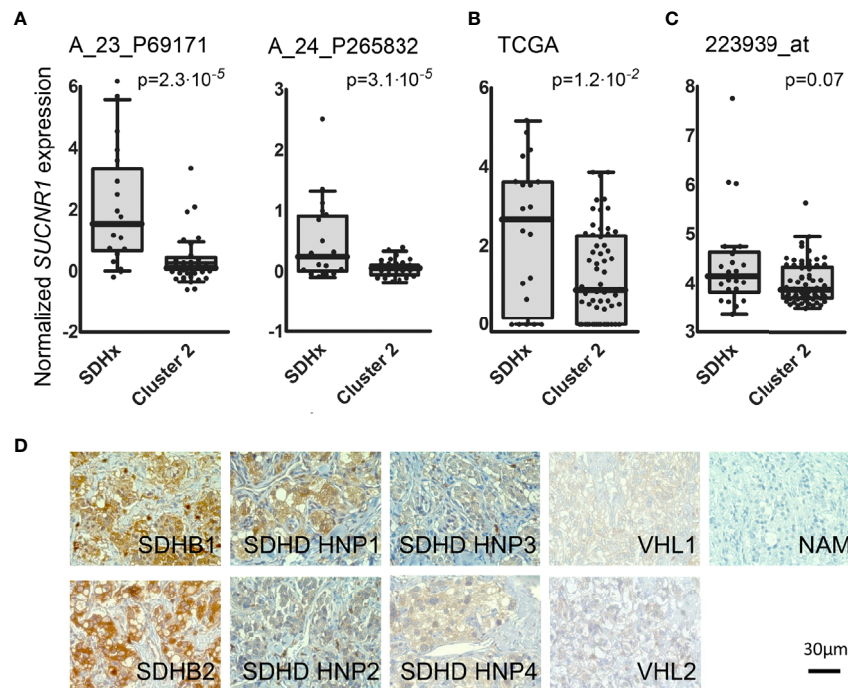


FIGURE 1 | (A) Box and whisker Tukey plots showing the expression of *SUCNR1* in PPGLs of three published series. Data from GSE19422 and GSE51081 (38, 39), showing two different probes for *SUCNR1*. SDHx (n = 19: 10 *SDHB*, 3 *SDHC*, 6 *SDHD*), cluster 2 (n = 37: 3 *FGFR1*, 7 *HRAS*, 3 *MAX*, 5 *NF1*, 16 *RET*, and 3 *TMEM127*). **(B)** Data from the TCGA project (41), SDHx (n = 20: 17 *SDHB*, 3 *SDHD*) and cluster 2 (n = 61: 2 *FGFR1*, 17 *HRAS*, 2 *MAX*, 22 *NF1*, 17 *RET*, and 1 *TMEM127*). **(C)** Data from E-MTAB-733 (40), SDHx (n = 23: 1 *SDHA*, 16 *SDHB*, 1 *SDHB+SDHA*, 2 *SDHC*, 3 *SDHD*) and cluster 2 (n = 67: 2 *FGFR1*, 6 *HRAS*, 2 *MAX*, 36 *NF1*, 17 *RET*, 1 *TMEM127*, and three tumors with mutations in two different drivers: *MAX+HRAS*, *NF1+FGFR1*, and *RET+SDHA*). One-tailed Mann-Whitney test was applied to test for significant differences. **(D)** *SUCNR1* protein expression determined by immunohistochemical staining in human PPGL tissue and normal adrenal medulla. Paraffin embedded PPGL samples from patients with mutations in succinate dehydrogenase B (*SDHB*, n = 2), succinate dehydrogenase D (*SDHD*, n = 4), the von-Hippel-Lindau gene (*VHL*, n = 2) as well as one sample of normal adrenal medulla (NAM) were used. *SDHD* PGLs were from the head and neck area (HNP).

To evaluate causality of *SDHB* dysfunction, *SDHB* was knocked out in hPheo1. Successful knockout and re-expression are shown by qRT-PCR and Western blot (**Figure 2B**). Respiration was vastly decreased in hPheo1-*SDHB*^{KO23} compared to the parental and -*SDHB*^{23Rec} cells (**Figure 2C**). Succinate to fumarate levels from cell extracts showed a mean 40-fold increase of succinate to fumarate (**Figure 2D**). Excess succinate was released to the media, as evident by a doubling of the succinate to fumarate ratio.

SDHB deficient hPheo1 showed significantly increased *SUCNR1* expression (p = 0.018, **Figure 2E**). *PTGS2/COX2* a downstream effector of *SUCNR1* signaling in inducible pluripotent neural stem cells (50) and retina in diabetic rats (29) was also significantly increased in hPheo1-*SDHB*^{KO23} and to a much smaller extent in -*SDHB*^{KO23Rec} (**Figure 2E**).

Succinate Promotes Proliferation via SUCNR1

To explore *SUCNR1* related effects in PPGL cells independent of intracellular succinate accumulation, we stably transfected PC12 cells with human *SUCNR1*. Confocal microscopy revealed a punctate staining pattern, which is in line with cell surface expression of the mCherry-h*SUCNR1* fusion protein, while

EGFP was equally distributed in control transfected cells, indicating cytosolic localization (**Figure 3A**). Western blot for mCherry and EGFP showed strong bands in the transfected cells, with no signal in the respective counterparts (**Figure 3B**).

Treatment of *SUCNR1*-transfected PC12 with 2, 10, or 20 mM succinate significantly increased cell viability compared to untreated controls after 24 and 48 h of treatment. Cell viability of EGFP-transfected PC12 did not change in response to succinate treatment (**Figure 3C**). Furthermore, *SUCNR1*-stimulation with 10 mM succinate significantly induced ERK-phosphorylation in *SUCNR1*-, but not EGFP-transfected cells (**Figure 3D**). Simultaneous treatment of *SUCNR1*-PC12 cells with 10 mM succinate and 10 nM of one of three candidate succinate receptor inhibitors successfully reversed the increase in relative viability of *SUCNR1*-PC12 treated with 10 mM succinate alone (**Figure 3E**).

DISCUSSION

SUCNR1 expression is induced by hypoxia, extracellular succinate, and loss of *SDHB* in hPheo1, and *SUCNR1* signaling increases viability in PC12 cells. Taken together, these data

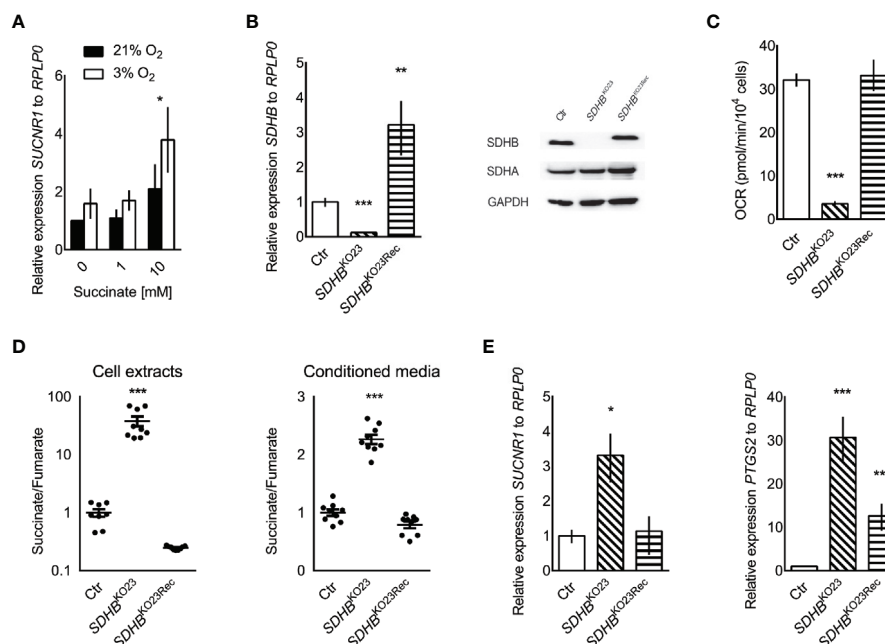


FIGURE 2 | (A) Relative *SUCNR1* mRNA expression in hPheo1 treated with succinate or oxygen deprivation ($n = 3$). Three-way ANOVA showed significant differences for oxygen ($p = 0.033$) and treatment ($p = 0.014$), after verifying there was no interaction between oxygen and treatment. Dunnett's *post-hoc* test was performed for the treatment main effect. The * above the 10 mM succinate bars reflects the significant difference from 0 mM, $p = 0.022$. **(B)** Relative expression of *SDHB* mRNA in hPheo1 parental cells (Ctrl), *SDHB* knockout (*SDHB*^{KO23}), and *SDHB* knockout cells re-expressing *SDHB* (*SDHB*^{KO23Rec}). Representative Western blot for *SDHB*, *SDHA*, and *GAPDH* in hPheo1-Ctrl, -*SDHB*^{KO23}, -*SDHB*^{KO23Rec} (right). *SDHB* protein expression was diminished in hPheo1-*SDHB*^{KO23} and normalized in -*SDHB*^{KO23Rec} with re-constitution of human *SDHB*-FLAG. **(C)** Basal oxygen consumption rate of hPheo1-Ctrl, -*SDHB*^{KO23}, -*SDHB*^{KO23Rec} as determined by Seahorse XF analyzer. Basal respiration measured as oxygen consumption rate was significantly decreased in *SDHB*^{KO23} and normalized with *SDHB* re-constitution ($n = 2$). **(D)** Succinate-to-fumarate ratios in cell extracts (left) of hPheo1-Ctrl, -*SDHB*^{KO23}, -*SDHB*^{KO23Rec} and conditioned media (right) ($n = 3$, each). Data are shown as mean \pm SEM. **(E)** Relative mRNA expression of *SUCNR1* and *PTGS2* in hPheo1-Ctrl, -*SDHB*^{KO23}, and -*SDHB*^{KO23Rec}. ANOVA with Dunnett's *post hoc* test for difference from Ctrl was performed for delta Cts. * $p \leq 0.05$, ** $p \leq 0.01$, *** $p \leq 0.001$ ($n = 3$).

suggest that accumulating succinate in *SDHx* PPGLs may have a previously unrecognized oncometabolic effect by stimulating SUCNR1 in an autocrine manner.

In several cell types and tissues, SUCNR1 expression has been induced or correlated with *SDHB* silencing, succinate treatment, or hypoxia (35, 51, 52). However, differences in susceptibility or interfering mechanisms may exist. In MTT sh*Sdhb* cells succinate only slightly accumulated. However, under hypoxia, an up to 30-fold increase in succinate to fumarate ratio was reached in sh*Sdhb*64. Nevertheless, expression of *Sucnr1* was not significantly induced. At an only slightly higher 40-fold increase seen in hPheo1 *SDHB*^{KO23}, *SUCNR1* was significantly up-regulated. Interestingly, in hPheo1 *SUCNR1* induction was also achieved by treatment with 10 mM extracellular succinate or 3% oxygen. If the discrepancy we observed between MTT and hPheo1 is due to cell specific reasons or the amount of succinate accumulation remains unclear. Other cell models with similarly or even more efficient succinate accumulation have been reported (48, 53, 54), however SUCNR1 expression has not been evaluated. Highly likely, extracellular succinate stimulation of the receptor leads to positive feedback on its expression, which can only be reached by substantial increase in

extracellular succinate due to severe *SDH* inhibition or hypoxia. Here we show that hPheo1 *SDHB*^{KO23} release excess succinate into the media, which is probably related to the amount of succinate accumulation. Surprisingly, *SUCNR1* was not elevated in *SDHD* abdominal and thoracic PGLs in our microarray study, while expression was increased in *SDHD* HNP and *SDHB* PPGLs (36). Succinate to fumarate levels have been shown to be lower in *SDHx* HNP compared to adrenal or extra-adrenal localization (11). Thus, additional factors likely influence *SUCNR1* expression in PPGL tissue. Potentially, tumor tissue pH and monocarboxylate transporter 1 expression level play an essential role, as these highly likely determine succinate release to the extracellular space (20, 21). Of note, hypoxia or HIF activation positively regulate monocarboxylate transporter 1 expression [summarized in (55)].

It will be of major interest for future studies to evaluate discrepancies between the models in more detail, also with respect to dysfunction of other *SDH* subunits. However, to date no comparable models with knockout of the different subunits is available (56).

Analysis of publically available data from three large mRNA expression studies showed a significant increase or strong trend

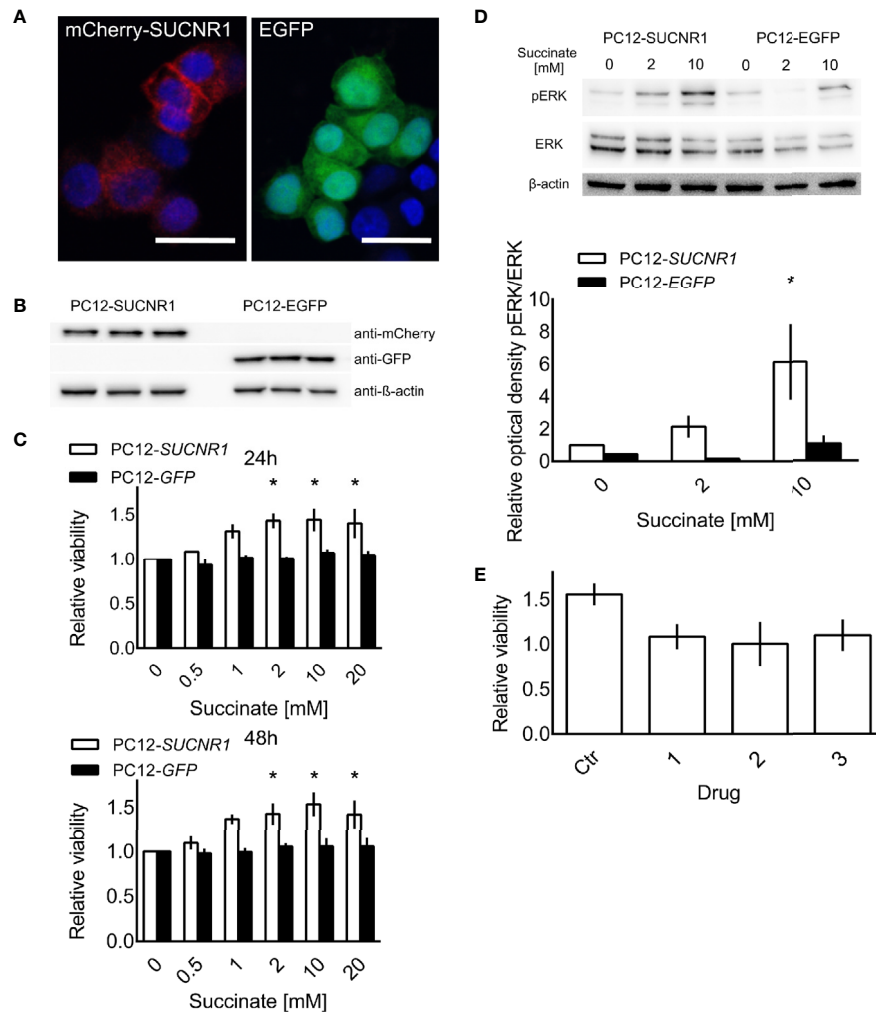


FIGURE 3 | PC12 cells transfected with a fusion protein of *mCherry* and *SUCNR1* or *EGFP*. **(A)** Confocal microscopy confirmed punctate *mCherry* signal in accordance with cell surface location typical for G-protein coupled receptors, while *EGFP* was equally distributed throughout the cells. **(B)** Western blot for *mCherry* and *GFP* confirmed successful transfection. **(C)** Cell viability of transfected cells was determined by XTT assay after 24 and 48 h of exposure to the indicated succinate concentrations. ANOVA with *post-hoc* Dunnet's test for difference from 0 mM succinate treatment was performed. * $p < 0.05$ ($n = 4$). **(D)** Representative Western blot showing increased ERK phosphorylation in *SUCNR1* transfected cells after 5 min exposure to 2 mM or 10 mM succinate, while no difference in phospho-ERK could be determined in *EGFP* transfected cells ($n = 3$). Mean optical density ratios of phospho-ERK to ERK \pm SEM of three independent experiments are shown as bar graph. Three-way ANOVA of the log transformed pERK/ERK ratios revealed significant interaction between cell type and succinate concentration ($p = 0.045$). ANOVA for the effect of treatment in PC12-SUCNR1 was significant at $p = 0.006$, with Dunnet's *post-hoc* test indicating a significant difference in phosphorylation at 10 mM succinate compared to control ($p = 0.023$). In PC12-EGFP cells, succinate had no effect on ERK phosphorylation ($p = 0.454$). **(E)** PC12-SUCNR1 cells were treated with candidate inhibitors **(A–C)** in presence and absence of succinate. The bars show the relative viability of cells treated with the drug or vehicle and succinate relative to drug or vehicle alone ($n = 2$). Data are shown as mean \pm SEM.

towards increased *SUCNR1* expression in *SDHx* compared to cluster 2 PPGLs (**Figures 1A–C**). Differences in composition of the *SDHx* cohorts with respect to exact mutation, level of succinate accumulation, and tumor location likely contribute to the variance between the cohorts.

While the stimulatory concentration of succinate in the millimolar range may appear high, such high levels can be expected in *SDHx* PPGLs (11). The median concentration of succinate in human *SDHx*-deficient PPGLs was close to 1 $\mu\text{g}/\text{mg}$ tissue. With the molecular weight of succinate of 118.09 g/

mol and an estimated density of PPGL tissue at the same level as normal adrenal [1.03 g/ml (57)], the tissue succinate content can be estimated at 8.7 mM. This is in the same range as the pro-proliferative dose of 2–20 mM used in our experiments.

Previously, ERK1/2 activation as well as induction of *PTGS2* expression and/or prostaglandin E2 release have been reported as downstream effectors of *SUCNR1* signaling (25, 29, 31, 50). Expression of *PTGS2/COX2* has been evaluated in PPGLs, however no clear relation with genetic background was evident

(58). As a hypoxia responsive gene, induction of *PTGS2* in hPheo1 *SDHB*^{KO23} may not entirely depend on SUCNR1 activation, yet may be worthwhile to further explore. Further roles of SUCNR1 on metastatic spread, immune-modulation and chemotaxis, or tumor angiogenesis, as observed in other tissues (30, 31, 59), remain to be evaluated in *SDHx* PPGLs.

Our data indicate that SUCNR1 mediated proliferation enhancement can be disrupted by targeted treatment with SUCNR1 inhibitors. Three compounds generated to inhibit SUCNR1 (Drugs 1, 2, 3) were available to us. Drug 1 corresponds to the previously described small molecule inhibitor 5 g, which shows excellent receptor binding capabilities and selectivity (37). Drugs 2 and 3 are new derivatives of Drug 1. Pharmacokinetic parameters of compounds closely related to drug 1, such as oral bioavailability and clearance (0.12–0.17 nmol/min/kg) are favorable. Plasma concentrations of 37–70 μ M have been reached. Selectivity was at least 100-fold increased over binding to the closely related GPR99 (37). It has been argued that newly developed SUCNR1 agonists may be superior to investigate the role of SUCNR1 as these agonists activate the SUCNR1 without the additional metabolic functions of succinate (60, 61). Regardless, the confounding effect of succinate on cell viability in PC12 cells should be negligible, since *EGFP*-transfected control cells were not influenced by succinate treatment. Expression of SUCNR1 was considerably higher in *SDHB* PPGL and *SDHD* HNP tissue than normal adrenal medulla. Thus, normal adrenal medulla will most likely not be affected by treatment with SUCNR1 inhibitors. However, vulnerability of normal adipocytes, hepatocytes, retinoblasts, or other SUCNR1 expressing cells to systemic application of SUCNR1-inhibitors remains to be evaluated together with potential immunomodulatory effects.

SUCNR1 inhibition may provide a promising new treatment approach for the aggressive and often inoperable *SDHx* tumors. Effectiveness of these novel drugs may likely be extended to unresectable or metastatic *SDH*-deficient renal cell carcinomas, gastrointestinal stroma tumors, thyroid, and pancreatic neuroendocrine tumors, or other conditions exhibiting disturbed SUCNR1-signaling due to hypoxia or hyperglycemia.

DATA AVAILABILITY STATEMENT

The raw data supporting the conclusions of this article will be made available by the authors, without undue reservation.

ETHICS STATEMENT

The studies involving human participants were reviewed and approved by the Eunice Kennedy Shriver National Institute of Child Health and Human Development's Institutional Review Board. The patients/participants provided their written informed consent to participate in this study.

AUTHOR CONTRIBUTIONS

Conceptualization, SF, KP, ZZ, and HL. Methodology and validation, DM, KHV, NB, SR, LA, RA, JF, MM, G-BG, and SF. Formal analysis, DM, JF, AM-M, BC, RW, and SF. Investigation, DM, KHV, NB, SR, LA, and SF. Resources, NB, SR, KHV, JN, MD, G-BG, PD, MM, RA, KP, and HL. Data curation, DM, NB, SR, AM-M, BC, JF, KHV, and SF. Writing—original draft preparation, DM and SF. Writing—review and editing, DM, NB, KHV, SR, SF, PD, HL, and KP. Visualization, DM, KHV, JF, and SF. Supervision, KP, HL, and SF. Funding acquisition, SF, KP, and HL. All authors contributed to the article and approved the submitted version.

FUNDING

This study was supported in part by the Intramural Research Program of the Eunice Kennedy Shriver NICHD, NIH, MD, and the University Medical Center Schleswig-Holstein, Lübeck, Germany. DM received a stipend for excellence in medicine from the University of Lübeck. NB, SR, MD, and PD were supported by a grant from the Paradifference foundation.

ACKNOWLEDGMENTS

We are grateful to Prof. Henriette Kirchner, Prof. Graeme Eisenhofer, Dr. Tillman Vollbrand, Dr. Helge Müller-Fielitz, Dr. Ralf Werner, Prof. Hendrik Ungefroren, Prof. Olaf Jöhren, Dr. Bjoern Schuster, and Linda Krobava for kindly sharing their expertise, materials, or equipment. Furthermore, we thank Sylvia Grammerstorf and Detlev Schult-Badusche for experimental support or advice.

SUPPLEMENTARY MATERIAL

The Supplementary Material for this article can be found online at: <https://www.frontiersin.org/articles/10.3389/fendo.2021.589451/full#supplementary-material>

Figure S1 | (A) Metabolite levels in MTT shSdhb and control cells under normoxia and at 1% and 10% oxygen. The normoxia control cells that were kept in parallel to the 1% oxygen condition are labelled N1, the control cells from the 10% oxygen condition are labelled N10. The succinate to citrate, fumarate to citrate, and succinate to fumarate levels are shown from top to bottom. The bars show means \pm SEM of n=4 (1% oxygen) and n=5 (10% oxygen) independent experiments. 2-way ANOVA showed significant differences between cell types and oxygen conditions. P-values for LDS post-hoc statistics of ANOVA for main effects are shown. Lower case letters indicate significant differences between oxygen concentrations for each cell type. Replication of x indicate 1: $p \leq 0.05$, 2: $p \leq 0.01$, 3: $p \leq 0.001$. Asterisks indicate significant difference between cell types within a given oxygen condition. * indicates $p \leq 0.05$, ** indicates $p \leq 0.01$, *** indicates $p \leq 0.001$. **(B)** Relative expression of *Sucnr1* to *Rplp0* in cells kept at 10% (top) and 1% (bottom) oxygen with respective normoxia controls. There was no statistic difference (n=3).

REFERENCES

- Pamporaki C, Hamplova B, Peitzsch M, Prejbisz A, Beuschlein F, Timmers H, et al. Characteristics of Pediatric vs Adult Pheochromocytomas and Parangliomas. *J Clin Endocrinol Metab* (2017) 102:1122–32. doi: 10.1210/jc.2016-3829
- Jochmanova I, Wolf KI, King KS, Nambuba J, Wesley R, Martucci V, et al. SDHB-related pheochromocytoma and paraganglioma penetrance and genotype-phenotype correlations. *J Cancer Res Clin Oncol* (2017) 143:1421–35. doi: 10.1007/s00432-017-2397-3
- Castro-Vega LJ, Letouze E, Burnichon N, Buffet A, Disderot PH, Khalifa E, et al. Multi-omics analysis defines core genomic alterations in pheochromocytomas and paragangliomas. *Nat Commun* (2015) 6:6044. doi: 10.1038/ncomms7044
- Curas-Freixes M, Inglada-Perez L, Mancikova V, Montero-Conde C, Leton R, Comino-Mendez I, et al. Recommendations for somatic and germline genetic testing of single pheochromocytoma and paraganglioma based on findings from a series of 329 patients. *J Med Genet* (2015) 52:647–56. doi: 10.1136/jmedgenet-2015-103218
- Schulte KM, Talat N, Galata G, Aylwin S, Izatt L, Eisenhofer G, et al. Genetics and the clinical approach to paragangliomas. *Horm Metab Res* (2014) 46:964–73. doi: 10.1055/s-0034-1383581
- Bourdeau I, Grunewald S, Burnichon N, Khalifa E, Dumas N, Binet MC, et al. A SDHC Founder Mutation Causes Parangliomas (PGLs) in the French Canadians: New Insights on the SDHC-Related PGL. *J Clin Endocrinol Metab* (2016) 101:4710–8. doi: 10.1210/jc.2016-1665
- Bausch B, Schiavi F, Ni Y, Welander J, Patocs A, Ngeow J, et al. Clinical Characterization of the Pheochromocytoma and Paranglioma Susceptibility Genes SDHA, TMEM127, MAX, and SDHAF2 for Gene-Informed Prevention. *JAMA Oncol* (2017) 3:1204–12. doi: 10.1001/jamaoncol.2017.0223
- Amato B, Serra R, Fappiano F, Rossi R, Danzi M, Milone M, et al. Surgical complications of carotid body tumors surgery: a review. *Int Angiol* (2015) 34:15–22.
- Main AM, Rossing M, Borgwardt L, Gronkaer Toft B, Rasmussen AKFeldt-Rasmussen U. Genotype-phenotype associations in PPGLs in 59 patients with variants in SDHX genes. *Endocr Connect* (2020) 9:793–803. doi: 10.1530/EC-20-0279
- Lendvai N, Pawlosky R, Bullova P, Eisenhofer G, Patocs A, Veech RL, et al. Succinate-to-fumarate ratio as a new metabolic marker to detect the presence of SDHB/D-related paraganglioma: initial experimental and ex vivo findings. *Endocrinology* (2014) 155:27–32. doi: 10.1210/en.2013-1549
- Richter S, Peitzsch M, Rapizzi E, Lenders JW, Qin N, de Cubas AA, et al. Krebs cycle metabolite profiling for identification and stratification of pheochromocytomas/parangliomas due to succinate dehydrogenase deficiency. *J Clin Endocrinol Metab* (2014) 99:3903–11. doi: 10.1210/jc.2014-2151
- Selak MA, Armour SM, MacKenzie ED, Boulahbel H, Watson DG, Mansfield KD, et al. Succinate links TCA cycle dysfunction to oncogenesis by inhibiting HIF- α prolyl hydroxylase. *Cancer Cell* (2005) 7:77–85. doi: 10.1016/j.ccr.2004.11.022
- Pollard PJ, Briere JJ, Alam NA, Barwell J, Barclay E, Wortham NC, et al. Accumulation of Krebs cycle intermediates and over-expression of HIF1 α in tumours which result from germline FH and SDH mutations. *Hum Mol Genet* (2005) 14:2231–9. doi: 10.1093/hmg/ddi227
- Gu C, Yang H, Chang K, Zhang B, Xie F, Ye J, et al. Melatonin alleviates progression of uterine endometrial cancer by suppressing estrogen/ubiquitin C/SDHB-mediated succinate accumulation. *Cancer Lett* (2020) 476:34–47. doi: 10.1016/j.canlet.2020.02.009
- Tseng PL, Wu WH, Hu TH, Chen CW, Cheng HC, Li CF, et al. Decreased succinate dehydrogenase B in human hepatocellular carcinoma accelerates tumor malignancy by inducing the Warburg effect. *Sci Rep* (2018) 8:3081. doi: 10.1038/s41598-018-21361-6
- Murphy MP, O'Neill LAJ. Krebs Cycle Reimagined: The Emerging Roles of Succinate and Itaconate as Signal Transducers. *Cell* (2018) 174:780–4. doi: 10.1016/j.cell.2018.07.030
- Zhao T, Mu X, You Q. Succinate: An initiator in tumorigenesis and progression. *Oncotarget* (2017) 8:53819–28. doi: 10.18632/oncotarget.17734
- He W, Miao FJ, Lin DC, Schwandner RT, Wang Z, Gao J, et al. Citric acid cycle intermediates as ligands for orphan G-protein-coupled receptors. *Nature* (2004) 429:188–93. doi: 10.1038/nature02488
- Ariza AC, Deen PM, Robben JH. The succinate receptor as a novel therapeutic target for oxidative and metabolic stress-related conditions. *Front Endocrinol (Lausanne)* (2012) 3:22. doi: 10.3389/fendo.2012.00022
- Prag HA, Gruszczczyk AV, Huang MM, Beach TE, Young T, Tronci L, et al. Mechanism of succinate efflux upon reperfusion of the ischaemic heart. *Cardiovasc Res* (2020) 148. doi: 10.1093/cvr/cvaa148
- Reddy A, Bozi LHM, Yaghi OH, Mills EL, Xiao H, Nicholson HE, et al. pH-Gated Succinate Secretion Regulates Muscle Remodeling in Response to Exercise. *Cell* (2020) 183:62–75. doi: 10.1016/j.cell.2020.08.039
- Ko SH, Choi GE, Oh JY, Lee HJ, Kim JS, Chae CW, et al. Succinate promotes stem cell migration through the GPR91-dependent regulation of DRP1-mediated mitochondrial fission. *Sci Rep* (2017) 7:12582. doi: 10.1038/s41598-017-12692-x
- Lei W, Ren W, Ohmoto M, Urban JF Jr., Matsumoto I, Margolske RF, et al. Activation of intestinal tuft cell-expressed Sucnr1 triggers type 2 immunity in the mouse small intestine. *Proc Natl Acad Sci U S A* (2018) 115:5552–7. doi: 10.1073/pnas.1720758115
- Mao H, Yang A, Zhao Y, Lei L, Li H. Succinate Supplement Elicited “Pseudohypoxia” Condition to Promote Proliferation, Migration, and Osteogenesis of Periodontal Ligament Cells. *Stem Cells Int* (2020) 2020:2016809. doi: 10.1155/2020/2016809
- de Castro Fonseca M, Aguiar CJ, da Rocha Franco JA, Gingold RN, Leite MF. GPR91: expanding the frontiers of Krebs cycle intermediates. *Cell Commun Signal* (2016) 14:3. doi: 10.1186/s12964-016-0126-1
- Gilissen J, Jouret F, Pirotte B, Hanson J. Insight into SUCNR1 (GPR91) structure and function. *Pharmacol Ther* (2016) 159:56–65. doi: 10.1016/j.pharmthera.2016.01.008
- Hamel D, Sanchez M, Duhamel F, Roy O, Honore JC, Noueihed B, et al. G-protein-coupled receptor 91 and succinate are key contributors in neonatal postcerebral hypoxia-ischemia recovery. *Arterioscler Thromb Vasc Biol* (2014) 34:285–93. doi: 10.1161/ATVBAHA.113.302131
- Sapieha P, Sirinyan M, Hamel D, Zaniolo K, Joyal JS, Cho JH, et al. The succinate receptor GPR91 in neurons has a major role in retinal angiogenesis. *Nat Med* (2008) 14:1067–76. doi: 10.1038/nm.1873
- Li T, Hu J, Du S, Chen Y, Wang S, Wu Q. ERK1/2/COX-2/PGE2 signaling pathway mediates GPR91-dependent VEGF release in streptozotocin-induced diabetes. *Mol Vis* (2014) 20:1109–21.
- Wu JY, Huang TW, Hsieh YT, Wang YF, Yen CC, Lee GL, et al. Cancer-Derived Succinate Promotes Macrophage Polarization and Cancer Metastasis via Succinate Receptor. *Mol Cell* (2020) 77:213–27.e5. doi: 10.1016/j.molcel.2019.10.023
- Mu X, Zhao T, Xu C, Shi W, Geng B, Shen J, et al. Oncometabolite succinate promotes angiogenesis by upregulating VEGF expression through GPR91-mediated STAT3 and ERK activation. *Oncotarget* (2017) 8:13174–85. doi: 10.18632/oncotarget.14485
- McCreath KJ, Espada S, Galvez BG, Benito M, de Molina A, Sepulveda P, et al. Targeted disruption of the SUCNR1 metabolic receptor leads to dichotomous effects on obesity. *Diabetes* (2015) 64:1154–67. doi: 10.2337/db14-0346
- Diehl J, Gries B, Pfeil U, Goldenberg A, Mermer P, Kummer W, et al. Expression and localization of GPR91 and GPR99 in murine organs. *Cell Tissue Res* (2016) 364:245–62. doi: 10.1007/s00441-015-2318-1
- Balbir A, Lee H, Okumura M, Biswal S, Fitzgerald RS, Shirahata M. A search for genes that may confer divergent morphology and function in the carotid body between two strains of mice. *Am J Physiol Lung Cell Mol Physiol* (2007) 292:L704–15. doi: 10.1152/ajplung.00383.2006
- Cervera AM, Apostolova N, Crespo FL, Mata M, McCreath KJ. Cells silenced for SDHB expression display characteristic features of the tumor phenotype. *Cancer Res* (2008) 68:4058–67. doi: 10.1158/0008-5472.CAN-07-5580
- Shankavaram U, Flidner SM, Elkahoul AG, Barb JJ, Munson PJ, Huynh TT, et al. Genotype and tumor locus determine expression profile of pseudohypoxic pheochromocytomas and paragangliomas. *Neoplasia* (2013) 15:435–47. doi: 10.1593/neo.122132
- Bhuniya D, Umrani D, Dave B, Salunke D, Kukreja G, Gundu J, et al. Discovery of a potent and selective small molecule hGPR91 antagonist. *Bioorg Med Chem Lett* (2011) 21:3596–602. doi: 10.1016/j.bmcl.2011.04.091

38. Lopez-Jimenez E, Gomez-Lopez G, Leandro-Garcia LJ, Munoz I, Schiavi F, Montero-Conde C, et al. Research resource: Transcriptional profiling reveals different pseudohypoxic signatures in SDHB and VHL-related pheochromocytomas. *Mol Endocrinol* (2010) 24:2382–91. doi: 10.1210/me.2010-0256
39. Qin N, de Cubas AA, Garcia-Martin R, Richter S, Peitzsch M, Menschikowski M, et al. Opposing effects of HIF1alpha and HIF2alpha on chromaffin cell phenotypic features and tumor cell proliferation: Insights from MYC-associated factor X. *Int J Cancer* (2014) 135:2054–64. doi: 10.1002/ijc.28868
40. Burnichon N, Vescovo L, Amar L, Libe R, de Reynies A, Venisse A, et al. Integrative genomic analysis reveals somatic mutations in pheochromocytoma and paraganglioma. *Hum Mol Genet* (2011) 20:3974–85. doi: 10.1093/hmg/ddr324
41. Fishbein L, Leshchiner I, Walter V, Danilova L, Robertson AG, Johnson AR, et al. Comprehensive Molecular Characterization of Pheochromocytoma and Paraganglioma. *Cancer Cell* (2017) 31:181–93. doi: 10.1016/j.ccell.2017.01.001
42. Calsina B, Castro-Vega LJ, Torres-Perez R, Inglada-Perez L, Curras-Freixes M, Roldan-Romero JM, et al. Integrative multi-omics analysis identifies a prognostic miRNA signature and a targetable miR-21-3p/TSC2/mTOR axis in metastatic pheochromocytoma/paraganglioma. *Theranostics* (2019) 9:4946–58. doi: 10.7150/thno.35458
43. Richter S, D'Antongiovanni V, Martinelli S, Bechmann N, Rivero M, Poitz DM, et al. Primary fibroblast co-culture stimulates growth and metabolism in Sdhb-impaired mouse pheochromocytoma MTT cells. *Cell Tissue Res* (2018) 374:473–85. doi: 10.1007/s00441-018-2907-x
44. Zetsche B, Heidenreich M, Mohanraju P, Fedorova I, Kneppers J, DeGennaro EM, et al. Multiplex gene editing by CRISPR-Cpf1 using a single crRNA array. *Nat Biotechnol* (2017) 35:31–4. doi: 10.1038/nbt.3737
45. Flidner SM, Engel T, Lendvai NK, Shankavaram U, Nolting S, Wesley R, et al. Anti-cancer potential of MAPK pathway inhibition in paragangliomas-effect of different statins on mouse pheochromocytoma cells. *PLoS One* (2014) 9: e97712. doi: 10.1371/journal.pone.0097712
46. Tan AS, Baty JW, Dong LF, Bezawork-Geleta A, Endaya B, Goodwin J, et al. Mitochondrial genome acquisition restores respiratory function and tumorigenic potential of cancer cells without mitochondrial DNA. *Cell Metab* (2015) 21:81–94. doi: 10.1016/j.cmet.2014.12.003
47. Flidner SM, Yang C, Thompson E, Abu-Asab M, Hsu CM, Lampert G, et al. Potential therapeutic target for malignant paragangliomas: ATP synthase on the surface of paraganglioma cells. *Am J Cancer Res* (2015) 5:1558–70.
48. Her YF, Nelson-Holte M, Majer LJ III. Oxygen Concentration Controls Epigenetic Effects in Models of Familial Paraganglioma. *PLoS ONE* (2015) 10(5):e0127471. doi: 10.1371/journal.pone.0127471
49. Flidner SMJ, Brabant G, Lehnert H. Pheochromocytoma and paraganglioma: genotype versus anatomic location as determinants of tumor phenotype. *Cell Tissue Res* (2018) 372:347–65. doi: 10.1007/s00441-017-2760-3
50. Peruzzotti-Jametti L, Bernstock JD, Vicario N, Costa ASH, Kwok CK, Leonardi T, et al. Macrophage-Derived Extracellular Succinate Licenses Neural Stem Cells to Suppress Chronic Neuroinflammation. *Cell Stem Cell* (2018) 22:355–68.e13. doi: 10.1016/j.stem.2018.01.020
51. Ortiz-Masia D, Gisbert-Ferrandiz L, Bauset C, Coll S, Mamie C, Scharl M, et al. Succinate Activates EMT in Intestinal Epithelial Cells through SUCNR1: A Novel Protagonist in Fistula Development. *Cells* (2020) 9:1104. doi: 10.3390/cells9051104
52. Lukyanova LD, Kirova YI, Germanova EL. Specific Features of Immediate Expression of Succinate-Dependent Receptor GPR91 in Tissues during Hypoxia. *Bull Exp Biol Med* (2016) 160:742–7. doi: 10.1007/s10517-016-3299-0
53. Cardaci S, Zheng L, MacKay G, van den Broek NJ, MacKenzie ED, Nixon C, et al. Pyruvate carboxylation enables growth of SDH-deficient cells by supporting aspartate biosynthesis. *Nat Cell Biol* (2015) 17:1317–26. doi: 10.1038/ncb3233
54. Letouze E, Martinelli C, Lorient C, Burnichon N, Abermil N, Ottolenghi C, et al. SDH mutations establish a hypermethylator phenotype in paraganglioma. *Cancer Cell* (2013) 23:739–52. doi: 10.1016/j.ccr.2013.04.018
55. Payen VL, Mina E, Van Hée VF, Porporato PE, Sonveaux P. Monocarboxylate transporters in cancer. *Mol Metab* (2020) 33:48–66. doi: 10.1016/j.molmet.2019.07.006
56. Martinelli S, Maggi M, Rapizzi E. Pheochromocytoma/paraganglioma preclinical models: which to use and why? *Endocr Connect* (2020) 9:R251. doi: 10.1530/ec-20-0472
57. Milo R, Jorgensen P, Moran U, Weber G, Springer M. BioNumbers—the database of key numbers in molecular and cell biology. *Nucleic Acids Res* (2010) 38:D750–3. doi: 10.1093/nar/gkp889
58. Ullrich M, Richter S, Seifert V, Hauser S, Calsina B, Martinez-Montes AM, et al. Targeting Cyclooxygenase-2 in Pheochromocytoma and Paraganglioma: Focus on Genetic Background. *Cancers (Basel)* (2019) 11:743. doi: 10.3390/cancers11060743
59. Krzak G, Willis CM, Smith JA, Pluchino S, Peruzzotti-Jametti L. Succinate Receptor 1: An Emerging Regulator of Myeloid Cell Function in Inflammation. *Trends Immunol* (2021) 42:45–58. doi: 10.1016/j.it.2020.11.004
60. Trauelsen M, Rexen Ulven E, Hjorth SA, Brvar M, Monaco C, Frimurer TM, et al. Receptor structure-based discovery of non-metabolite agonists for the succinate receptor GPR91. *Mol Metab* (2017) 6:1585–96. doi: 10.1016/j.molmet.2017.09.005
61. Rexen Ulven E, Trauelsen M, Brvar M, Luckmann M, Bielefeldt LO, Jensen LKI, et al. Structure-Activity Investigations and Optimisations of Non-metabolite Agonists for the Succinate Receptor 1. *Sci Rep* (2018) 8:10010. doi: 10.1038/s41598-018-28263-7

Conflict of Interest: The authors declare that the research was conducted in the absence of any commercial or financial relationships that could be construed as a potential conflict of interest.

Copyright © 2021 Matlac, Hadrava Vanova, Bechmann, Richter, Folberth, Ghayee, Ge, Abunimer, Wesley, Aherrahrou, Dona, Martinez-Montes, Calsina, Merino, Schwaninger, Deen, Zhuang, Neuzil, Pacak, Lehnert and Flidner. This is an open-access article distributed under the terms of the Creative Commons Attribution License (CC BY). The use, distribution or reproduction in other forums is permitted, provided the original author(s) and the copyright owner(s) are credited and that the original publication in this journal is cited, in accordance with accepted academic practice. No use, distribution or reproduction is permitted which does not comply with these terms.



Seven Novel Genes Related to Cell Proliferation and Migration of VHL-Mutated Pheochromocytoma

Shuai Gao^{1†}, Longfei Liu^{2†}, Zhuolin Li¹, Yingxian Pang², Jiaqi Shi¹ and Feizhou Zhu^{1,3*}

¹ Department of Biochemistry and Molecular Biology, School of Life Sciences, Central South University, Changsha, China,

² Department of Urology, Xiangya Hospital, Central South University, Changsha, China, ³ Hunan Key Laboratory of Animal Models for Human Diseases, Central South University, Changsha, China

OPEN ACCESS

Edited by:

Farhadul Islam,
University of Rajshahi, Bangladesh

Reviewed by:

Yannick Arlot,
UMR-CNRS, France
Chunzhang Yang,
National Cancer Institute,
United States

*Correspondence:

Feizhou Zhu
zhufeizhou@csu.edu.cn

[†]These authors have contributed
equally to this work

Specialty section:

This article was submitted to
Neuroendocrine Science,
a section of the journal
Frontiers in Endocrinology

Received: 25 August 2020

Accepted: 09 February 2021

Published: 22 March 2021

Citation:

Gao S, Liu L, Li Z, Pang Y, Shi J and
Zhu F (2021) Seven Novel Genes
Related to Cell Proliferation and
Migration of VHL-Mutated
Pheochromocytoma.
Front. Endocrinol. 12:598656.
doi: 10.3389/fendo.2021.598656

Pheochromocytoma, as a neuroendocrine tumor with the highest genetic correlation in all types of tumors, has attracted extensive attention. Von Hippel Lindau (VHL) has the highest mutation frequency among the genes associated with pheochromocytoma. However, the effect of VHL on the proteome of pheochromocytoma remains to be explored. In this study, the VHL knockdown (VHL-KD) PC12 cell model was established by RNA interference (shRNA). We compared the proteomics of VHL-KD and VHL-WT PC12 cell lines. The results showed that the expression of 434 proteins (VHL shRNA/WT > 1.3) changed significantly in VHL-KD-PC12 cells. Among the 434 kinds of proteins, 83 were involved in cell proliferation, cell cycle and cell migration, and so on. More importantly, among these proteins, we found seven novel key genes, including Connective Tissue Growth Factor (CTGF), Syndecan Binding Protein (SDCBP), Cysteine Rich Protein 61 (CYR61/CCN1), Collagen Type III Alpha 1 Chain (COL3A1), Collagen Type I Alpha 1 Chain (COL1A1), Collagen Type V Alpha 2 Chain (COL5A2), and Serpin Family E Member 1 (SERPINE1), were overexpressed and simultaneously regulated cell proliferation and migration in VHL-KD PC12 cells. Furthermore, the abnormal accumulation of HIF2 α caused by VHL-KD significantly increased the expression of these seven genes during hypoxia. Moreover, cell-counting, scratch, and transwell assays demonstrated that VHL-KD could promote cell proliferation and migration, and changed cell morphology. These findings indicated that inhibition of VHL expression could promote the development of pheochromocytoma by activating the expression of cell proliferation and migration associated genes.

Keywords: pheochromocytoma, Von Hippel-Lindau (VHL), connective tissue growth factor (CTGF), syndecan binding protein (SDCBP), cellular communication network factor 1 (CCN1), collagen type III alpha 1 chain (COL3A1), collagen type V alpha 2 chain (COL5A2), serpin family E member 1 (SERPINE1)

INTRODUCTION

Pheochromocytoma and paraganglioma (PPGL) are rare neuroendocrine tumors with a incidence of about six patients per million, of which approximately 10% of patients are diagnosed as malignant tumors (1, 2). Although the malignancy rate of PPGL was not high, but it had relatively high genetic relevance and germline mutation rate (3). According to the statistics, about 40% of PPGL were related to germline mutations (4, 5). So far, about 20 susceptibility genes were found in PPGL, which could be divided into three different clusters: the Cluster 1, which was related to the pseudo-hypoxia signaling pathway, including VHL, SDHx, FH, PHD2, and HIF2 α , which could be divided into two subgroups: the tricarboxylic acid (TCA) cycle and the VHL/HIF axis (6–8); the Cluster 2, which was related to kinase signaling pathways including RET, NF1, MAX, KIF1B, H-RAS, and TMEM127; and the Cluster 3 was related to the Wnt signaling pathway, including CSDE1 and MAML3 fusion gene (5, 9–13).

Among the PPGL susceptibility genes, the genes involved in the VHL/HIF axis had the highest mutation frequency (14, 15). The pVHL was a component of the ubiquitin ligase complex, where VHL recognized the substrate. In addition to pVHL, the ubiquitin ligase complex also contained elongin B, elongin C, Cul2, and Rbx1 (16). Moreover, pVHL played an important role in the formation of extracellular matrix and epithelial differentiation (17), and was necessary for the interaction between epithelial cells and extracellular matrix (18). The abnormal function of pVHL prevented the ubiquitin ligase complex from ubiquitinating the α -subunit of the heterodimeric transcription factor HIF (hypoxia-inducible factor), thereby preventing the degradation of HIF α in the proteasome (19, 20). Some studies reviewed the molecular functions of pVHL, indicating that pVHL could regulate many processes such as cell cycle (21), mRNA stability, and hypoxia induced gene expression (16, 22). Hypoxia inducible-factor 2 α (HIF2 α) inhibition was necessary for pVHL to inhibit tumor (23). Meanwhile, there were three kinds of HIF α proteins in human, including hypoxia-inducible factor 1 α (HIF1 α), HIF2 α , and hypoxia-inducible factor 3 α (HIF3 α) (24), in which mutations in HIF2 α or downstream pseudo-hypoxia signaling pathway-related genes were susceptible to PPGL (25).

Moreover, HIF2 α mutations were found in a new unique type of syndrome. The new syndrome disease carrying PPGL-somatostatinoma-polycythemia greatly promoted our understanding of the key molecular mechanisms of PPGL (26, 27). Melanie J et al. reported that a gain-of-function missense mutation occurred in HIF2 α and impaired the hydroxylation of HIF2 α protein. This mutation not only maintained the stable conformation of HIF2 α , but also caused the onset of polycythemia (28). More gain-of-function missense mutations in HIF2 α were found in PPGL associated with polycythemia (29). HIF2 α was also considered to be a key regulator of erythropoiesis (30). However, many researchers successively reported that HIF2 α mutations were found in PPGL patients with or without polycythemia and somatostatinoma (27, 31–35). The patients' multiple organ involvement and distant metastasis

indicated that the HIF2 α mutation occurred in the early life or embryonic development stage. And the different periods of HIF2 α somatic mutations in pregnancy might affect the later phenotype of the syndrome (36). At the same time, Lorenzo et al. described a new germline mutation of HIF2 α in PGLs patients (37). On the other hand, HIF2 α was necessary for the synthesis of catecholamines. The analysis of the patient's clinical manifestations and HIF2 α imbalance reflected the role of HIF2 α in preferential norepinephrine synthesis. So HIF2 α mutation might provide more guidance for the molecular typing and prognosis of PPGL (38, 39). Furthermore, studies showed that overexpression of HIF2 α might lead to the formation of diffuse clusters and the appearance of pseudopodia (40), and enhance cell proliferation and metastatic load (25, 41). Therefore, HIF2 α played an important role in pheochromocytoma. The discovery of new downstream genes driven by HIF2 α might provide new ideas for the treatment of pheochromocytoma.

HIF2 α stabilization was also found in patients with VHL mutation (42). There were many reports on the function of pVHL, and it was reported that pVHL could cause abnormal accumulation of HIF2 α thereby activating the expression of downstream target genes of HIF2 α . In this study, we used the latest high-sensitivity proteomics platform of isobaric labels tandem mass tags (TMT) to discover the novel proteins involved in pVHL/HIF2 α axis. This will help us to understand the pathogenic mechanism of VHL dysfunction, guide the treatment of clinical diseases and optimize the prognosis.

MATERIALS AND METHODS

Tumor Tissue Samples

From December 2017 to June 2018, 30 cases of tumor tissue and para-carcinoma medulla samples were collected from PPGL patients undergoing laparoscopic surgery in Xiangya Hospital, Hunan, China. Through imaging examinations (computed tomography and color Doppler ultrasound) and laboratory examinations, all patients were diagnosed as PPGL. All PPGL samples confirmed by pathological examination were stored at -80°C for later use. Subsequently, Sanger and next-generation sequencing confirmed VHL mutations in four patients who had not received any treatment before surgery. All patients signed an informed consent form before surgery and the study was approved by the Ethical Committee of the School of Life Sciences, Central South University.

Cell Culture and Proliferation Assay

The rat adrenal pheochromocytoma PC12 cell line was obtained from the Advanced Research Center of Central South University (Changsha, China). The cells were transported on dry ice, and after receiving, the cells were resuscitated according to standard methods, sub-cultured, and cryopreserved (43, 44). The frozen cells were stored in liquid nitrogen and the recovered PC12 cells were routinely inoculated into RPMI-1640 medium (GIBCO, Carlsbad, CA, USA) containing 10% fetal bovine serum (FBS)

(GIBCO, Carlsbad, CA, USA), penicillin (100 U/ml), and streptomycin (100 µg/ml). The cells were maintained in humidified incubator containing 5% CO₂ at 37°C for routine culture. In order to analyze the proliferation of the cells, the cells were seeded in six-well plates with 1×10^5 cells per well. The cells were trypsinized every other day for 3 consecutive days and counted with CellDrop BF counter (Denovix). To simulate a hypoxic environment, different types of PC12 cells were cultured in a hypoxic incubator containing 94% N₂, 5% CO₂, and 1% O₂ for 24 h or 21% O₂, and then the downstream experiments were performed immediately.

VHL RNAi

According to VHL target gene sequence and RNAi sequence design principle, three shRNA sequences were designed by GeneChem Inc. (Shanghai, China), and shRNA with the best kinetic parameters were selected for subsequent experiments. The shRNA target sequence was as follows: Negative Control (NC): 5'-TTCTCCGAACGTGTCACGT-3'; VHL-LV-94: 5'-CAGGTCGCTCTATGAAGACTT-3'; VHL-LV-95: 5'-GTGCATCCCTCAATGTTGAT-3'; VHL-LV-96: 5'-CTGCCTTTGTGGCTCAACTTT-3'. The lentiviral vector system consisted of three plasmids: GV112, pHelper 1.0, and pHelper 2.0 vectors (provided by GeneChem Inc.). Among them, the clone sites of GV112 were AgeI and EcoRI. Then the NC and three target sequences were inserted into the GV112 vector by double enzyme digestion and T4 DNA ligase, and the recombinant plasmid was extracted and verified by Sanger sequencing. All enzymes were purchased from Thermo Fisher Scientific. Next, the recombinant GV112, pHelper 1.0, and pHelper 2.0 were co-transfected into 293T cells for lentivirus packaging (45). The lentiviral liquids were collected, and the quality was tested for later use.

The sensitivity of different cells to lentivirus was different, so pre-experiment should be carried out before transfection to determine the multiplicity of infection (MOI = (Virus titer × Virus volume)/cell number). The PC12 cells were seeded in a six-well plate and cultured until 50% confluence the day before transfection. On the next day, when the cells were cultured to the appropriate density, the transfection experiment was carried out. Then, 1.5 µg/ml puromycin (Sigma, USA) was used to select stable expression clones, and the knockdown efficiency was verified by RT-qPCR and Western blotting. The cell line with the best silencing effect was used in subsequent experiments.

Quantitative Real-Time PCR

After grinding the frozen clinical tissue with liquid nitrogen (the cell line goes directly to the next step), RNA was extracted by the TRIzol method, and then the mRNA was reverse transcribed into cDNA (Thermo Scientific, USA) using the RevertAid First Strand cDNA Synthesis Kit (#K1622). Then, the Bio-Rad CFX96 real-time PCR system (Bio-Rad, CA, USA) was used to perform SYBR Green real-time quantitative PCR. The relative expression of mRNA transcripts in carcinoma and para-cancerous tissues was determined by SYBR[®] premix Ex Taq II Kit (Takara, Beijing, China) and target gene specific primers were listed in **Table S1**. The relative expression of different target genes was analyzed by Livak method (46).

Western Blotting Assay

The total cell protein was lysed and extracted with RIPA buffer (PMSF, Solarbio, China) containing 1 mm of phenylmethanesulfonyl fluoride, and then quantified using the BCA protein assay kit (Beyotime, Shanghai, China). Subsequently, the equal molecular proteins from the lysates were separated using 12% SDS-PAGE gel and transferred to the polyvinylidene fluoride membranes (Millipore Corp, Billerica, MA, USA). After blocking with 5% skimmed milk in Tris buffer for 2 h at room temperature, the membranes were incubated in the target primary antibody at 4°C overnight (ABclonal Technology, Wuhan, China). After incubating the secondary antibody, the protein level was detected by the enhanced ECL luminescence reagent on a chemiluminescence imager (SmartChemi420, Sage Creation Science Co. Ltd., Beijing).

Protein Extraction and Trypsin Digestion

Three parallel groups of negative control cells and LV-95 cells were sent for mass spectrometry detection. By counting with a hemocytometer, the number of cells in each dish was about $3\sim5 \times 10^5$ /ml. The samples were homogenized three times in the ice-cold lysis buffer (8 M urea, 1% Protease Inhibitor Cocktail) using an Ultrasonic Cell Disruptor (Scientz). After centrifugation at 4°C for 10 min, the cell debris was removed, and the cell supernatant was collected and the protein concentration was determined with the BCA kit according to the instructions (Beyotime Biotechnology, China). For digestion, the protein solution was reduced with 5 mM dithiothreitol for 30 min at 56°C and alkylated with 11 mM iodoacetamide in the dark at room temperature for 15 min. The protein samples were diluted by adding 100 mM tetraethyl ammonium bromide (TEAB) to urea concentration of less than 2 M. Finally, trypsin was added at a mass ratio of trypsin to protein of 1:50, and the first digestion was carried out overnight, and then at a ratio of trypsin to protein of 1:100 for the second digestion for 4 h.

After trypsinization, the peptides were desalted using a Strata XC18 SPE column (Phenomenex) and vacuum dried. Peptides were reconstituted in 0.5 M TEAB and processed according to the manufacturer's protocol for TMT kit (Thermo Scientific, USA). The tryptic peptides were fractionated into different components by high pH reverse-phase HPLC using Thermo Betasil C18 column (5 µm particles, 10 mm ID, 250 mm length).

LC-MS/MS Analysis and Database Search

The peptides were dissolved in the mobile phase A [0.1% (v/v) formic acid aqueous solution] of liquid chromatography, and then separated using the nanoElute ultra-high-performance liquid chromatography (UHPLC) system. Mobile phase A was an aqueous solution containing 0.1% formic acid, and mobile phase B was an acetonitrile solution containing 0.1% formic acid. The peptides were processed from NSI sources, and then tandem mass spectrometry (MS/MS) was performed in Q ExactiveTM Plus (Thermo) connected to online UHPLC. The applied electrospray voltage was 2.0 kV. The m/z scan range was 350 to 1,800 for full scan, and intact peptides were detected in the Orbitrap with a resolution of 70,000. Then used the NCE to set 28 to the selected

peptides for MS/MS and detected these fragments in Orbitrap with a resolution of 17,500. A data-dependent procedure alternated between one MS scan and the subsequent 20 MS/MS scans with an interval of 15.0 s. The automatic gain control (AGC) was set to 5E4, and fixed first mass was set as 100 m/z.

Database Search

We used Maxquant search engine (v.1.5.2.8) to process the obtained MS/MS data. Tandem mass spectra were searched against human UniProt database concatenated with reverse decoy database. Trypsin/P was designated as a lyase, allowing up to four missing cleavages. In the first search, the mass tolerance of precursor ions was set to 20 ppm, and 5 ppm in the Main search, and the mass tolerance of fragment ions was set to 0.02 Da. The carbamoyl group on Cys was designated as a fixed modification, and acetylation modification and oxidation on Met were specified as variable modifications. FDR was adjusted to <1% and the lowest score for modified peptides was set >40. Subsequently, the data searched in the database were respectively annotated with GO, domain, KEGG Pathway, and Subcellular Localization.

Gene Ontology, Kyoto Encyclopedia of Genes and Genomes, and Protein Domain Enrichment Analysis

Gene Ontology (GO) annotation was derived from the UniProt-GOA database (<http://www.ebi.ac.uk/GOA/>), and GO enrichment analysis was performed with InterProScan platform (v.5.14-53.0 <http://www.ebi.ac.uk/interpro/>). Firstly, the identified protein ID was converted into UniProt ID, and then mapped to GO IDs through protein ID. If the UniProt-GOA database didn't annotate some identified proteins, based on the protein sequence alignment method, InterProScan software was used to annotate the GO function of the protein. Secondly, GO annotations of proteins were divided into three categories: biological processes, cell composition, and molecular functions. Moreover, the KAAS server (v.2.0 http://www.genome.jp/kaas-bin/kaas_main) was used to perform the "Kyoto Encyclopedia of Genes and Genomes" (KEGG) annotation, and the KEGG database was used for pathway enrichment analysis. Furthermore, The InterPro database (<http://www.ebi.ac.uk/interpro/>) was used to analyze the enrichment of differentially expressed protein functional domains. Finally, the Fischer exact double-ended test method was used to test the differentially expressed proteins in the background of the identified protein, and the enrichment test with a corrected *P*-value of less than 0.05 was considered statistically significant.

Enrichment-Based Clustering

Further hierarchical clustering was performed based on the functional classification of differentially expressed proteins. Firstly, we collated all the categories and their *P* value obtained after enrichment, and then filtered for those categories that are enriched in at least one of the clusters with a *P* value <0.05. Then the filtered *P* value matrix was transformed by the function $x = -\log_{10}(P\text{-value})$. Finally, for each functional category, these *x* values were converted to *z*. Then, these *z*-scores were clustered by one-way hierarchical clustering (Euclidean distance, average linkage

clustering) in Genesis. The cluster membership was visualized by using the heat map of "Heatmap. 2" function in the "gplots" R-package.

The *P* value was calculated by two-sample two-tailed t-test method. In terms of specification, the modulus (VHL shRNA/WT) where the differential expression change exceeds 1.3 was used as the change threshold for significant up or down regulation. To study the relationship between different proteins, all differentially expressed proteins (Fold change >1.3 or <0.769, VHL shRNA/WT) were searched against the STRING database version 11 to understand the protein-protein interactions. The protein-protein interaction network chart was plotted according to the following rules: only the interactions between proteins belonging to the search data set are selected to exclude external candidates; the STRING defined a metric called "confidence score," which was used to define the confidence of the interaction, and we selected the confidence score > 0.7 (high confidence) for all interactions; the confidence score of the protein was higher, indicating that the protein were more important in the network. In addition, we labeled the different functions and types of proteins to distinguish the different functions of different proteins.

Scratch and Transwell Assays

The cells were plated in 6 cm petri dish with 1×10^6 cells per well. Then scratched each petri dish with a 200 μ l pipette tip and Images were taken with inverted microscope on the same day and for the next 2 days. The Image J software developed by the National Institutes of Health (NIH) was used to analyze the changes in the scratched area.

In the migration test, 5×10^5 cells were seeded in serum-free media in the upper well of an 8 μ m pore transwell (BD), and the medium containing 20% FBS was placed at the bottom of the well. The cells were fixed with 4% paraformaldehyde and stained with crystal violet after 48 h and five random 10 \times images were taken from each well for quantification.

Sanger Sequencing and Bioinformatics Prediction

The DNA of the samples was detected by Sanger sequencing to determine the mutation sites. Then the Protein Variation Effect Analyzer (PROVEAN: http://provean.jcvi.org/seq_submit.php) online prediction software was used to filter sequence variants to identify non-synonymous or indel variants that were predicted to be functionally important.

Statistical Analysis

All experiments were verified more than three times for biological replicates and each subgroup was also repeated at least three times. The Graphpad prism 8.0 software (GraphPad Software Inc., San Diego, CA, USA) was used for variance analysis. All data were expressed as mean \pm standard error (SEM). The one-way ANOVA with a *post-hoc* test method (Student-Newman-Keuls test) were used to analyze the differences between the mean values. The probability value of less than 0.05 was considered statistically significant.

RESULTS

VHL Mutations in PPGL and Construction of VHL-KD PC12 Cell Line

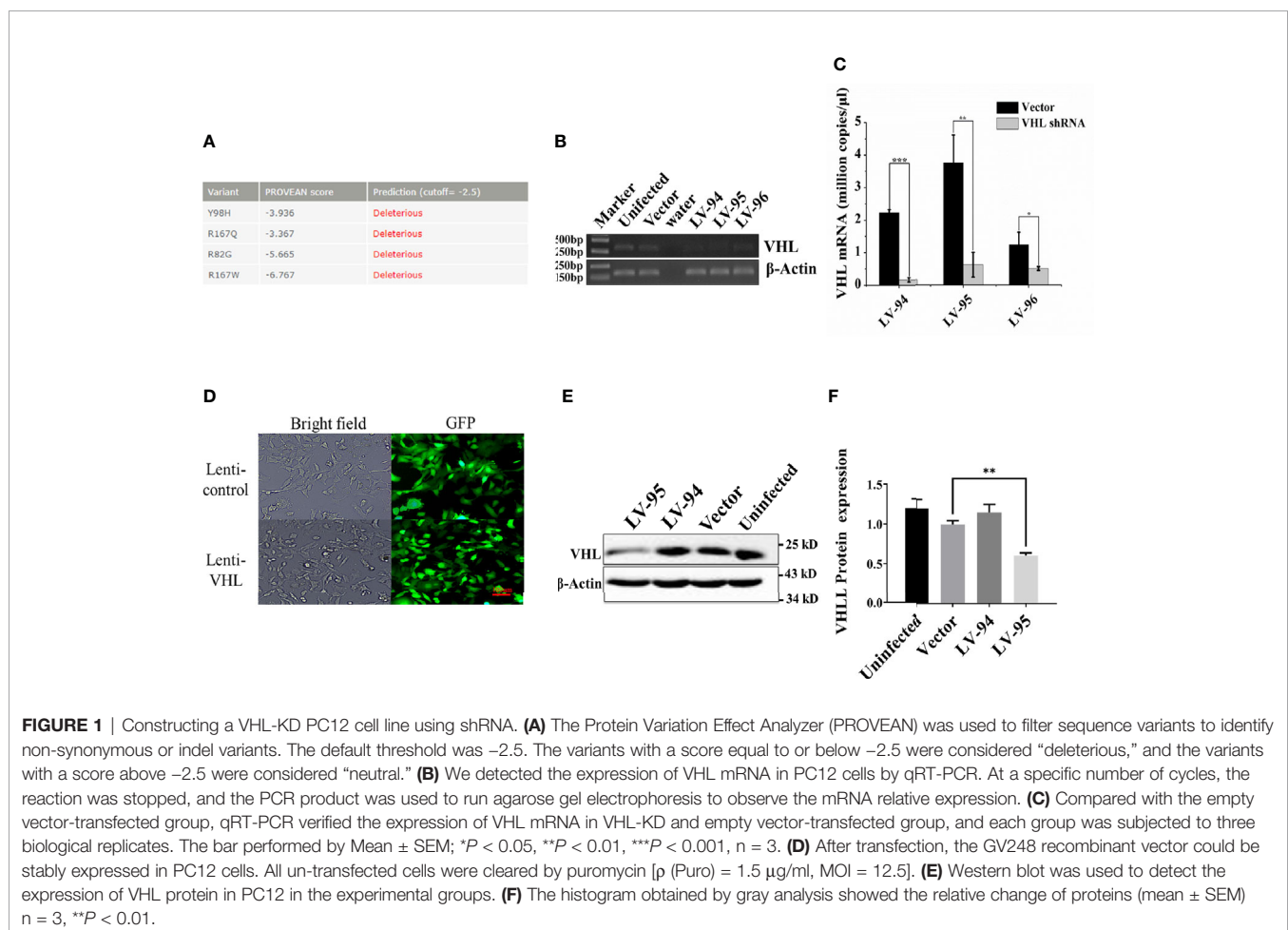
Since VHL mutation was the most common type of mutation in PPGL genes, we collected four clinical samples with VHL mutations, and the specific clinical information and mutation sites were shown in **Table 1**. The PROVEAN was used to predict the hazard of the four mutations, and the predicted scores were shown in **Figure 1A**. To study the influence of VHL mutations

on the development of pheochromocytoma, we constructed stable VHL-KD PC12 cell line model and evaluated the efficiency of VHL-KD at mRNA and protein levels. Firstly, to ensure the optimal growth state of cells during the VHL-KD process, we carried out preliminary experiments to optimize the transfection conditions. After transfection and puromycin screening, the VHL shRNA mediated by recombinant plasmid GV248 was stably expressed in the PC12 cells. The GV248 vector had the GFP fluorescent protein gene, which could monitor transfection efficiency of the recombinant vector in the PC12

TABLE 1 | Characteristics and mutation sites of four patients with VHL-mutated pheochromocytomas.

Serial No.	Gender	Age	Diagnosis & location	Other disease	Blood pressure	Immunohistochemical index	Mutant gene	Mutation site
1	Female	61	PCC (Right)	Sudden blindness	156/76	CgA (++), Syn (+), S-100 (+), SF-1 (-), Ki67 (<1%+), inhibin (-), Melan-A (-), P53 (-)	VHL	NM_000551.3: c.292T>C, p.Y98H
2	Male	32	PCC (Double)	Hepatic nodules	140/87	CgA++, Syn+, S-100-, SF-1, Ki67 < 1%, inhibin-, Melan-A-, P53-	VHL	NM_000551.3: c.500G>A, p.R167Q
3	Female	51	PCC (Left)	PNET*	141/84	CgA+++, Syn++, S-100+, SF-1+, Ki67 < 1%+, inhibin-, Melan-A-, P53-	VHL	NM_000551.3: c.244C>G, p.R82G
4	Male	49	PCC (Double)	None	129/88	CgA (++), Syn (++), S-100 (++), Ki67 (2%+), inhibin (+), Melan-A (-), P53 (-)	VHL	NM_000551.3: c.499C>T, p.R167W

*PNET, Primitive Neuroectodermal Tumor.



cells (**Figure 1D**). The specific information of GV248 carrier could be obtained from **Table S2**. After transfection, the expression of VHL mRNA was significantly down-regulated in the three RNAi groups. However, the interference efficiencies of three kinds of shRNA targeting three segments of VHL mRNA were different, and the interference efficiencies of LV-94 and LV-95 were more significant (**Figures 1B, C**). To further verify the efficiency of RNAi at protein level, western blot confirmed that only LV-95 shRNA could successfully inhibit the expression of pVHL (**Figures 1E, F**).

pVHL Regulating Multiple Cell Functions

To explore the biological processes regulated by pVHL, we carried out mass spectrometry analysis. We identified a total of 5,819 quantifiable proteins through the TMT-labeled proteomics quantitative platform. Among them, compared with the VHL-WT group, 248 proteins in the VHL-KD group were up-regulated, while 186 proteins were down-regulated ($P < 0.05$, **Figure 2A, Table S3**). These proteins were depicted in the quantitative volcanic distribution of differential proteins (**Figure 2B**, Fold Change >1.3 or <0.769 , $P < 0.05$). Moreover, GO analysis annotated these proteins were divided into three major categories: biological processes, cell composition, and molecular functions, demonstrating the biological effects of proteins from different perspectives. Among them, the proteins related to cell proliferation, cell growth, and extracellular matrix were significantly enriched in these three functional categories (**Figure 2C**). Meanwhile, our results showed that the genes regulating cell growth, proliferation, differentiation, cell viability, and response to nutrients were significantly different in the VHL-KD group, and the functional enrichment analysis of the up-regulated proteins also showed that the enriched proteins were mainly involved in cell growth, proliferation, differentiation, and migration (**Figure 2D**).

A total of 405 differentially expressed proteins were searched and included in the interaction network. Protein interaction analysis showed that most of the proteins related to proliferation, migration, and development in the VHL-KD group were significantly increased, but phosphorylation, ubiquitination, and ribosome-related proteins were significantly reduced in the VHL-KD group. Meanwhile, the up-regulations of cell surface receptor proteins, neurite outgrowth proteins, and axonogenesis proteins might promote synapseogenesis and enhance signal transmission and communication between cells (**Figure 3**).

The Seven Novel Genes Up-Expressed in Pheochromocytoma Tumor

In order to study the specific mechanism of pVHL affecting cell biological functions, we first collected the functional classification information of all proteomes and the corresponding enrichment P value (Fisher's exact test), and then screened the significantly enriched functional classification (P -value <0.05) in at least one protein group. For the P -value obtained by Fisher's exact test, the bubble chart showed the functional classification of significant enrichment of differential proteins and the results were shown in

Figure 2D. As shown in the figure, the differentially expressed proteins mainly tended to the types of cell proliferation and migration. Therefore, we aimed to investigate the differentially expressed proteins associated with cell proliferation and migration. For biological process (BP), we selected 47 proteins related to cell proliferation, migration, and growth from BP group; for molecular function (MF), we selected 17 proteins related to growth factor binding, insulin-like growth factor binding, and peptidase regulatory activity from MF group. Furthermore, we selected 57 proteins related to extracellular matrix and extracellular space from the CC group as cell components (CC) while the screening workflow was shown in **Table S4**. In order to find differentially expressed proteins with important regulatory functions, we used the Venny Diagram online software (Venny-v.2.0) to select 10 differentially expressed proteins in these three parts (MF, CC, and BP groups) (**Figure 4A**). In order to further prove the clinical significance and application value of these proteins, we collected the tumor tissues of four patients with VHL mutation pheochromocytoma to verify the expression of these genes *in vivo*. We found that seven genes, including connective tissue growth factor (CTGF), Syndecan Binding Protein (SDCBP), Cysteine Rich Protein 61 (CYR61/CCN1), Type III Collagen A 1 Chain (COL3A1), Type I Collagen A 1 Chain (COL1A1), Type V Collagen A 2 Chain (COL5a2), and Serpin Family E Member 1 (SERPINE1), were significantly up-regulated in these tumor samples, which proved that VHL mutation activated Expression of these genes in pheochromocytoma. (**Figure 4B**). The up-regulation of seven genes in tumor tissues indicated that they played an important role in tumorigenesis and development. Meanwhile, western blot further confirmed the conclusions obtained by qRT-PCR (**Figures 4C, D**). The information of the seven genes in the proteomics quantitative analysis was shown in **Table 2**. In order to explore whether the overexpression of these genes was related to hypoxia-inducible factor (HIF), we detected HIF α and its downstream proteins vascular endothelial growth factor A (VEGFA) and glucose transporter 1 (Glut1) in VHL mutated carcinoma and para-carcinoma tissues. We found that in tumor tissues, HIF2 α accumulated significantly, while VEGF and Glut1 were significantly overexpressed at both the mRNA and protein levels (**Figures 4B–D**).

HIF2 α Regulated the Overexpression of these Seven Novel Genes

We further explored the mechanism of pVHL regulating these seven novel genes. Similar to other work, we found that HIF2 α accumulated when VHL was knocked down (**Figure 5B**). In the case of abnormal accumulation of HIF2 α , VEGF and Glut1 were significantly overexpressed (**Figures 5A, B**). To explore the role of HIF2 α in the expression of these seven genes, we treated VHL-KD cells with hypoxia and observed the expression levels of these seven genes. After 24 h of hypoxia, the expression of six genes including CTGF, SDCBP, CCN1, COL3A1, COL1A1, and SERPINE1 significantly increased in the cells. Western blot showed no significant change of COL5a2 expression (**Figure 5B, C**) maybe due to its low expression in the cell. Therefore, HIF-2 α might mediate the expression of these seven genes.

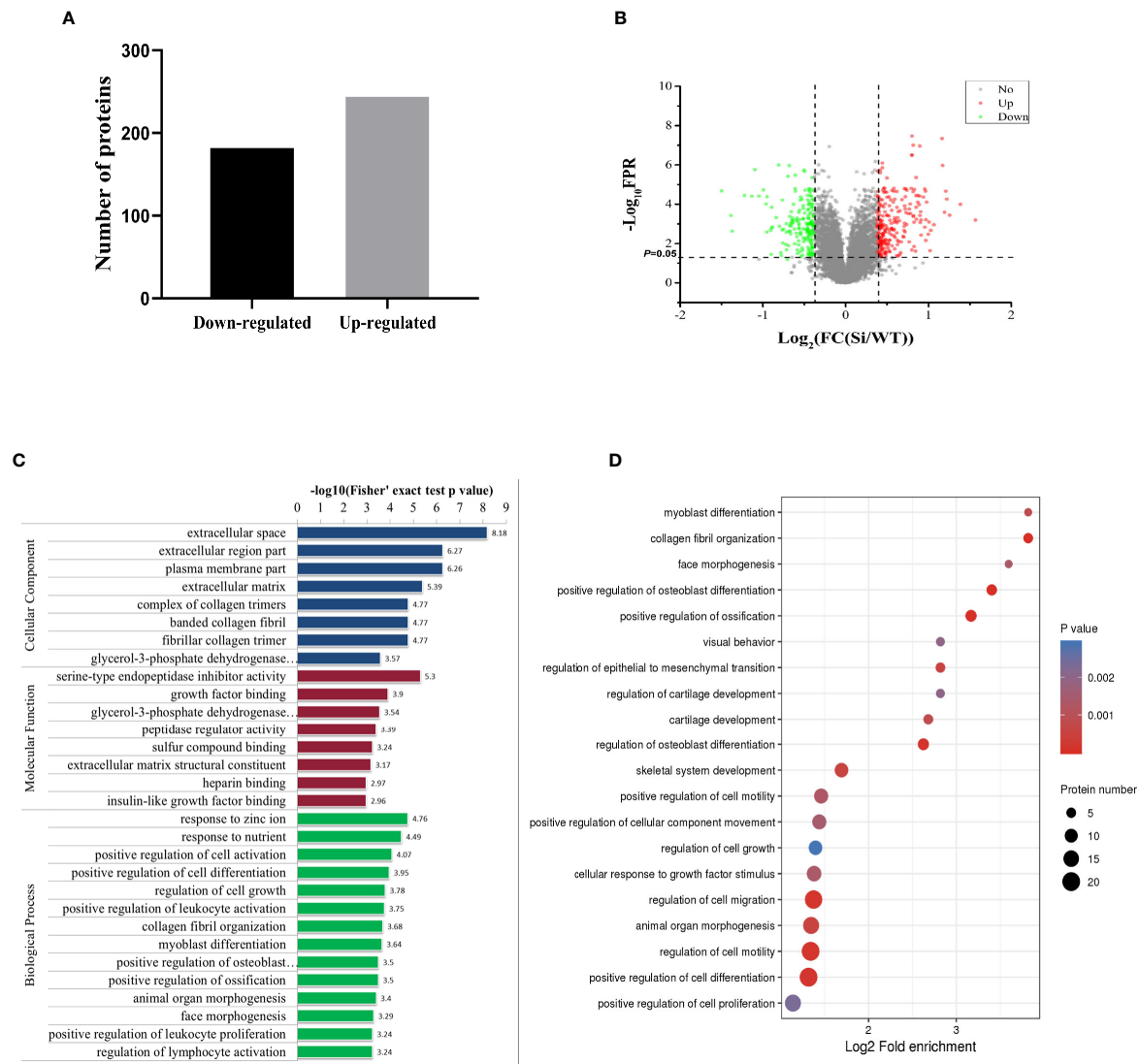


FIGURE 2 | Proteomics analysis of VHL-KD PC12 cell line. **(A)** A bar graph showed the differential protein analyzed by TMT labeling quantitatively. **(B)** The volcano map of differentially expressed proteins. The abscissa denotes the ratios of differential expression proteins in the VHL-KD PC12 cell line vs those in the empty vector-transfected cell line; the ordinate represents the P -value between the two groups. **(C)** Differential protein was analyzed by GO function enrichment, and GO annotations were divided into three categories: Biological Process, Cellular Component, and Molecular Function. **(D)** The three main categories of differential proteins obtained by GO classification were further functionally analyzed. The circle in the figure indicated the number of differential proteins. The shade of the circle color represented the size of the P -value. The darker the color of the circle represented the smaller the P -value; the lighter the color of the circle represented the larger the P -value.

VHL-KD Changes Cell Morphology and Promotes Cell Proliferation and Migration

Since the discovered seven novel genes were related to cell proliferation and migration, we wanted to know whether VHL-KD would promote proliferation and migration. We observed that the morphology of VHL-KD cells changed, and the neurites of VHL-KD cells were longer than those of uninfected and empty vector transfected cells (**Figure 6A**). Furthermore, VHL-KD cells proliferated faster than empty vector-transfected cells (**Figure 6B**). Scratch and transwell assays showed that VHL-KD cells had

stronger migration ability as compared to empty vector-transfected (**Figures 6C–F**).

DISCUSSION

As a rare neuroendocrine tumor, PPGL were mostly benign and could be cured by surgery (47). However, due to the limitations of precise diagnostic tools and effective treatment methods, metastatic PPGL had become a major challenge in the medical

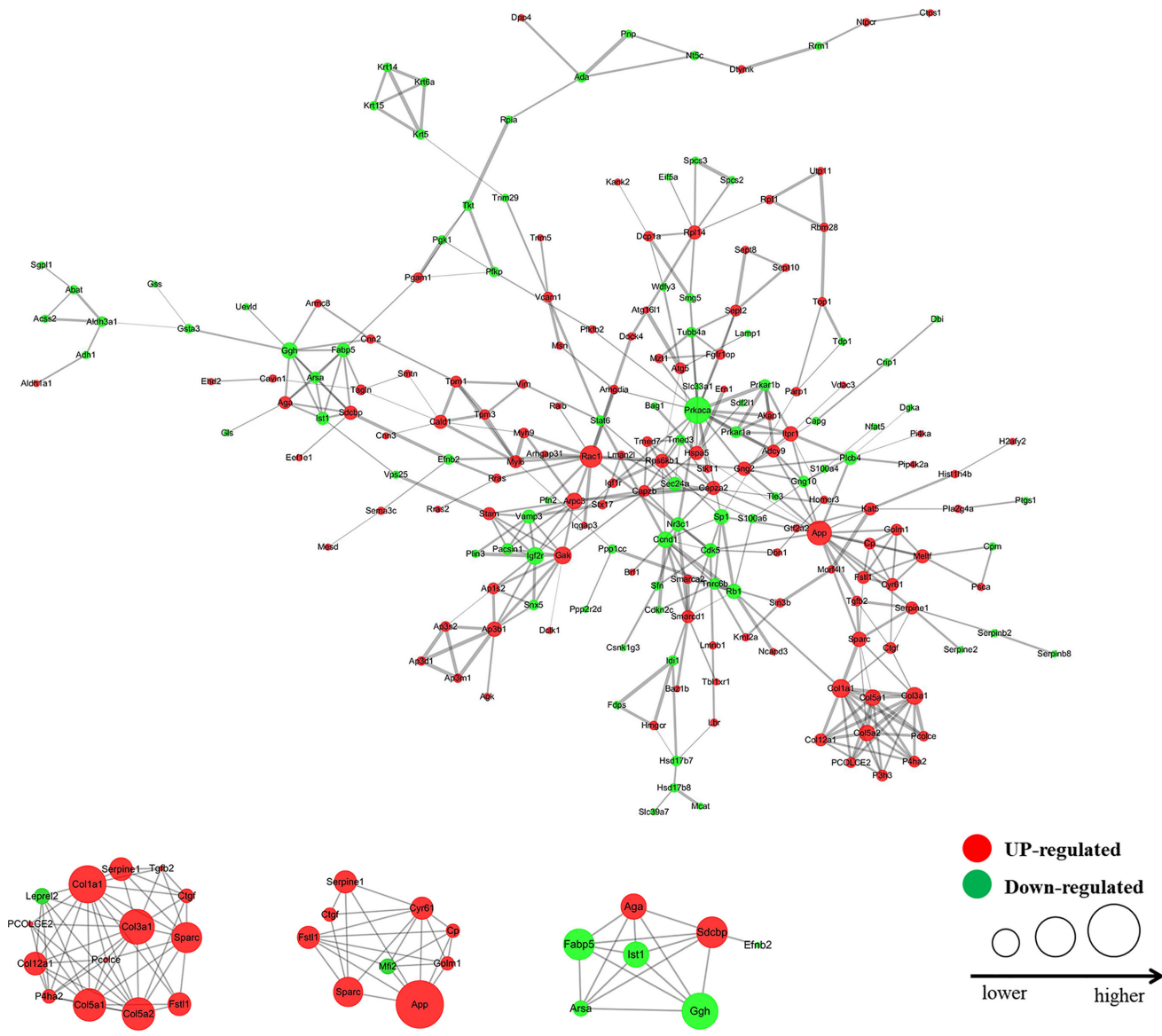


FIGURE 3 | Interaction network diagram of the protein with fold change >1.3 (VHL shRNA/WT). The interactive network of 83 proteins and their differential expression in the VHL-KD cells vs those in the empty vector-transfected cells.

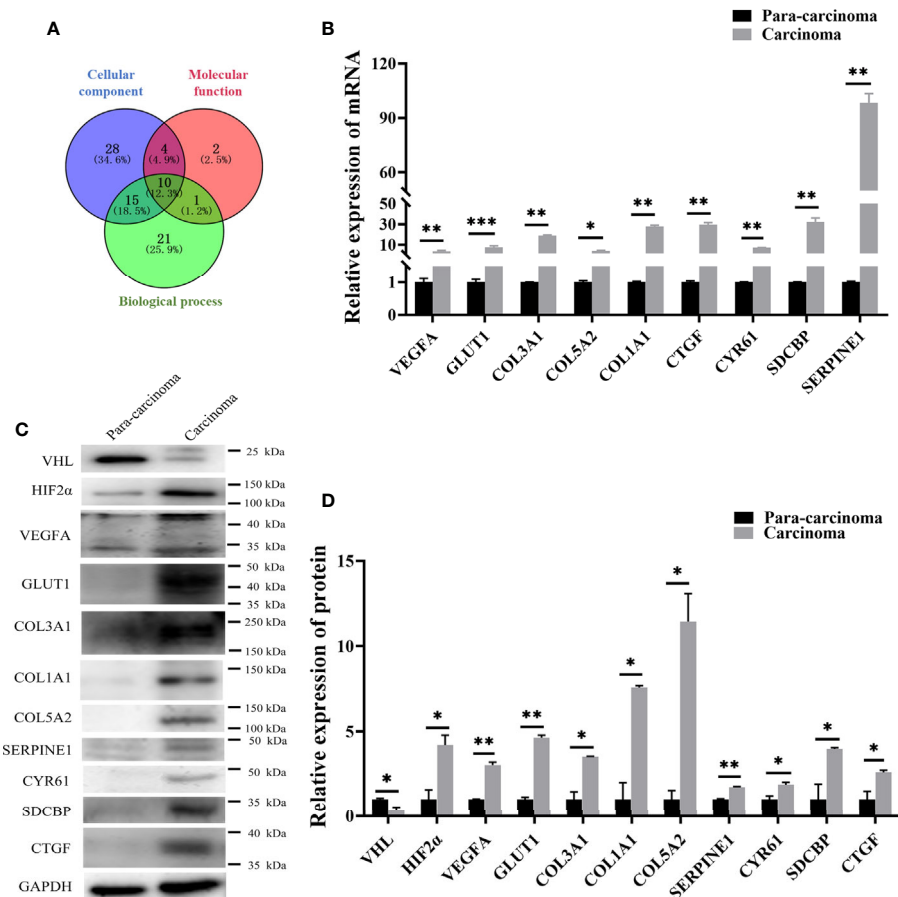


FIGURE 4 | qRT-PCR and western blot confirmed that seven genes screened by proteomics analysis were also significantly up-regulated in pheochromocytoma tumors. **(A)** Venn diagram was used to screen the co-existing proteins among three groups of proteins. **(B)** qRT-PCR detected expression of seven genes in PCC carcinoma and para-carcinoma tissues. *significance between carcinoma vs. para-carcinoma group. * $P < 0.05$, ** $P < 0.01$, *** $P < 0.001$, $n = 4$. **(C)** Western blot was used to detect protein expression in clinical tissue samples. * $P < 0.05$, ** $P < 0.01$, $n = 4$. **(D)** The histogram obtained by gray analysis showed the relative change of proteins (mean \pm SEM), $n = 3$, * $P < 0.05$, ** $P < 0.01$.

field (48, 49). Nowadays, more and more attention had been paid to the targeted therapy of PPGL (50). Therefore, optimizing the diagnostic efficiency of metastatic PPGL and finding more effective biological target molecules had gradually become the trend of clinical and basic research (51). In this study, the most relevant tumor malignant indicators and essential biological characteristics were used as screening criteria, and high-throughput technology was used to comprehensively evaluate the molecular mechanism of tumor pathogenesis. As we know, targeted therapy needs long-term and painstaking exploration to obtain more effective treatments (52).

As the key protein of VHL syndrome, pVHL regulated the expression of different tumor genes (53). The patients with VHL germline mutations were susceptible to VHL disease, which was an autosomal dominant syndrome (54). The multiple subtypes of VHL disease indicated that pVHL had multiple cellular functions (55). Other related studies also showed that VHL was involved in other functions besides the regulation mechanism of HIF1 α -mediated proteasome degradation induced by hypoxia (19).

Chitrakar et al. found that in Th17 cells, VHL was involved in the regulation of a variety of cellular pathways (56), including glycolytic pathways that were indirectly or directly inhibited by protein-coding genes (57). Furthermore, the VHL also controlled the function of innate immune cells (58), and the interleukin 33 receptor directly interacted with VHL (59). Our results suggested that pVHL was related to interleukin-related proteins. In order to study the role of pVHL in hypoxia induced pathway, we carried out the whole protein quantitative analysis. Our study showed that the differentially expressed proteins caused by VHL inactivation were mainly concentrated in clusters related to proliferation and migration. The deregulation of HIF2 α could promote tumor development (60), but HIF2 α had an undeveloped function that was largely independent of ARNT, which could affect gene transcription, cell differentiation, proliferation, and tumor metastasis and growth (61, 62). Sun et al. reported that VHL mutation promoted the proliferation, migration, and tumorigenesis of clear cell renal cell carcinoma (ccRCC) cells through the bridging function of SALL4 (63) and

TABLE 2 | Specific information on differential expression of seven proteins in proteomics.

Protein accession	Gene name	Ratio (shRNA/WT)	q-value*	Biological process	Cellular component	Molecular function
Q9R1E9	Connective Tissue Growth Factor (CTGF)	1.763	0.000422	regulation of cell death and growth; regulation of G0 to G1 transition; regulation of cell differentiation and motility.	extracellular matrix; intracellular membrane-bounded organelle	fibronectin binding; carbohydrate derivative binding; growth factor activity; growth factor binding;
Q9JI92	Syndecan Binding Protein (SDCBP)	2.093	0.001103	regulation of vesicle-mediated transport; positive regulation of cell migration; positive regulation of cell proliferation;	extracellular exosome; nucleoplasm; nuclear outer membrane-endoplasmic reticulum membrane network;	cell adhesion molecule binding; insulin-like growth factor binding;
Q66HT5	Cysteine Rich Protein 61 (CYR61)	2.286	0.000256	positive regulation of cell migration; angiogenesis; regulation of cell growth;	extracellular matrix;	integrin binding; cell adhesion molecule binding; structural molecule activity;
P13941	Collagen Alpha-1 (III) Chain (COL3A1)	2.313	2.17E-05	nervous system development; negative regulation of cell development; regulation of cell migration;	supramolecular complex; extracellular matrix component;	cell adhesion molecule binding; growth factor binding; growth factor binding;
P02454	Collagen Alpha-1 (I) Chain (COL1A1)	1.832	3.66E-05	positive regulation of canonical Wnt signaling pathway response to transforming growth factor beta; positive regulation of epithelial to mesenchymal transition;	membrane-bounded organelle; secretory vesicle; extracellular matrix component;	extracellular matrix structural constituent;
F1LQ00	Collagen Type V Alpha 2 Chain (COL5A2)	1.875	0.000243	negative regulation of cell differentiation; cellular response to oxygen-containing compound;	proteinaceous extracellular matrix; supramolecular complex;	structural molecule activity; SMAD binding;
F1LM16	Serpin Family E Member 1 (SERPINE1)	1.343	0.005075	positive regulation of cell migration; positive regulation of vasculature development positive regulation of chemotaxis;	extracellular exosome; extracellular vesicle	protease binding; peptidase inhibitor activity

*q-value indicate the p-value after FDR correction.

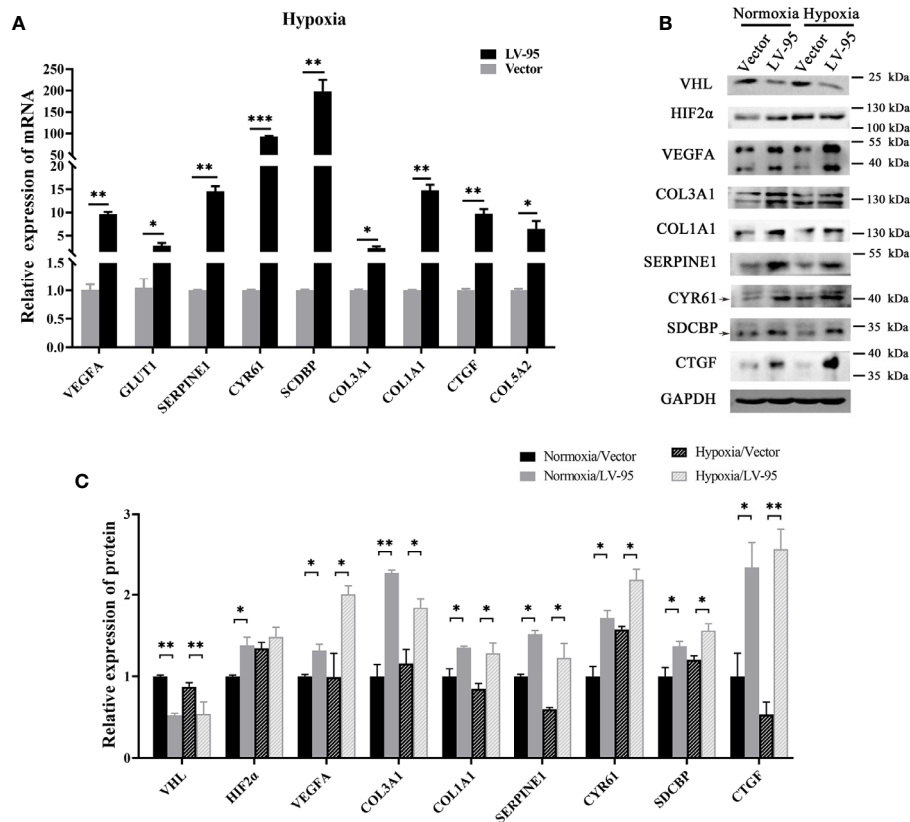


FIGURE 5 | HIF-2α may mediate the overexpression of these seven genes. **(A)** The VHL-KD cell line (LV-95) and the empty vector-transfected cell line (Vector) were treated with hypoxia, and then qRT-PCR was used to detect the mRNA expression of seven target genes in the cells (mean ± SEM), $n = 3$, $^*P < 0.05$, $^{**}P < 0.01$, $^{***}P < 0.001$. **(B, C)** The western blot was used to detect the change of protein expression in cells when VHL is knocked down; the histogram indicated the multiple of protein changes (mean ± SEM), $n = 3$, $^{**}P < 0.01$.

inhibited the senescence of ccRCC cells (64). Kondo et al. proved that pVHL achieved tumor suppression by inhibiting HIF2α (23). Our results conferred the seven downstream genes related to cell proliferation and migration regulated by the VHL/HIF2α axis.

From the complicated network controlled by pVHL, we found seven novel genes related to cell proliferation and migration. Firstly, our results showed that SERPINE1 expression was significantly up-regulated in the VHL-KD PC12 cell line, suggesting its distinctive biological significance. In a series of cell biology and molecular biology experiments, Yang et al. proved that overexpression of SERPINE1, which promoted the proliferation, invasion, and migration of ccRCC cells, was used as an independent prognostic factor for patients with gastric cancer (65). Secondly, our results showed that the expression of SDCBP was significantly increased *in vivo*. Related studies reported that the metastasis and spread of cancer cells were indirectly completed by many discrete processes, such as invasion, intravascular invasion, and angiogenesis (66), and SDCBP was a unique gene that promoted metastasis (67). Moreover, preclinical studies confirmed that inhibiting SDCBP from a genetic or pharmacological perspective could effectively

inhibit cell metastasis (68). The expression of CTGF in our results was also significantly increased. Therefore, in our findings, the overexpression of SDCBP might promote the metastasis of pheochromocytoma. The low expression of CTGF was associated with the high overall survival rates of neuroblastoma patients, indicating the important role of CTGF in tumors (69). CTGF promoted the deposition of extracellular matrix and the proliferation of fibroblasts, thereby causing vascular diseases (70). Moreover, the phase-dependent regulation of CTGF was crucial for the malignancy of competent cancer cells (71). We discovered three collagen family proteins which were significantly up-regulated in PCC carcinoma. In liver cancer, there were relatively many studies on the function of COL1A1. Ma et al. proved that COL1A1, which promoted the HCC cell proliferation and invasion and the formation of tumor balls, was significantly up-regulated in liver cancer and enhanced carcinogenicity (72). Additionally, COL1A1 highly expressed in human breast and gastric cancer, while COL1A2 highly expressed in gastric cancer, and affected the prognosis (73, 74). As members of the collagen family, both COL3A1 and COL5A2 had significant value in the prognosis of gastric cancer (75). In our research results, they were significantly

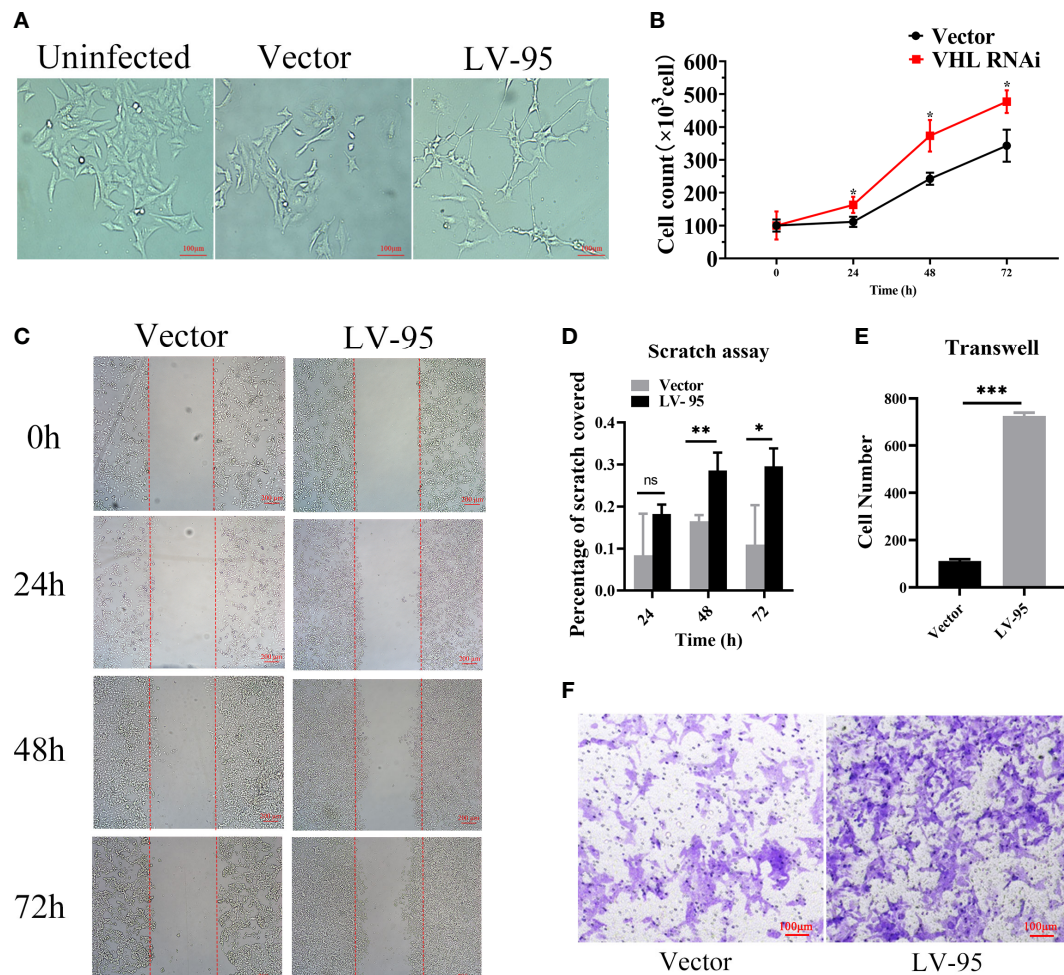


FIGURE 6 | VHL-KD changed the cell morphology and promoted the proliferation and migration of PC12 cells. **(A)** Phase contrasted 10 \times images of VHL-KD (LV-95) and empty vector-transfected (Vector) PC12 cells. **(B)** Growth chart of VHL-KD and VHL empty vector-transfected cells, * $P < 0.05$. **(C, D)** Phase-contrast micrographs illustrating migration by wound healing of PC12 cells transduced with empty vector or VHL shRNA. Images were taken at different time points after wounding, as indicated. $n = 3$, ns: non significant, * $P < 0.05$, ** $P < 0.01$. **(E, F)** Down: Micrographs illustrating trans-migration of PC12 cells transduced with empty vector or VHL shRNA. Up: Bar graphs indicated trans-migration relative to empty vector transduced cells. *** $P < 0.001$.

overexpressed in pheochromocytoma tissues and cell lines. Finally, the enrichment of CYR61 was very significant in VHL-KD cells. Mustafa Ilhan et al. demonstrated that overexpression of CYR61 promoted Notch1-induced migration, invasion, and anchorage-independent growth of the normal breast cancer cell line MCF10A, suggesting its importance in cancer progression (76). Thus, it could be concluded that the above seven genes regulated the proliferation, invasion, and metastasis of various tumors, suggesting that they could provide potential biomarkers and therapeutic targets for effective treatment of PPGL patients.

In conclusion, we found that the inactivation of pVHL in pheochromocytoma led to the up-regulation of the seven novel genes, such as CTGF, SDCBP, CYR61, COL3A1, COL1A1, COL5A2, and SERPINE1. The seven novel genes were closely related to cell proliferation, migration, and differentiation. Therefore, our results indicated that the seven proteins might

serve as important diagnostic and therapeutic candidates for pheochromocytoma.

DATA AVAILABILITY STATEMENT

The original contributions presented in the study are publicly available, and the original data can be found on the Internet through the data set identifier of PXD021190: <http://www.ebi.ac.uk/pride>.

ETHICS STATEMENT

The studies involving human participants were reviewed and approved by the Ethics Committee of the School of Life Sciences,

Central South University. The patients/participants provided their written informed consent to participate in this study.

AUTHOR CONTRIBUTIONS

FZ and LL designed and supervised the experiments and modified and contributed towards writing the manuscript. SG performed the experiments and wrote the initial manuscript. ZL helped with the experiments and cell modeling. JS and YP collected clinical samples and helped with data. All authors contributed to the article and approved the submitted version.

FUNDING

This work was supported by Natural Science Foundation of Hunan Province (No. 2018JJ6133), Innovation Driven Program

of Central South University (No. 020CX046), Changsha Municipal Natural Science Foundation (No. kq2007062), and Funds for the Shenghua Yuying talents program of Central South University.

ACKNOWLEDGMENTS

The author would like to thank pheochromocytoma patients for their cooperation and support.

SUPPLEMENTARY MATERIAL

The Supplementary Material for this article can be found online at: <https://www.frontiersin.org/articles/10.3389/fendo.2021.598656/full#supplementary-material>

REFERENCES

- Withey SJ, Perrio S, Christodoulou D, Izatt L, Carroll P, Velusamy A, et al. Imaging Features of Succinate Dehydrogenase-deficient Pheochromocytoma-Paranglioma Syndromes. *Radiographics* (2019) 39(5):1393–410. doi: 10.1148/rg.2019180151
- Schreiner F, Beuschlein F. Disease monitoring of patients with pheochromocytoma or paraganglioma by biomarkers and imaging studies. *Best Pract Res Clin Endocrinol Metab* (2020) 34(2):101347. doi: 10.1016/j.beem.2019.101347
- Buffet A, Burnichon N, Favier J, Gimenez-Roqueplo AP. An overview of 20 years of genetic studies in pheochromocytoma and paraganglioma. *Best Pract Res Clin Endocrinol Metab* (2020) 34(2):101416. doi: 10.1016/j.beem.2020.101416
- Favier J, Amar L, Gimenez-Roqueplo AP. Paraganglioma and phaeochromocytoma: from genetics to personalized medicine. *Nat Rev Endocrinol* (2015) 11(2):101–11. doi: 10.1038/nrendo.2014.188
- Nölting S, Ullrich M, Pietzsch J, Ziegler CG, Eisenhofer G, Grossman A, et al. Practicing Clinician in the Era of Precision Medicine. *Cancers (Basel)* (2019) 11(10):1505–31. doi: 10.3390/cancers11101505
- Song Y, Huang J, Shan L, Zhang HT. Analyses of Potential Predictive Markers and Response to Targeted Therapy in Patients with Advanced Clear-cell Renal Cell Carcinoma. *Chin Med J (Engl)* (2015) 128(15):2026–33. doi: 10.4103/0366-6999.161353
- Bender BU, Gutsche M, Gläsker S, Müller B, Kirste G, Eng C, et al. Differential genetic alterations in von Hippel-Lindau syndrome-associated and sporadic pheochromocytomas. *J Clin Endocrinol Metab* (2000) 85(12):4568–74. doi: 10.1210/jcem.85.12.7015
- Taïeb D, Pacak K. New Insights into the Nuclear Imaging Phenotypes of Cluster 1 Pheochromocytoma and Paraganglioma. *Trends Endocrinol Metab* (2017) 28(11):807–17. doi: 10.1016/j.tem.2017.08.001
- Luchetti A, Walsh D, Rodger F, Clark G, Martin T, Irving R, et al. Profiling of somatic mutations in phaeochromocytoma and paraganglioma by targeted next generation sequencing analysis. *Int J Endocrinol* (2015) 2015:138573. doi: 10.1155/2015/138573
- Vicha A, Musil Z, Pacak K. Genetics of pheochromocytoma and paraganglioma syndromes: new advances and future treatment options. *Curr Opin Endocrinol Diabetes Obes* (2013) 20(3):186–91. doi: 10.1097/MED.0b013e32835fcc45
- Majewska A, Budny B, Ziemnicka K, Ruchała M, Wierzbicka M. Head and Neck Paragangliomas-A Genetic Overview. *Int J Mol Sci* (2020) 21(20):7669–79. doi: 10.3390/ijms21207669
- Nölting S, Grossman AB. Signaling pathways in pheochromocytomas and paragangliomas: prospects for future therapies. *Endocr Pathol* (2012) 23(1):21–33. doi: 10.1007/s12022-012-9199-6
- Guo Z, Lloyd RV. Pheochromocytomas and Paragangliomas: An Update on Recent Molecular Genetic Advances and Criteria for Malignancy. *Adv Anat Pathol* (2015) 22(5):283–93. doi: 10.1097/pap.0000000000000086
- Peng S, Zhang J, Tan X, Huang Y, Xu J, Silk N, et al. The VHL/HIF Axis in the Development and Treatment of Pheochromocytoma/Paraganglioma. *Front Endocrinol* (2020) 11:586857. doi: 10.3389/fendo.2020.586857
- Fishbein L, Leshchiner I, Walter V, Danilova L, Robertson AG, Johnson AR, et al. Comprehensive Molecular Characterization of Pheochromocytoma and Paraganglioma. *Cancer Cell* (2017) 31(2):181–93. doi: 10.1016/j.ccell.2017.01.001
- Kaelin WJ Jr. Molecular basis of the VHL hereditary cancer syndrome. *Nat Rev Cancer* (2002) 2(9):673–82. doi: 10.1038/nrc885
- Davidowitz EJ, Schoenfeld AR, Burk RD. VHL induces renal cell differentiation and growth arrest through integration of cell-cell and cell-extracellular matrix signaling. *Mol Cell Biol* (2001) 21(3):865–74. doi: 10.1128/mcb.21.3.865-874.2001
- Ohh M, Yach RL, Loneragan KM, Whaley JM, Stemmer-Rachamimov AO, Louis DN, et al. The von Hippel-Lindau tumor suppressor protein is required for proper assembly of an extracellular fibronectin matrix. *Mol Cell* (1998) 1(7):959–68. doi: 10.1016/s1097-2765(00)80096-9
- Zhang J, Zhang Q. VHL and Hypoxia Signaling: Beyond HIF in Cancer. *Biomedicines* (2018) 6(1):35–47. doi: 10.3390/biomedicines6010035
- Semenza GL. Hypoxia-inducible factor 1 (HIF-1) pathway. *Sci STKE* (2007) 2007(407):cm8. doi: 10.1126/stke.4072007cm8
- Atkins DJ, Gingert C, Justenhoven C, Schmahl GE, Bonato MS, Brauch H, et al. Concomitant deregulation of HIF1alpha and cell cycle proteins in VHL-mutated renal cell carcinomas. *Virchows Arch* (2005) 447(3):634–42. doi: 10.1007/s00428-005-1262-y
- Chen F, Kishida T, Duh FM, Renbaum P, Orcutt ML, Schmidt L, et al. Suppression of growth of renal carcinoma cells by the von Hippel-Lindau tumor suppressor gene. *Cancer Res* (1995) 55(21):4804–7. doi: 10.1007/BF01517220
- Kondo K, Kim WY, Lechpammer M, Kaelin WJ Jr. Inhibition of HIF2alpha is sufficient to suppress pVHL-defective tumor growth. *PLoS Biol* (2003) 1(3):E83. doi: 10.1371/journal.pbio.0000083
- Gonzalez FJ, Xie C, Jiang C. The role of hypoxia-inducible factors in metabolic diseases. *Nat Rev Endocrinol* (2018) 15(1):21–32. doi: 10.1038/s41574-018-0096-z
- Bechmann N, Moskopp ML, Ullrich M, Calsina B, Wallace PW, Richter S, et al. HIF2α supports pro-metastatic behavior in pheochromocytomas/paragangliomas. *Endocr Relat Cancer* (2020) 27(11):625–40. doi: 10.1530/erc-20-0205
- Jochmanova I, Lazurova I. A new twist in neuroendocrine tumor research: Pacak-Zhuang syndrome, HIF-2α as the major player in its pathogenesis and

- future therapeutic options. *Biomed Pap Med Fac Univ Palacky Olomouc Czech* (2014) 158(2):175–80. doi: 10.5507/bp.2014.021
27. Pacak K, Jochmanova I, Prodanov T, Yang C, Merino MJ, Fojo T, et al. New syndrome of paraganglioma and somatostatinoma associated with polycythemia. *J Clin Oncol* (2013) 31(13):1690–8. doi: 10.1200/jco.2012.47.1912
 28. Percy MJ, Furlow PW, Lucas GS, Li X, Lappin TR, McMullin MF, et al. A gain-of-function mutation in the HIF2A gene in familial erythrocytosis. *N Engl J Med* (2008) 358(2):162–8. doi: 10.1056/NEJMoa073123
 29. Taïeb D, Barlier A, Yang C, Pertuit M, Tchoghandjian A, Rochette C, et al. Somatic gain-of-function HIF2A mutations in sporadic central nervous system hemangioblastomas. *J Neurooncol* (2016) 126(3):473–81. doi: 10.1007/s11060-015-1983-y
 30. Percy MJ, Beer PA, Campbell G, Dekker AW, Green AR, Oscier D, et al. Novel exon 12 mutations in the HIF2A gene associated with erythrocytosis. *Blood* (2008) 111(11):5400–2. doi: 10.1182/blood-2008-02-137703
 31. Taïeb D, Yang C, Delenne B, Zhuang Z, Barlier A, Sebag F, et al. First report of bilateral pheochromocytoma in the clinical spectrum of HIF2A-related polycythemia-paraganglioma syndrome. *J Clin Endocrinol Metab* (2013) 98(5):E908–13. doi: 10.1210/jc.2013-1217
 32. Yang C, Sun MG, Matro J, Huynh TT, Rahimpour S, Prchal JT, et al. Novel HIF2A mutations disrupt oxygen sensing, leading to polycythemia, paragangliomas, and somatostatinomas. *Blood* (2013) 121(13):2563–6. doi: 10.1182/blood-2012-10-460972
 33. Favie J, Buffet A, Gimenez-Roqueplo AP. HIF2A mutations in paraganglioma with polycythemia. *N Engl J Med* (2012) 367(22):2161. doi: 10.1056/NEJMc1211953
 34. Comino-Méndez I, de Cubas AA, Bernal C, Álvarez-Escolá C, Sánchez-Malo C, Ramírez-Tortosa CL, et al. Tumoral EPAS1 (HIF2A) mutations explain sporadic pheochromocytoma and paraganglioma in the absence of erythrocytosis. *Hum Mol Genet* (2013) 22(11):2169–76. doi: 10.1093/hmg/ddt069
 35. Toledo RA, Qin Y, Srikantan S, Morales NP, Li Q, Deng Y, et al. In vivo and in vitro oncogenic effects of HIF2A mutations in pheochromocytomas and paragangliomas. *Endocr Relat Cancer* (2013) 20(3):349–59. doi: 10.1530/erc-13-0101
 36. Richter S, Qin N, Pacak K, Eisenhofer G. Role of hypoxia and HIF2 α in development of the sympathoadrenal cell lineage and chromaffin cell tumors with distinct catecholamine phenotypic features. *Adv Pharmacol (San Diego Calif)* (2013) 68:285–317. doi: 10.1016/b978-0-12-411512-5.00014-2
 37. Lorenzo FR, Yang C, Ng Tang Fui M, Vankayalapati H, Zhuang Z, Huynh T, et al. A novel EPAS1/HIF2A germline mutation in a congenital polycythemia with paraganglioma. *J Mol Med (Berlin Germany)* (2013) 91(4):507–12. doi: 10.1007/s00109-012-0967-z
 38. Tian H, Hammer RE, Matsumoto AM, Russell DW, McKnight SL. The hypoxia-responsive transcription factor EPAS1 is essential for catecholamine homeostasis and protection against heart failure during embryonic development. *Genes Dev* (1998) 12(21):3320–4. doi: 10.1101/gad.12.21.3320
 39. Nilsson H, Jögi A, Beckman S, Harris AL, Poellinger L, Pahlman S. HIF-2 α expression in human fetal paraganglia and neuroblastoma: relation to sympathetic differentiation, glucose deficiency, and hypoxia. *Exp Cell Res* (2005) 303(2):447–56. doi: 10.1016/j.yexcr.2004.10.003
 40. Huang CC, Wang SY, Lin LL, Wang PW, Chen TY, Hsu WM, et al. Glycolytic inhibitor 2-deoxyglucose simultaneously targets cancer and endothelial cells to suppress neuroblastoma growth in mice. *Dis Models Mech* (2015) 8(10):1247–54. doi: 10.1242/dmm.021667
 41. Giatromanolaki A, Sivridis E, Fiska A, Koukourakis MI. Hypoxia-inducible factor-2 α (HIF-2 α) induces angiogenesis in breast carcinomas. *Appl Immunohistochem Mol Morphol AIMM* (2006) 14(1):78–82. doi: 10.1097/01.pai.0000145182.98577.10
 42. Capodimonti S, Teofili L, Martini M, Cenci T, Iachininoto MG, Nuzzolo ER, et al. Von hippel-lindau disease and erythrocytosis. *J Clin Oncol* (2012) 30(13):e137–9. doi: 10.1200/jco.2011.38.6797
 43. Bourkoulas A, Mavrogonatou E, Pavli P, Petrou PS, Douvas AM, Argitis P, et al. Guided cell adhesion, orientation, morphology and differentiation on silicon substrates photolithographically micropatterned with a cell-repellent cross-linked poly(vinyl alcohol) film. *BioMed Mater* (2018) 14(1):014101. doi: 10.1088/1748-605X/aae7ba
 44. Murray KA, Gibson MI. Post-Thaw Culture and Measurement of Total Cell Recovery Is Crucial in the Evaluation of New Macromolecular Cryoprotectants. *Biomacromolecules* (2020) 21(7):2864–73. doi: 10.1021/acs.biomac.0c00591
 45. Broussau S, Jabbour N, Lachapelle G, Durocher Y, Tom R, Transfiguración J, et al. Inducible packaging cells for large-scale production of lentiviral vectors in serum-free suspension culture. *Mol Ther* (2008) 16(3):500–7. doi: 10.1038/sj.mt.6300383
 46. Livak KJ, Schmittgen TD. Analysis of relative gene expression data using real-time quantitative PCR and the 2 \times (-Delta Delta C(T)) Method. *Methods* (2001) 25(4):402–8. doi: 10.1006/meth.2001.1262
 47. Khorram-Manesh A, Ahlman H, Nilsson O, Odén A, Jansson S. Mortality associated with pheochromocytoma in a large Swedish cohort. *Eur J Surg Oncol (EJSO)* (2004) 30(5):556–9. doi: 10.1016/j.ejso.2004.03.006
 48. Ding XF, Chen J, Zhou J, Chen G, Wu YL. Never-in-mitosis A-related kinase 8, a novel target of von-Hippel-Lindau tumor suppressor protein, promotes gastric cancer cell proliferation. *Oncol Lett* (2018) 16(5):5900–6. doi: 10.3892/ol.2018.9328
 49. Goncalves J, Lussey-Lepoutre C, Favier J, Gimenez-Roqueplo AP, Castro-Vega LJ. Emerging molecular markers of metastatic pheochromocytomas and paragangliomas. *Ann Endocrinol (Paris)* (2019) 80(3):159–62. doi: 10.1016/j.jando.2019.04.003
 50. Nölting S, Grossman A, Pacak K. Metastatic Pheochromocytoma: Spinning Towards More Promising Treatment Options. *Exp Clin Endocrinol Diabetes* (2019) 127(2-03):117–28. doi: 10.1055/a-0715-1888
 51. Sarkadi B, Meszaros K, Krencz I, Canu L, Krokker L, Zakarias S, et al. Glutaminases as a Novel Target for SDHB-Associated Pheochromocytomas/Paragangliomas. *Cancers (Basel)* (2020) 12(3):599–623. doi: 10.3390/cancers12030599
 52. Lee YT, Tan YJ, Oon CE. Molecular targeted therapy: Treating cancer with specificity. *Eur J Pharmacol* (2018) 834:188–96. doi: 10.1016/j.ejphar.2018.07.034
 53. Crespigio J, Berbel LCL, Dias MA, Berbel RF, Pereira SS, Pignatelli D, et al. Von Hippel-Lindau disease: a single gene, several hereditary tumors. *J Endocrinol Invest* (2018) 41(1):21–31. doi: 10.1007/s40618-017-0683-1
 54. Chittiboina P, Lonser RR. Von Hippel-Lindau disease. *Handb Clin Neurol* (2015) 132:139–56. doi: 10.1016/b978-0-444-62702-5.00010-x
 55. Tarade D, Ohh M. The HIF and other quandaries in VHL disease. *Oncogene* (2018) 37(2):139–47. doi: 10.1038/onc.2017.338
 56. Mehdi A, Riazalhosseini Y. Epigenome Aberrations: Emerging Driving Factors of the Clear Cell Renal Cell Carcinoma. *Int J Mol Sci* (2017) 18(8):1774–806. doi: 10.3390/ijms18081774
 57. Chitrakar A, Budda SA, Henderson JG, Axtell RC, Zenewicz LA. E3 Ubiquitin Ligase Von Hippel-Lindau Protein Promotes Th17 Differentiation. *J Immunol* (2020) 205(4):1009–23. doi: 10.4049/jimmunol.2000243
 58. Zhang W, Li Q, Li D, Li J, Aki D, Liu YC. The E3 ligase VHL controls alveolar macrophage function via metabolic-epigenetic regulation. *J Exp Med* (2018) 215(12):3180–93. doi: 10.1084/jem.20181211
 59. Li Q, Li D, Zhang X, Wan Q, Zhang W, Zheng M, et al. E3 Ligase VHL Promotes Group 2 Innate Lymphoid Cell Maturation and Function via Glycolysis Inhibition and Induction of Interleukin-33 Receptor. *Immunity* (2018) 48(2):258–70.e5. doi: 10.1016/j.immuni.2017.12.013
 60. Liu C, Liu L, Wang K, Li XF, Ge LY, Ma RZ, et al. VHL-HIF-2 α axis-induced SMYD3 upregulation drives renal cell carcinoma progression via direct trans-activation of EGFR. *Oncogene* (2020) 39(21):4286–98. doi: 10.1038/s41388-020-1291-7
 61. Persson CU, von Stedingk K, Fredlund E, Bexell D, Pahlman S, Wigerup C, et al. ARNT-dependent HIF-2 transcriptional activity is not sufficient to regulate downstream target genes in neuroblastoma. *Exp Cell Res* (2020) 388(2):111845. doi: 10.1016/j.yexcr.2020.111845
 62. Hoefflin R, Harlander S, Schäfer S, Metzger P, Kuo F, Schönenberger D, et al. HIF-1 α and HIF-2 α differently regulate tumour development and inflammation of clear cell renal cell carcinoma in mice. *Nat Commun* (2020) 11(1):4111. doi: 10.1038/s41467-020-17873-3
 63. Chen L, Zhan CZ, Wang T, You H, Yao R. Curcumin Inhibits the Proliferation, Migration, Invasion, and Apoptosis of Diffuse Large B-Cell Lymphoma Cell Line by Regulating MiR-21/VHL Axis. *Yonsei Med J* (2020) 61(1):20–9. doi: 10.3349/ymj.2020.61.1.20
 64. Sun J, Tang Q, Gao Y, Zhang W, Zhao Z, Yang F, et al. VHL mutation-mediated SALLA overexpression promotes tumorigenesis and vascularization of clear cell renal cell carcinoma via Akt/GSK-3 β signaling. *J Exp Clin Cancer Res* (2020) 39(1):104. doi: 10.1186/s13046-020-01609-8

65. Yang JD, Ma L, Zhu Z. SERPINE1 as a cancer-promoting gene in gastric adenocarcinoma: facilitates tumour cell proliferation, migration, and invasion by regulating EMT. *J Chemother* (2019) 31(7-8):408–18. doi: 10.1080/1120009x.2019.1687996
66. Leung K. Microbubbles conjugated with anti-matrix metalloproteinase 2 mouse monoclonal antibody sc-13595. In: . *Molecular Imaging and Contrast Agent Database (MICAD)*. Bethesda (MD: National Center for Biotechnology Information (US (2004).
67. Das SK, Maji S, Wechman SL, Bhoopathi P, Pradhan AK, Talukdar S, et al. MDA-9/Syntenin (SDCBP): Novel gene and therapeutic target for cancer metastasis. *Pharmacol Res* (2020) 155:104695. doi: 10.1016/j.phrs.2020.104695
68. Das SK, Kegelman TP, Pradhan AK, Shen XN, Bhoopathi P, Talukdar S, et al. Suppression of Prostate Cancer Pathogenesis Using an MDA-9/Syntenin (SDCBP) PDZ1 Small-Molecule Inhibitor. *Mol Cancer Ther* (2019) 18(11):1997–2007. doi: 10.1158/1535-7163.Mct-18-1019
69. Chen B, Ding P, Hua Z, Qin X, Li Z. Analysis and identification of novel biomarkers involved in neuroblastoma via integrated bioinformatics. *Invest New Drugs* (2020) 9(1):52–65. doi: 10.1007/s10637-020-00980-9
70. Zhou SN, Zhang J, Ren QY, Yao RF, Liu P, Chang B. Early intervention with Di-Dang Decoction prevents macrovascular fibrosis in diabetic rats by regulating the TGF- β 1/Smad signalling pathway. *Chin J Natural Med* (2020) 18(8):612–9. doi: 10.1016/s1875-5364(20)30073-x
71. Kim KH, Lee SJ, Kim J, Moon Y. Dynamic Malignant Wave of Ribosome-Insulted Gut Niche via the Wnt-CTGF/CCN2 Circuit. *iScience* (2020) 23(5):101076. doi: 10.1016/j.isci.2020.101076
72. Ma HP, Chang HL, Bamodu OA, Yadav VK, Huang TY, Wu ATH, et al. Collagen 1A1 (COL1A1) Is a Reliable Biomarker and Putative Therapeutic Target for Hepatocellular Carcinogenesis and Metastasis. *Cancers (Basel)* (2019) 11(6):786–800. doi: 10.3390/cancers11060786
73. Meng C, He Y, Wei Z, Lu Y, Du F, Ou G, et al. MRTF-A mediates the activation of COL1A1 expression stimulated by multiple signaling pathways in human breast cancer cells. *BioMed Pharmacother* (2018) 104:718–28. doi: 10.1016/j.biopha.2018.05.092
74. Li J, Ding Y, Li A. Identification of COL1A1 and COL1A2 as candidate prognostic factors in gastric cancer. *World J Surg Oncol* (2016) 14(1):297. doi: 10.1186/s12957-016-1056-5
75. Shen H, Wang L, Chen Q, Xu J, Zhang J, Fang L, et al. The prognostic value of COL3A1/FBN1/COL5A2/SPARC-mir-29a-3p-H19 associated ceRNA network in Gastric Cancer through bioinformatic exploration. *J Cancer* (2020) 11(17):4933–46. doi: 10.7150/jca.45378
76. Ilhan M, Kucukkose C, Efe E, Gunyuz ZE, Firatligil B, Dogan H, et al. Pro-metastatic functions of Notch signaling is mediated by CYR61 in breast cells. *Eur J Cell Biol* (2020) 99(2-3):151070. doi: 10.1016/j.ejcb.2020.151070

Conflict of Interest: The authors declare that the research was conducted in the absence of any commercial or financial relationships that could be construed as a potential conflict of interest.

Copyright © 2021 Gao, Liu, Li, Pang, Shi and Zhu. This is an open-access article distributed under the terms of the Creative Commons Attribution License (CC BY). The use, distribution or reproduction in other forums is permitted, provided the original author(s) and the copyright owner(s) are credited and that the original publication in this journal is cited, in accordance with accepted academic practice. No use, distribution or reproduction is permitted which does not comply with these terms.



Identification of Clinical Relevant Molecular Subtypes of Pheochromocytoma

Umair Ali Khan Saddozai¹, Fengling Wang¹, Muhammad Usman Akbar², Lu Zhang¹, Yang An¹, Wan Zhu³, Longxiang Xie¹, Yongqiang Li^{1*}, Xinying Ji^{1*} and Xiangqian Guo^{1*}

¹ Department of Preventive Medicine, Institute of Biomedical Informatics, Cell Signal Transduction Laboratory, Bioinformatics Center, School of Basic Medical Sciences, Henan University, Kaifeng, China, ² Gomal Center of Biochemistry and Biotechnology, Gomal University, Dera Ismail Khan, Pakistan, ³ Department of Anesthesia, Stanford University, Stanford, CA, United States

OPEN ACCESS

Edited by:

Alfred King-yin Lam,
Griffith University, Australia

Reviewed by:

David Vaudry,
Institut National de la Santé et de la
Recherche Médicale (INSERM),
France

Md Farhadul Islam,
Griffith University, Australia

*Correspondence:

Yongqiang Li
liyongqiang@vip.henu.edu.cn
Xinying Ji
10190096@vip.henu.edu.cn
Xiangqian Guo
xqguo@henu.edu.cn

Specialty section:

This article was submitted to
Neuroendocrine Science,
a section of the journal
Frontiers in Endocrinology

Received: 13 September 2020

Accepted: 10 May 2021

Published: 21 June 2021

Citation:

Saddozai UAK, Wang F, Akbar MU, Zhang L, An Y, Zhu W, Xie L, Li Y, Ji X and Guo X (2021) Identification of Clinical Relevant Molecular Subtypes of Pheochromocytoma. *Front. Endocrinol.* 12:605797. doi: 10.3389/fendo.2021.605797

Pheochromocytoma (PCC) is a rare neuroendocrine tumor of the adrenal gland with a high rate of mortality if diagnosed at a late stage. Common symptoms of pheochromocytoma include headache, anxiety, palpitation, and diaphoresis. Different treatments are under observation for PCC but there is still no effective treatment option. Recently, the gene expression profiling of various tumors has provided new subtype-specific options for targeted therapies. In this study, using data sets from TCGA and the GSE19422 cohorts, we identified two distinct PCC subtypes with distinct gene expression patterns. Genes enriched in Subtype I PCCs were involved in the dopaminergic synapse, nicotine addiction, and long-term depression pathways, while genes enriched in subtype II PCCs were involved in protein digestion and absorption, vascular smooth muscle contraction, and ECM receptor interaction pathways. We further identified subtype specific genes such as *ALK*, *IGF1R*, *RET*, and *RSPO2* for subtype I and *EGFR*, *ESR1*, and *SMO* for subtype II, the overexpression of which led to cell invasion and tumorigenesis. These genes identified in the present research may serve as potential subtype-specific therapeutic targets to understand the underlying mechanisms of tumorigenesis. Our findings may further guide towards the development of targeted therapies and potential molecular biomarkers against PCC.

Keywords: pheochromocytoma, prognosis, molecular subtype, mutation, subtype specific treatment

INTRODUCTION

Pheochromocytoma (PCC) is a type of tumor with catecholamine secretion derived from the chromaffin cells of the sympathoadrenal system (1–4). The majority of PCC arises within the adrenal medulla where the chromaffin cells are located in abundance (4). However, a small number of them are found in extra-adrenal sites (such as neck, mediastinum, abdomen, pelvis, and organ of Zuckerkandl) and are termed Paragangliomas (4, 5). The annual incidence rate of PCC is 1–4/10⁶ of the population while the recurrence rate is 4.6–6.5% (5, 6). In females the tendency for PCC progression (55.2%) is slightly higher than in males (44.8%). PCC occurs most frequently in aged individuals around 40–50 years old (7, 8). The most common signs and symptoms include

hypertension, palpitation, headache, pallor, and sweating because of excessive catecholamine secretion. While the less common signs and symptoms are fever, nausea, weight loss, constipation, flushing, and fatigue (9). The metastases rate is about 10-15% in pheochromocytoma patients (10), but only a few patients are suitable candidates for surgical resection of the tumor in this case (11). Although the survival advantage of surgical debulking is not proven, it can significantly reduce organ damage, catecholamine secretion, and the required dosage of alpha and beta blockades. The decreased tumor burden as a result of surgical resection can also assist in successive radiotherapy or chemotherapy (9). Different methodologies are under process for guiding the treatment of cancers including the recently developed gene expression profiling methods used against gastric cancer, breast cancer, and uterine carcinosarcomas (12–18). The successful categorization of cancers into different molecular subtypes help cancer patients to receive better diagnosis and get more effective therapy for cancers (19). Therefore, the characterization of PCC into molecular subgroups will provide a better understanding of the underlying mechanisms of disease and thus will lead to a better and more precise treatment for PCC in the future. In the current study, by using gene expression profiling method, we successfully defined two distinct solid subtypes of PCC with enriched different potential genes and pathways. Our findings will accelerate the understanding of PCC pathogenesis and provide opportunities for effective subtype-specific therapies.

MATERIALS AND METHODS

Determination and Validation of Molecular Subtypes of PCC

TCGA and Gene Expression Omnibus (GEO) databases were checked to obtain the Expression profiling data of clinical PCC cases. Two datasets, including one dataset from TCGA (154 cases) and the other dataset of GSE19422 from GEO (63 samples), were collected and used to define the molecular subtypes of PCC. After filtering individual expression datasets with standard deviation, the transformation of the data was done by gene-based centering. To identify the molecular subtypes, both datasets were separately run on Consensus clustering (R package Consensus clustering Plus) (20) with a set of parameters, including 80% sample resampling, distance (1-Pearson correlation), 80% gene resampling, maximum evaluated k of 12, agglomerative hierarchical clustering algorithm, and 1000 iterations. Finally, the R package cluster (silhouette width) was used to determine the accuracy of subtype assignment from Consensus Clustering Plus (21).

Reproducibility Measurement of PCC Molecular Subtypes

Subclass Mapping (SubMap) implemented in Gene Pattern was used to determine the reproducibility of PCC molecular subtypes between TCGA and GSE19422 cohorts. SubMap analysis was

achieved with parameters of (num. marker. genes=300, num.perm=1000 and num.per.fisher=1000) (22).

Gene Ontology and Gene Set Enrichment (GSEA) Analysis

Subtype-specific genes were identified by SAM (23) and SAMseq (24) with a false discovery rate of less than 0.05. GO and KEGG pathway analyses were performed using DAVID Bioinformatics resources online version 6.7 (<https://david.ncicrf.gov/>). GSEA (25) analysis was carried out to examine the expression of gene patterns and pathways of each subtype. Furthermore, therapeutic genes of each PCC subtype were explored through the TARGET V2 database (<http://www.broadinstitute.org/cancer/cga/target>).

Statistical Analysis

For the evaluation of statistical significance between the clinical factors and subtypes of PCC, Fisher exact tests and chi-square test were applied and a *p-value* value less than 0.05 was considered to be significant. The survival curve was also calculated by log-rank test and Kaplan-Meier plot through Graphpad Prism 7 software.

RESULTS

Consensus Clustering Identifies Two Different PCC Molecular Subtypes

PCC subtypes were identified using the gene expression profiling data of PCC with consensus clustering. Initially, the TCGA cohort (154 PCC samples) was revealed to have two optimal molecular subtypes based on the curve of empirical cumulative distribution (CDF) (Figures 1A–C). Subtype assignment was confirmed through silhouette width analysis. Out of 154 samples, 114 samples were found to have positive silhouette value, which was used for further analysis. In 114 samples, subtype I gathered 69 samples while 45 samples belonged to subtype II (Figure 1D).

Further Validation of PCC Molecular Subtypes in an Independent Dataset

For further confirmation of PCC subtypes identified in the TCGA cohort, a GEO dataset (GSE19422) with 63 PCC cases was analyzed. Consensus clustering identified two distinct molecular subtypes in the GSE19422 dataset as well (Figure 2). As in the TCGA dataset, positive silhouette cases were obtained and used for further analysis in GSE19422.

Reproduced Molecular Subtypes in Independent PCC Cohorts by SubMap Analysis

The correlation of two distinct molecular subtypes of PCC in independent datasets was measured through SubMap analysis. The result of SubMap analysis revealed a significant correlation between A1-A2 subtypes of TCGA with the B1-B2 of GSE19422 (Figure 3), indicating the common and reproducible PCC molecular subtype across different cohorts.

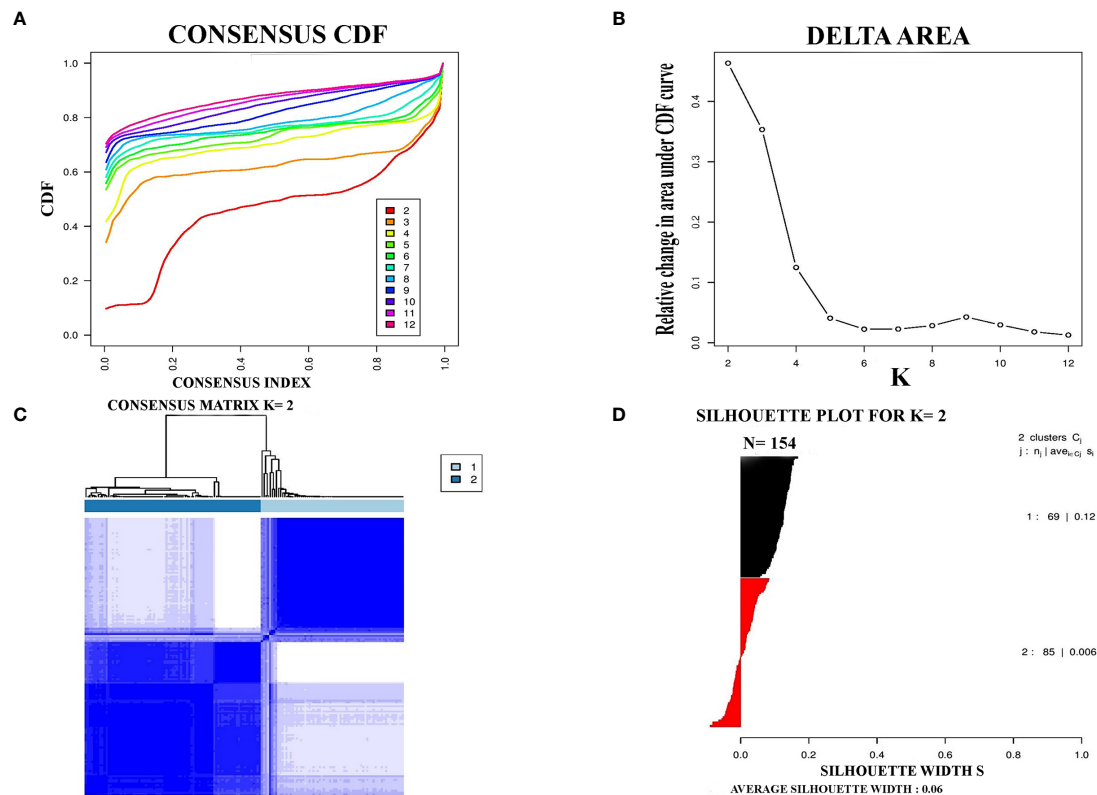


FIGURE 1 | Represented two molecular subtypes in TCGA cohort of PCC. **(A)** The optimal number of PCC molecular subtypes was determined through Empirical cumulative distribution plot. **(B)** The increasement of area under the CDF curve with the increased expected number of molecular subtypes. **(C)** Consensus clustering matrix for the two distinct subtypes of PCC. **(D)** Silhouette plot based on Consensus clustering assignment.

Clinical Characteristics of PCC Molecular Subtypes

To understand the clinical characteristics of PCC molecular subtypes, the relationship between molecular subtypes and clinical factors was checked in the TCGA cohort. Notably, the laterality rate of subtype II PCC was found to be higher on the left side of patients (24/45) than subtype I PCC (34/69) (**Supplementary Table S1**, $P = 0.2057$). Furthermore, it is noteworthy to highlight that the detection rate of the disease during the initial screening was found to be higher in subtype I PCC patients (37/69) than in subtype II PCC patients (22/45) ($P = 0.5883$). The mean age at diagnosis was found to be higher in Subtype I PCCs (48.4 years) as compared to Subtype II PCCs (41.8 years) ($P=0.02^*$). The median overall survival (OS) time in patients of Subtype I PCCs was recorded as 736 days, which was slightly shorter than the patients with Subtype II PCCs who had an OS time period of 944 days. However, survival curve analysis (Kaplan-Meier plots) showed no significant difference in survival between the two PCC subtypes. In addition to the survival rate, there was no significant difference found based on the patient's sex among the two subtypes ($P = .5248$) as well as their success in primary therapy outcome ($P = 0.6136$) (**Supplementary Table S1**).

Functional Analysis of PCC Subtype-Specific Genes

SAMseq analysis was performed in the TCGA dataset to analyze differentially expressed genes between two PCC molecular subtypes. A total of 6813 genes were found to have differential expression between the subtypes, among which 2840 genes were overexpressed in subtype I while 3973 genes had higher expression in subtype II (**Supplementary Table S2**). KEGG and GO analyses were performed on the Top 1000 overexpressed genes from each PCC subtype to obtain further biological information about the subtypes. GO analysis revealed 187 biological processes enriched in subtype I, including Nervous system-associated genes (4.5%) (**Supplementary Table S3**). KEGG analysis of subtype I overexpressing genes revealed 23 different pathways that belonged to Neuroactive ligands receptor interaction, cAMP signaling pathways, and Calcium signaling pathways, (**Figure 4A**). Whereas 259 biological processes and 26 KEGG pathways were significantly enriched in subtype II PCCs. These pathways included Vascular Smooth Muscle Contraction, ECM Receptor Interaction, and Hedgehog Signaling Pathway. (**Figure 4B**). In addition, GSEA analysis in the TCGA cohort demonstrated gene sets enriched with significant biological pathways were found to be abundant only in subtype II. These

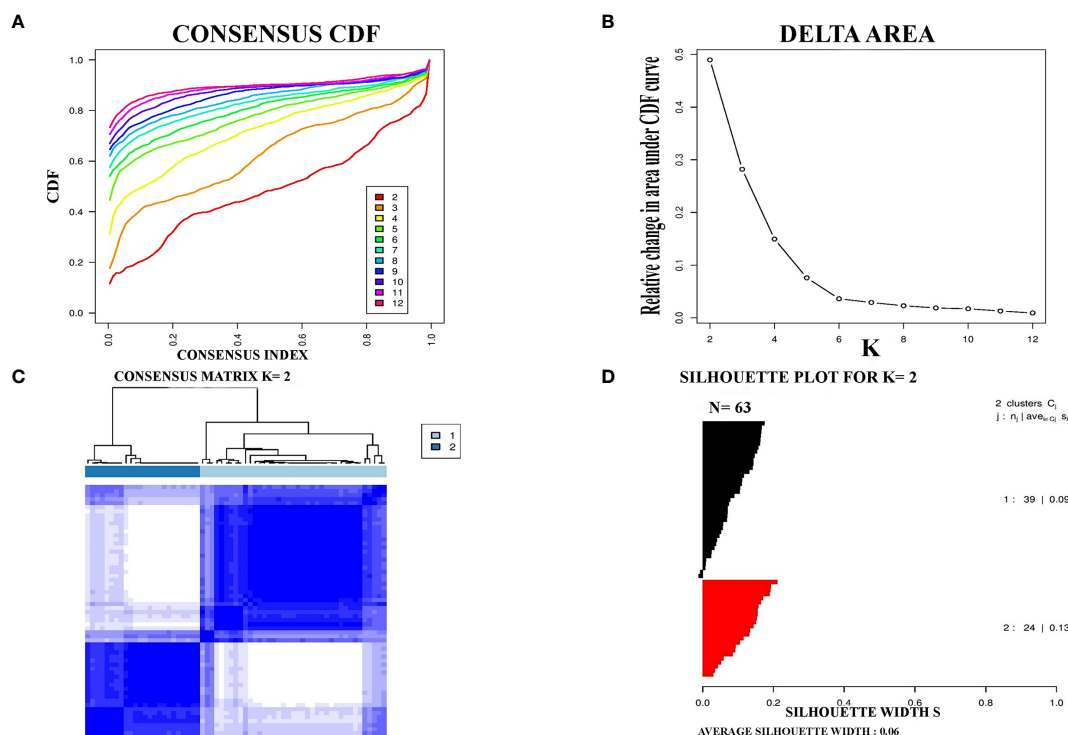


FIGURE 2 | Identification of two molecular subtypes in GSE19422 cohort of PCC. **(A)** The optimal number of PCC molecular subtypes was defined through Empirical cumulative plot. **(B)** Comparative increase in the area under the CDF curve with the increasing expected number of molecular subtypes. **(C)** Consensus clustering matrix of the two PCC subtypes. **(D)** Silhouette plot of PCC samples based on Consensus clustering assignment.

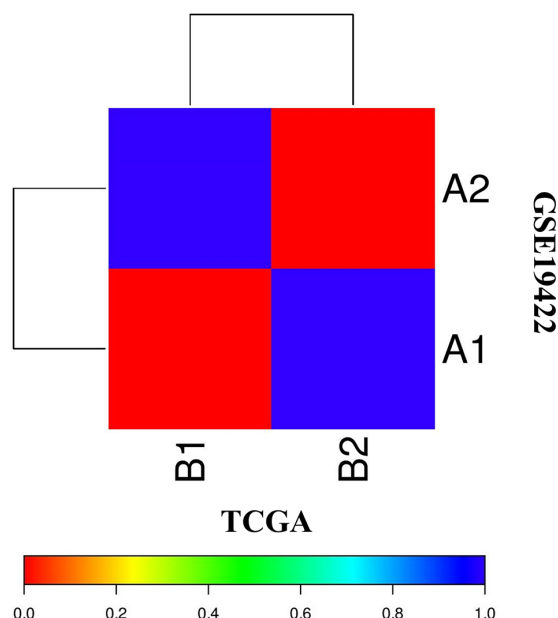


FIGURE 3 | SubMap association between the two molecular subtypes from the two independent datasets of TCGA and GSE19422 presents a significant correlation. FDR-corrected p-value denoted the correlation significance.

pathways for subtype II include Hedgehog signaling pathways, Vascular smooth interaction, ECM interaction, and TGF Beta signaling pathway (**Figure 5**).

Clinical Implication of PCC Subtyping

The purpose of molecular subtyping of PCC was to search and identify therapeutic routes and to employ those specified routes further in clinical studies and discourses. Overexpressed genes in each PCC subtype were obtained and compared with the target database (that contains target genes and functional inhibitors) for the determination of therapeutic molecules (26). Further studies may be carried out on the targeted genes to translate them into potential clinical stages (27–29).

We have found seven subtype-specific target genes which would give relative benefits to the PCC patients from distinct subtypes. Given in **Table 1**, subtype I PCCs benefit from four target genes, namely *ALK*, *IGF1R*, *RET*, and *RSPO2*, while subtype II contains three target genes: *EGFR*, *ESR1*, and *SMO*.

DISCUSSION

PCC is a type of catecholamine-secreting neuroendocrine tumors, most of which arise from chromaffin cells of the adrenal medulla. About 15–20% of these PCC tumors belong to an extra-adrenal origin and are termed as paraganglioma (PGL)

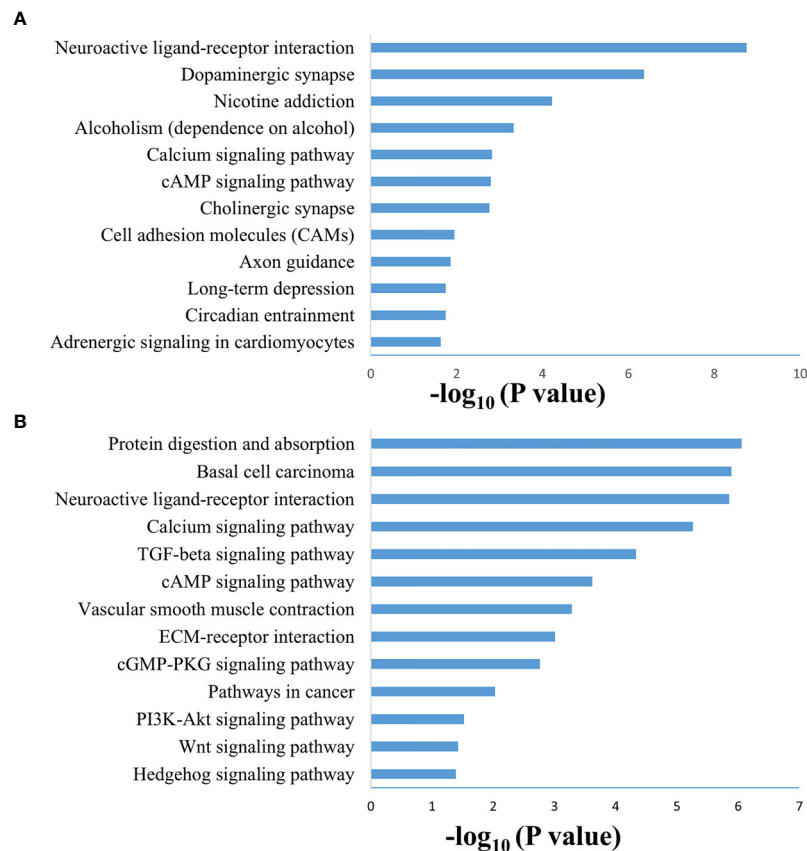


FIGURE 4 | Enriched biological pathways found through the analysis of overexpression of genes individual PCC subtypes. **(A)** KEGG pathway through the gene overexpression profile analysis in subtype I. **(B)** KEGG pathway through the gene overexpression profile analysis subtype II.

(30). Due to excessive secretion of catecholamines, both forms of tumors (adrenal and extra-adrenal) have similar clinical symptoms and are only distinguished based on potential differences in prognosis (31). Most of the PCCs are benign, although metastasis may develop in patients with specific backgrounds (32, 33). At present, different studies have debated PCC treatment. Patients at the same stage may still respond to treatment differently due to the molecular heterogeneity even if they were administered the identical treatment (34, 35). Molecular subtyping approaches based on gene expression profiling of tumors has greatly guided the medical community in introducing subtype specific diagnostic techniques and targeted therapies (20). The subtype-based targeted therapies in clinical trials of breast cancer is a good example of molecular prognostic and treatment of malignancies. The positive response of HER2-positive breast cancer patients towards subtype specific therapies is an example for the future directions of the current study (36). Using the gene expression profiling method, it is possible to get a better understanding of the heterogeneity of PCCs, and also provides the opportunity to develop subtype-specific therapeutic strategies.

In this study, we identified two molecular subtypes of PCC (also confirmed previously by Fishbian et al.) (37). The Gene set

enrichment and Gene ontology analyses of the identified subtypes revealed the overexpression of certain genes and pathways specific to each subtype (**Supplementary Table S4**). The subtype I PCCs include the overexpressed genes involved in pathways of Dopaminergic synapse, Nicotine addiction, and Long-term depression. The *SALL4* involved in the proliferation of cancer was also found to be overexpressed within subtype I (**Figure 5**). *SALL4* gene is involved in the maintenance of pluripotency and self-renewal of embryonic stem cells (38, 39). Expression of *SALL4* has been reported in various cancers such as precursor B-cell lymphoblastic lymphoma (40, 41), acute myeloid leukemia (42), myelodysplastic syndromes (43), breast cancer (44), chronic myeloid leukemia (45), lung cancer (46, 47), endometrial cancer (48), liver cancer (49, 50) gastrointestinal carcinoma (51–53), glioma (54), germ cell tumor, and yolk sac tumor (55, 56). In subtype II PCCs, enriched genes and pathways include the overexpression of smooth muscle-specific markers and the genes involved in the lymph node. Overexpressed pathways in subtype II include protein digestion and absorption pathway, Vascular smooth muscle contraction pathway, and ECM-receptor interaction pathway. The overexpressed gene in this subtype include *Twist1* (**Figure 5**). The consistent significance of *Twist1* gene in cancer biology

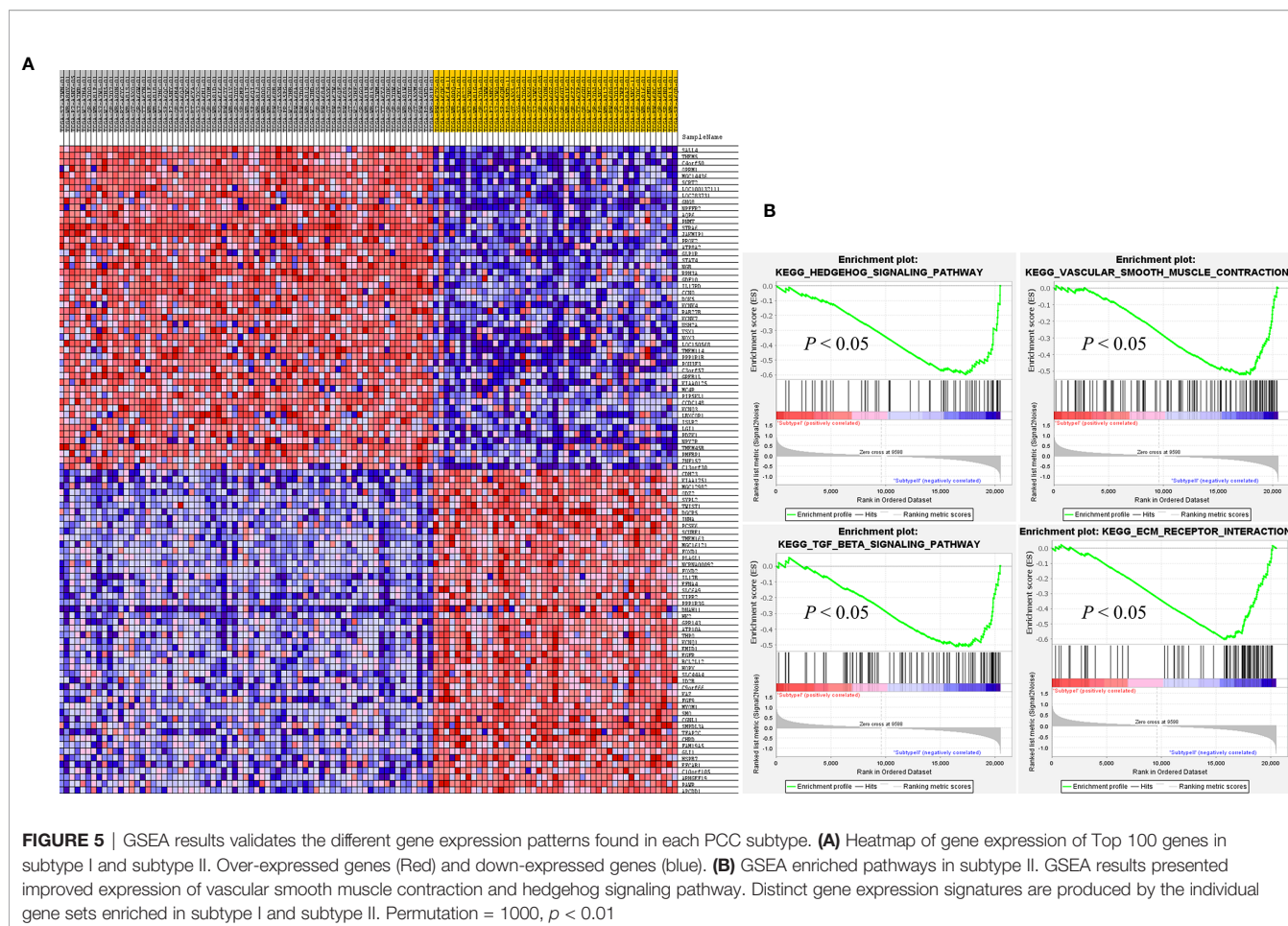


TABLE 1 | Target genes enriched in each molecular subtype.

Gene overexpressed	Examples of Potential Therapeutic Agents	
Subtype I	<i>ALK</i>	Crizotinib, ALK inhibitors
	<i>IGF1R</i>	IGF1R Inhibitor
	<i>RET</i>	Sorafenib, vandetinib, RET Inhibitors
	<i>RSPO2</i>	WNT inhibitors
Subtype II	<i>EGFR</i>	Erlotinib, Gefitinib, EGFR Inhibitors
	<i>ESR1</i>	Hormonal therapy
	<i>SMO</i>	Vismodegib, hedgehog inhibitors

involves its overexpression which is linked to metastasis, therapeutic failure, recurrence, and inferior prognosis (57). The role of *Twist1* has already been shown to serve as a useful prognostic factor predicting poor outcome in breast cancer (58), nasopharyngeal cancer (59), ovarian cancer (60) and cervical cancer (61). Expression of these distinct genes and pathways in each subtype will provide a better way to understand PCC at the subtype level and to develop subtype-specific treatment.

After analyzing the overexpressed genes and pathways in each subtype, we further checked these overexpressed genes in the TARGET database and identified seven known target genes for each subtype. Subtype I PCCs have four overexpressed genes,

namely *ALK*, *IGF1R*, *RET*, and *RSPO2*, while subtype II includes *EGFR*, *ESR1*, and *SMO*. In most types of cancers, overexpression of the *IGF1R* gene is found to be a typical hallmark (62). In addition, *IGF1R* has an important role in invasion, metastasis, and angiogenesis (63–65). Its overexpression has also been found in pheochromocytoma and paraganglioma with a high risk of metastasis (66).

Blocking the *IGF1R* via antisense therapy (67), anti IGF1R antibodies (68–70), dominant negative IGF1R (71), and small-molecule inhibitors has proven efficacious in the treatment of various cancers. A preclinical study found Cixutumumab effective against prostate cancer as it caused significant delaying of the androgen resistance by blocking IGF1R in disease (72, 73). Recent studies have suggested linsitinib (OSI-906) as a promising drug for PCC patients, when used alone or combined with mTOR inhibitors (74). Therefore, IGF1R inhibitors may play a significant role in subtype I of PCC.

The overexpression of *EGFR* has been observed to play a key role in tumorigenesis (75). Targeting *EGFR* using different approaches has proven effective in the treatment of various solid tumors such as head and neck, colorectal, pancreatic, and non-small lung cancer (NSCLC) (76–80). Gefitinib, the first FDA-approved anti-EGFR drug (81, 82), has been shown to prevent autophosphorylation of *EGFR* in many tumor cell lines

and xenografts (83). It inhibits the cell growth in HER2-overexpressing breast cancer cells (84, 85). Similarly, Erlotinib is another FDA-approved drug that acts as an inhibitor of *EGFR* (86, 87) and has been proven effective in the treatment of NSCLC and metastatic pancreatic cancer when used in combination with gemcitabine (76, 80). Gene expression analysis revealed the role of the *EGFR* gene in subtype II patients of the PCC cohort. Based on the *EGFR*'s role in cancer and the availability of anti-*EGFR* inhibitors, patients of subtype II may benefit from anti-*EGFR* inhibitors.

In conclusion, we have characterized two distinct molecular subtypes of PCC in two independent cohorts. Differentially expressed genes found in the two subtypes provide an insight into the underlying mechanisms of tumorigenesis and progression in a subtype-specific manner. Targeted therapies against molecular targets identified in the present study may help better understand the disease prognosis and aid in developing specified therapies against individual subtypes of PCC.

DATA AVAILABILITY STATEMENT

The datasets presented in this study can be found in online repositories. The names of the repository/repositories and accession number(s) can be found in the article/**Supplementary Material**.

REFERENCES

- Portela-Gomes GM, Stridsberg M, Grimelius L, Falkmer UG, Falkmer S. Expression of Chromogranins A, B, and C (Secretogranin II) in Human Adrenal Medulla and in Benign and Malignant Pheochromocytomas. An Immunohistochemical Study With Region-Specific Antibodies. *APMIS* (2004) 112:663–73. doi: 10.1111/j.1600-0463.2004.t01-1-apm1121005.x
- Allibhai Z, Rodrigues G, Brecevic E, Neumann HP, Winquist E. Malignant Pheochromocytoma Associated With Germline Mutation of the *SDHB* Gene. *J Urol* (2004) 172:1409–10. doi: 10.1097/01.ju.0000137892.89141.6a
- De Toma G, Letizia C, Cavallaro G, Cavallaro G, Giacchino V, Mosiello G, et al. Malignant Pheochromocytoma. Personal Experience and Review of the Literature. *Ann Ital Chir* (2002) 73:413–8.
- Thompson LD. Pheochromocytoma of the Adrenal Gland Scaled Score (PASS) to Separate Benign From Malignant Neoplasms. A Clinicopathologic and Immunophenotypic Study of 100 Cases. *Am J Surg Pathol* (2002) 26:551–66. doi: 10.1097/00000478-200205000-00002
- Adler JT, Meyer-Rochow GY, Chen H, Benn DE, Robinson BG, Sippel RS, et al. Pheochromocytoma: Current Approaches and Future Directions. *Oncologist* (2008) 13:779–93. doi: 10.1634/theoncologist.2008-0043
- Tang SH, Chen A, Lee CT, Yu DS, Chang SY, Sun GH. Remote Recurrence of Malignant Pheochromocytoma 14 Years After Primary Operation. *J Urol* (2003) 169:269. doi: 10.1097/00005392-200301000-00066
- Lenders JW, Eisenhofer G, Mannelli M, Pacak K. Pheochromocytoma. *Lancet* (2005) 366:665–75. doi: 10.1016/S0140-6736(05)67139-5
- Adas M, Koc B, Adas G, Yalcin O, Celik S, Kemik O. Pitfalls in the Diagnosis of Pheochromocytoma: A Case Series and Review of the Literature. *J Epidemiol Res* (2016) 2:49–55. doi: 10.5430/jer.v2n2p49
- Chen H, Sippel RS, O'Dorisio MS, Vinik AI, Lloyd RV, Pacak K. North American Neuroendocrine Tumor Society (Nanets). The North American Neuroendocrine Tumor Society Consensus Guideline for the Diagnosis and Management of Neuroendocrine Tumors: Pheochromocytoma, Paraganglioma, and Medullary Thyroid Cancer. *Pancreas* (2010) 39:775–83. doi: 10.1097/MPA.0b013e3181ebb4f0
- Pacak K, Wimalawansa SJ. Pheochromocytoma and Paraganglioma. *Endocrinol Pract* (2015) 21:406–12. doi: 10.4158/EP14481.RA
- Pacak K, Linehan WM, Eisenhofer G, Walther MM, Goldstein DS. Recent Advances in Genetics, Diagnosis, Localization, and Treatment of Pheochromocytoma. *Ann Intern Med* (2001a) 134:315–29. doi: 10.7326/0003-4819-134-4-200102200-00016
- Bertucci F, Finetti P, Rougemont J, Charafe-Jauffret E, Cervera N, Tarpin C, et al. Gene Expression Profiling Identifies Molecular Subtypes of Inflammatory Breast Cancer. *Cancer Res* (2005) 65(6):2170–8. doi: 10.1158/0008-5472.CAN-04-4115
- Sorlie T, Perou CM, Tibshirani R, Aas T, Geisler S, Johnsen H, et al. Gene Expression Patterns of Breast Carcinomas Distinguish Tumor Subclasses With Clinical Implications. *Proc Natl Acad Sci U.S.A.* (2001) 98(19):10869–74. doi: 10.1073/pnas.191367098
- Lei Z, Tan IB, Das K, Deng N, Zouridis H, Pattison S, et al. Identification of Molecular Subtypes of Gastric Cancer With Different Responses to PI3-Kinase Inhibitors and 5-Fluorouracil. *Gastroenterology* (2013) 145(3):554–65. doi: 10.1053/j.gastro.2013.05.010
- Cristescu R, Lee J, Nebozhyn M, Kim KM, Ting JC, Wong SS, et al. Molecular Analysis of Gastric Cancer Identifies Subtypes Associated With Distinct Clinical Outcomes. *Nat Med* (2015) 21(5):449–56. doi: 10.1038/nm.3850
- Saddozai UAK, Wang F, Cheng Y, Lu Z, Akbar MU, Zhu W, et al. Gene Expression Profile Identifies Distinct Molecular Subtypes and Potential Therapeutic Genes in Merkel Cell Carcinoma. *Trans Oncol* (2020) 13(11):100816. doi: 10.1016/j.tranon.2020.100816
- Wang F, Zhongyi Y, Jiajia L, Junfang X, Yifang D, Xiaoxiao S. Gene Expression Profiling Reveals Distinct Molecular Subtypes of Oesophageal Squamous Cell Carcinoma in Asian Population. *Neoplasia* (2019) 21:571–81. doi: 10.1016/j.neo.2019.03.013
- Flynn A, Dwight T, Harris J, Benn D, Zhou L, Hogg A, et al. Pheo-Type: A Diagnostic Gene-expression Assay for the Classification of Pheochromocytoma and Paraganglioma. *J Clin Endocrinol Metab* (2016) 110(3):1034–43. doi: 10.1210/nc.2015-3889
- Goldhirsch A, Wood WC, Coates AS, Gelber RD, Thürlimann B, Senn HJ. Strategies for Subtypes—Dealing With the Diversity of Breast Cancer:

AUTHOR CONTRIBUTIONS

Term Definition Conceptualization: XG. Methodology: XG. Software: XG. Validation: US, XG. Formal analysis: US, XG, FW, ZL. Investigation: US, XG. Resources: XG, XJ, YL. Data Curation: US, XG. Writing - Original Draft: US, MA, WZ, XG. Writing - Review and Editing: US, MA, WZ, XG, XJ, LX, YA. Visualization: US. Supervision: XG, XJ, YL. Project administration: XG, XJ, YL. Funding acquisition: XG. All authors contributed to the article and approved the submitted version.

FUNDING

This work was supported by the program for Innovative Talents of Science and Technology in Henan Province (No. 18HASTIT048). The funding bodies were not involved in the study design, data collection, analysis and interpretation of data, or writing of this manuscript.

SUPPLEMENTARY MATERIAL

The Supplementary Material for this article can be found online at: <https://www.frontiersin.org/articles/10.3389/fendo.2021.605797/full#supplementary-material>

- Highlights of the St. Gallen International Expert Consensus on the Primary Therapy of Early Breast Cancer. *Ann Oncol* (2011) 22(8):1736–47. doi: 10.1093/annonc/mdr304
20. Wilkerson MD, Hayes DN. Consensus Cluster Plus; a Class Discovery Tool With Confidence Assessments and Item Tracking. *Bioinformatics* (2010) 26:1572–3. doi: 10.1093/bioinformatics/btq170
 21. Rousseeuw PJ. Silhouettes; a Graphical Aid to the Interpretation and Validation of Cluster Analysis. *J Comput Appl Math* (1987) 20:53–65. doi: 10.1016/0377-0427(87)90125-7
 22. Hoshida Y, Brunet JP, Tamayo P, Golub TR, Mesirov JP. Subclass Mapping: Identifying Common Subtypes in Independent Disease Data Sets. *PloS One* (2007) 2:e1195. doi: 10.1371/journal.pone.0001195
 23. Tusher VG, Tibshirani R, Chu G. Significance Analysis of Microarrays Applied to the Ionizing Radiation Response. *Proc Natl Acad Sci USA* (2001) 98:5116–21. doi: 10.1073/pnas.091062498
 24. Li J, Tibshirani R. Finding Consistent Patterns; a Nonparametric Approach for Identifying Differential Expression in RNA-Seq Data. *Stat Methods Med Res* (2013) 22:519–36. doi: 10.1177/0962280211428386
 25. Subramanian A, Tamayo P, Mootha VK, Mukherjee S, Ebert BL, Gillette MA. Gene Set Enrichment Analysis; a Knowledge-Based Approach for Interpreting Genome-Wide Expression Profiles. *Proc Natl Acad Sci* (2005) 102:15545–50. doi: 10.1073/pnas.0506580102
 26. Van Allen EM, Wagle N, Stojanov P, Perrin DL, Cibulskis K, Marlow S. Whole-Exome Sequencing and Clinical Interpretation of Formalin Fixed, Paraffin-Embedded Tumor Samples to Guide Precision Cancer Medicine. *Nat Med* (2014) 20:682–8. doi: 10.1038/nm.3559
 27. Moroni M, Veronese S, Benvenuti S, Marrapese G, Sartore-Bianchi A, Di-Nicolantonio F. Gene Copy Number for Epidermal Growth Factor Receptor (EGFR) and Clinical Response to Anti-EGFR Treatment in Colorectal Cancer; a Cohort Study. *Lancet Oncol* (2005) 6:279–86. doi: 10.1016/S1470-2045(05)70102-9
 28. Lehmann BD, Bauer JA, Chen X, Sanders ME, Chakravarthy AB, Shyr Y. Identification of Human Triple-Negative Breast Cancer Subtypes and Preclinical Models for Selection of Targeted Therapies. *J Clin Invest* (2011) 121:2750–67. doi: 10.1172/JCI45014
 29. Paez JG, Jänne PA, Lee JC, Tracy S, Greulich H, Gabriel S. EGFR Mutations in Lung Cancer; Correlation With Clinical Response to Gefitinib Therapy. *Science* (2004) 304:1497–500. doi: 10.1126/science.1099314
 30. Lenders JW, Eisenhofer G, Mannelli M, Pacak K. Pheochromocytoma. *Lancet* (2005) 366(9486):665–75. doi: 10.1016/S0140-6736(05)67139-5
 31. Omura M, Saito J, Yamaguchi K, Kakuta Y, Nishikawa T. Prospective Study on the Prevalence of Secondary Hypertension Among Hypertensive Patients Visiting a General Outpatient Clinic in Japan. *Hypertens Res* (2004) 27(3):193–202. doi: 10.1291/hyres.27.193
 32. Ayala-Ramirez M, Feng L, Johnson MM, Ejaz S, Habra MA, Rich T, et al. Clinical Risk Factors for Malignancy and Overall Survival in Patients With Pheochromocytomas and Sympathetic Paragangliomas: Primary Tumor Size and Primary Tumor Location as Prognostic Indicators. *J Clin Endocrinol Metab* (2011) 96:717–25. doi: 10.1210/jc.2010.1946
 33. Eisenhofer G, Lenders JW, Siebert G, Bornstein SR, Friberg P, Milosevic D, et al. Plasma Methoxytyramine: A Novel Biomarker of Metastatic Pheochromocytoma and Paraganglioma in Relation to Established Risk Factors of Tumour Size, Location and SDHB Mutation Status. *Eur J Cancer* (2012) 48:1739–49. doi: 10.1016/j.ejca.2011.07.016
 34. Gerlinger M, Rowan AJ, Horswell S, Math M, Larkin J, Endesfelder D, et al. Intratumor Heterogeneity and Branched Evolution Revealed by Multiregion Sequencing. *N Engl J Med* (2012) 366:883–92. doi: 10.3410/f.14001976.792252863
 35. Navin N, Kendall J, Troge J, Andrews P, Rodgers L, McIndoo J, et al. Tumor Evolution Inferred by Single Cell Sequencing. *Nature* (2011) 472:90–4. doi: 10.1038/nature09807
 36. Piccart-Gebhart MJ, Procter M, Leyland-Jones B. Trastuzumab After Adjuvant Chemotherapy in HER2-Positive Breast Cancer. *N Engl J Med* (2005) 353:1659–72. doi: 10.1056/NEJMoa052306
 37. Fishbein L, Leshchiner I, Walter V, Danilova L, Robertson AG, Johnson AR, et al. Comprehensive Molecular Characterization of Pheochromocytoma and Paraganglioma. *Cancer Cell* (2017) 2:181–93. doi: 10.1016/j.ccell.2017.01.001
 38. Yang L, Chai TC, Fowles Z, Alipio Z, Xu D, Fink LM, et al. Genome-Wide Analysis Reveals Sall4 to be a Major Regulator of Pluripotency in Murine Embryonic Stem Cells. *Proc Natl Acad Sci USA* (2008) 105:19756–61. doi: 10.1073/pnas.0809321105
 39. Zhang WL, Tam GQ, Tong Q, Wu Q, Chan HY, Soh BS, et al. SALL4 Modulates Embryonic Stem Cell Pluripotency and Early Embryonic Development by the Transcriptional Regulation of Pou5f1. *Nat Cell Biol* (2006) 8:1114–23. doi: 10.1038/ncb1481
 40. Ueno J, Lu J, He J, Li A, Zhang X, Ritz J, et al. Aberrant Expression of SALL4 in Acute B Cell Lymphoblastic Leukemia: Mechanism, Function, and Implication for a Potential Novel Therapeutic Target. *Exp Hematol* (2014) 42(308):307–16. doi: 10.1016/j.exphem.2014.01.005
 41. Cui W, Kong NR, Ma Y, Amin HM, Lai R, Chai L. Differential Expression of the Novel Oncogene, SALL4, in Lymphoma, Plasma Cell Myeloma, and Acute Lymphoblastic Leukemia. *Mod Pathol* (2006) 19:1585–92. doi: 10.1038/modpathol.3800694
 42. Ma Y, Cui W, Yang J, Qu J, Di C, Amin HM, et al. SALL4, a Novel Oncogene, Is Constitutively Expressed in Human Acute Myeloid Leukemia (AML) and Induces AML in Transgenic Mice. *Blood* (2006) 108:2726–35. doi: 10.1182/blood-2006-02-001594
 43. Wang F, Guo Y, Chen Q, Yang Z, Ning N, Zhang Y, et al. Stem Cell Factor SALL4, a Potential Prognostic Marker for Myelodysplastic Syndromes. *J Hematol Oncol* (2013) 6:73. doi: 10.1186/1756-8722-6-73
 44. Kobayashi D, Kuribayashi K, Tanaka M, Watanabe N. SALL4 Is Essential for Cancer Cell Proliferation and is Overexpressed at Early Clinical Stages in Breast Cancer. *Int J Oncol* (2011) 38:933–9. doi: 10.3892/ijo.2011.929
 45. Lu J Y, Ma Y, Kong N, Alipio Z, Gao C, Krause DS, et al. Dissecting the Role of SALL4, a Newly Identified Stem Cell Factor, in Chronic Myelogenous Leukemia. *Leukemia* (2011) 25:1211–3. doi: 10.1038/leu.2011.65
 46. Kobayashi D, Kuribayashi K, Tanaka M, Watanabe N. Overexpression of SALL4 in Lung Cancer and Its Importance in Cell Proliferation. *Oncol Rep* (2011) 26:965–70. doi: 10.3892/or.2011.1374
 47. Fujimoto M, Sumiyoshi S, Yoshizawa A, Sonobe M, Kobayashi M, Mori Yoshi K, et al. SALL4 Immunohistochemistry in non-Small-Cell Lung Carcinomas. *Histopathology* (2014) 64:309–11. doi: 10.1111/his.12241
 48. Li A, Jiao Y, Yong KJ, Wang F, Gao C, Yan B, et al. SALL4 Is a New Target in Endometrial Cancer. *Oncogene* (2013) 34(1):63–72. doi: 10.1038/ncr.2013.529
 49. Oikawa T, Kamiya A, Zeniya M, Chikada H, Hyuck AD, Yamazaki Y, et al. Sal-Like Protein 4 (SALL4), a Stem Cell Biomarker in Liver Cancers. *Hepatology* (2013) 57:1469–83. doi: 10.1002/hep.26159
 50. Zeng SS, Yamashita T, Kondo M, Nio K, Hayashi T, Hara Y, et al. The Transcription Factor SALL4 Regulates Stemness of EpCAM-Positive Hepatocellular Carcinoma. *J Hepatol* (2014) 60:127–34. doi: 10.1016/j.jhep.2013.08.024
 51. Zhang L, Xu Z, Xu X, Zhang B, Wu H, Wang M, et al. SALL4, a Novel Marker for Human Gastric Carcinogenesis and Metastasis. *Oncogene* (2013) 33(48):5491–500. doi: 10.1038/ncr.2013.495
 52. Rieger LS, Schaapveld M, Janus CPM, Krol ADG, van der Maazen RWM, Roesink J, et al. Overall and Disease-Specific Survival of Hodgkin Lymphoma Survivors Who Subsequently Developed Gastrointestinal Cancer. *Cancer Med* (2018) 8(1):190–9. doi: 10.1002/cam4.1922
 53. Forghanifard MM, Moghbeli M, Raeisossadati R, Tavassoli A, Mallak AJ, Boroumand-Noughabi S, et al. Role of SALL4 in the Progression and Metastasis of Colorectal Cancer. *J Biomed Sci* (2013) 20:6. doi: 10.1186/1423-0127-20-6
 54. Zhang L, Yan Y, Jiang Y, Cui Y, Zou Y, Qian J, et al. The Expression of SALL4 in Patients With Gliomas: High Level of SALL4 Expression Is Correlated With Poor Outcome. *J Neurooncol* (2014) 121(2):261–8. doi: 10.1007/s11060-014-1646-4
 55. Miettinen M, Wang Z, McCue M, Sarlomo-Rikala M, Rys J, Biernat W, et al. SALL4 Expression in Germ Cell and Non-Germ Cell Tumors: A Systematic Immunohistochemical Study of 3215 Cases. *Am J Surg Pathol* (2014) 38:410–20. doi: 10.1097/PAS.0000000000000116
 56. Wang F, Liu A, Peng Y, Rakheja D, Wei L, Xue D, et al. Diagnostic Utility of SALL4 in Extragonadal Yolk Sac Tumors: An Immunohistochemical Study of 59 Cases With Comparison to Placental-Like Alkaline Phosphatase, Alpha-Fetoprotein, and Glypican-3. *Am J Surg Pathol* (2009) 33:1529–39. doi: 10.1097/PAS.0b013e3181ad25d5
 57. Ansieau S, Morel AP, Hinkal G, Bastid J, Puisieux A. Twisting an Embryonic Transcription Factor Into an Oncoprotein. *Oncogene* (2010) 29:3173–84. doi: 10.1038/ncr.2010.92

58. Martin TA, Goyal A, Watkins G, Jiang WG. Expression of the Transcription Factors Snail, Slug, and Twist and Their Clinical Significance in Human Breast Cancer. *Ann Surg Oncol* (2005) 12:488–96. doi: 10.1245/ASO.2005.04.010
59. Song LB, Liao WT, Mai HQ, Zhang HZ, Zhang L, Li MZ, et al. The Clinical Significance of Twist Expression in Nasopharyngeal Carcinoma. *Cancer Lett* (2006) 242:258–65. doi: 10.1016/j.canlet.2005.11.013
60. Kajiyama H, Hosono S, Terauchi M, Shibata K, Ino K, Yamamoto E, et al. Twist Expression Predicts Poor Clinical Outcome of Patients With Clear Cell Carcinoma of the Ovary. *Oncology* (2006) 71:394–401. doi: 10.1159/000107108
61. Shibata K, Kajiyama H, Ino K, Terauchi M, Yamamoto E, Nawa A, et al. Twist Expression in Patients With Cervical Cancer Is Associated With Poor Disease Outcome. *Ann Oncol* (2008) 19:81–5. doi: 10.1093/annonc/mdm344
62. Werner H. Tumor Suppressors Govern Insulin-Like Growth Factor Signaling Pathways: Implications in Metabolism and Cancer. *Oncogene* (2012) 31:2703–14. doi: 10.1038/onc.2011.447
63. Baserga R. The IGF-I Receptor in Cancer Research. *Exp Cell Res* (1999) 253:1–6. doi: 10.1006/excr.1999.4667
64. Raju U, Molkentine D, Valdecanas DR, Deorukhkar A, Mason KA, Buchholz TA, et al. Inhibition of EGFR or IGF-1R Signaling Enhances Radiation Response in Head and Neck Cancer Models But Concurrent Inhibition has No Added Benefit. *Cancer Med* (2014) 4:65–74. doi: 10.1002/cam4.345
65. Samani AA, Yakar S, LeRoith D, Brodt P. The Role of the IGF System in Cancer Growth and Metastasis: Overview and Recent Insights. *Endocrine Rev* (2007) 28:20–47. doi: 10.1210/er.2006-0001
66. Fernandez MC, Martin A, Venara M, Calcagno MdeL, Sansó G, Quintana S, et al. Overexpression of the Insulin-Like Growth Factor 1 Receptor (IGF-1R) Is Associated With Malignancy in Familial Pheochromocytomas and Paragangliomas. *Clin Endocrinol* (2013) 79:623–30. doi: 10.1111/cen.12205
67. Resnicoff M, Tjuvajev J, Rotman HL, Abraham D, Curtis M, Aiken R, et al. Regression of C6 Rat Brain Tumors by Cells Expressing an Antisense Insulinlike Growth Factor I Receptor RNA. *J Exp Ther Oncol* (1996) 1:385–9.
68. Cohen BD, Baker DA, Soderstrom C, Tkalecic G, Rossie AM, Miller P, et al. Combination Therapy Enhances the Inhibition of Tumor Growth With the Fully Human Anti-Type 1 Insulin-Like Growth Factor Receptor Monoclonal Antibody CP-751,871. *Clin Cancer Res* (2005) 11:2063–73. doi: 10.1158/1078-0432.CCR-04-1070
69. Beadling C, Patterson J, Justusson E, Nelson D, Pantaleo MA, Hornick JL, et al. Gene Expression of the IGF Pathway Family Distinguishes Subsets of Gastrointestinal Stromal Tumors Wild Type for KIT and PDGFRA. *Cancer Med* (2013) 2:21–31. doi: 10.1002/cam4.57
70. Wang Y, Hailey J, Williams D, Wang Y, Lipari P, Malkowski M, et al. Inhibition of Insulin-Like Growth Factor-I Receptor (IGF-IR) Signaling and Tumor Cell Growth by a Fully Human Neutralizing anti-IGF-IR Antibody. *Mol Cancer Ther* (2005) 4:1214–21. doi: 10.1158/1535-7163.MCT-05-0048
71. Sachdev D, Hartell JS, Lee AV, Zhang X, Yee D. A Dominant Negative Type I Insulin-Like Growth Factor Receptor Inhibits Metastasis of Human Cancer Cells. *J Biol Chem* (2004) 279:5017–24. doi: 10.1074/jbc.M305403200
72. de Bono JS, Attard G, Adjei A, Pollak MN, Fong PC, Haluska P, et al. Potential Applications for Circulating Tumor Cells Expressing the Insulin-Like Growth Factor-I Receptor. *Clin Cancer Res* (2007) 13:3611–6. doi: 10.1158/1078-0432.CCR-07-0268
73. Plymate SR, Haugk K, Coleman I, Woodke L, Vessella R, Nelson P, et al. An Antibody Targeting the Type I Insulin-Like Growth Factor Receptor Enhances the Castration-Induced Response in Androgen-Dependent Prostate Cancer. *Clin Cancer Res* (2007) 13:6429–39. doi: 10.1158/1078-0432.CCR-07-0648
74. De Martino MC, Richard A, Feelders Dogan F, Van-koetsveld P, Krijger RD, Janssen J, et al. Expression of IGF/mTOR Pathway Components in Human Pheochromocytomas and In Vitro Inhibition of PC12 Rat Pheochromocytoma Cell Growth by mTOR Inhibitors Alone and in Combination With the Dual IGF1-R/INS-R Antagonist OSI-906. *Endocrine Abstracts* (2014) 35:P62. doi: 10.1530/endoabs.35.P62
75. Wells A. EGF Receptor. *Int J Biochem Cell Biol* (1999) 31:637–43. doi: 10.1016/S1357-2725(99)00015-1
76. Bareschino MA, Schettino C, Troiani T, Martinelli E, Morgillo F, Ciardiello F. Erlotinib in Cancer Treatment. *Ann Oncol* (2007) 18:35–41. doi: 10.1093/annonc/mdm222
77. Giaccone G, Gonzalez-Larriba JL, Van Oosterom AT, Alfonso R, Smit EF, Martens M, et al. Combination Therapy With Gefitinib, an Epidermal Growth Factor Receptor Tyrosine Kinase Inhibitor, Gemcitabine and Cisplatin in Patients With Advanced Solid Tumors. *Ann Oncol* (2004) 15:831–8. doi: 10.1093/annonc/mdh188
78. Petrelli F, Borgonovo K, Cabiddu M, Ghilardi M, Barni S. Cetuximab and Panitumumab in KRAS Wild-Type Colorectal Cancer: A Meta-Analysis. *Int J Colorectal Dis* (2011) 26:823–33. doi: 10.1007/s00384-011-1149-0
79. Petrelli F, Barni S. Anti-EGFR—targeting Agents in Recurrent or Metastatic Head and Neck Carcinoma: A Meta-Analysis. *Head Neck* (2011) 34(11):1657–64. doi: 10.1002/hed.21858
80. Rocha-Lima CM, Soares HP, Raez LE, Singal R. EGFR Targeting of Solid Tumors. *Cancer. Contr* (2007) 14:295–304. doi: 10.1177/107327480701400313
81. Fukuoka M, Yano S, Giaccone G, Tamura T, Nakagawa K, Douillard JY, et al. Multi-Institutional Randomized Phase II Trial of Gefitinib for Previously Treated Patients With Advanced Non-Small-Cell Lung Cancer (the IDEAL 1 Trial). *J Clin Oncol* (2003) 21:2237–46. doi: 10.1200/JCO.2003.10.038
82. Kris MG, Natale RB, Herbst RS, Lynch TJ Jr, Prager D, Belani CP, et al. Efficacy of Gefitinib, an Inhibitor of the Epidermal Growth Factor Receptor Tyrosine Kinase, in Symptomatic Patients With Non-Small Cell Lung Cancer: A Randomized Trial. *JAMA* (2003) 290:2149–58. doi: 10.1001/jama.290.16.2149
83. Wakeling AE, Barker AJ, Davies DH, Brown DS, Green LR, Cartledge SA, et al. Specific Inhibition of Epidermal Growth Factor Receptor Tyrosine Kinase by 4-Anilinoquinazolines. *Breast Cancer Res Treat* (1996) 38:67–73. doi: 10.1007/BF01803785
84. Moulder SL, Yakes FM, Muthuswamy SK, Bianco R, Simpson JF, Arteaga CL. Epidermal Growth Factor Receptor (HER1) Tyrosine Kinase Inhibitor ZD1839 (Iressa) Inhibits HER2/neu (erbB2)-Overexpressing Breast Cancer Cells In Vitro and In Vivo. *Cancer Res* (2001) 61:8887–95.
85. Normanno N, Maiello MR, De LA. Epidermal Growth Factor Receptor Tyrosine Kinase Inhibitors (EGFR-TKIs): Simple Drugs With a Complex Mechanism of Action? *J Cell Physiol* (2003) 194:13–9. doi: 10.1002/jcp.10194
86. Moyer JD, Barbacci EG, Iwata KK, Arnold L, Boman B, Cunningham A, et al. Induction of Apoptosis and Cell Cycle Arrest by CP-358,774, an Inhibitor of Epidermal Growth Factor Receptor Tyrosine Kinase. *Cancer Res* (1997) 57:4838–48.
87. Ranson M. Epidermal Growth Factor Receptor Tyrosine Kinase Inhibitors. *Br J Cancer* (2004) 90:2250–5. doi: 10.1038/sj.bjc.6601873

Conflict of Interest: The authors declare that the research was conducted in the absence of any commercial or financial relationships that could be construed as a potential conflict of interest.

Copyright © 2021 Saddozai, Wang, Akbar, Zhang, An, Zhu, Xie, Li, Ji and Guo. This is an open-access article distributed under the terms of the Creative Commons Attribution License (CC BY). The use, distribution or reproduction in other forums is permitted, provided the original author(s) and the copyright owner(s) are credited and that the original publication in this journal is cited, in accordance with accepted academic practice. No use, distribution or reproduction is permitted which does not comply with these terms.

Advantages of publishing in Frontiers



OPEN ACCESS

Articles are free to read
for greatest visibility
and readership



FAST PUBLICATION

Around 90 days
from submission
to decision



HIGH QUALITY PEER-REVIEW

Rigorous, collaborative,
and constructive
peer-review



TRANSPARENT PEER-REVIEW

Editors and reviewers
acknowledged by name
on published articles

Frontiers

Avenue du Tribunal-Fédéral 34
1005 Lausanne | Switzerland

Visit us: www.frontiersin.org

Contact us: frontiersin.org/about/contact



REPRODUCIBILITY OF RESEARCH

Support open data
and methods to enhance
research reproducibility



DIGITAL PUBLISHING

Articles designed
for optimal readership
across devices



FOLLOW US

@frontiersin



IMPACT METRICS

Advanced article metrics
track visibility across
digital media



EXTENSIVE PROMOTION

Marketing
and promotion
of impactful research



LOOP RESEARCH NETWORK

Our network
increases your
article's readership